COMPRES

Community Facilities and Infrastructure Development for High-Pressure Mineral Physics and Geosciences: COMPRES II

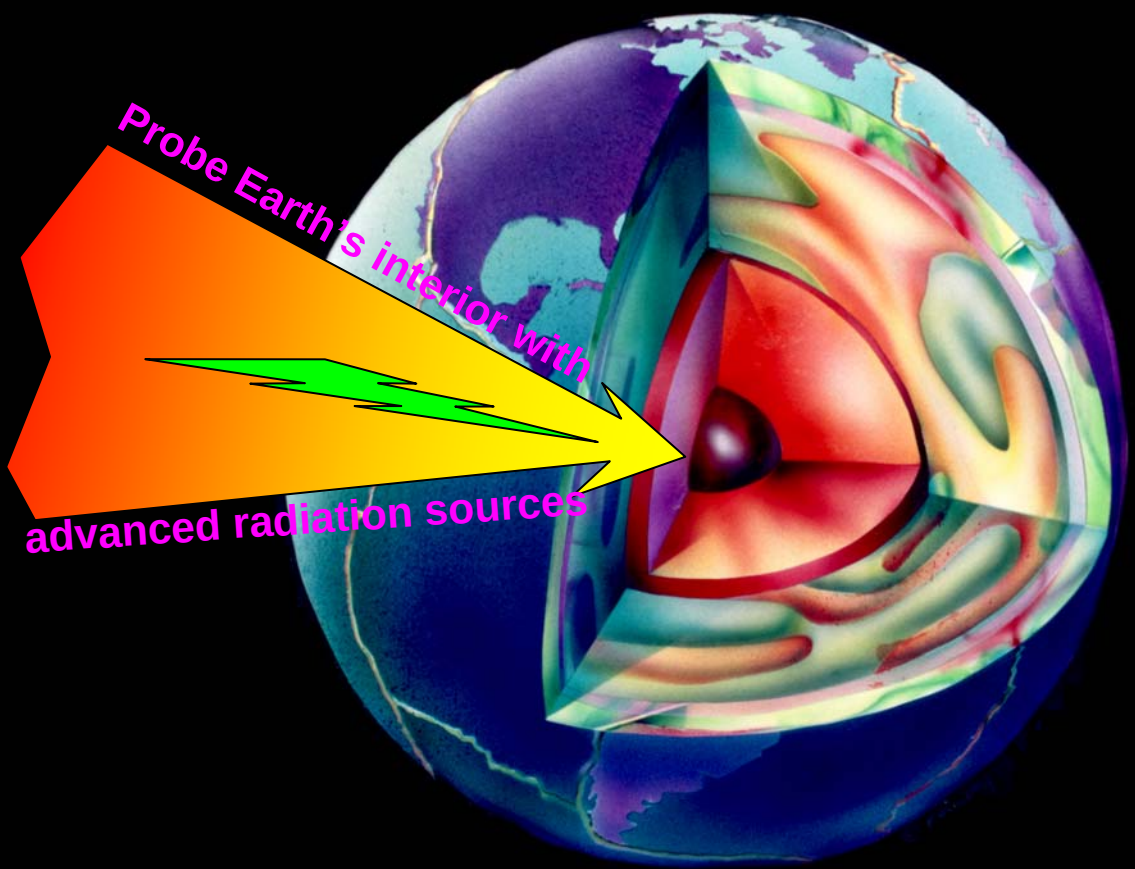

Proposal to NSF 2007-2012

Part C: Research Accomplishments

8 August 2006

Part C: Review of Accomplishments

This Review of Accomplishments is a compilation of one page summaries [One-Pagers] which report highlights of the scientific and technological achievements of students, staff and faculty researchers using COMPRES-supported facilities, data produced from COMPRES programs, and infrastructure development projects supported by COMPRES in its first four years from 2002-2006.

We have adopted the "One-Pager" format developed by IRIS in its 2005 proposal to attractively feature this research. Many students, staff and faculty in the COMPRES community contributed the One-Pagers which appear in this section of the proposal. We thank them for their contributions to high-pressure mineral physics.

Cation distribution in a Fe-bearing K-feldspar from Itrongay, Madagascar. A combined neutron- and X-ray single crystal diffraction study.

Sonia Ackermann *Department of Earth Sciences, University of Basel, Bernoullistr. 30, CH-4056 Basel, Switzerland*,
Martin Kunz *ALS, LBL, MS 4R 0230, 1 Cyclotron Rd, Berkeley CA 94720, USA*,
Thomas Armbruster *Laboratory for Chemical and Mineralogical Crystallography University of Bern, Freiestrasse 3, CH-3012 Bern, Switzerland*,
Jürg Schefer *Laboratory for Neutron Scattering, ETHZ & PSI, CH-5232 Villigen, Switzerland*,
Henry Hänni *Swiss Gemmological Institute, Falknerstrasse 9, CH-4001 Basel, Switzerland*

We determined the cation distribution and ordering of Si, Al and Fe on the tetrahedral sites of a monoclinic low-sanidine from Itrongay, Madagascar, by combined neutron- and X-ray single-crystal diffraction. The cation distribution was determined by means of a simultaneous refinement using neutron- and X-ray data, as well as by combining scattering densities obtained from separate refinements with chemical data from a microprobe experiment. The two methods give the same results and show that Fe is fully ordered on T1, whereas Al shows a high degree of disorder. Based on this and previously published temperature-dependent X-ray data, we conclude that it is preferential ordering of Fe on T1 even at high temperature, rather than a high diffusion kinetics of Fe, which causes this asymmetry in ordering behaviour between Al and Fe. The preferential ordering of Fe relative to Al is in line with its 25 percent larger ionic radius.

	occupancies from simultaneous refinement	occupancies from separate refinement
T1 Si	0.65 (2)	0.65 (3)
T1 Al	0.33 (2)	0.32 (3)
T1 Fe	0.02 (2)	0.023(9)
T2 Si	0.88 (2)	0.88 (3)
T2 Al	0.12 (2)	0.113 (9)
T2 Fe	0.00 (2)	0.000 (2)

This work was partially performed at TriCS / SINQ at the Paul Scherrer Institute in Villigen, Switzerland, Proposal Number II / 03 S-5. Martin Kunz is supported by COMPRES, the Consortium for Materials Properties Research in Earth Sciences under NSF Cooperative Agreement EAR 01-35554. Thomas Armbruster acknowledges support from the ‘Schweizerische Nationalfonds’.

High Pressure X-ray Diffraction of Iron Nitrides and Earth's Anisotropic Inner Core

J.F. Adler and Q. Williams, *UC Santa Cruz*

At modest pressures and reducing conditions, nitrogen becomes compatible within solid phases due to the formation of nitrides. Indeed, the composition of iron-rich meteorites indicates that ~0.5 wt% nitrogen could have been incorporated in Earth's core during accretion. Accordingly, we have examined the behavior of h.c.p. Fe_7N_3 and c.c.p. Fe_4N under compression to 51 GPa. We find that the bulk modulus of each phase is close to that of iron, but that the response to compression of Fe_7N_3 is dramatically more anisotropic than that of iron. Thus, if nitrogen partitions into the solid phase at inner core/outer core conditions, a mixture of iron and iron nitride (or a solid solution between the two) could easily generate the observed anisotropy of the inner core: a result in accord with the possible nitrogen abundance in the bulk of Earth's core.

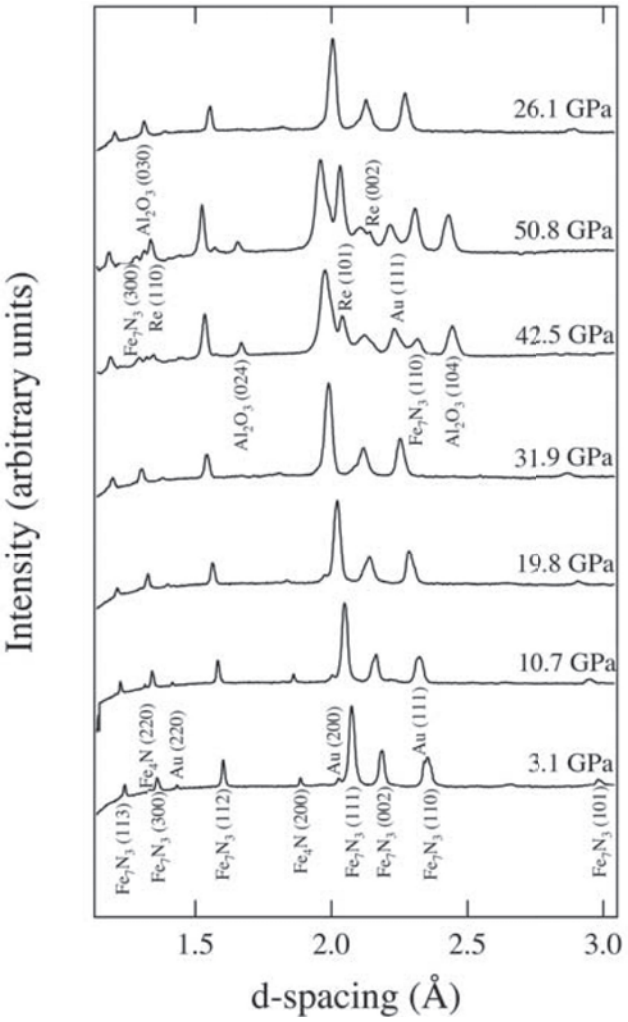

X-ray diffraction patterns of iron nitride. The top pattern was collected during decompression

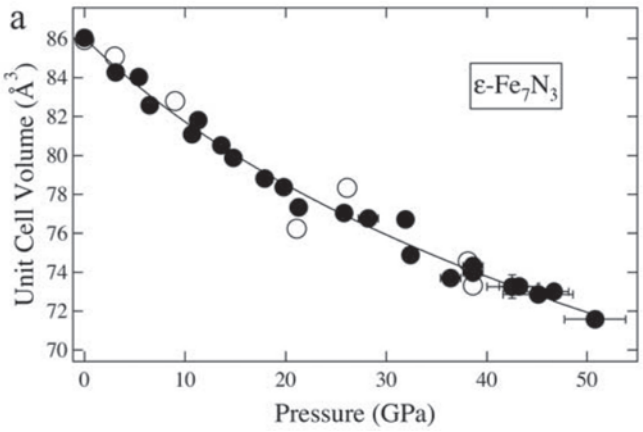

Unit cell volume vs. pressure for Fe_7N_3. Open symbols are on decompression.

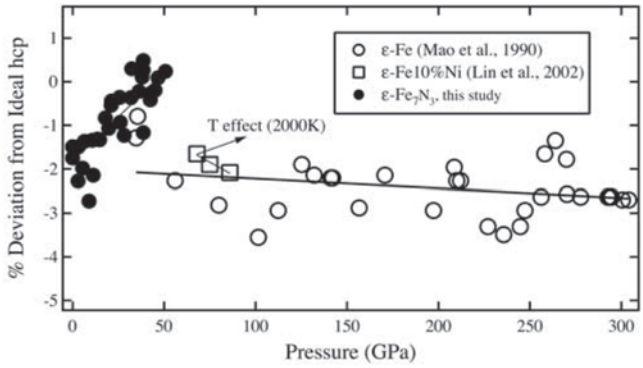

Percent deviation of Fe_7N_3 from the ideal hcp structure relative to iron and an iron-nickel alloy: this deviation is expected to be correlated with anisotropy.

Adler, J.F. and Q. Williams, A high-pressure X-ray diffraction study of iron nitrides: Implications for Earth's core, *Journal of Geophysical Research*, 110, B01203, doi:10.1029/2004JB003103, 2005

Work supported by NSF grant EAR-0310342. This study was conducted at Beamline 10-2 of the Stanford Synchrotron Radiation Laboratory.

Local and long-range order in ferroelastic lead phosphate at high pressure

Ross J. Angel *Virginia Polytechnic Institute and State University*
Ulrich Bismayer *Universitaet Hamburg*
William G. Marshall *Rutherford Appleton Laboratory*

Lead orthophosphate, $Pb_3(PO_4)_2$, undergoes a phase transition from C2/c to symmetry at a pressure of 1.8 GPa at room temperature. Structures determined from neutron powder diffraction data indicated that the phase includes disordered positions for several atoms. Observation of X-ray diffuse scattering from the phase at high pressure suggests that this disorder is static and arises from the presence of several orientations of ordered microdomains of monoclinic local structure, and thus there is no significant change in the local structure at the phase transition (Angel et al., 2004). This is in contrast to the high-temperature phase in which the disorder is dynamic in nature.

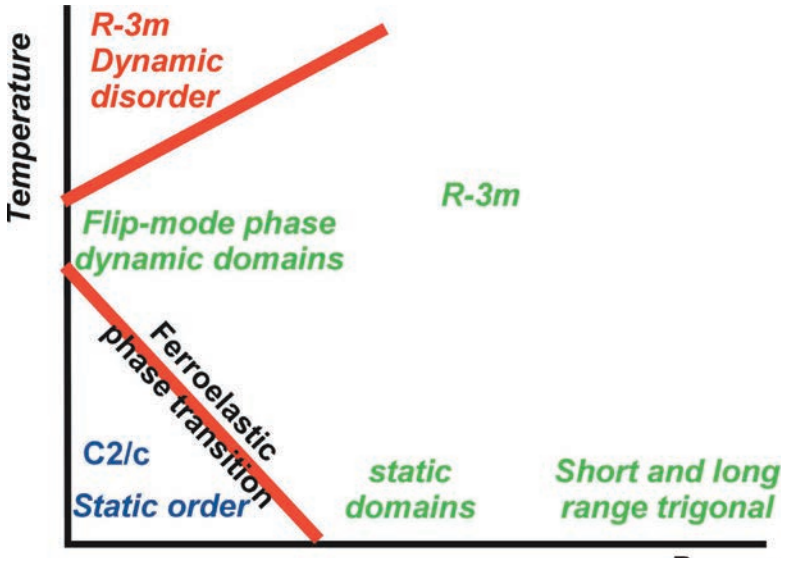

Variation of pressure and temperature in pure lead phosphate. Local environments persist through phase transition. Above transition structure is statically disordered and then becomes ordered.

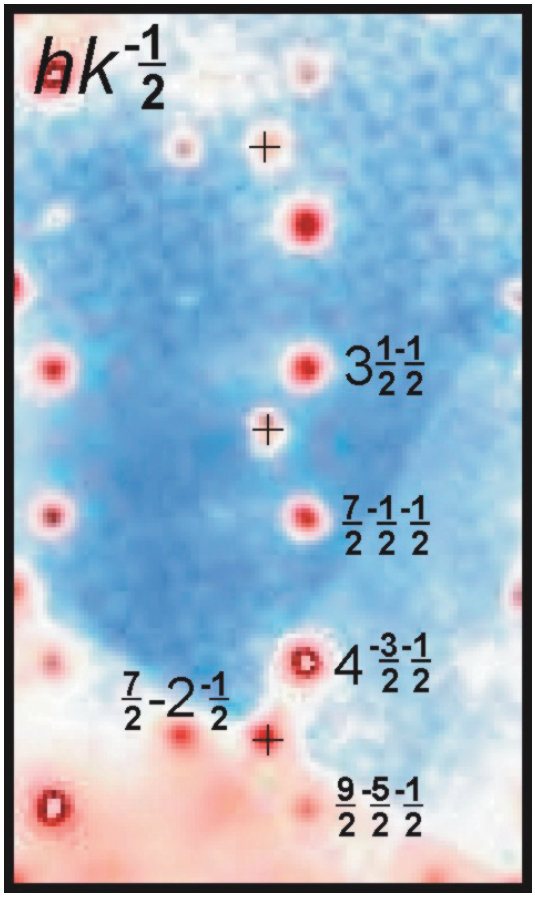

hk-½ reciprocal lattice section collected from a single crystal of $Pb_3(As_{0.52},P_{0.48}O_4)_2$ shows diffuse maxima that are indexed with half integer indices of the R3m unit cell (Angel et al., 2004).

Angel, R. J., U. Bismayer and W. G. Marshall. (2004). Local and long-range order in ferroelastic lead phosphate at high pressure. *Acta Crystallography*, B60, 1–9.

We would like to acknowledge COMPRES (Consortium for Materials Properties Research in Earth Sciences Foundation Cooperatives Agreement EAR 01-35554) for financial support.

Acoustic anomalies accompanying structural changes in $GeSe_2$ glass with pressure

Sytle M. Antao, Liping Wang, Baosheng Li, Jiuhua Chen, John B. Parise *Stony Brook University*
C. J. Benmore *Argonne National Laboratory*

Phase transitions in $GeSe_2$, an archetypal network glass containing both edge and corner sharing tetrahedra, are followed using ultrasonic measurements, at room temperature and pressure up to 9.6 GPa, using a DIA-type, large-volume multi-anvil apparatus in conjunction with in situ energy dispersive X-radiation techniques at X17B2 beamline of the NSLS at Brookhaven National Laboratory. The P-wave velocity increases gradually with pressure while the S-wave velocity decreases anomalously up to 4.5 GPa, and then increases to 9.6 GPa (Figure 1). We attribute this anomaly to changes in the structure of the glass. On decompression, the P and S velocities decrease irreversibly to ambient pressure because of permanent densification. SiO_2 glasses were found to exhibit an anomalous minima in both P and S wave velocities around 3 GPa (e.g., Zha et al. 1994). However, in this study, the minima was observed only for the S wave at about 4.5 GPa. Mei et al. (2005) reported a volume decrease of about 15% up to 3 GPa, and only about 3% from 3 to 9 GPa. Raman results showed that the number of edge sharing tetrahedra changes from 34% at ambient P to ~18% at 3 GPa, and the ratio of edge/corner sharing tetrahedra essentially remains the same beyond 3 GPa (Petri et al. 2000; Wang et al. 2005). The mechanism of close packing of the network maybe by conversion of edge-sharing to corner-sharing tetrahedra at low pressure (0-3 GPa) and by distortion of tetrahedra at higher pressure (3-9 GPa). The variation of Poisson's ratio, σ, is displayed in Figure 1c. The σ starts from 0.03 at 1 GPa, and then increases to 0.34 at 4.5 GPa, beyond which, it becomes nearly pressure independent. A similar trend was observed for SiO_2 glass that becomes pressure independent above 23 GPa (Zha et al. 1994). Most metals have σ between 0.25 and 0.35, while liquids have σ = 0.5. With increasing pressure, the ductility of $GeSe_2$ glass is similar to the typical value for metals.

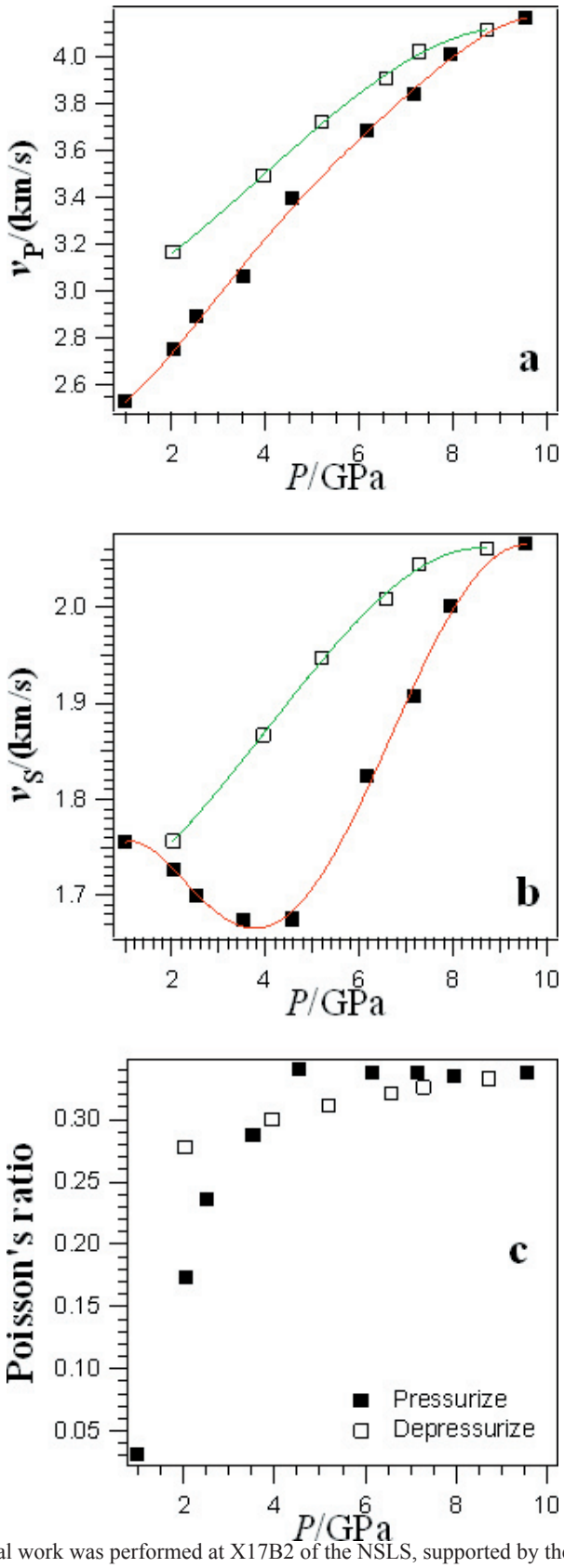

Variations with pressure for (a) v_P (b) v_S, and (c) and Poisson's ratio.

Mei, Q., Benmore, C. J., Hart, R. T., Bychkov, E., Salmon, P. S., Martin, C. D., Michel, F. M., Antao, S. M., Chupas, P. J., Lee, P. L., Shastri, S. D., Parise, J. B., Leinenweber, K., Amin, S., and Yarger, J. L. . (2005) Topology changes in glassy $GeSe_2$ under pressure. In Preperation.

Petri, I., Salmon, P. S., and Fischer, H. E. (2000) Defects in a disordered world: The structure of glassy $GeSe_2$. *Physical Review Letters*, 84, 2413-2416.

Wang, F., Mamedov, S., Boolchand, P., Goodman, B., and Chandrasekhar, M. (2005) Pressure Raman effects and internal stress in network glasses. *Physical Review B*, 71, 174201.

Zha, C. S., Hemley, R. J., Mao, H. K., Duffy, T. S., and Meade, C. (1994) Acoustic velocities and refractive-index of SiO_2 glass to 57.5-GPa by brillouin-scattering. *Physical Review B*, 50, 13105-13112.

This study was supported by NSF grant EAR-0510501. The experimental work was performed at X17B2 of the NSLS, supported by the U.S. Department of Energy, Division of Materials Sciences and Division of Chemical Sciences, under Contract No. DE-AC02-98CH10886. This research was partially supported by COMPRES, the Consortium for Materials Properties Research in Earth Sciences under NSF Cooperative Agreement EAR 01-35554.

High-temperature elasticity, cation disorder and magnetic transition in magnesioferrite

Sytle M. Antao, John B. Parise, Robert C. Liebermann *Stony Brook University*
Ian Jackson *Australian National University*

Acoustic anomalies in magnesioferrite, $MgFe_2O_4$, are followed using ultrasonic measurements, at 300 MPa and temperatures up to 700 ºC, in a gas-medium high-pressure apparatus. The experimental path for the high-T ultrasonic-data collection consists of four heating and cooling cycles carried out on the sample held at 300 MPa. In general, there is a smooth and consistent trend of decreasing velocities with increasing temperature (Figure 1). For T < 400 ºC, this trend is linear with δKS/δT of approximately – 0.032 and – 0.026 GPa K^{-1} for the (1c, 2h) and (2c, 3h) datasets, respectively, while the δG/δT values are approximately - 0.011 GPa K^{-1} for both datasets. A significant discontinuity between 350 and 400 ºC is evident only in the results from the second heating cycle. This discontinuity probably represents the Curie transition that was observed by thermal analyses at about 360 ºC (Antao et al. 2005). At 600 ºC, the S wave was unobserved. On heating to temperatures > 650 ºC, the P-wave signal quality progressively deteriorates and the travel-times become more strongly temperature-sensitive. Signal quality is recovered on subsequent cooling below ~ 500 ºC. The dramatic decrease of V_P with increasing temperature beyond 550 ºC is probably associated with the onset of appreciable cation mobility (Antao et al. 2005). A close correlation is observed between results obtained during any given cooling cycle and the immediately subsequent heating cycle. However, travel-times measured during cooling from temperatures near 700 ºC are systematically greater than those for the preceding heating cycle. On recovery at room temperature following the final cooling cycle (4c), V_P and V_S are found to have decreased by 1.2% and 0.8%, respectively, relative to the corresponding quantities measured after cooling cycle 1c.

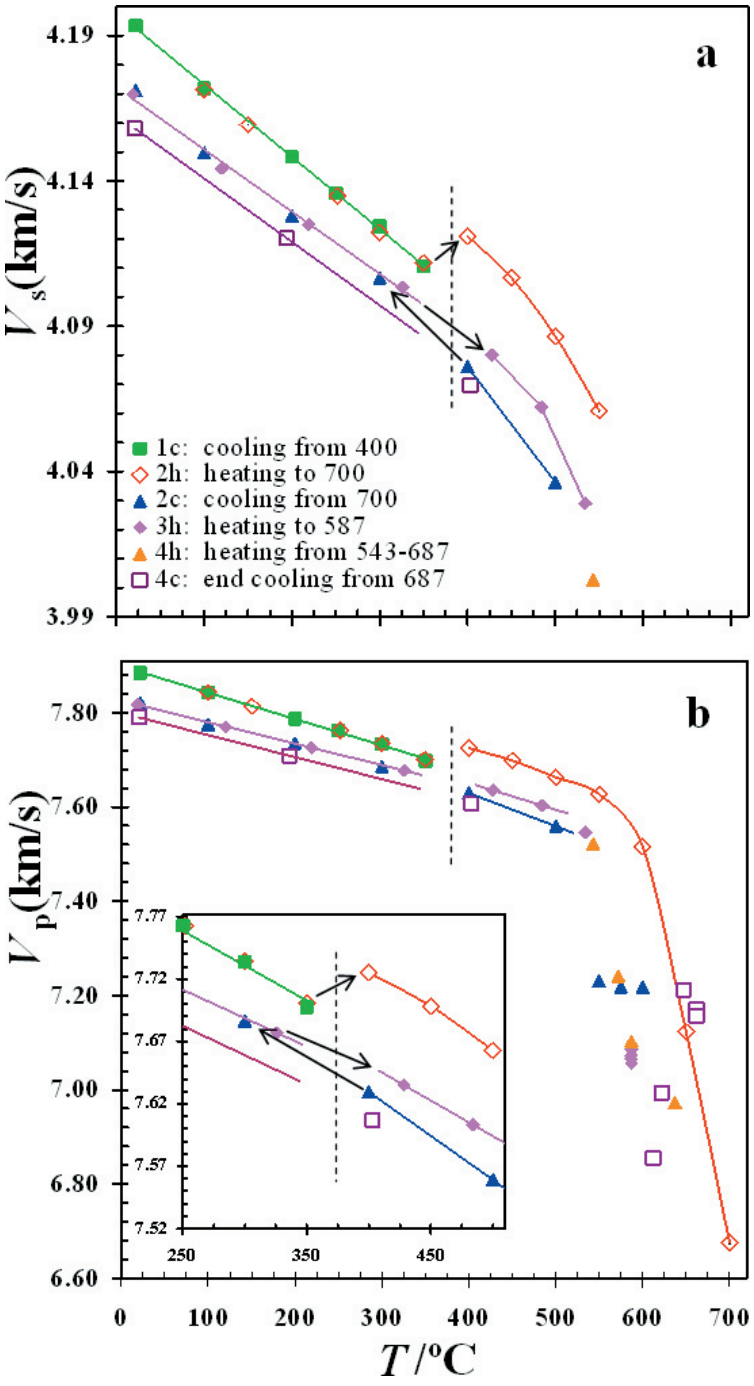

Variation of the velocity vs. temperature for (a) S waves and (b) P waves in magnesioferrite held at a constant pressure of 300 MPa. The insert in (b) displays V_P in the vicinity of the magnetic transition. A dashed line is drawn near the magnetic transition, T_c. Data from 550 ºC onwards slowly start to move towards smaller values. The S wave is unobserved at and beyond 600 ºC, where V_P markedly decreases.

Antao, S. M., Hassan, I., and Parise, J. B. (2005) Cation ordering in magnesioferrite, $MgFe_2O_4$, to 982 °C using in situ synchrotron X-ray powder diffraction. *American Mineralogist*, 90, 219-228.

The experimental work was performed in the high pressure laboratory at the Australian National University with the assistance of Craig Saint and Lara Weston. This study was supported by NSF grants EAR-0510501 and NSF-INT 0233849.

Brillouin Scattering with Synchrotron Radiation at the GSECARS, Advanced Photon Source: A COMPRES Infrastructure Development Project

Jay D Bass1, Guoyin Shen2,3, Mark Rivers2

1: Geology Dept, Univ. of Illinois, 1301 W Green St, Urbana, IL 61801 jaybass@uiuc.edu ; 217-333-1018
2: GSECARS, University of Chicago, 5640 S. Ellis Ave, Chicago, IL 60637
3: Now at HPCAT, sector 16 of the APS. gshen@hpcat.aps.anl.g

A Brillouin spectrometer has been installed and successfully tested at the 13-BM-D station (GSECARS) of the Advanced Photon Source (APS). This is a unique facility which opens a new area of in-situ studies for materials at extreme conditions. Now it is possible to perform simultaneous measurements of density (by x-ray diffraction) and sound velocities (by Brillouin scattering) of transparent single-crystal and polycrystalline materials at high pressure and temperature. This allows the determination of an absolute pressure scale, which is one of the outstanding technical challenges in experimental mineral physics today. The equation of state, acoustic velocities and, hence, elastic moduli of materials as a function of pressure and temperature can now be determined without resort to a secondary pressure standard, such as ruby fluorescence scale, or the EOS of Au, Pt, MgO and other commonly used standard materials.. The experimental data collected simultaneously with high resolution x-ray diffraction and Brillouin spectroscopy from the same sample area and in the same P-T environment provides essential information for comparing with mineral physics results with seismic observations, and for modeling the composition and evolution of the Earth.

Interfacing an elaborate Brillouin system with the x-ray optics in the beam line hutch, and being about to operate it from outside the hutch, were to of many experimental challenges faced in this project. The Brillouin system is compatible with powder (polycrystalline) and single-crystal x-ray diffraction techniques, while not interfering with other experimental techniques performed on the beamline.

Pilot high-pressure experiments measuring sound velocities and densities of samples in a diamond anvil cell were performed on single-crystal NaCl (B1), polycrystalline NaCl (B2) to 73 GPa, and single crystal MgO at high temperature to 600°C and high pressure.

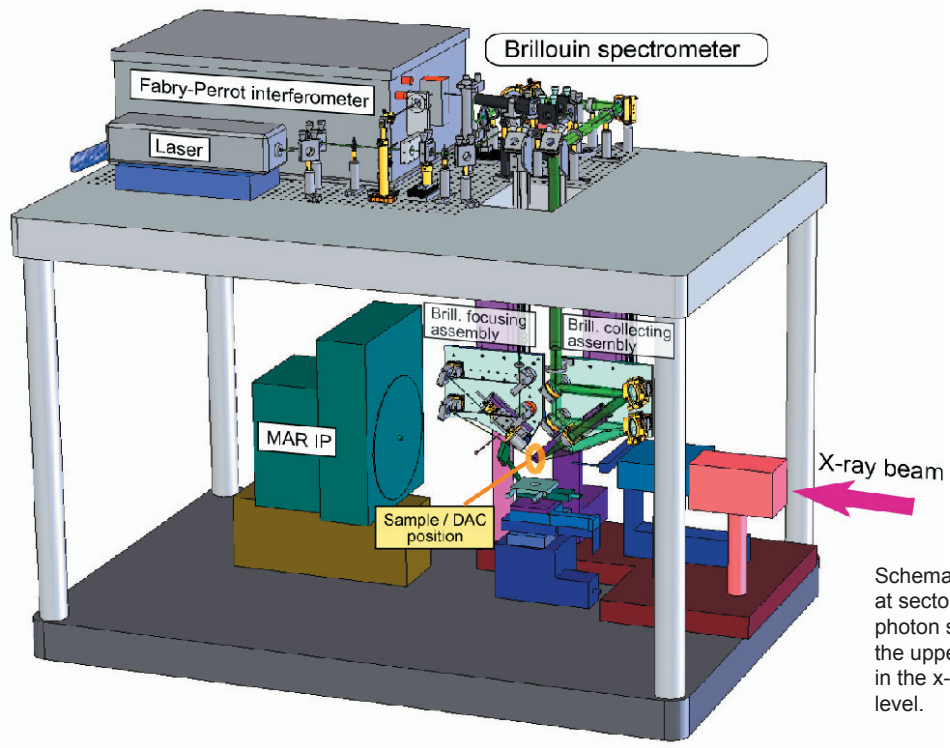

Schematic diagram of the Brillouin spectrometer at sector 12-BM-D of GSECARS, Asvanced photon source. Most of the Brillouin optics are on the upper level, whereas the sample is in placed in the x-ray beam for all experiments on the lower level.

Sinogeikin, SV, J D Bass, V Prakapenka, D L Lakshtanov, G Shen, C Sanches-Valle, M Rivers. (2006) A Brillouin spectrometer interfaced with synchrotron X-radiation for simultaneous x-ray density and acoustic velocity measurements. Submitted, *Rev. Sci. Instr*.

Bass J.D, SV Sinogeikin, D Lakshtanov, V Prakapenka, G Shen (2005) Brillouin Scattering and Synchrotron X-Ray Measurements at GSECARS, Advanced Photon Source: Simultaneous Measurements of Sound Velocities and Density, *Fall AGU meeting*, San Francisco CA.

Sinogeikin, SV, D Lakshtanov, C Sanches-Valle, V Prakapenka, G Shen, E Gregoryanz, JD Bass (2005) Elastic moduli and equation of state of NaCl to 30 GPa by simultaneous x-ray density and Brillouin sound velocity and measurements. *Fall AGU meeting*, San Francisco CA.

D Lakshtanov SV Sinogeikin, C Sanches-Valle, V Prakapenka, G Shen3, E Gregoryanz4, JD Bass (2005) Aggregate Elastic Moduli and Equation of State of B2 Phase of NaCl to 73 GPa by Simultaneous Synchrotron X-ray Diffraction and Brillouin Scattering Measurements. *Fall AGU meeting,* San Francisco CA.

Supported by the NSF under grant EAR-0135642, the Elasticity Grand Challenge.

Short and Long Range Order Using Neutron Diffraction, Pair Distribution Function Analysis and NMR Spectorscopy

Julien Bréger, Nicolas Dupré, John B. Parise and Clare P. Grey• *Stony Brook University*
Peter J. Chupas, Peter L. Lee • *APS, Argonne National Laboratory*

Thomas Proffen • *Los Alamos*

The local environments and short-range ordering in condensed matter are best addressed using X-ray total scattering techniques (Bragg + diffuse). Supplementing X-ray studies with neutron scattering and NMR, especially in those cases where X-ray scattering contrast is poor (Al/Si disorder for example) provides new insights. As a proof of concept experiment we have used neutron diffraction and isotopic substitution (NDIS) techniques to "mask" scattering from one or two components of the structure and thereby greatly simplify the task of interpreting short range structure (Figure 1). This approach is particularly useful in combination with modeling Reverse Monte Carlo (RMC) calculations. Our initial results suggest the approach will be useful to study order-disorder in systems, including glasses and possibly melts. The material chosen for proof of concept study, $LiNi_{0.5}Mn_{0.5}O_2$, a layered structure potentially useful in battery applications and with considerable Li/Ni/Mn disorder between metal sites. This was prepared as $^{6}Li(NiMn)_{0.5}O_2$, $^{7}Li(NiMn)_{0.5}O_2$, and $^{7}Li(NiMn)_{0.5}O_2$ enriched with ^{62}Ni (denoted as $^{7}LiZERONi_{0.5}Mn_{0.5}O_2$), so that the resulting scattering length of Ni atoms is null. PDF analysis of the neutron data revealed considerable local distortions in the layers that were not captured in the Rietveld refinements performed using the Bragg diffraction data alone. RMC calculations using large clusters of 2400-3456 atoms, built to investigate cation ordering provided results consistent with a nonrandom distribution of Ni, Mn, and Li cations in the transition metal layers; both the Ni and Li atoms are, on average, close to more Mn ions than predicted based on a random distribution of these ions in the transition metal layers. These results are not obtained from analysis of the Bragg data alone and suggest when appropriate mixtures of isotopes are available (readily available mixtures providing null contrast) NDIS coupled with RMC can provide insight into the local order. Following up on these results in systems under high pressure is a priority for future work.

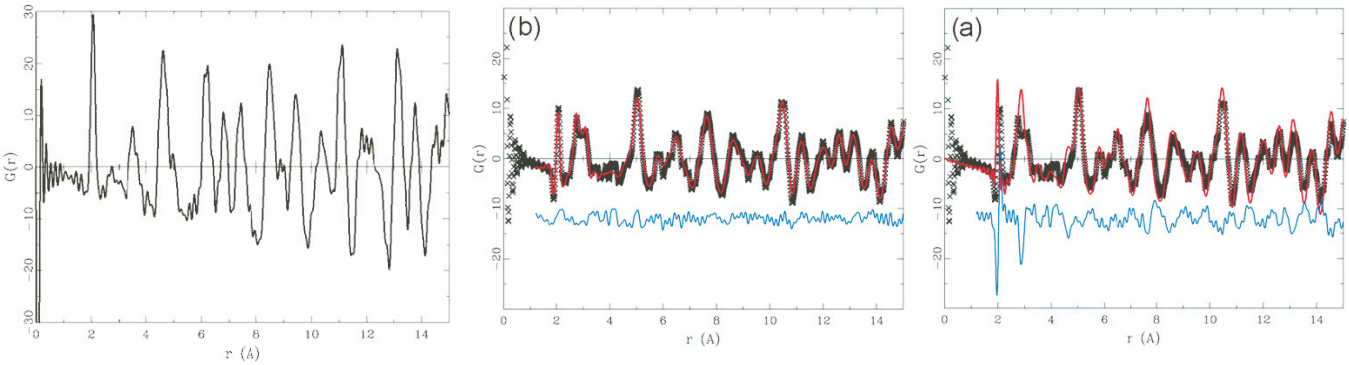

Figure 1 (left) Differential Ni PDF obtained from the PDF data of $^{7}Li(natNiMn)_{0.5}O_2$ and $^{7}Li(ZERONiMn)_{0.5}O_2$. (right) Reverse Monte Carlo (RMC) results for $^{7}LiNi_{0.5}Mn_{0.5}O_2$ pristine material; (a) is the fit before the RMC calculations with the initial random cluster model, and (b) is after. The black crosses represent the experimental data, and the solid red line is the calculated PDF. The difference between the calculated and experimental patterns is shown in blue.

Breger, J.; Dupre, N.; Chupas, P. J.; Lee, P. L.; Proffen, Th.; Parise, J. B.; Grey, C. P. (2005) Short- and Long-Range Order in the Positive Electrode Material, $Li(NiMn)_{0.5}O_2$: A Joint X-ray and Neutron Diffraction, Pair Distribution Function Analysis and NMR Study *J. Am. Chem. Soc*. 127, 7529-7537

This study was supported U.S. DOE under Contract No. DE-AC03-76SF00098. Travel support for one trip to Los Alamos partially provided to JB by COMPRES (EAR 01-35554). Use of the Advanced Photon Source and LANSCE neutron source was supported by the U. S. Department of Energy, Office of Science, Office of Basic Energy Sciences.

Investigation of Quartz Deformation and Phase Transformation Behavior Using the D-DIA Apparatus

Pamela C. Burnley, Dongmei Zhang, and Beth Lavoie, *Department of Geosciences, Georgia State University*

An understanding of the influence of phase transformation and other metamorphic reactions on the rheological properties of rocks is of interest to geophysicists and geologists studying deformation in all parts of the Earth. In particular, it has been proposed that reactions may concentrate shear strain (for review see [Rutter and Brodie, 1995]) and it has been demonstrated that transformation during deformation can produce mechanical instabilities [e.g. Burnley et al., 1991; Green and Burnley, 1989; Jung et al., 1994; Zhang et al., 2004]. We are conducting experiments using the D-DIA that will allow us to observe how both stress and strain evolve in materials that are actively deforming while transforming. We plan to study reconstructive transformations in olivine, calcite, quartz, and jadeite. Our initial experiments have focused on the deformation of quartz and the quartz-coesite transformation. However, before we can understand how phase transformation affects deformation behavior, we must first understand the deformation behavior of the parent phase alone. The differential stress in a sample being deformed in the D-DIA can be measured by comparing the d-spacing of x-ray reflections parallel to and perpendicular to the direction of the maximum compressive stress. The d-spacings combined with single crystal elastic constants yield a differential stress for each reflection (Singh et al., 1998). During elastic deformation the differential stresses measured from different x-ray reflections generally agree (e.g. Li et al., 2004). However, once the sample yields and ductile deformation begins, the differential stresses associated with each reflection begin to diverge (e.g. Li et al., 2004). This effect has also been observed in neutron scattering experiments on deforming metals (e.g. Clausen et al., 1999; Daymond et al.,1997), MgO (Li et al., 2004) and in olivine (Mei et al., 2005). In our D-DIA experiments on the deformation of polycrystalline alpha quartz, we observed a flow strength of 0.1(0.1)GPa for the (112) reflection versus a flow strength of 0.7 (0.2) GPa for the (100) reflection (Figure 1). The cause of these differences is not well understood and the interpretation of the single crystal differential stresses in terms of the over all load that the specimen supports is also not clear – especially for materials where the differences between reflections is very large. What is clear is that we now have access to an entirely new and different class of information about how polycrystalline materials deform. In our ongoing studies, we are focusing on developing a technique for directly measuring the overall external load supported by the sample and comparing the pattern of differential stresses between samples that contain only one phase (e.g. alpha quartz) and partially transformed samples that contain two phases (e.g. alpha quartz and coesite).

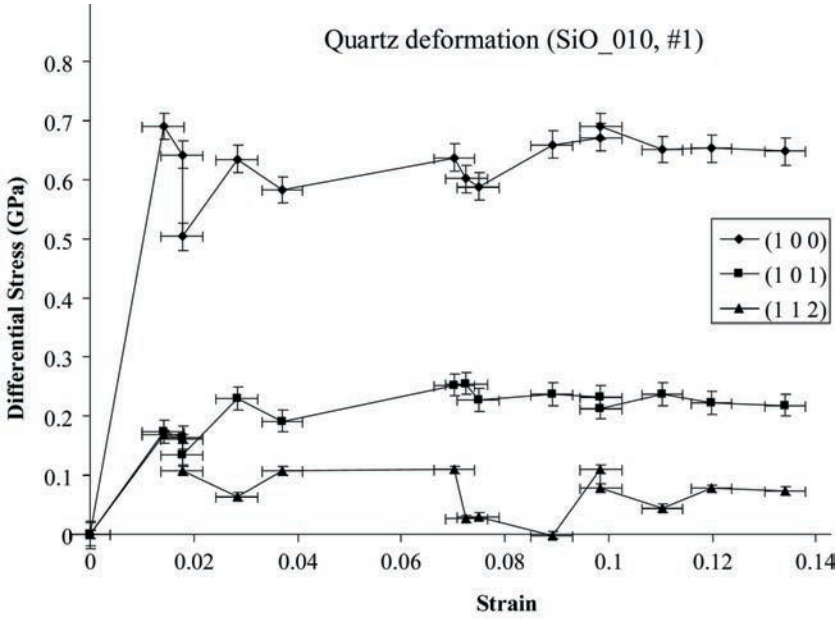

Stress strain curves for deformation of quartz at 800 C and 2 GPa at 10-5/s in the D-DIA apparatus. Error bars show precision of measurements, systematic uncertainty in stress is estimated to be about ±0.1 GPa for (101) and (112) and ±0.2 GPa for (100).

Clausen, B. Lorentzen. T. Bourke, M. A.M. and Daymond, M.R., (1999) *Mater. Sci. Eng. A* 259(1), 19.

Daymond, M.R. Bourke, M.A.M., Von Dreele, R. B., Clausen, B. and Lorentzen, T. J. (1997) *Appl. Phys*. 82(4), 1554

S. Mei, W. B. Durham, and D. L. Kohlstedt (2005) *Eos Trans. AGU* 86(52), Fall Meet. Suppl., Abstact MR13B-08

Singh, A.K., Balasingh, C., Hao, H.-K, Hemley, R. Shu, J. (1998) *Appl. Phys*. 83, 7567

Li, L. Weidner, D.J., Chen, J. Vaughan, M.T., Davis, M. and Durham, W. B. (2004) *Journal of Applied Physics*, 95, 12, 8357-8365

The work supported by NSF grant EAR-0136107 to PCB. Experiments were carried out at the X-17B2 beamline of the National Synchrotron Light Source (NSLS) which is supported by the US Department of Energy, Division of Materials Sciences and Division of Chemical Sciences under Contract No. DE-AC02-76CH00016 and by COMPRES, the Consortium for Materials Properties Research in Earth Sciences under contract number NSF Cooperative Agreement EAR 01-35554.

Finite element modeling of elastic volume changes in fluid inclusions: Comparison with experiment

Pamela. C. Burnley *Department of Geosciences, Georgia State University, Atlanta, GA Phone: (404)463-9551, FAX: (404)651-1376, E-mail: Burnley@GSU.edu*
Christian Schmidt *GeoForschungsZentrum Potsdam, Potsdam, Germany*

Inclusions within mineral grains are nearly ubiquitous in rocks of all types. Whether they are crystalline, glass, fluid, or, gas, inclusions contain information about either the environment of formation of the host mineral grain or conditions since the mineral grain was formed. If the temperature or pressure changes after the inclusion host system forms, differences in thermal expansion or compressibility between the two will create differential stresses in the host and may cause it to permanently deform. Understanding the mechanics of the inclusion-host system can be important for interpreting measurements made on the inclusion as well as for deducing information about the geologic history of a sample. We have used finite element modeling (FEM) to successfully reproduce elastic volume changes of synthetic fluid inclusions in quartz pressurized in a hydrothermal diamond anvil cell (HDAC) at external pressures up to 250 MPa. At higher pressures, the synthetic inclusions are somewhat stiffer than would be predicted by linear elasticity due to the effect of pressure on the elastic moduli. The finite element models were created to reproduce the inclusion's approximate shape, and crystallographic orientation within the host, which is elastically anisotropic. The models successfully predict changes in fluid inclusion volume measured using the HDAC, which gives us confidence that FEM may be used to predict the elastic behavior of inclusions in other situations. The figure below shows: 1) a photomicrograph of synthetic inclusion I, 2) 1/8th of the 3D finite element model mesh for an inclusion with dimensions 1.5 x 12 x 24. The white region is the inclusion. The remainder of the model is related to the part shown by reflection through three orthogonal mirror planes. 3) a plot comparing the percent volume change of synthetic inclusion I to calculated volume changes from finite element models with dimensions 12 x 24 and thickness between 1.3 and 1.7. A good match is obtained for the model 1.5 units thick. Note that the volume change of the model is strongly sensitive to thickness.

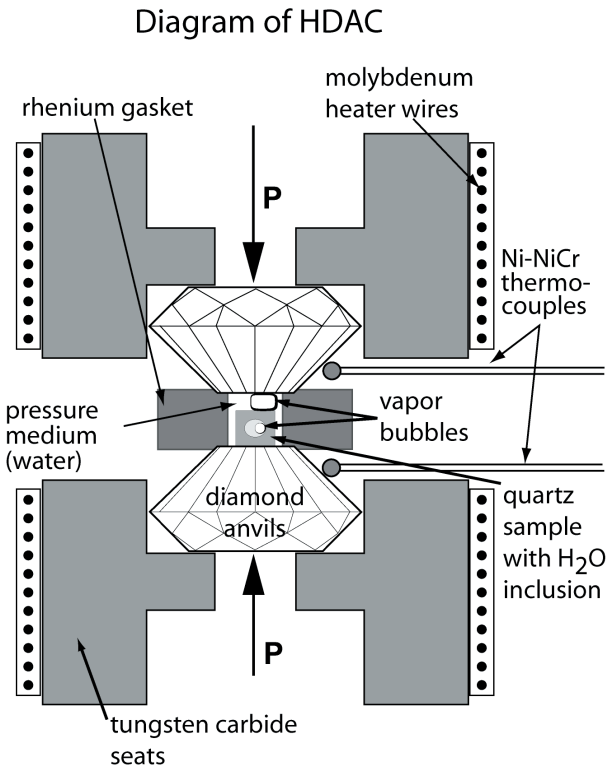

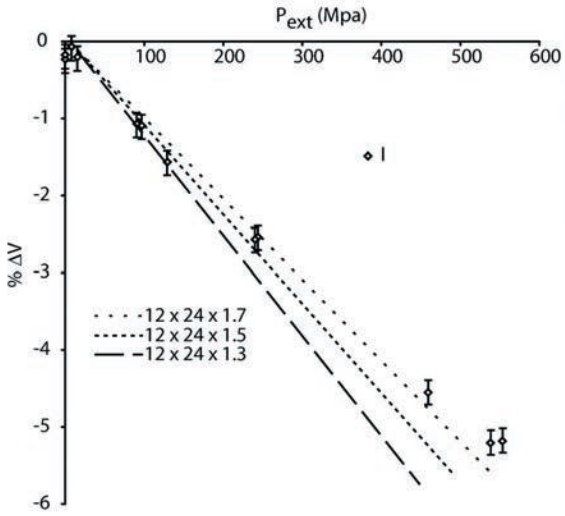

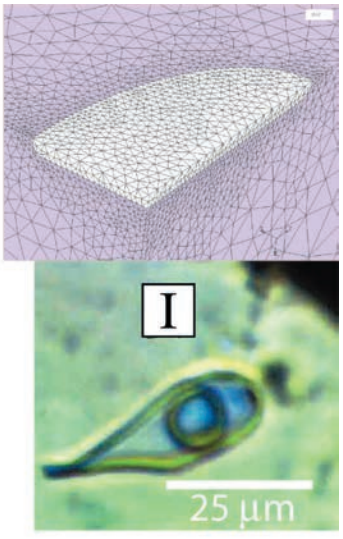

Acknowledgements: The work supported by NSF grant EAR-0136107 to PCB.

Laser Heated Diamond Anvil Cell at the Advanced Light Source

W. A. Caldwell, M. Kunz, R. S. Celestre, J. M. Glossinger, A. A. MacDowell, M. J. Walter, D. Walker, H. A. Padmore, R. Jeanloz, and S. M. Clark

The laser heating system for the diamond anvil cell at endstation 2 of beamline 12.2.2 of the Advanced Light Source in Berkeley, CA has been constructed and is available for high-pressure high-temperature experiments. The endstation couples a high-brilliance synchrotron x-ray source with an industrial strength laser to heat and probe samples at high pressure in the diamond anvil cell, as shown schematically in Figure 1. The system incorporates an 80 watt Nd:YLF (cw) laser operated in TEM01 mode. Double-sided heating is achieved by splitting the laser beam into 2 paths that are directed through the opposing diamond anvils. X-ray transparent mirrors steer the laser beams coaxial with the x-ray beam from the superbend magnet (energy range 6-35 KeV) and direct the emitted light from the heated sample into two separate spectrometers for temperature measurement by spectroradiometry. Objective lenses focus the laser beam to a size of 30 micron diameter (FWHM) in the sample region. An x-ray spot size of 10 micron diameter (FWHM) has been achieved with the installation of a pair of focusing Kirkpatrick-Baez mirrors. A unique aperture configuration has produced an x-ray beam profile that has very low intensity in the tails. The main thrust of the program is aimed at producing in-situ high-pressure high-temperature x-ray diffraction data, but other modes of operation, such as x-ray imaging have been accomplished.

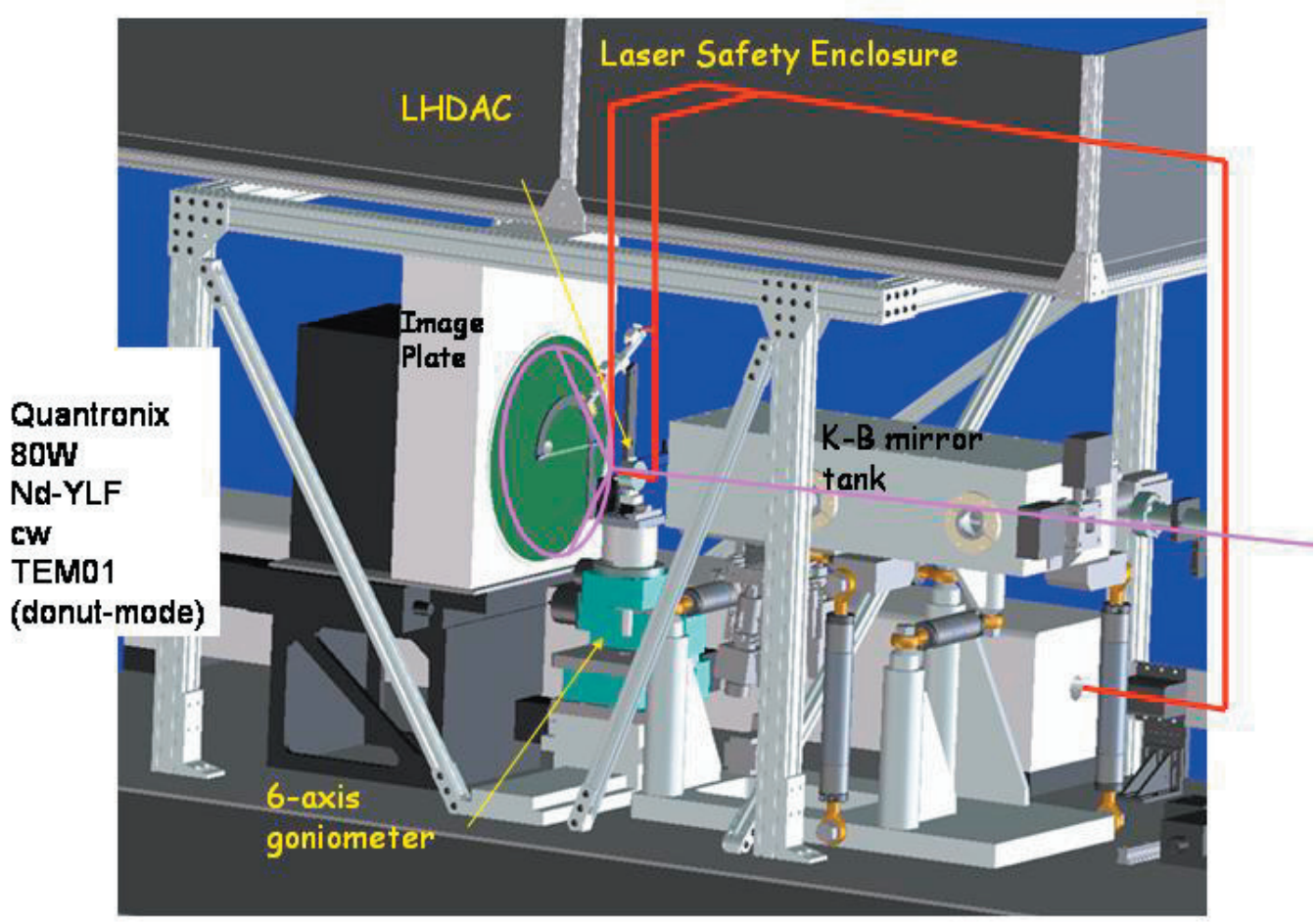

W.A. Caldwell et al., Fall Meeting of the American Geophysical Union, San Francisco, CA (2005).

This work was supported by COMPRES, the Consortium for Materials Properties Research in Earth Sciences under NSF Cooperative Agreement EAR 01-35554.

The Advanced Light Source is supported by the Director, Office of Science, Office of Basic Energy Sciences, Materials Sciences Division, of the U.S. Department of Energy under Contract No. DE-AC03-76SF00098 at Lawrence Berkeley National Laboratory.

Oxygen fugacity at high pressure: Equations of state of metal – oxide pairs.

A. J. Campbell1, L. Danielson2, K. Righter2, Y. Wang3, G. Davidson1 and H. Nguyen1, *1Dept. of Geology, University of Maryland, College Park, MD 20742 (ajc@umd.edu); 2Johnson Space Center, NASA, Houston, TX 77058; Center for Advanced Radiation Sources, University of Chicago, Argonne, IL 60439.*

Introduction: Oxygen fugacity (fO_2) varies by orders of magnitude in nature, and can induce profound changes in the chemical state of a substance, and also in the chemical equilibrium of multicomponent systems. fO_2 is a principal controlling factor for redox equilibria and valences of elements that are stable in more than one oxidation states (e.g., [1]). In experimental studies, fO_2 are usually determined relative to a particular metal-oxide buffer (e.g., Fe-FeO, Ni-NiO, Co-CoO, Re-ReO_2), but the application of experimental results is weakened by the fact that the pressure-induced relative changes between these buffer systems are imprecisely known. To better understand the pressure effect on the Gibbs free energy (dG = VdP) of buffer equilibria such as $M + (x/2)\ O_2 = MO_x$, we measure the equations of state of metal-oxide buffer pairs simultaneously. This minimizes systematic biases that might appear between studies, improving the precision of the ΔV data used to determine the high pressure fO_2 buffers. This work utilizes special beamline specific multi-anvil assemblies that were developed by a COMPRES project.

Experimental: Mixtures of fine-grained Ni-NiO, Fe-$Fe_{1-x}O$ and Re-ReO_2 and NaCl, (pressure standard) were loaded into a boron nitride capsule which was machined to fit within a specially developed beamline version of a 14/8 assembly developed by the COMPRES multi-anvil assembly initiative (Fig. 1A; [2]). The octahedron is extrusion molded $MgAl_2O_4$ (spinel) which, together with the BN capsule, graphite furnace and an outer forsterite sleeve, is more transparent to x-rays than standard assemblies. More standard features of the assembly are a Type C W-Re thermocouple, TZM sleeves around the alumina thermocouple sheaths, pyrophyllite gaskets, and laser-cut paper on opposing cubes. The octahedral assemblies were loaded into the multi-anvil press at GSECARS, Sector 13 of the Advanced Photon Source [3], and pressurized for in situ, high-P,T X-ray diffraction using synchrotron radiation. Diffraction patterns were collected at a series of P,T points for each sample; in this way the molar volume of the metal and metal oxide in each buffer pair were determined under identical P,T conditions, allowing intercalibration of their equations of state. Temperature was cycled at each of several hydraulic load settings. The pressure varied slightly with the changing temperature, because of competing effects of gasket softening and thermal pressure.

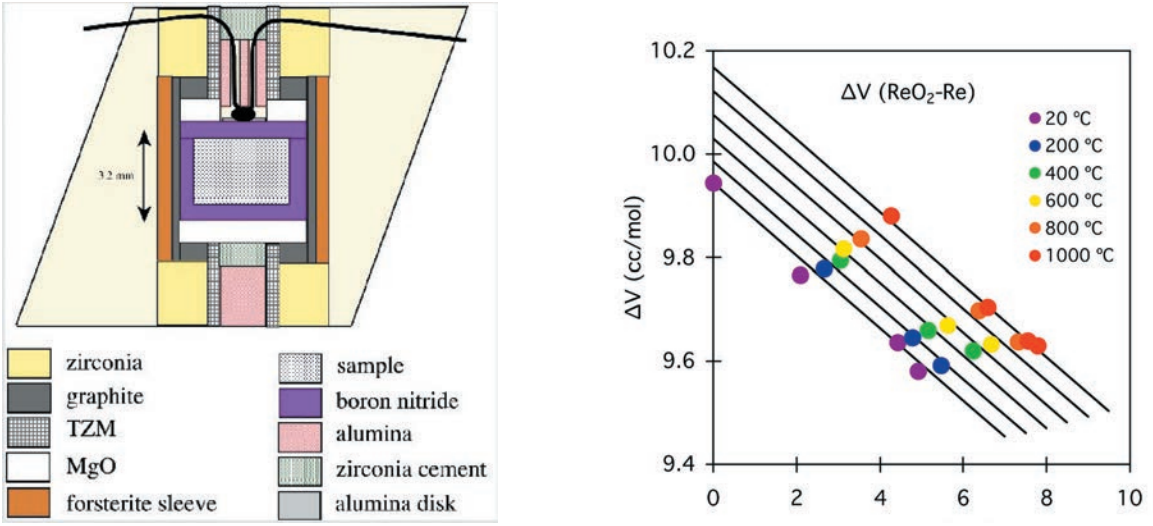

Figure 1A) High pressure assembly used for in situ experiments. B) ΔV (ReO_2=Re) as a function of pressure and temperature. Solid lines are a fit to a simple expression: $\Delta V_{RRO} = A*P + B*\Delta T$. The r.m.s. value for this fit is 0.02 cm^3/mol, or 0.2%.

Results: The bulk modulus, K_T, of ReO_2 (orthorhombic phase) was determined to be 180±4 GPa, based on a fit of the high-P,T data to a thermal equation of state [4]. The volume difference between ReO_2 and Re (ΔV_{RRO}) is shown as a function of pressure and temperature in Fig. 1B. These data can be used to evaluate the ΔG of the Re-ReO_2 buffer at high pressures, by integrating the $\int \Delta V_{RRO}\ dP$ term in the equation above. The difference between the IW [5] and RRO buffers ($\log(fO_2)_{RRO}$-$\log(fO_2)_{IW}$) remains nearly the same (within 0.1 log units) even when extrapolated to 20 GPa, over $1000 \leq T \leq 2200$. This is a useful result, because it indicates that relative fO_2 values determined in previous high pressure experiments using either the IW or RRO buffers are readily comparable, and not subject to a significant systematic error from different pressure effects on the two buffers. This is not a general result appropriate to all fO_2 buffers, but a coincidence in high-pressure effects on the IW and RRO buffers (supported by NASA Cosmochemistry RTOP to KR and NSF grant EAR0600140 to AJC).

[1] Righter K. and Drake M. J. (2003) In *The Mantle and Core* **(Ed. R. Carlson), Elsevier, pp. 425-449.**

[2] Leinenweber K. et al. (2006), *High Pressures*, submitted;

[3] Uchida T. et al. (2002) *J. Phys. Condens. Matter*, 14, 11517-11523;

[4] Anderson et al. (1989) J. Ap. Phys., 65, 1534. [5] Fei Y. (1996) In *Mineral Spectroscopy* (Eds. M. D. Dyar et al.), Geochemical Soc., pp. 243-254; Uchida T. et al. (2001) *J. Geophys. Res*., 106, 21799-21810.

High Pressure XRD Study of Mixed-stacking Nano-ZnS

Bin Chen, Hengzhong Zhang, Jill Banfield, *University of California, Berkeley*

Studies of high pressure induced structural changes of mixed-stacking ZnS nanoparticles using diamond anvil cells were carried out to 28.6 GPa on Beamlines X17C and X17B3, National Synchrotron Light Source, Brookhaven National Laboratory. When pressure rises to ~15 GPa the mixed-stacking structure of AB-ABC is lost (Fig. 1). A high-pressure phase begins to form above ~16 GPa. The high-pressure phase is stable at pressure up to 28.6 GPa, the highest pressure attained in this study, and is quenchable to room pressure. This is another evidence that high-pressure compression may be used to create materials with novel structures. It has been reported that both sphalerite and wurtzite ZnS nanoparticles transform to the NaCl phase under compression and return to sphalerite phase upon decompression. Apparently the high-pressure phase observed in this study is not the NaCl structure. The phase identification is in process. TEM measurements are planned. We are studying further to find out why the high-pressure behavior of the mixed cubic and hexagonal stacking structure of n-ZnS is so different from that of the pure cubic and hexagonal structures. This work is being Representative XRD patterns of mixed-stacking n-ZnS in compression written up for journal publication.

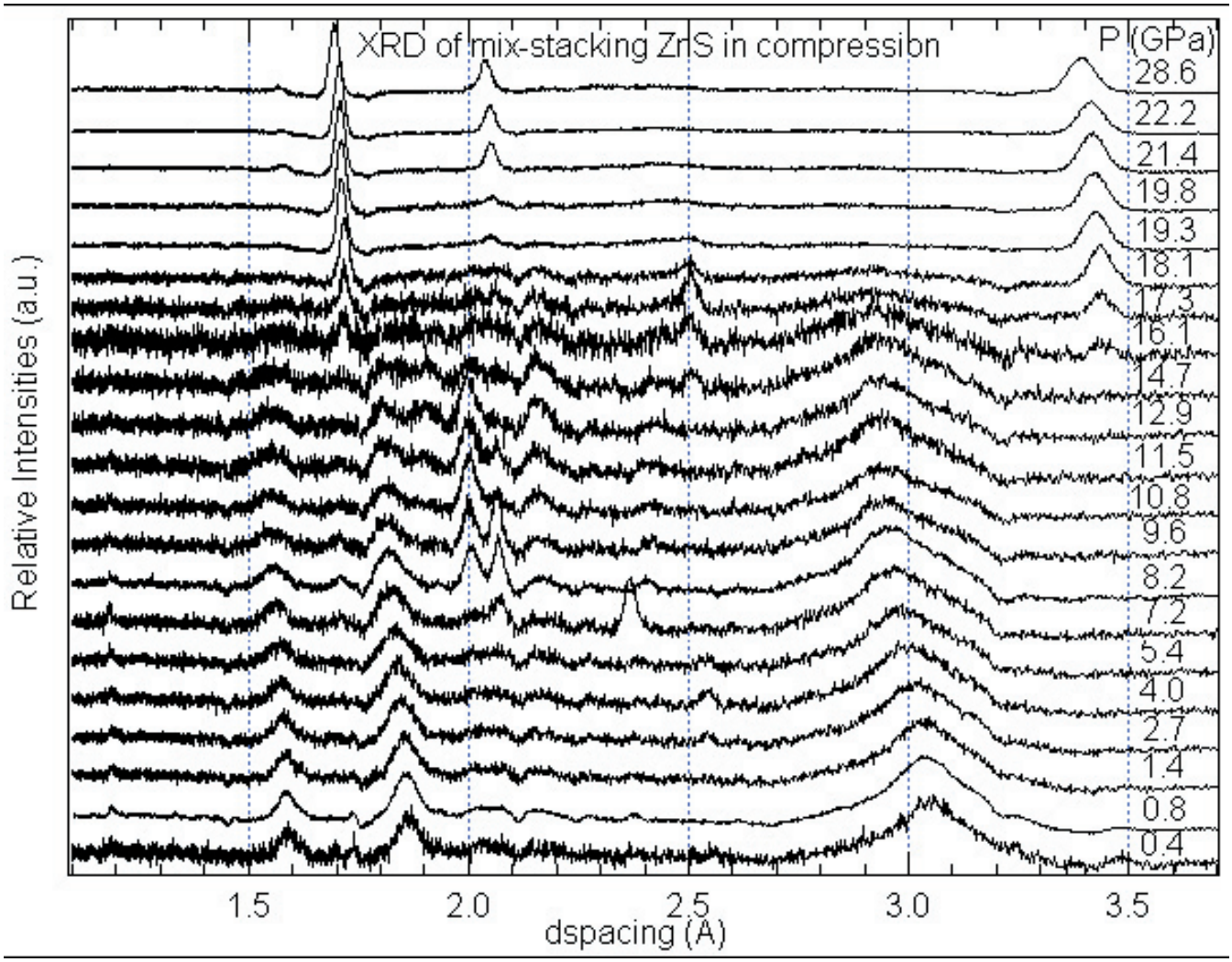

Representative XRD patterns of mixed-stacking n-ZnS in compression

This work was supported by the U.S. Department of Energy (Grant # DE-FG03-01ER15218) and the National Science Foundation (Grant # EAR-0123967).

High-Pressure Infrared and Powder X-ray Study of Topaz-OH

Jianrong Chen, George A. Lager *Department of Geography and Geosciences, University of Louisville, Louisville, KY*
Zhenxian Liu, Jingzhu Hu *Geophysical Laboratory, Carnegie Institution of Washington, Washington, D.C.*
Peter Ulmer *Institute for Mineralogy and Petrography, Swiss Federal Institute of Technology, CH-8092 Zurich, Switzerland*

High-pressure mid-infrared (IR) and powder X-ray data were collected for topaz-OH [$Al_2F_{2-x}(OH)_x(SiO_4)$] (x = 2) to ~10 GPa at the U2A and X17C beam lines (NSLS), respectively, using argon (IR) and methanol-ethanol (X-ray) as pressure-transmitting media. In the structure of topaz-OH, the hydrogen atoms are disordered, reside in a rather rigid cavity and form weak to moderate-strength hydrogen bonds to oxygen atoms within the cavity. The bulk modulus determined from a Birch-Murnaghan fit to energy-dispersive X-ray powder data is K_0 = 144.4 (4) GPa with K′ ≡ 4. Comparison to F-rich-topaz (x = 0.5) (K_0 = 154 (2) GPa; Komatsu et al. 2003) shows that substitution of the larger OH ion for F decreases the bulk modulus. IR spectra of topaz-OH in the OH stretching region are characterized by two strong vibrational modes. Both OH frequencies decrease slightly (20-40 cm^{-1}) with pressure but at significantly different rates, consistent with results from a recent Raman study of the same phase to 17.3 GPa (Komatsu et al. 2005). Based on neutron powder data collected at ambient pressure (Chen et al. 2005), hydrogen bond distances range from 2.038 to 2.263 Å for OH1 and from 2.253 to 2.541 Å for OH2. The lower frequency mode, which can be assigned to OH1, decreases at a greater rate with pressure by a factor of ~2. In contrast to topaz-OH, OH vibrational modes in F-rich topaz show a small, positive shift in frequency with pressure (Bradbury and Williams 2003). Differences in the pressure dependency of the OH modes due to F/OH substitution will be further investigated using a theoretical approach.

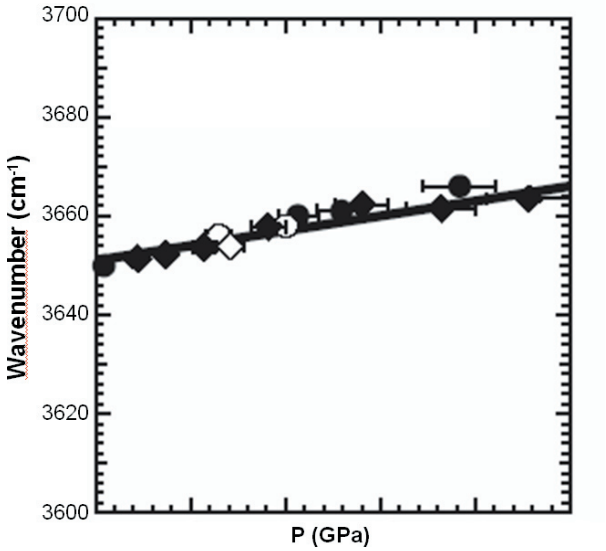

Mode shift of the F-rich topaz hydroxyl-stretching vibration (from Bradbury and Williams 2003).

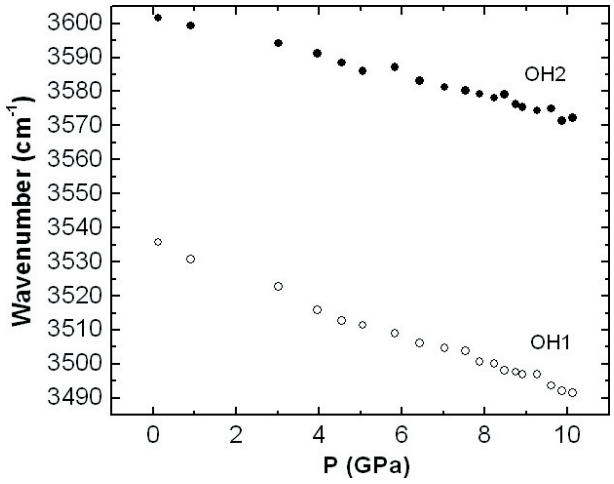

Mode shift of the topaz-OH hydroxyl-stretching vibrations

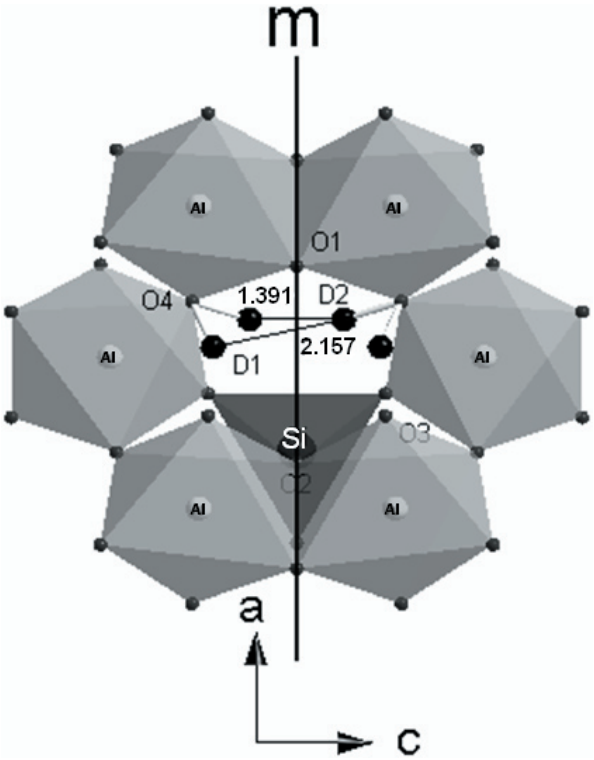

(010) projection of the topaz-OD structure showing the two half-occupied D-atom positions (space group *Pbnm*). Interatomic distances for D2• • • D2 (1.391 Å) and D1• • •D2 (2.157 Å) are indicated on the diagram (Chen et al. 2005).

Bradbury S.E. and Williams Q. (2003) Contrasting bonding behavior of two hydroxyl-bearing metamorphic minerals under pressure: Clinozoisite and topaz. *American Mineralogist* 88, 1460-1470.

Chen, J., Lager, G.A., Kunz, M., Hansen, T.C., and Ulmer, P. (2005) A Rietveld refinement using neutron powder diffraction data of a fully deuterated topaz, $Al_2(SiO_4)(OD)_2$. *Acta Crystallographica*, E61, i253-i255.

Komatsu, K., Kuribayashi, T., and Kudoh, Y. (2005) Effect of temperature and pressure on the crystal structure of topaz, $A1_2SiO_4(OH,F)_2$. J*ournal of Mineralogical and Petrological Sciences*, 98, 167-180, 2003.

Komatsu K., Kagi H., Okada T., Kuribayashi T, Parise J.B., and Kudoh Y. (2005) Pressure dependence of the OH-stretching mode in F-rich natural topaz and topaz-OH. *American Mineralogist* 90, 266-270.

This research was supported by the National Science Foundation through grant EAR-0337534 to GAL.

Density measurements of molten materials at high pressure using synchrotron x-ray radiography: Melting volume of FeS

Jiuhua Chen, Tony Yu, Christopher E. Young, Donald J. Weidner, Liping Wang, Michael T. Vaughan
Stony Brook University

A new technique for density measurement of molten materials in a multi-anvil press using synchrotron x-ray radiography is described. This technique takes advantage of a linear conversion of x-ray intensity to radiograph brightness, and records two-dimensional variations in transmitted x-ray intensities across a reference sphere in the sample on a single exposure. Comparing with the existing technique of one-dimensional scan using a small beam of x-rays for the melt density measurement at high pressure, this method gains a shorter data collection time and larger data coverage (two-dimensional). Melting volume of FeS at 4.1 GPa is determined to be 0.28 cm^3/mol and slope of the melting curve is estimated to be 41°C/GPa. This experiment demonstrates an accuracy of 1% for the density measurement with respect to x-ray diffraction method for crystalline phase.

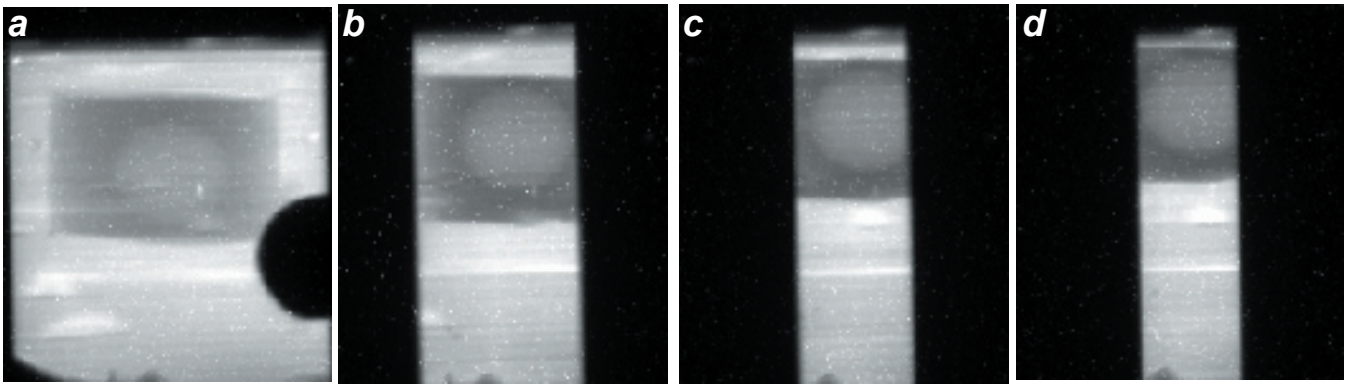

X-ray radiograph images of high pressure cell between the WC anvils at a) ambient condition; b) 1.7 GPa and room temperature; c) 4.1 GPa and room temperature; and d) 4.1 GPa and 1300°C. The round shape dark area on the right of plate a) is the image of the thermocouple junction next to the sample. As pressure increases, the anvil gap becomes tighter and therefore the visible image becomes narrower. The round shape image is from the reference sphere embedded in the sample

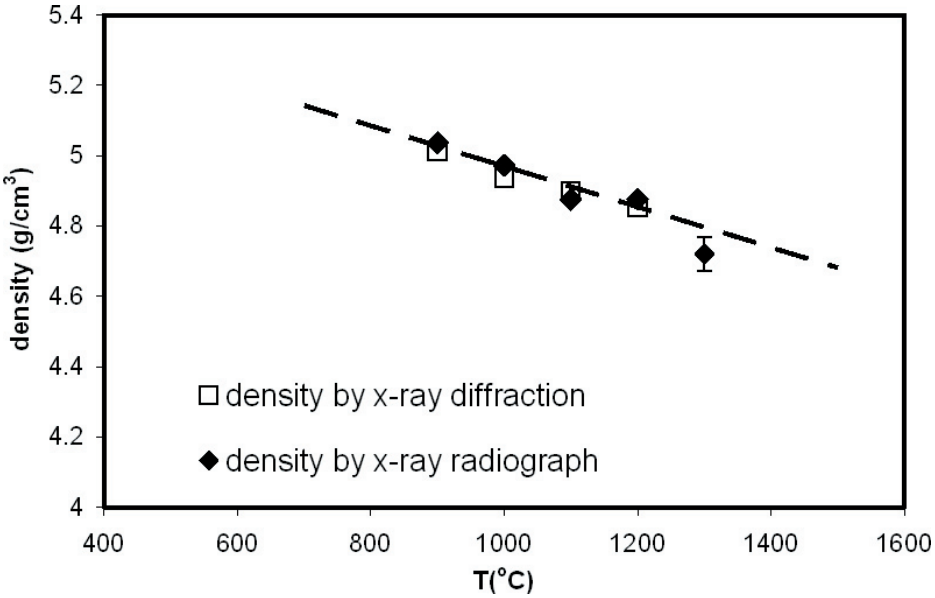

Measured densities of FeS as function of temperature at 4.1 GPa. Bar attached to the symbol represents an estimated experimental error. The straight line represents a linear fit to the density data of crystalline phase from radiograph method. Melting occurs at 1300°C.

Chen, Jiuhua, Donald J. Weidner, Liping Wang, Michael T. Vaughan, and Christopher E. Young, *Density measurements of molten materials at high pressure using synchrotron x-ray radiography: Melting volume of FeS, in Advances in High-Pressure Technology for Geophysical Applications*, Eds. J. Chen, Y. Wang, T.S. Duffy, G. Shen and L.F. Dobrzhinetskaya, ELSEVIER, Amsterdam, pp. 185-194 (2005).

This study was supported by the National Science Foundation under grants EAR039879 to JC. The in situ x-ray experiments were carried out at the X-17B2 beamline of the National Synchrotron Light Source (NSLS) which is supported by the US Department of Energy, Division of Materials Sciences and Division of Chemical Sciences under Contract No. DE-AC02-76CH00016 and by COMPRES, the Consortium for Materials Properties Research in Earth Sciences under contract number NSF Cooperative Agreement EAR 01-35554.

Natural occurrence and synthesis of two new post-spinel polymorphs of chromite

Ming Chen, Xiande Xie, *Guangzhou Institite of Geochemistry, Chinese Academy of Sciences, China*
Jinfu Shu, Ho-kwang Mao, and Russell J. Hemley, *Geophysical laboratory, Carnegie Institution of Washington, USA*

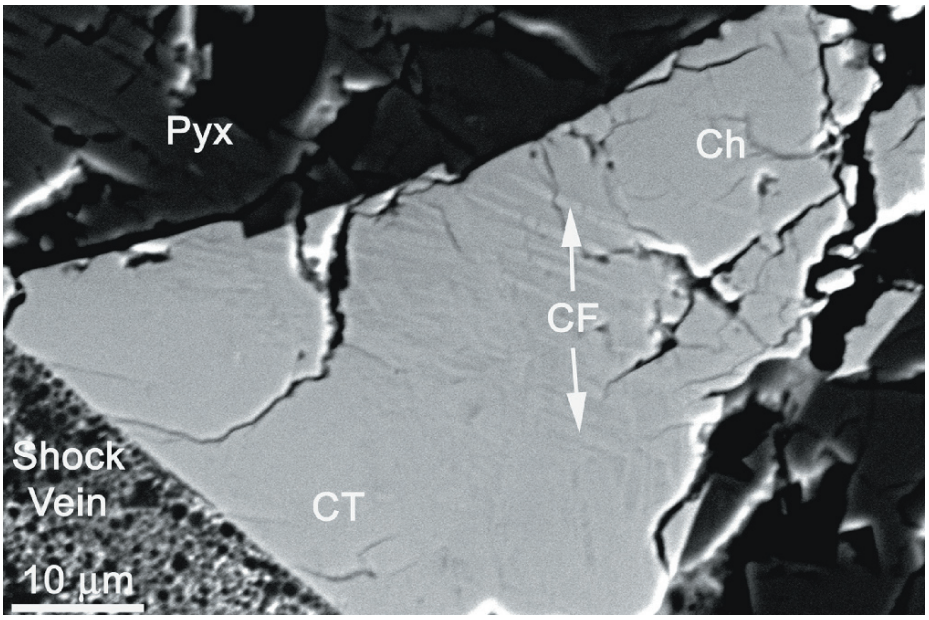

A high-pressure polymorph of chromite, the first natural sample with the calcium ferrite structure, has been discovered in the shock veins of the Suizhou meteorite. Synchrotron x-ray diffraction analyses reveal an orthorhombic $CaFe_2O_4$-type (CF) structure. The unit-cell parameters are a = 8.954(7) Å, b = 2.986(2) Å, c = 9.891(7) Å, V = 264.5(4) Å3 (Z=4) with space group Pnma. The new phase has a density of 5.62 g/cm3, which is 9.4 % denser than chromite-spinel. Laser-heated diamond anvil cell experiments were performed to establish that chromite-spinel transforms to CF at 12.5 GPa and then to the recently discovered $CaTi_2O_4$-type (CT) structure above 20 GPa. With the ubiquitous presence of chromite, the CF and CT phases may be among the important index minerals for natural transition sequence and P-T conditions in mantle rocks, shock-metamorphosed terrestrial rocks and meteorites.

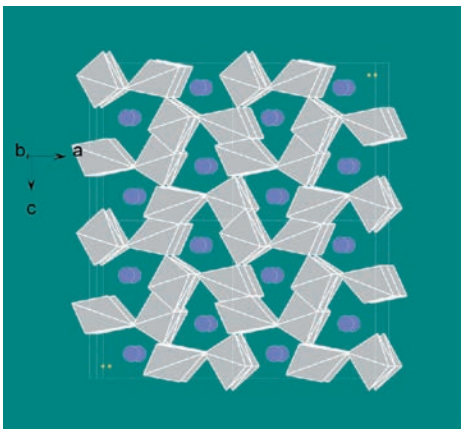

$CaFe_2O_4$-structure

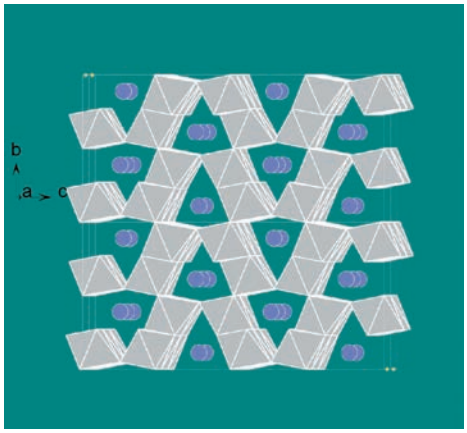

$CaTi_2O_4$-structure

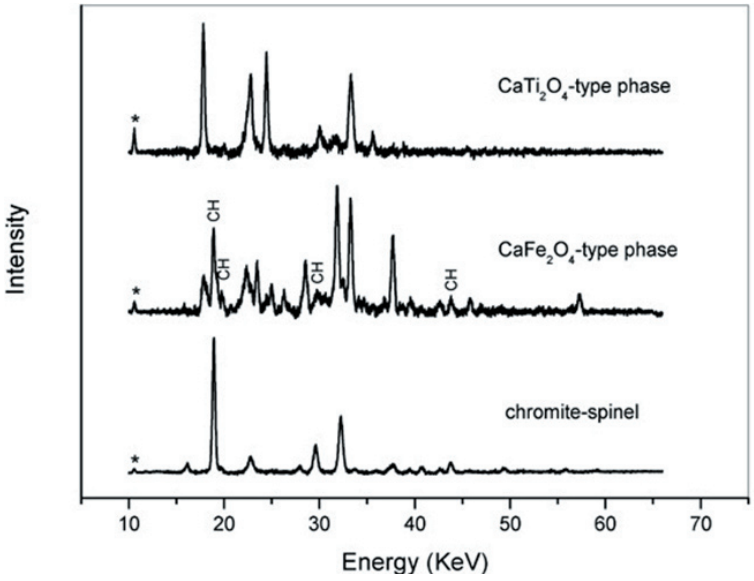

M. Chen et al, *PNAS*, 100, pp 14651-14654, 2003

The experiments were performed at beamline X17C of NSLS, Brookhaven National Laboratory, USA

Size dependence of the pressure-induced γ to α structural phase transition in iron oxide nanocrystals

S.M. Clark1, S.G. Prilliman2, C.K. Erdonmez2 and A.P. Alivisatos2,3

1Advanced Light Source, Lawrence Berkeley National Laboratory, MS6R2100, Berkeley, CA 94720
2Department of Chemistry, University of California, Berkeley, CA 94720
3Materials Science Division, Lawrence Berkeley National Laboratory, Berkeley, CA 94720

The size trend for the pressure-induced γ-Fe_2O_3 (maghemite) to α-Fe_2O_3 (hematite) structural phase transition in nanocrystals has been observed. The transition pressure was found to increase with decreasing nanocrystal size: 7 nm nanocrystals transformed at 27±2GPa, 5 nm at 34±3GPa and 3 nm at 37±2GPa. Annealing of a bulk sample of γ-Fe_2O_3 was found to reduce the transition pressure from 35±2 to 24±2GPa. The bulk modulus was determined to be 262±6GPa for 7 nm nanocrystals of γ-Fe_2O_3, which is significantly higher than for the value of 190±6GPa that we measured for bulk samples. For α-Fe_2O_3, the bulk moduli for 7 nm nanocrystals (336±5) and bulk (300±30) were found to be almost the same within error. The bulk modulus for the γ phase was found to decrease with decreasing particle size between 10 and 3.2 nm particle size. Values for the ambient pressure molar volume were found within 1% to be: 33.0 cm^3/mol for bulk γ-Fe_2O_3, 32.8 cm^3/mol for 7 nm diameter γ-Fe_2O_3 nanocrystals, 30.7 cm^3/mol for bulk α-Fe_2O_3 and 30.6 cm^3/mol for α-Fe_2O_3 nanocrystals.

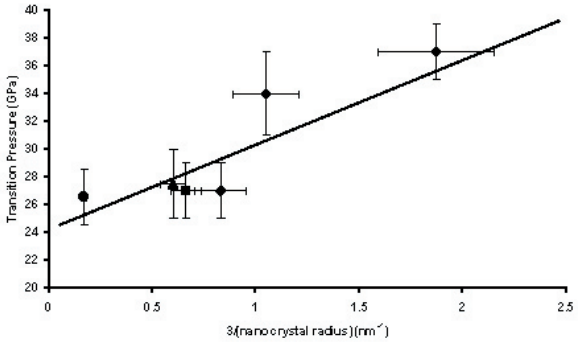

Variation of transition pressure as a function of surface to volume ratio for γ -Fe_2O_3. The diamonds are our data, the square is from Jiang et al. [20], the triangle is from Zhao et al. and the circle is from Wang and Saxena. The line is a guide for the eye.

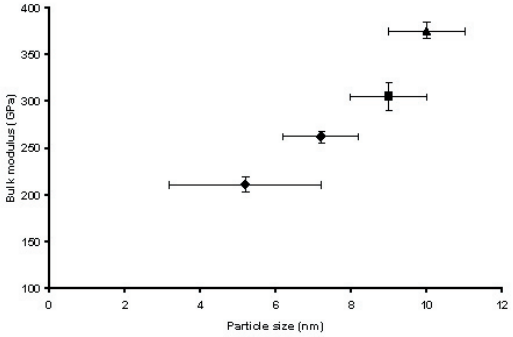

Variation of bulk modulus with nanocrystal size for γ-Fe_2O_3. Diamonds are our data, the square is from Jiang et al. and the triangle is from Zhao et al.

S.M. Clark, S.G. Prilliman, C.K. Erdonmez and A.P. Alivisatos, Size dependence of the pressure-induced γ to α structural transition in iron oxide nanocrystals, *NanoTechnology*, 16 2813-2818 (2005).

We would like to thank Rich Celestre, Alastair Macdowell and Edward Domining for help on beamline 7.2.2. and Raymond Jeanloz for helpful discussions. We would like to thank J. Rockenberger and J. Kwong for help with making the samples. The Advanced Light Source is supported by the Director, Office of Science, Office of Basic Energy Sciences, Materials Sciences Division, of the U.S. Department of Energy under Contract No. DE-AC03-76SF00098 at Lawrence Berkeley National Laboratory.

A new paradigm to extend diffraction measurements beyond the Megabar regime.

S.M. Clark *Advanced Light Source, Lawrence Berkeley National Laboratory, 1 Cyclotron Road, MS6R2100, Berkeley, CA 94720-8226, USA* **and R. Jeanloz** *University of California, Department of Earth and Planetary Science, Berkeley, CA94720-4767, USA*

The possibility of using x-ray diffraction to precisely monitor crystal structure at the extremes of pressure and temperature produced by shock-wave loading is explored. A summary of the advantages of using various x-ray sources for this work and an outline of the necessary experimental layout is given. The conclusion is that it seems likely that x-ray diffraction measurements from shocked materials could be used for structure determination at extreme conditions of pressure and temperature from powder and amorphous materials. X-ray free-electron lasers appear to offer the only monochromatic sources with sufficient flux per pulse to allow single-pulse data collection. Alternative, polychromatic sources with sufficient x-ray flux per shot need to be developed for single-shot structural studies using single crystals. This paradigm shift in the way we approach the determination of crystal structure under extreme conditions offers the only prospect available to extend measurements into the tens of Megabar regime.

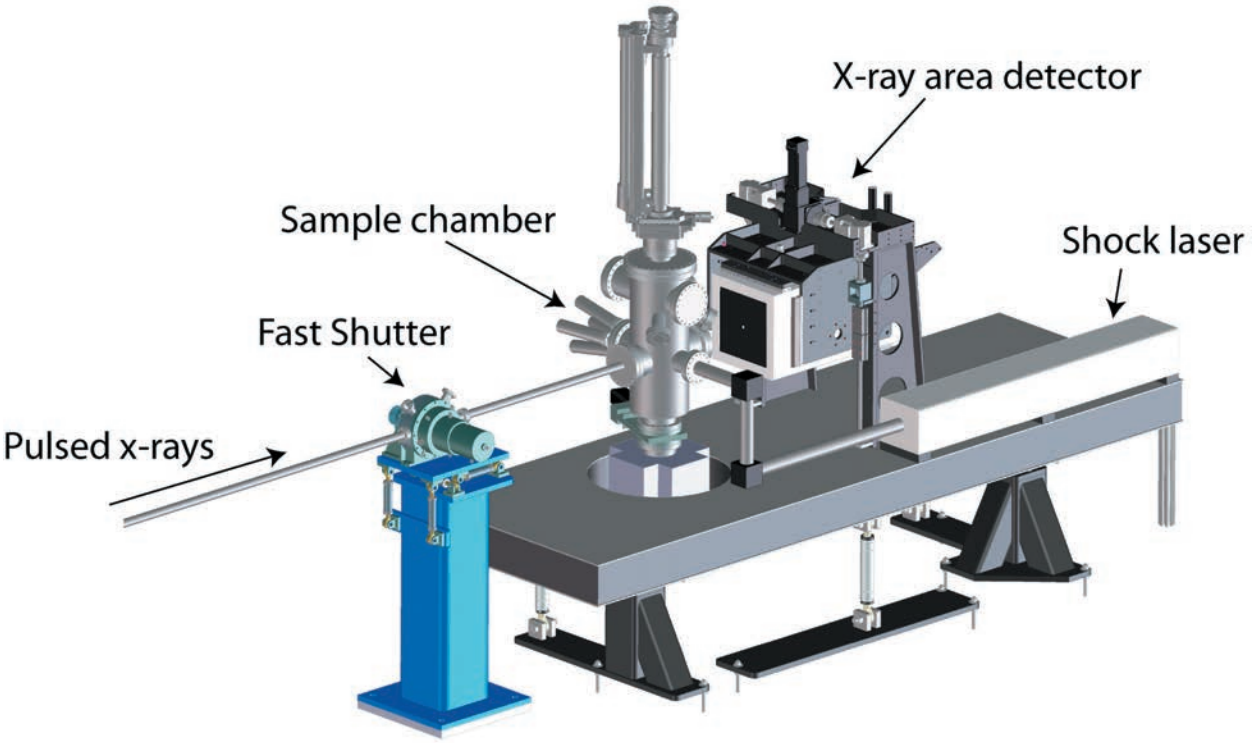

Schematic outline of the proposed experimental layout for diffraction measurements from samples under shock compression.

S.M. Clark and R. Jeanloz, A new paradigm to extend diffraction measurements beyond the megabar regime *J. Synch. Rad*. 12(5) 632-636 (2005).

We would like to thank the many colleagues who have contributed to the generation of these ideas, in particular Bill Nellis, Howard Padmore, Gilbert Collins, Phil Heimann and Dick Lee. We would like to thank Martin Kunz for help with the diffraction measurements, and Greg Morrison for producing the figure. The Advanced Light Source is supported by the Director, Office of Science, Office of Basic Energy Sciences, Materials Sciences Division, of the U.S. Department of Energy under Contract No. DE-AC03-76SF00098 at Lawrence Berkeley National Laboratory.

Title: Elastic behavior and strength of Al_2O_3 fiber/Al matrix composite and implications for equation of state measurements in the diamond anvil cell

Nathalie Conil and Abby Kavner
University of California, Los Angeles

Understanding the strength and elastic behavior of an intermixed phase assemblage is vital for the interpretation of mineral behavior at high pressures and temperatures. To examine pressure relationships in a mixed phase assemblage, we performed room temperature/high pressure radial x-ray diffraction measurements on a controlled geometry bimaterial composite consisting of oriented Al_2O_3 fibers embedded in an aluminum matrix. Lattice strains of each material were measured as a function of orientation with respect to the fiber alignment, and as a function of orientation with respect to the major principal stress axis of the diamond cell, and as a function of pressure up to 15 GPa. The results show that both Al and Al_2O_3 elastically support a differential stress, but the hydrostatic pressures determined from the average lattice strains of Al and Al_2O_3 are not in general equal, with the pressure of Al_2O_3 higher than Al by an average of 0.5 GPa throughout the measured range. The geometric relationship between the composite material and the principal stress axis of the diamond cell plays a role in establishing both the absolute and relative strain response of the composite sample. A comparison of the two composite geometries under the same diamond cell compression show that when the fibers are oriented vertically along the diamond cell axis, both the differential stress and pressure supported by Al_2O_3 is higher than Al. When the fibers are oriented horizontally along the radial direction, the pressure supported by Al and Al_2O_3 is similar, and the differential stress supported by both materials is higher than the vertical case. Many in situ measurements of high pressure mineral phase stability and elasticity are performed using intermixed phases—the unknown and a reference marker. Measurement of properties relies on the assumptions that the reference material has an accurate and well-calibrated equation of state and that the pressures of the two materials are identical in the high pressure sample chamber. This latter assumption is clearly violated in our experiments. Therefore, it is important to account for potential pressure effects due to sample geometry when making in situ x-ray measurements of equations of state and phase transformations.

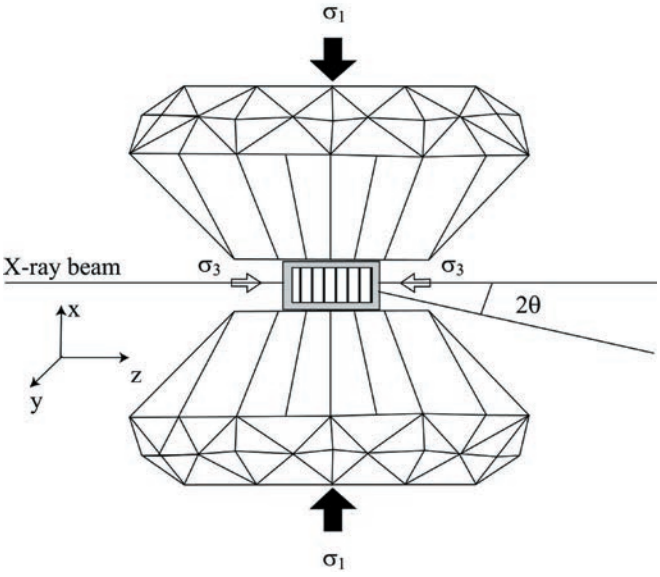

The relationship between theexperimental geometries: X-ray diffraction orientation, diamond anvil cell axis, and the composite material fiber alignment.

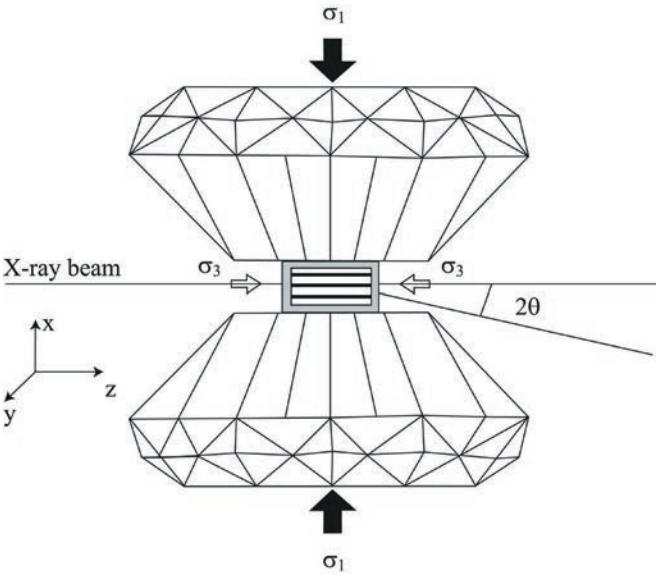

Aluminum and Alumina strain as a function of minimum and maximum stress, for two different sample orientations—fibers oriented horizontally (left) and vertically (right).

N. Conil and A. Kavner: "Elastic behavior and strength of A1$_2$O$_3$ fiber/A1 matrix composite and implications for equation of state measurements in the diamond anvil cell", in press, *Journal of Applied Physics*

Work Performed: at NSLS X17C; NSF-EAR: 0440332

Using the D-DIA to measure the stress in forsterite at high pressure and temperature

Hélène Couvy *Université de Lille and Universitaet Bayreuth (now at Stony Brook University)*
Patrick Cordier *Université de Lille*
Falko Langenhorst *Universitaet Bayreuth*

The rheological parameters of forsterite (Mg_2SiO_4) have been measured using Deformation-DIA high-pressure apparatus coupled with synchrotron. The purpose of this experiment was to measure more accurately the stress level previously determined in forsterite samples deformed in shear configuration using Kawai type multi anvil press [1]. In this previous study, forsterite has been deformed at 11 GPa and 1400°C by relaxation and a low stress level of few hundred MPa has been determined from dislocation densities . Using the D-Dia press coupled with synchrotron, a forsterite sample has been deformed at 4 GPa and 1300°C. The strain and strain rate has been determined equivalent to 10% and 10-5s-1 respectively, using radiograph imaging. The differential stress has been measured using energy dispersive X-ray diffraction. During deformation at steady state, it remains below to 500 MPa. This is in good agreement with the stress level determined previously.

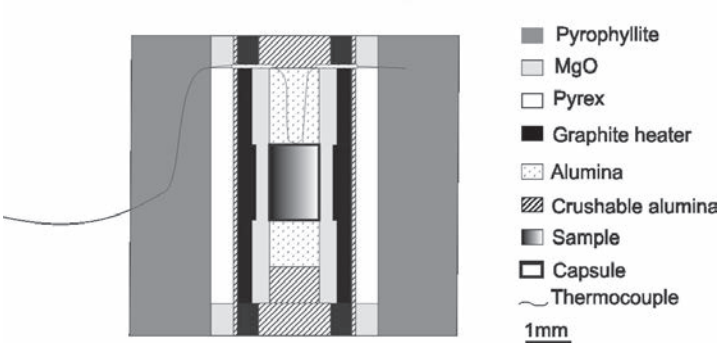

Cross sectional view of the D-DIA cell assembly

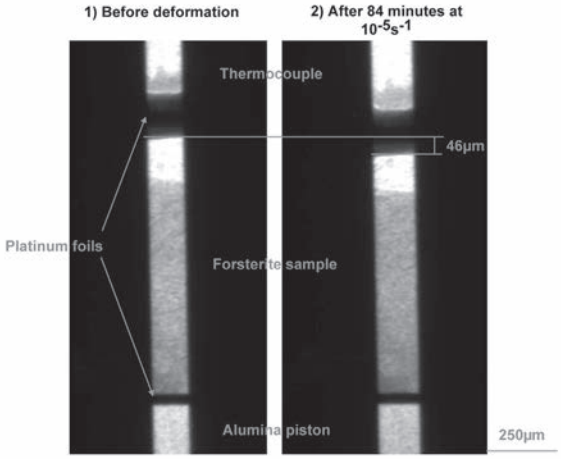

Radiographic images of forsterite sample before and after 84 min of deformation at 4 GPa and 1300°C

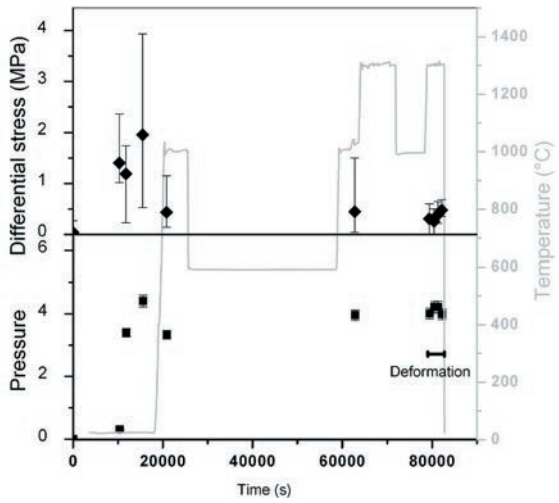

Pressures and differential stress calculated from lattice strains on the forsterite sample. Hydrostatic pressure: black squares. Differential stress: open diamond. In dot gray line, the temperature path. The plotted values of stress are an average of the calculated values from the different diffraction peaks. The error bars represent the range of the values from these peaks

Couvy, H., Frost, D.J., Heidelbach, F., Nyilas, K., Ungár, T., Mackwell, S.J., Cordier, P. (2004): Shear deformation experiments of forsterite at 11 GPa-1400°C in the multianvil apparatus. *Eur. J. Mineral*., 16, 877-889.
Couvy, H. (2005): *Experimental deformation of forsterite, wadsleyite and ringwoodite: Implications for seismic anisotropy of the Earth's mantle*. Thesis. Universitaet Bayreuth, Bayreuth and Université des Sciences et Technologies de Lille, Villeneuve d'Ascq.

The in situ X-ray experiments were carried out at the X-17B2 beamline of the National Synchrotron Light Source (NSLS) which is supported by the US Department of Energy, Division of Materials Sciences and Division of Chemical Sciences under Contract No. DE-AC02-76CH00016 and by COMPRES, the Consortium for Materials Properties Research in Earth Sciences under contract number NSF Cooperative Agreement EAR 01-35554. We thank L. Wang, J.Chen, D. Weidner and P. Raterron for assistance in conducting the in-situ X-ray D-DIA experiment on beamline X17B2.

Rheological properties of α and β-Mn_2GeO_4 as structural analogues of dominant mantle's minerals

Hélène Couvy, Donald Weidner and Jiuhua Chen *Stony Brook University*

In this current project, rheological properties of dominant phases of the upper mantle and the transition zone (olivine and wadsleyite $(Fe,Mg)_2SiO_4$) are addressed through the rheological properties of structural analogues. Knowledge of the rheological properties of wadsleyite are lacking because quantitative deformation experiments under the pressure range of this phase are technically limited. These properties are essential for a better understanding of the dynamics of mantle convection. Structural analogues of $(Fe,Mg)_2SiO_4$ are then necessary to study the rheology of the zones of interest. Mn_2GeO_4 presents alpha-beta phase transitions within the pressure range of the deformation-DIA (D-DIA) high pressure apparatus and it is generally considered as a structural analogue of Mg_2SiO_4 (end member of olivine). In order to study the rheological properties of alpha- and beta-Mn_2GeO_4 over pressure and temperature ranges of their stability field, shear deformation experiments are performed using the D-DIA press coupled with the synchrotron light source.

In preliminary experiments, a shear deformation cell has been developed and tested in-situ. Full diffraction rings have been collected on an imaging plate using a monochromatic beam and variations of d(hkl) in function the diffraction vector have enabled the determination of the form of the stress field. Samples are deformed mainly under simple shear configuration with a small compressional component. Shear rate and shear strain can be determined using rhenium foil placed in the sample as a strain marker and using X-ray radiograph imaging greater than 100% and of 10-6s-1 can be easily achieved.

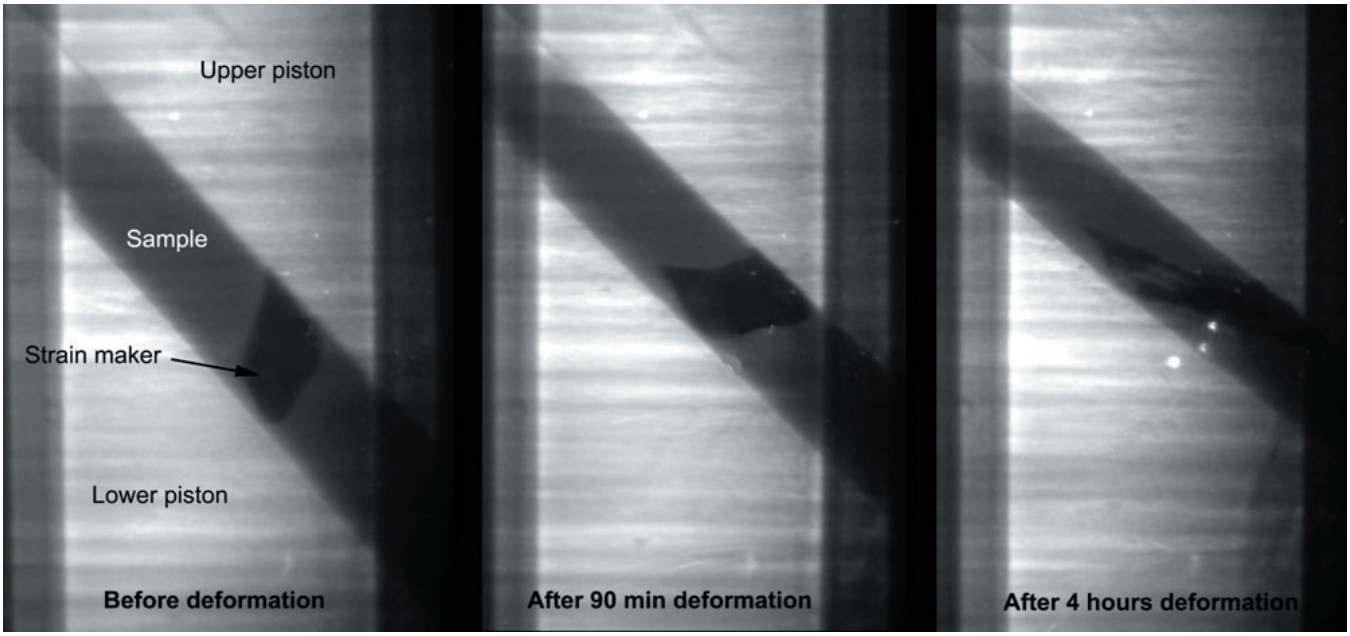

X-ray radiographic images of shear deformed α-Mn_2GeO_4 sample. From left to right: before deformation, after 90 minutes deformation and after 4 hours deformation at 3 GPa, 1000°C and about 10-6s-1

The in situ X-ray experiments were carried out at the X-17B2 beamline of the National Synchrotron Light Source (NSLS) which is supported by the US Department of Energy, Division of Materials Sciences and Division of Chemical Sciences under Contract No. DE-AC02-76CH00016 and by COMPRES, the Consortium for Materials Properties Research in Earth Sciences under contract number NSF Cooperative Agreement EAR 01-35554. We thank L. Wang for assistance in conducting the in-situ X-ray D-DIA experiment on beamline X-17B2.

vestigations of planetary differentiation from high P-T phase equilibria of natural materials

Lisa R. Danielson, Kevin Righter *NASA Johnson Space Center;* **Yanbin Wang** *GSECARS, APS, University of Chicago,* **and Kurt Leinenweber** *Arizona State University*

Chondritic material is thought to be the fundamental building blocks of terrestrial planets and planetessimals. Therefore, crystallization of chondritic material can be used to simulate an accreting and segregating bulk planet. Although chondritic and peridotitic phase equilibria below 20 GPa have been studied in detail (Zhang and Herzberg, 1994; Agee et al., 1995; Wasserman et al., 2001; Litasov and Ohtani, 2002; Asahara et al., 2004; Danielson et al., 2004; Lee et al., 2004; Nishiyama et al., 2004), experiments above 20 GPa, and particularly ≥27 GPa, are lacking. Because this pressure range represents the transition into the Earth's lower mantle, experiments conducted in this pressure range are critical to understanding early crystallization of the deepest planetary mantles. Therefore, the objective of this study is to conduct in situ measurements of the liquidus phases and temperatures for a number of planetary mantle analog materials at pressures above 20 GPa.
Experiments were carried out at the Large Volume Press at the Advanced Photon Source, Argonne National Laboratory. Energy dispersive X-ray diffraction data were collected between 1500 °C and 2200 °C. A 3mm TEL beamline modified "Fei-type" assembly was used in experiments and developed by Leinenweber and Soignard as part of the COMPRES cooperative agreement (figure inset below). X-ray windows are a slit in the Re furnace and alumina plugs in the lanthanum chromite. The view through the slit can be seen in the radiography image of the uncompressed or heated assembly below, left – the darker grey regions in the column are areas of more Re foil overlap. A 1:1 by weight mixture of MgO and diamond powder was used as a pressure standard and packed between the capsule and thermocouple and/or under the capsule.

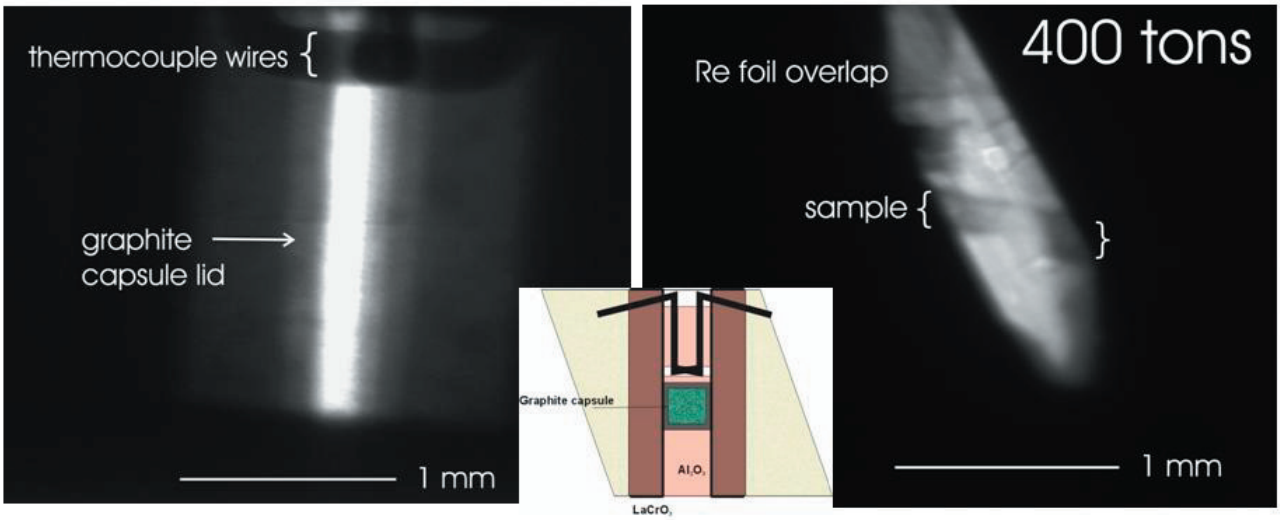

The assembly is extremely robust, which is necessary for the collection of sample and pressure standard XRD spectra at intervals between the subsolidus and superliquidus; the time at temperatures above 1500 °C and above 400 tons was ~ 55 minutes, and 14 minutes above 2000 °C. The radiography image above right shows the end result of compression to 400 tons and heating to a peak temperature of 2200 °C. Development and testing of these assemblies is critical to the success of this project. It is expected that this assembly will be necessary for at least two more beamline sessions to complete the study.

Agee et al. (1995) *J. Geophys. Res*., 100, 17725-17740.
Asahara et al. (2004) *Phys. Earth Planet. Int*., 143-144, 421-432.
Danielson et al. (2004) *Eos Trans. AGU*, 85(47), Fall Meet. Suppl., V43C-1432.
Litasov and Ohtani (2002) *Phys. Earth Planet. Int*, 134, 105-127.
Lee et al. (2004) *Earth Planet. Sci. Lett*, 223, 381-393.
Nishiyama et al. (2004) *Phys. Earth Planet. Int*., 143-144, 185-199.
Zhang and Herzberg (1994) *J. Geophys. Res*, 99, 17729-17742.

This study is supported in part by a NASA RTOP to Kevin Righter.

Ultrasonic Measurements of the Sound Velocities in Polycrystalline San Carlos Olivine in Multi-Anvil, High-Pressure Apparatus

Kenneth L. Darling, Jennifer Kung, Baosheng Li, and Robert C. Liebermann *Stony Brook University*
Gabriel D. Gwanmesia Delaware State University

Sound velocities in polycrystalline San Carlos olivine have been measured to pressures of 7 GPa at room temperature in a 1000-ton uniaxial, split-cylinder apparatus (USCA-1000) of the Kawai multi-anvil type. These velocities and elastic moduli are in good agreement with those calculated from single-crystal moduli determined by previous investigators. In preliminary experiments in a DIA-type, cubic anvil apparatus (SAM-85), ultrasonic interferometric techniques were used in conjunction with synchrotron X-radiation to determine the elastic properties of San Carlos olivine under simultaneous high pressures and temperatures. We demonstrate the feasibility of such experiments even in specimens which have undergone plastic deformation at elevated pressures and temperatures.

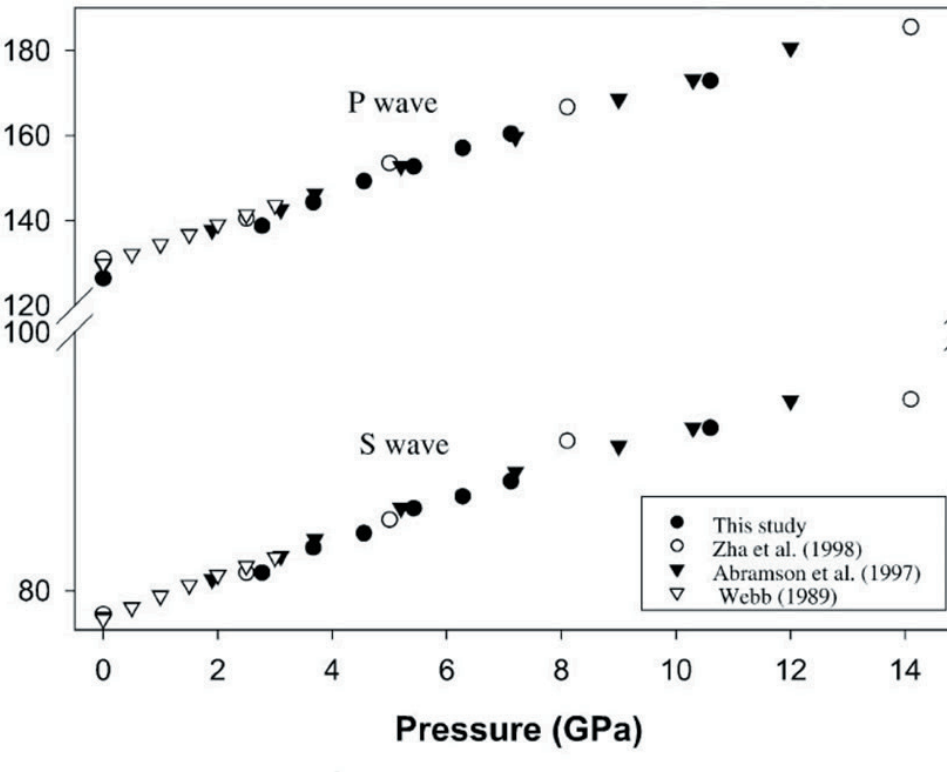

P and S-wave velocities for polycrystalline specimens of San Carlos olivine at high pressure and room temperature.

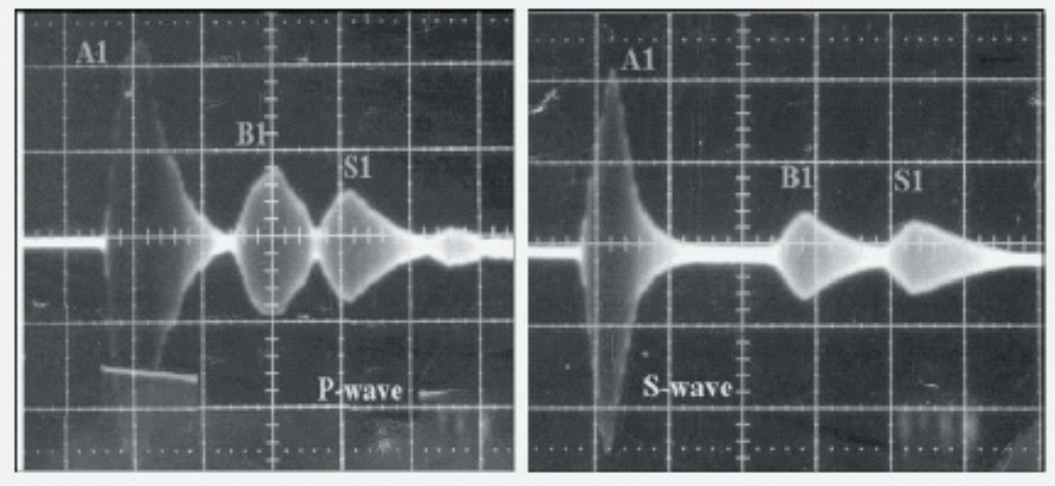

P and S-waves from polycrystalline specimen S3419 at 10.6 GPa in SAM-85 showing echoes from the WC anvil (A1), the alumina buffer-rod (B1) and specimen (S1).

Reference: Darling, K.L., G.D. Gwanmesia, J. Kung, B. Li, and R.C. Liebermann, Ultrasonic measurements of the sound velocities in polycrystalline San Carlos olivine in multi-anvil, high-pressure apparatus, *Phys. Earth Planet. Interiors*, 143-144, 19-31, 2004.

This study was supported by the National Science Foundation under grants EAR 99-80491 and 02-29704 to RCL. The insitu ultrasonic and X-ray experiments were carried out at the X-17B2 beamline of the National Synchrotron Light Source (NSLS) which is supported by the US Department of Energy, Division of Materials Sciences and Division of Chemical Sciences under Contract No. DE-AC02-76CH00016 and by COMPRES, the Consortium for Materials Properties Research in Earth Sciences under contract number NSF Cooperative Agreement EAR 01-35554.

Synchrotron Infrared and Raman Spectroscopy of Microdiamonds from Erzgebirge, Germany

Larissa F. Dobrzhinetskaya *Dept. of Earth Sciences, University of California, Riverside* **Junfeng Zhang** *Institute of Geophysics and Planetary Physics, University of California, Riverside* **Harry W. Green II** *Dept. of Earth Sciences and Institute of Geophysics and Planetary Physics, University of California, Riverside* • **Zhenxian Liu, Russell J. Hemley** • *Geophysical Laboratory, Carnegie Institution of Washington* **Pierre Cartigny** • *Université de Paris, France* **Dalila Tchkhetia** • *Vernadsky Institute of Geochemistry and Analytical Chemistry, Moscow, Russia*

Over the last decade, microdiamonds of 1- to 300-μm size have been found in ultra-high-pressure metamorphic rocks with crustal affinities within the Paleozoic-Mesozoic collisional orogenic belts of Kazakhstan (Kokchetav massif), China (Dabie and Qiadam territories), Norway (Western Gneiss Region), Germany (Erzgebirge massif), Greece (Rhodope), and Russia (Ural Mountains). This is the first study of the Erzgebirge diamonds from Germany with aid of synchrotron infrared absorption, Raman scattering, and fluorescence spectroscopy. Infrared absorption features associated with C-C, C-H bonds, molecular H_2O, OH-- and CO_3-2-radicals, and N-impurities were observed in the diamonds. The results suggest that a C-O-H supercritical fluid is the most likely growth medium for these diamonds from ultrahigh-pressure metamorphic terranes. Investigation of the nitrogen impurities suggests that the Erzgebirge diamonds belong to the Type 1b-1aA, which is similar to metamorphic diamonds from the Kokchetav massif and Norway, and differentiates them from other nitrogen-bearing diamonds from kimberlitic sources (type 1aAB). The amount of nitrogen impurities suggests that the Erzgebirge diamonds had a short residence time in a high-pressure and high-temperature environment, which therefore suggests a possibility for very fast exhumation.

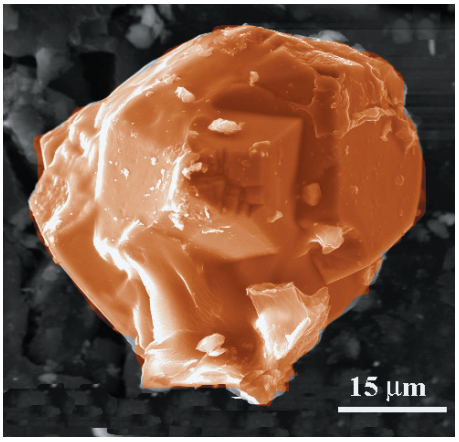

Secondary electron image of diamond from Erzgebirge, Gremany.

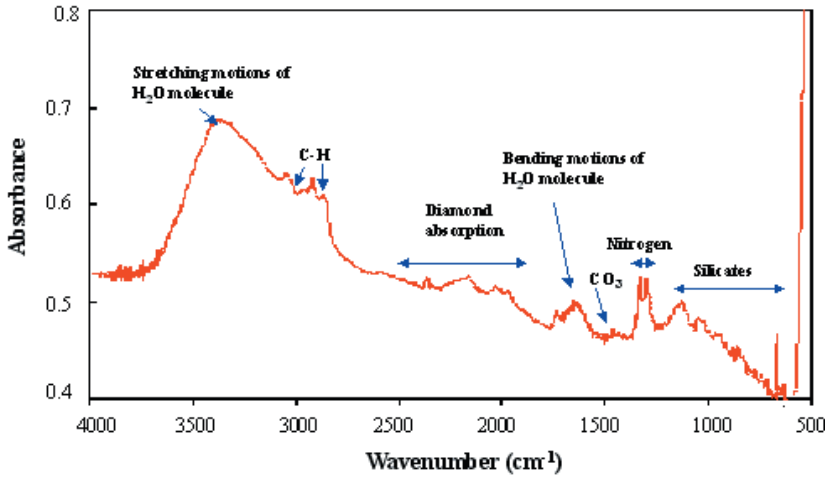

Synchrotron IR spectrum of the microdiamond shown to the left.

Dobrzhinetskaya, L.F., Liu, X., Cartigny, P., Zhang, J., Tchkhetia, D., Hemley, R. and Green II, H.W., Synchrotron Infrared and Raman Spectroscopy of Microdiamonds from Erzgebirge, Germany. Submitted to *Earth and Planetary Science Letters*, 2006

Research is supported: International Division of the U.S. NSF, grant EAR 0229666, and Pacific Rim Program of the University of California to LD and HWG. IR measurements were performed at the U2A beamline at NSLS of Brookhaven National Laboratory, the U.S. Department of Energy (DOE), contract DE-AC02-98CH10886. The U2A beamline is supported by COMPRES, the Consortium for Materials Properties Research in Earth Sciences under the U.S. NSF Cooperative Agreement Grant (EAR 01-35554) and DOE (CDAC, contract No. DE-FC03-03N00144).

Elasticity of Olivine $(Mg,Fe)_2SiO_4$ polymorphs: Current understanding and implications for mantle composition

Thomas S. Duffy and Zhu Mao, *Dept. of Geosciences, Princeton University, Princeton, NJ*

The elastic properties of mantle minerals are of critical importance for interpreting radial and lateral seismic velocity variations and seismic anisotropy in the Earth's mantle. To properly understand seismic observations, it is necessary to determine the variation of elastic properties as a function of at least five major variables: composition, structure, pressure, temperature, and hydration. The $(Mg.Fe)_2SiO_4$ system contains three polymorphs whose compositional variation is mainly restricted to Mg-Fe substitution. Due to their importance for upper mantle seismic discontinuities, their elastic properties have been well studied at high pressures and temperatures. There is also growing recognition that significant hydration of olivine can occur at high P-T conditions. For these reasons the olivine system is ideal for an evaluation of the status of our understanding of mantle mineral elasticity.

Ambient P-T data on the effect of Fe on aggregate elasticity of olivine polymorphs reveals that the α- and γ-phases exhibit parallel modulus-density trends but wadsleyite appears to be more strongly affected by Fe content. Individual Cijs show a linear dependence on Fe content but it is notable that off-diagonal moduli remain rather poorly constrained (~5-10%). Bulk modulus (K) – density plots show that trends connecting different polymorphs at a given Mg/(Mg+Fe) content also describe high P and T behavior (Fig. 1). In other words, density and composition are sufficient to constrain K regardless of P,T and the polymorph involved. Shear moduli show systematic deviations from Birch's Law that are generally consistent across the compositional range (Fig. 2). The effects of hydration can be described from the modulus -density trend shifted to account for the reduction in mean atomic weight accompanying hydration. These systematic relations provide a basis for examination of how olivine content estimated from seismic velocity jumps depend on changes in iron partitioning, hydration, and non-linear yield of the high-pressure phase across the transition.

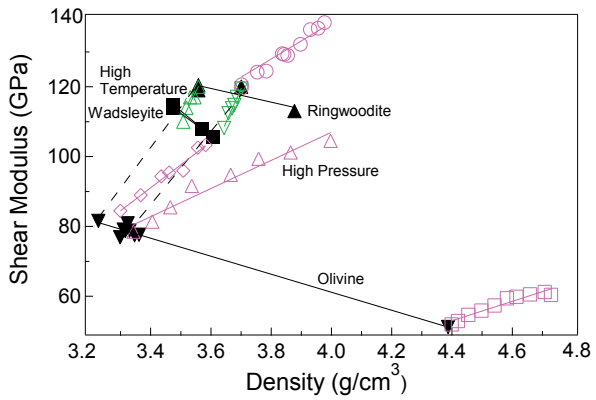

Figure 1. Birch plot show variation of bulk modulus with density for $(Mg,Fe)_2SiO_4$ polymorphs from single-crystal elasticity data.

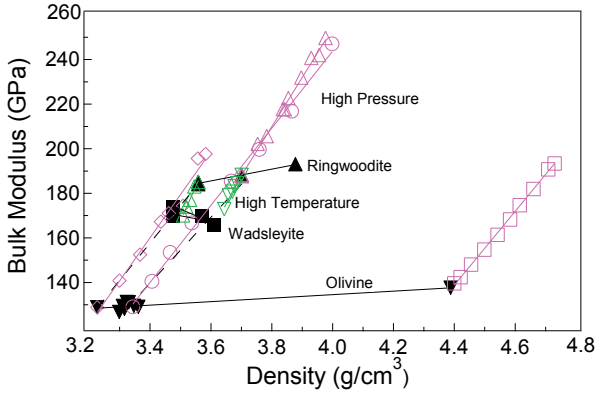

Figure 2. Birch plot show variation of shear modulus with density for $(Mg,Fe)_2SiO_4$ polymorphs from single-crystal elasticity data.

Pressure Calibration at High Temperatures

Yingwei Fei *Carnegie Institution of Washington*

A correct pressure scale is fundamentally important for interpreting geophysical observations using laboratory experimental data obtained at high pressure and temperature. It also allows us to make comparisons of high-pressure results produced in different laboratories using different experimental and analytical techniques. Metals such as Au, Pt, W, Mo, Pd, Ag, and Cu, whose equations of state are established based on shock compression experiments and thermodynamic data, are commonly used as pressure standards in high-pressure experiments. Commonly used non-metal pressure standards include MgO and NaCl. Accurate determination of pressure at high temperature is more difficult because of large uncertainty in calculating the thermal pressure. Commonly used pressure standards such as Au, Pt, MgO, NaCl generally do not predict the same pressures under the same experimental conditions. In some cases, the calculated pressures based on different standards could differ as much as 4 GPa (Figure 1).

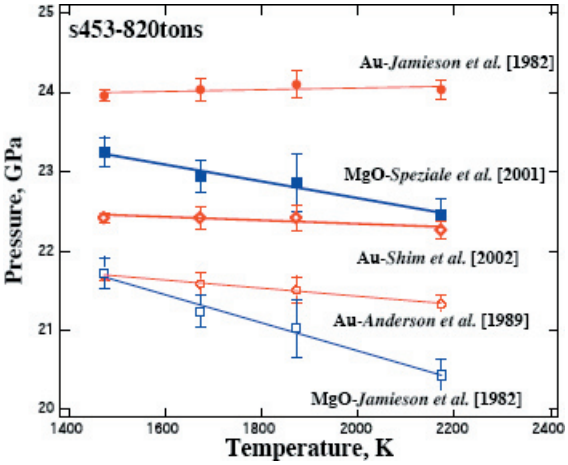

Fig. 1. Calculated pressures using MgO and Au pressure scales at high temperatures. Solid circles, open diamonds, and open circles represent pressures calculated from Au scales by Jamieson et al. (1982), Shim et al. (2002), and Anderson et al. (1989), respectively. Solid and open squares represent pressure from MgO scales by Speziale et al. (2001) and Jamieson et al. (1982), respectively.

With recent advances in synchrotron radiation and high-pressure techniques, it is possible to evaluate and compare pressure scales over a wide range of pressure and temperature. We established a self-consistent pressure scale through in situ X-ray diffraction measurements of the primary pressure standards such as MgO, Au, and Pt in a multi-anvil apparatus up to 28 GPa and 2300 K and in a externally-heated diamondanvil cell up to 100 GPa and 1100 K. The recommended model parameters for the thermal equation of state of MgO, Au, and Pt are listed in Table 1. These equations of state predict consistent pressures. Details are described in the published paper by Fei et al. (2004).

Table 1. Model parameters for the equations of state of MgO, Au, and Pt

Parameters	MgO[1]	Au[2]	Pt[3]
V_0, Å^3	74.71(1)	67.850(4)	60.38(1)
K_{0T}, GPa	160.2(2)	167(3)	273(3)
$K_{0T'}$	3.99(1)	5.0(2)	4.8(3)
θ_0, K	773	170	230
γ_0	1.524(25)	2.97(3)	2.69(3)
q_0	1.65(40)	0.7(3)	0.5(5)
q_1	11.8(2)	0	0
3R, J/gK	0.12664	0.12500	0.12786

[1]All parameters are from Speziale et al. (2001) ($q = q_0(V/V_0)^q1$). [2]All parameters except q value are from Shim et al. (2002). [3]Fei et al. (2004).

Reference:
Fei, Y., J. Li, K. Hirose, W. Minarik, J. Van Orman, C. Sanloup, W. van Westrenen, T. Komabayashi, K. Funakoshi, A critical evaluation of pressure scales at high temperatures by in situ X-ray diffraction measurements, *Phys. Earth Planet Inter.*, 143/144, 516-526, 2004.

This study was supported by NSF grants to YF (EAR9873577) and to COMPRES, the Consortium for Materials Properties Research in Earth Sciences under contract number EAR013554.

Elasticity of Polycrystalline Pyrope ($Mg_3Al_2Si_3O_{12}$) to 9 GPa and 1000°C

Gabriel D. Gwanmesia *Delaware State University*
Jianzhong Zhang *Stony Brook University and Los Alamos National Laboratory*
Kenneth Darling, Jennifer Kung, Baosheng Li, Liping Wang, Robert C. Liebermann *Stony Brook University*
Daniel Neuville *Laboratoire de Physique du Globe de Paris*

Acoustic wave velocities for synthetic polycrystalline pyrope ($Mg_3Al_2Si_3O_{12}$) were measured to 9 GPa, and temperatures up to 1000˚C by ultrasonic interferometry combined with energy-dispersive synchrotron X-ray diffraction in a cubic anvil DIA-type apparatus (SAM-85). Specimen lengths at high pressures (P) and temperatures (T) are directly measured by X-radiagraphic methods. Elastic wave travel times and X-ray diffraction data were collected after heating and cooling at high pressures to minimize effect of non-hydrostatic stress on the measurements. A linear fit to the high P and T data set yields the elastic bulk and shear moduli [KS =175 (2) GPa; G = 91 (1) GPa], and their pressure and temperature derivatives [KS' = 3.9 ± 0.3; G' = 1.7 ± 0.2, and (∂KS/∂T)P = -18 (2) MPa/K; (∂G/∂T)P = -10 (1) MPa/K]. In a separate analysis, the pressure-volume-temperature data collected during these acoustic experiments were fit to a high temperature Birch-Murnaghan (HTBM) equation [with K' fixed at 4.3] and to each isothermal P-V-T data yielding (∂KT/∂T)P= -24 (7) MPa/K, and (∂KT/∂T)P = –23 (3) MPa/K, respectively, and the thermal expansion (in K-1) = 2.65 (27) x 10-5 + 5.33 (383) x 10-9T. Comparison of Py100 data with those other Py-Mj compositions indicates that the thermoelastic properties are insensitive to majorite content in the garnet along the pyrope-majorite join.

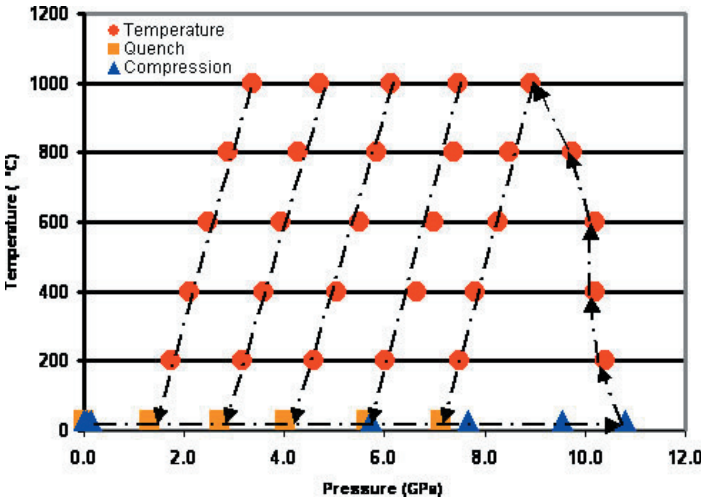

Typical P-T path for ultrasonic experiments at high P & T, in conjunction with synchrotron X-radiation , From work on pyrope by Gwanmesia et al (2005)

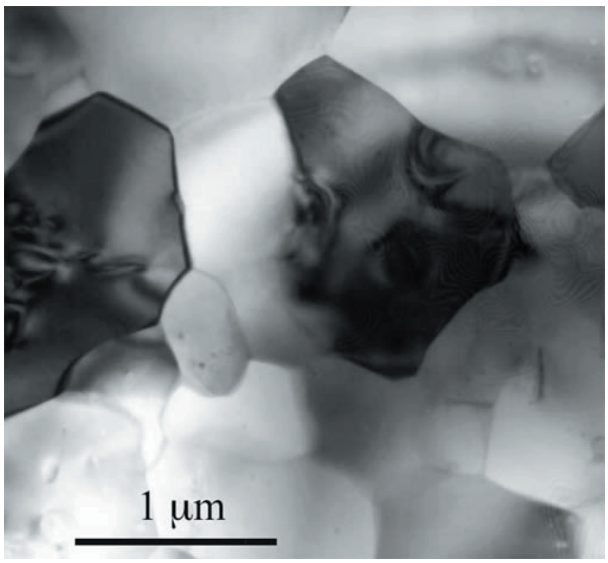

Transmission electron micrograph of pyrope polycrystalline specimen synthesized at high P&T for ultrasonic experiments.

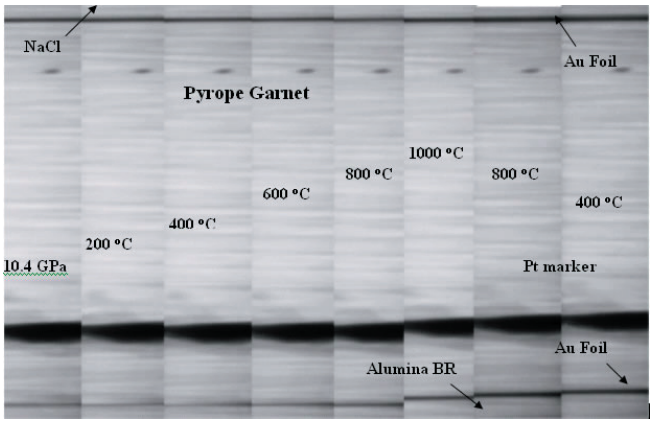

X-ray images of sample recorded at maximum pressure of 10.4 GPa, according to NaCl pressure scale, and at various temperatures during the first heating cycle up to 1000ºC. Also shown are images for two cooling temperatures 800ºC and 400ºC. From top: Al_2O_3 buffer rod, Au foil, sample (with residual platinum foil marker towards bottom of sample used for easy location of sample during high P and T ultrasonic study), Au foil and NaCl.

Reference: Gwanmesia, G.D., J. Zhang, K. Darling, J. Kung, B. Li, L. Wang, R.C. Liebermann, and D. Neuville, Elasticity of Polycrystalline Pyrope ($Mg_3Al_2Si3O_{12}$) to 9 GPa and 1000°C *Physics of Earth and Planetary Interiors*, in press, 2005.

This research was supported by National Science Foundation under grants EAR-0106528 to GDG and EAR-0135431 to GDG under the Elasticity Grand Challenge project. The in-situ ultrasonic experiments were carried out at the X-17B2 beamline of the National Synchrotron Light Source (NSLS), which is supported by the US Department of Energy, Division of Materials Sciences and Division of Chemical Sciences under No. DE-AC02-76CH00016, and COMPRES, the Consortium for Materials Properties Research in Earth Sciences under NSF Cooperative Agreement EAR 01-35554.

Static Strength of Tungsten to 69 GPa

Duanwei He and Thomas S. Duffy, *Princeton University*

The yield strengths of incompressible metals (e.g. W, Re) are of considerable importance for optimizing the design and operation of high-pressure apparatus. Strength properties are also of interest due to the growing applications of dynamic isentropic compression techniques. Here, the strength of tungsten was determined under static high pressures to 69 GPa using x-ray diffraction techniques in a diamond anvil cell. Analysis of x-ray diffraction peak broadening and measurement of peak shifts associated with lattice strains are directly compared under uniaxial compression in a diamond anvil cell. Our results demonstrate the consistency of the two approaches, and shows that the yield strength of tungsten increases with compression, reaching a value of 5.3 GPa at the highest pressure. The obtained yield strength of tungsten is also compared with previous experimental data involving shock wave and static compression measurements, and with theoretical predictions. The high-pressure strength of tungsten is comparable to that of other dense metals such as Re and Mo, and ratio of yield strength to shear modulus is about 0.02 for all these materials between 20-70 GPa. The static strength of tungsten is much greater than values observed for W under shock loading but is very similar to values observed under quasi-isentropic loading.

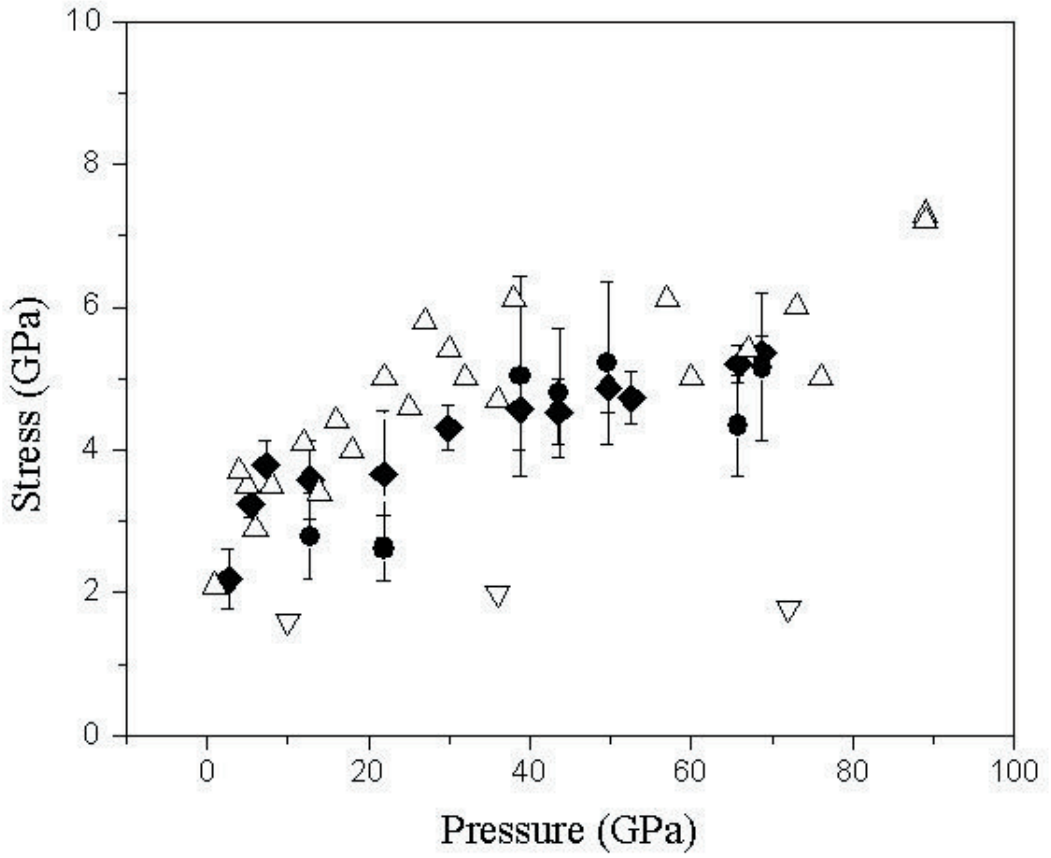

Differential stress and microscopic deviatoric stress of tungsten as a function of pressure (solid symbols) compared with yield strengths determined under shock loading (inverted triangles) and dynamic isentropic loading (triangles).

He, D. W., and T. S. Duffy, Static strength of tungsten to 69 GPa, *Physical Review B*, in press, 2006.

This research was supported by the NSF and DOE. Experiments were conducted at the X17C beamline of NSLS which is supported by COMPRES, the Consortium for Material Property Research in the Earth Sciences under NSF Cooperative Agreement EAR01-35554.

Strength and equation of state of boron suboxide (B_6O) from radial x-ray diffraction in a diamond cell

Duanwei He, Sean R. Shieh, and Thomas S. Duffy, *Princeton University*

Boron compounds such as boron suboxide (B_6O) have generated considerable interest as strong, lightweight solids. Using radial x-ray diffraction techniques together with lattice strain theory, the behavior of boron suboxide (B_6O) was investigated under non-hydrostatic compression up to 65.3 GPa in a diamond anvil cell. The bulk modulus derived from nonhydrostatic compression data varies from 363 GPa to 124 GPa depending on the orientation of the diffraction planes with respect to the loading axis. The ratio of differential stress to shear modulus ranges from 0.021 to 0.095 at pressures of 9.3-65.3 GPa. Together with estimates of the high-pressure shear modulus, a lower bound to the yield strength is 26-30 GPa at the highest pressure. The yield strength of B_6O is about a factor of 2 larger than other strong solids such as Al_2O_3 and B_4C. The ratio of yield stress to shear modulus derived from lattice strain theory is also consistent with the result obtained by the analysis of x-ray peak width. This ratio might be a good qualitative indicator of hardness as it reflects the contributions of both plastic and elastic deformation.

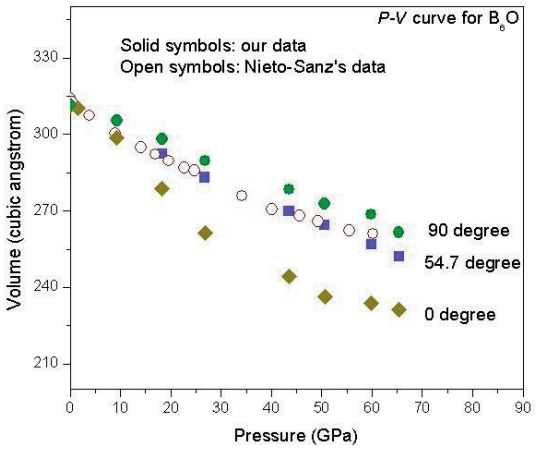

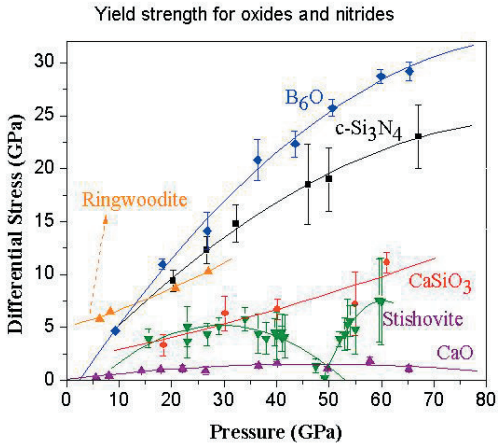

The left figure shows the quasi-hydrostatic compression curve of B_6O from radial diffraction. The figure on the right shows the differential stress supported by B_6O under non-hydrostatic compression.

He, D. W., S. R. Shieh and T. S. Duffy, Equation of state and strength of boron suboxide from radial x-ray diffraction in a diamond cell under nonhydrostatic compression, *Physical Review B*, 70, 184121, 2004

A synchrotron Mössbauer spectroscopy study of $(Mg,Fe)SiO_3$ perovskite up to 120 GPa

Jennifer M. Jackson* *and Jay D. Bass University of Illinois at Urbana-Champaign*
Wolfgang Sturhahn and Jiyong Zhao *IXN, Advanced Photon Source*
Guoyin Shen *GSECARS - University of Chicago*
Michael Y. Hu *HP-CAT, Advanced Photon Source*
Daniel Errandonea *University of Valencia*
Yingwei Fei *Carnegie Institution of Washington*

***Present address:** *Carnegie Institution of Washington*

The electronic environment of the Fe nuclei in two silicate perovskite samples, $Fe_{0.05}Mg_{0.95}SiO_3$ (Pv05) and $Fe_{0.1}Mg_{0.9}SiO_3$ (Pv10), have been measured to 120 GPa and 75 GPa, respectively, at room temperature using diamond anvil cells and synchrotron Mössbauer spectroscopy (SMS). Such investigations of extremely small and dilute ^{57}Fe-bearing samples have become possible through the development of SMS. Our results are explained in the framework of the "three-doublet" model, which assumes two Fe^{2+}-like sites and one Fe^{3+}-like site that are well distinguishable by the hyperfine fields at the location of the Fe nuclei. Our results show that at pressures extending into the lowermost mantle the fraction of Fe^{3+} remains essentially unchanged, indicating that pressure alone does not alter the valence states of iron in $(Mg,Fe)SiO_3$ perovskite. The quadrupole splittings of all Fe sites first increase with increasing pressure, which suggests an increasingly distorted (noncubic) local iron environment. Above pressures of 40 GPa for Pv10 and 80 GPa for Pv05, the quadrupole splittings are relatively constant, suggesting an increasing resistance of the lattice against further distortion. Around 70 GPa, a change in the volume dependence of the isomer shift could be indicative of the endpoint of a continuous transition of the Fe^{3+} from a high-spin to a low-spin state (Jackson et al. 2005).

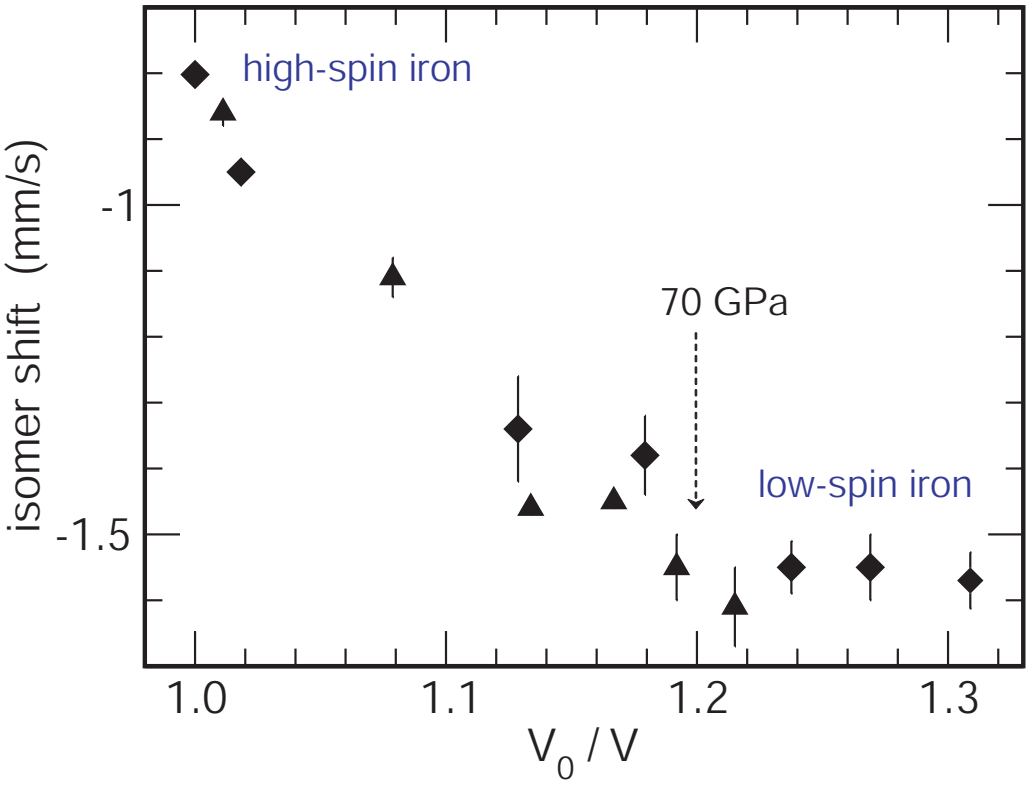

Volume dependence of the isomer shift of the Fe^{3+} site relative to the Fe^{2+} sites from fits of the time spectra for Pv10 (triangles) and Pv05 (diamonds). A change in the volume dependence of the isomer shift around $V_0/V = 1.2$ (a pressure of about 70 GPa) could be indicative of the endpoint of a continuous transition of the Fe^{3+} ions from a high-spin to a low-spin state.

Jackson, J.M., W. Sturhahn, G. Shen, J. Zhao, M.Y. Hu, D. Errandonea, J.D. Bass, and Y. Fei (2005): A synchrotron Mössbauer spectroscopy study of $(Mg,Fe)SiO_3$ perovskite up to 120 GPa. *American Mineralogist*, 90, 199-205.

Support for this work was provided by COMPRES, the NSF, and the DOE under contract no. W-31-109-Eng-38.

Sound velocities and elasticity of aluminous $MgSiO_3$ perovskite to 45 GPa: Implications for lateral heterogeneity in Earth's lower mantle

Jennifer M. Jackson*, *Stanislav V. Sinogeikin, and Jay D. Bass, University of Illinois at Urbana-Champaign*
Jianzhong Zhang, *Los Alamos National Laboratory*
Jinfu Shu, *Carnegie Institute of Washington*

***Present address:** *Carnegie Institution of Washington*

Brillouin scattering measurements on aluminous magnesium silicate perovskite, arguably the most abundant phase in Earth, have been performed to 45 GPa in a diamond anvil cell at room temperature, using methanol-ethanol-water and neon as pressure transmitting media. The experiments were performed on a polycrystalline sample of aluminous $MgSiO_3$ perovskite containing 5.1±0.2 wt.% Al_2O_3., representing the first Brillouin scattering measurements at high-pressure on a dense, chemically complex, polycrystalline silicate characteristic of Earth's lower mantle. The pressure derivatives of the adiabatic bulk (K_{0S}) and shear (μ_{0S}) moduli are 3.7±0.3 and 1.7±0.2, respectively. These measurements allow us to evaluate whether the observed lateral variations of seismic wave speeds in Earth's lower mantle are due at least in part to a chemical origin. Our results indicate that a difference in the aluminum content of silicate perovskite, reflecting a variation in overall chemistry, is a plausible candidate for such seismic heterogeneity.

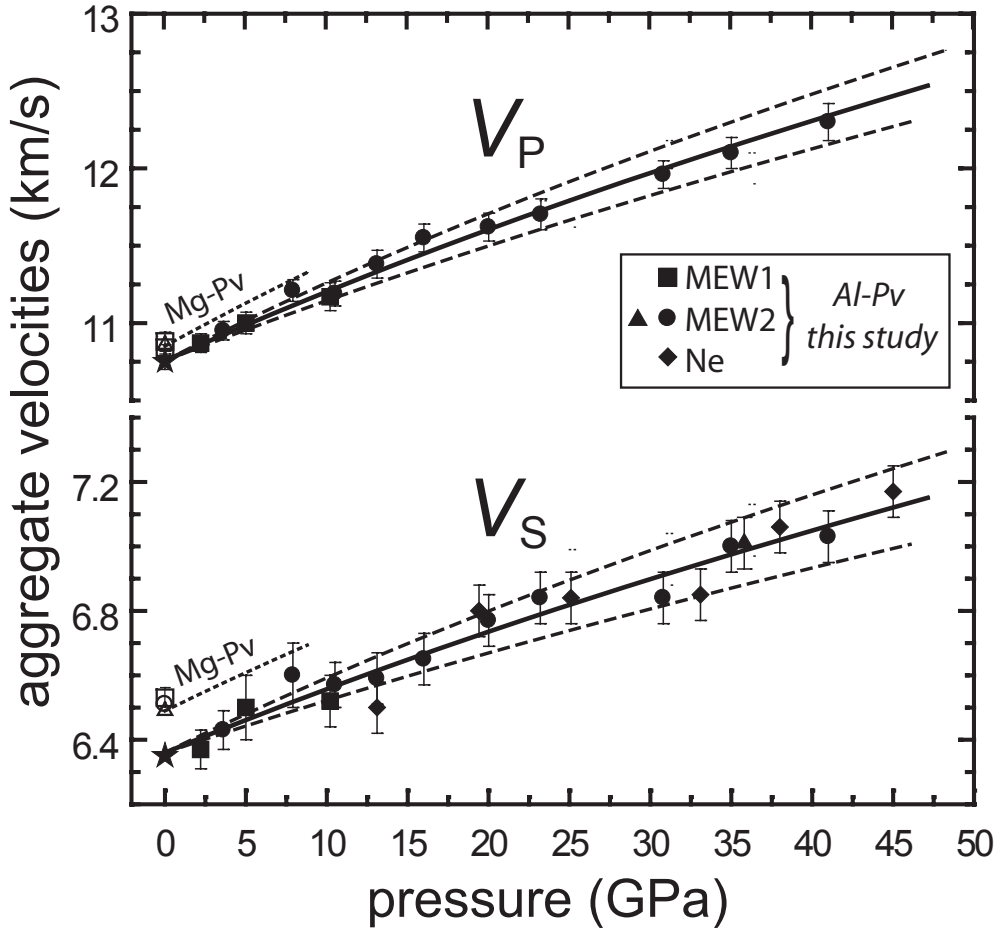

Aggregate sound velocities of polycrystalline Al-Pv from room pressure (stars, *Jackson et al*. [2004]) to 45 GPa. The solid black lines are calculated from the best-fit elastic moduli (3rd order finite strain EOS), and the long-dashed lines represent the error determined from these fits. See *Jackson et al*. (2005) for more details.

Jackson, J.M., J. Zhang, and J.D. Bass (2004): Sound velocities and elasticity of aluminous $MgSiO_3$ perovskite: Implications for aluminum heterogeneity in Earth's lower mantle, *GRL*, 2004GL019918.

Jackson, J.M., J. Zhang, J. Shu, S.V. Sinogeikin, and J.D. Bass (2005): High-pressure sound velocities and elasticity of aluminous $MgSiO_3$ perovskite to 45 GPa: Implications for lateral heterogeneity in Earth's lower mantle, *GRL*, 2005GL023522.

This research was funded by the NSF under grants EAR 0003383 and 0135642 (JDB) and by the Mineralogical Society of America Grant for Student Research in Mineralogy and Petrology (JMJ).

Single-crystal X-ray diffraction study of wüstite-$Fe_{0.93}O$ to 50 GPa

Steven D. Jacobsen* *Carnegie Institution of Washington, Geophysical Laboratory*
***Present address**: Northwestern University, Department of Geological Sciences*
Jung-Fu Lin *Lawrence Livermore National Laboratory*

In this study, monochromatic synchrotron X-ray radiation at ~40 keV was used to obtain zone-axis type diffraction patterns from five simultaneously loaded single-crystals of (Mg,Fe)O with variable compositions to 51 GPa in a helium pressure medium. Here we present results on the wüstite sample of $Fe_{0.93}O$ composition. The experiments were preformed on the 13-BMD beamline of GSECARS, Advanced Photon Source. At each pressure, six to ten reflections of *h*00 and *hk*0 classes were available for indexing. The cubic (B1) to rhombohedral phase transition was observed at about 22 GPa by splitting of the cubic 220 reflection. Equation of state parameters for the rhombohedral phase of $Fe_{0.93}O$ are K_0 = 134(4) GPa assuming K' is equal to 4.0, compared with K_0 = 146(2) GPa for the cubic phase of $Fe_{0.93}O$. Other developments in megabar single-crystal diffraction techniques were presented at a COMPRES sponsored workshop at APS and published in a special issue of *J. Synchr. Rad*. (see Dera et al. 2005).

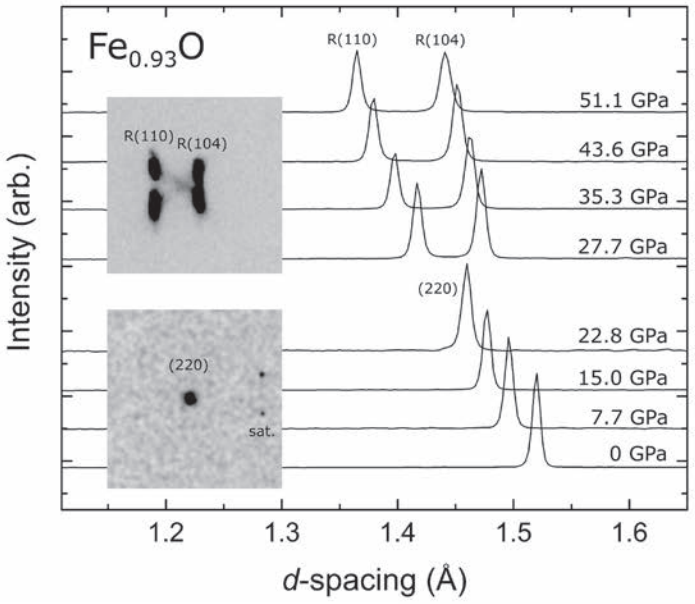

Evolution of the 220 reflection in $Fe_{0.93}O$.

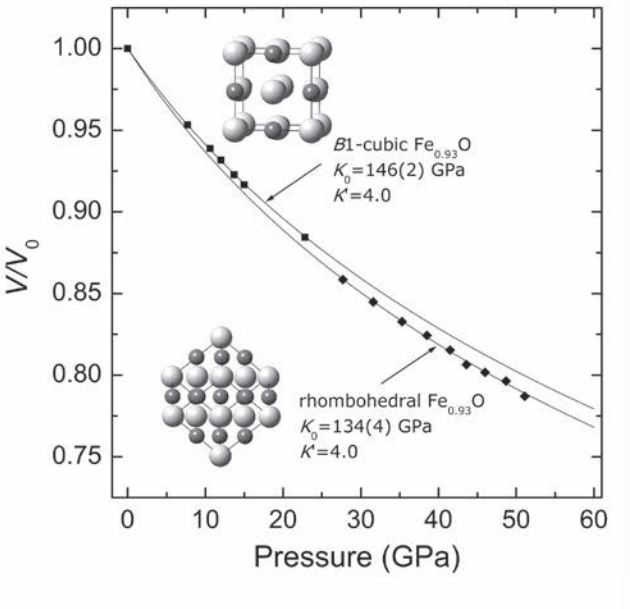

Equation of state of $Fe_{0.93}O$.

Dera, P., C.T. Prewitt, and S.D. Jacobsen (2005) Structure Determination by Single-Crystal X-ray Diffraction at Megabar Pressures. J*ournal of Synchrotron Radiation*, 12, 547-548.

Jacobsen, S.D., J.F. Lin, R.J. Angel, G. Shen, V.B. Prakapenka, P. Dera, H.-K. Mao, and R.J. Hemley (2005) Single-crystal synchrotron X-ray diffraction study of wüstite and magnesiowüstite at lower-mantle pressures. *Journal of Synchrotron Radiation*, 12, 577–583.

We wish to thank G. Shen, V.B. Prakapenka, P. Dera, R.J. Angel, S.J. Mackwell, C.T. Prewitt, H.K. Mao, and R.J. Hemley for support, assistance, and discussions. Supported in part by NSF-EAR 0440112 to SDJ and the Carnegie/DOE Alliance Center. GSECARS is supported by NSF-EAR 0217473, DOE DE-FG02-94ER14466 and the State of Illinois. Use of the APS was supported by DOE W-31-109-Eng-38.

A gigahertz ultrasonic interferometer for the diamond anvil cell

Steven D. Jacobsen* *Carnegie Institution of Washington, Geophysical Laboratory*
***Present address:** *Northwestern University, Department of Geological Sciences*

A broadband (0.5-2.0 GHz) ultrasonic interferometer is being developed for single-crystal elasticity measurements in the diamond anvil cell. Subsequent to the pioneering developments made by Spetzler (1993; 1996)[1], ultrasonic interferometry in the diamond cell had been achieved at hydrostatic pressures up to about 4 GPa with P-waves. During the initial years of the Elasticity Grand Challenge of the COMPRES Initiative, an improved interferometer developed by Jacobsen et al. (2002; 2004)[2] at Bayerisches Geoinstitut in Bayreuth was re-located to the US with an expanded pressure range of ~10 GPa and with both P- and S-wave capabilities. The GHz-interferometer has since been used to study micro-crystals of high-pressure phases as thin as ~30-µm thickness and in determining the full elastic tensor (C_{ijkl}) of optically opaque minerals at high pressures including magnetite, wüstite, and other oxide spinels (see Jacobsen et al. 2005 and references therein).

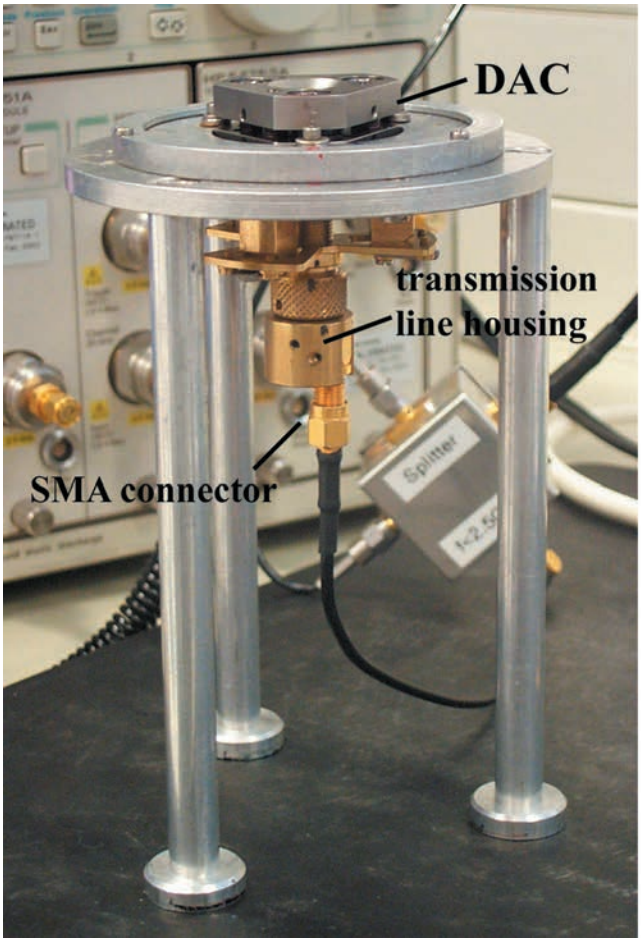

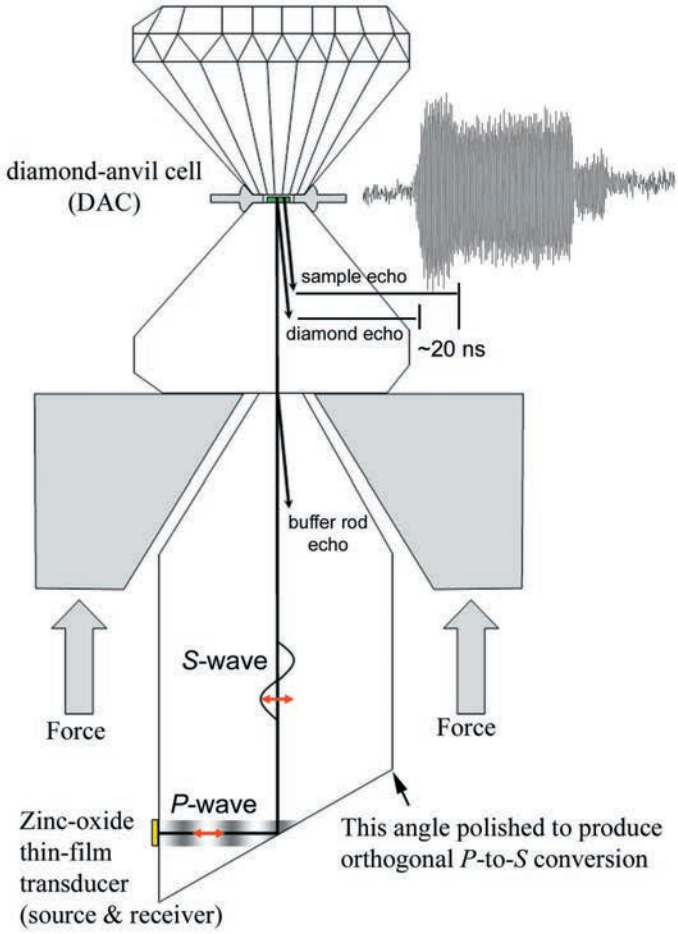

[1](PAGEOPH 141, 341-377; PEPI 98, 93-99), [2](JGR 107(B2), 2037; PNAS 101, 5867–5871).

Jacobsen, S.D., H.J. Reichmann, A. Kantor, and H. Spetzler (2005) A gigahertz ultrasonic interferometer for the diamond-anvil cell and high-pressure elasticity of some iron-oxide minerals. In: J. Chen et al. (Eds.) *Adv. in High-Pressure Technology for Geophys. Applications*, Elsevier, Amsterdam, pp. 25-48.

Many people have been involved in the (ongoing) development of GHz-ultrasonic interferometry, including H.A. Spetzler, H.J. Reichmann, J.R. Smyth, G. Chen, W.A. Bassett, R. Angel, H. Schulze, K. Mueller, S. Lindenhardt, K. Klasinski, S.J. Mackwell, A. Kantor (Ph.D. student) and many others. Upon arrival at the Geophysical Laboratory, Jacobsen and the GHz-ultrasonic laboratory was supported through NSF-EAR 0135540, "Collaborative Research: Elasticity Grand Challenge of the COMPRES Initiative" to R.J. Hemley and H.K. Mao, and subsequently by the Carnegie/DOE Alliance Center (CDAC) and a Carnegie Fellowship. The GHz-laboratory is currently funded through NSF-EAR 0440112 to SDJ.

Sound velocities and elastic constants of hydrous Fo_{90} ringwoodite

Steven D. Jacobsen* *Carnegie Institution of Washington, Geophysical Laboratory*
***Present address**: Northwestern University, Department of Geological Sciences*
***J*oseph R. Smyth** *University of Colorado, Department of Geological Sciences*

The sound velocities and single-crystal elastic constants of ringwoodite (Fo_{90} composition) containing ~1 wt% H_2O have been determined to 9.2 GPa using GHz-ultrasonic interferometry in the diamond-anvil cell. The aggregate moduli and pressure derivatives are K_{S0} = 177(4) GPa, K' = 5.3(4), G_0 = 103(1) GPa, and G' = 2.0(2). The incorporation of 1wt% H_2O into Fo_{90} ringwoodite reduces K_{S0} and G_0 by 6% and 14%, respectively compared with anhydrous Fe-bearing ringwoodite (Sinogeikin et al. 2003, PEPI 136, 41-66). Elevated pressure derivatives bring calculated P-velocities up to anhydrous values within uncertainty above about 12 GPa, whereas S- velocities remain 1-2% slower at transition zone pressures. Corresponding V_P/V_S ratios are elevated by 2-3%, which may be the best seismic indicator of hydration in the mantle transition zone.

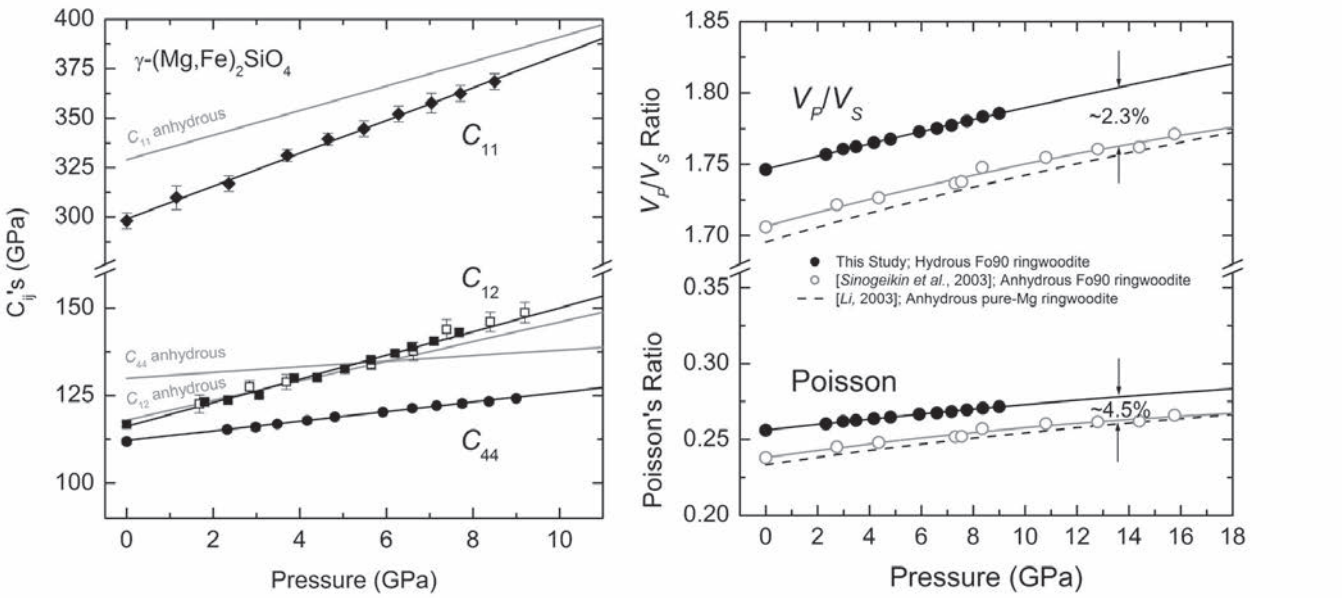

LEFT: Elastic constants (C_{ij}) of hydrous ringwoodite (symbols) compared with anhydrous ringwoodite from Sinogeikin et al. (2003) (grey curves). RIGHT: V_P/V_S ratio and Poisson's ratio.

Jacobsen, S.D. and J.R. Smyth (2004) High-pressure elasticity of Fo_{90} hydrous ringwoodite. *Eos Trans. AGU*, 85(47), Fall Meet. Suppl., Abstract T41B-1188.

Jacobsen, S.D. and J.R. Smyth (2006) Effect of water on the sound velocities of ringwoodite in the transition zone. In: S.D. Jacobsen and S. van der Lee (Eds.) *Earth's Deep Water Cycle*, American Geophysical Union Monograph, in press.

Support during various stages of this study was provided by Fellowships from the Alexander von Humblodt Foundation (SDJ and JRS) and the Carnegie Institution of Washington (SDJ). Also funded in part by NSF-EAR 0440112 to SDJ and NSF-EAR 0337611 to JRS, CDAC, and the Bayerisches Geoinstitut Visitors Program.

High-pressure phase in SrF_2 by laser heating at NSLS X17B3

Fuming Jiang, Atsushi Kubo, and Thomas S. Duffy, *Princeton University*

There has been considerable interest in understanding phase transition sequences in divalent metal fluorides AF_2 (A = Pb, Ca, Sr, Ba, etc.) as a function of pressure. These materials have applications as scintillators, luminescent materials, and ionic conductors. A cubic (fluorite-type) to orthorhombic (cotunnite-type) phase transformation at high pressures has been observed in these materials. Further phase transitions and metallization are expected at higher pressures. In this study we examined SrF_2 using the laser-heated diamond anvil cell at beamline X17B3 at the NSLS. Pure SrF_2 was mixed with platinum and insulated from the diamonds using NaCl layers. The sample was directly compressed to 60 GPa and then heated. Before heating, broad diffraction lines are observed which are distinct from the low-pressure fluorite-type phase indicating that a room-temperature transition had occurred. After 3 minutes of heating many new diffraction lines appear, and the pattern appears related to that prior to heating. The new diffraction peaks can be fit to a hexagonal unit cell. The observed peaks are similar to those of the post-cotunnite phase observed in BaF_2 at lower pressures (12 GPa) (Leger et al., 1995). Upon further compression and heating to 92 GPa, the diffraction pattern is largely unchanged. Future work will focus on profile refinements of the powder patterns and further experiments to constrain the phase boundary.

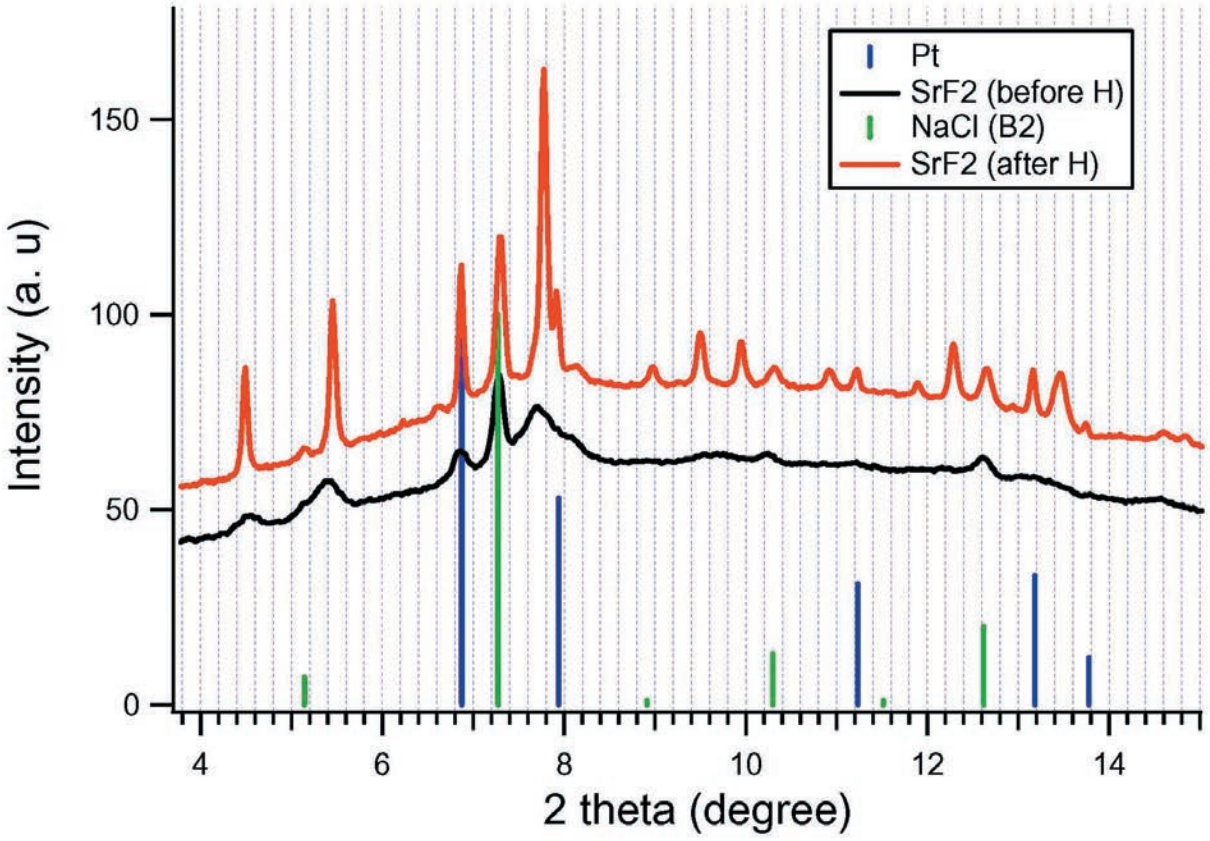

Diffraction patterns obtained at X17B3 from SrF_2 prior to heating (black) and after heating (red). The blue and green vertical bars show expected diffraction peak positions for Pt and CsCl-type phase of NaCl.

This research was supported by the NSF and DOE. Experiments were conducted at the X17B3 beamline of NSLS which is supported by COMPRES, the Consortium for Material Property Research in the Earth Sciences under NSF Cooperative Agreement EAR01-35554.

Measurement of water content of olivine using synchrotron IR spectroscopy

Haemyeong Jung *Inst. Geophysics & Planetary Physics,* **Zhenxian Liu** *National Synchrotron Light Source, Brookhaven National Laboratory, Upton, NY ,* **Harry W. Green II** *Inst. Geophysics & Planetary Physics and Dept. Earth Sciences University of California, Riverside*

Water is known to change many physical properties of olivine such as solidus, electrical conductivity, dislocation mechanisms and seismic wave velocity, which can affect the dynamics, evolution and seismic anisotropy of the upper mantle. Pressure can also affect these properties, hence it is critical to differentiate between these effects. As a consequence, it is important to carefully verify whether high-pressure experiment products are dry or have measurable water contents. We have measured the water content of nominally-dry olivine deformed at pressures of P = 2 – 3.1 GPa and temperature of 1570 K as part of a project to differentiate between water and pressure as the cause of certain lattice preferred orientations in olivine.

Measuring the water content using conventional FTIR microscopy is not simple when the sample size is less than ~ 30 mm. However, measurement of water content of a small sample can be done easily using synchrotron IR spectroscopy because the synchrotron IR beam has a higher signal to noise ratio and higher spatial resolution. Samples were polished well on both sides.

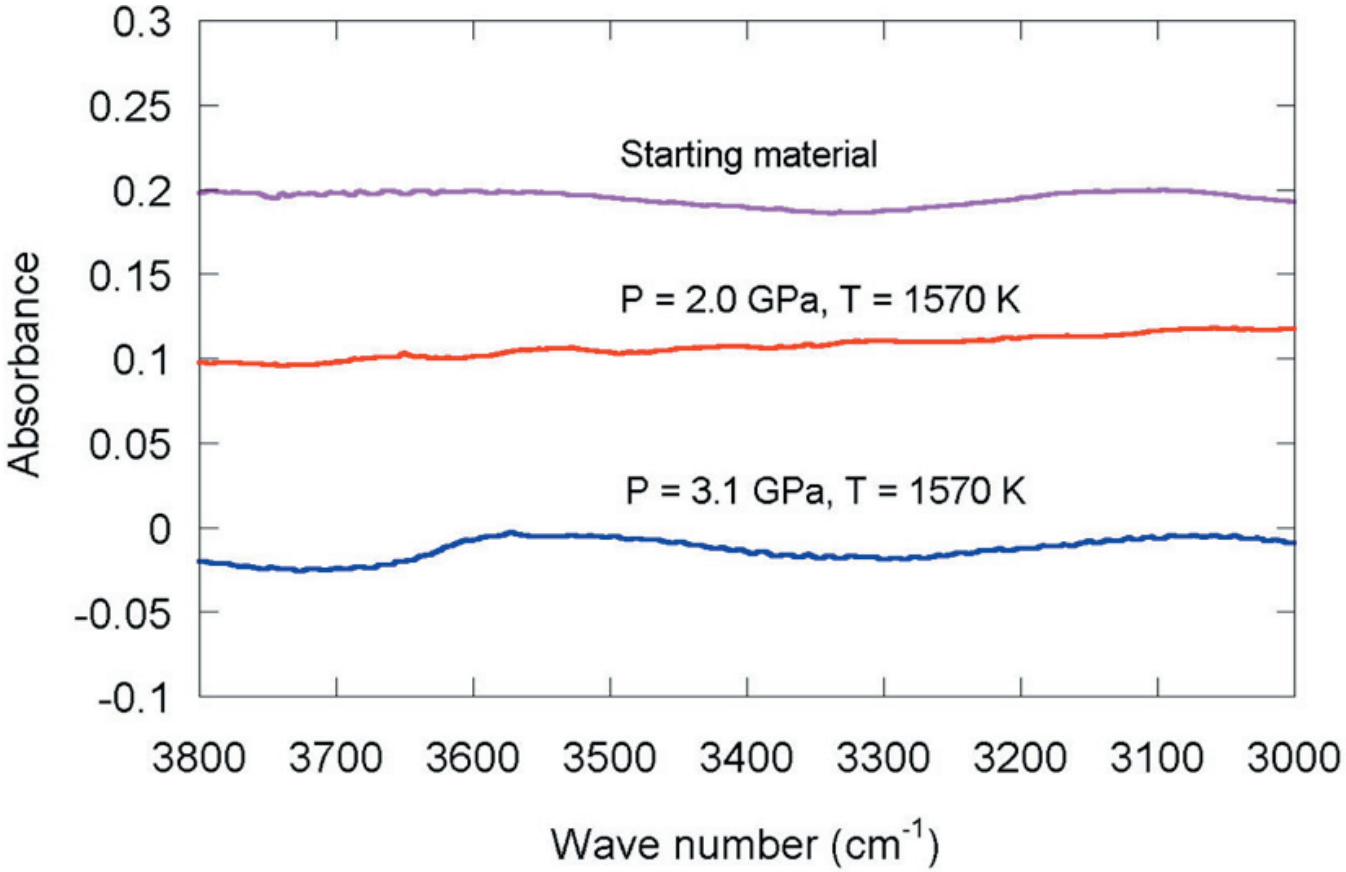

Synchrotron IR spectra of olivine taken at U2A beam line at the Brookhaven National Laboratory. We used an IR beam with a diameter of 20 mm. The spectra show that the water content of the specimens is undetectable for both starting material and experimental samples.

Green II, H. W. and H. Jung, Fluids, faulting and flow, *Elements*, Vol. 1, 31-37, 2005;
H. Jung and HW Green, II , unpublished results

This study was performed as part of a pilot project conducted at NSLS as part of the COMPRES IR Spectroscopy Workshop, September, 2005.

A New System for Detecting Acoustic Emissions in Multianvil Experiments: Application to Deep Seismicity in the Earth

Haemyeong Jung *Inst Geophysics & Planetary Physics,* **Yingwei Fei** *Geophysical Laboratory,* **Paul G. Silver** *Dept. Terrestrial Magnetism,* **Harry W. Green**, *II Inst Geophysics & Planetary Physics and Dept. Earth Sciences, University of California, Riverside, CA*

One of the major goals in the experimental study of deep earthquakes is to identify slip instabilities at high pressure and high temperature (HPHT) that might be responsible for the occurrence of earthquakes. Detecting acoustic emissions from a specimen during faulting provides unique constraints on the instability process. Due to technical challenges, there have been few studies reporting acoustic emissions under HPHT conditions, and all these studies have used at most two acoustic sensors during the experiments. Such techniques preclude accurate location of the acoustic emission source region and thus limit the ability to distinguish real signal from noise that may be coming from outside the sample. We have developed a new system for detecting acoustic emissions at HPHT. Here we present a 4-channel acoustic emission detecting system working in the HPHT octahedral multianvil apparatus. Each channel has high resolution (12 bit) and a sampling rate of 30 MHz. In experiments at pressures up to 6 GPa, and temperatures up to 770 ºC, we have observed acoustic emissions under various conditions. Analyzing these signals, we are able to show that this system permits us to distinguish between signal and noise, locate the source of the acoustic emission, and obtain reliable data on the radiation pattern. This system has greatly improved our ability to study faulting instabilities under high pressure and high temperature.

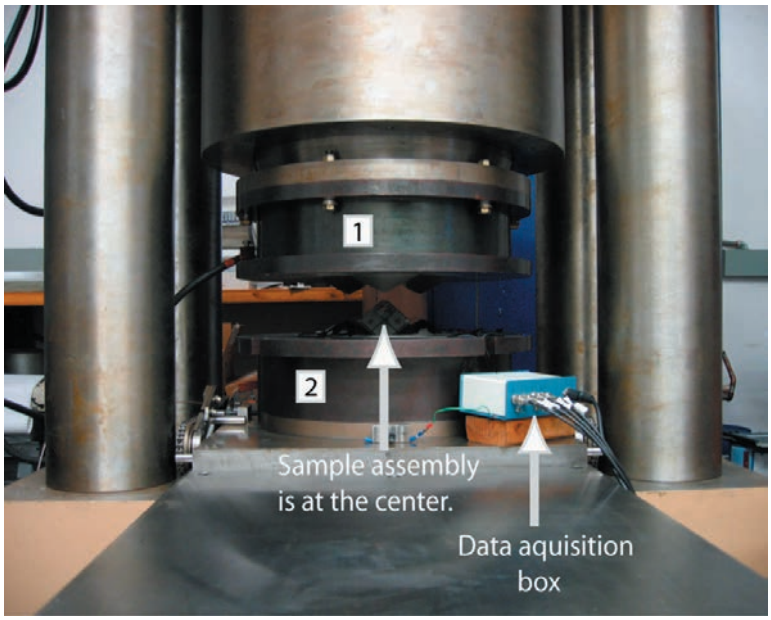

Fig. 1. A multianvil apparatus (Presnall Press). (1) Top pressure ram, (2) Bottom pressure ram. Loaded sample at room pressure. Sample assembly is located at the center. Four acoustic sensors are attached to the outer truncated edges of the Tungsten Carbide (WC) cubes. (Jung et al., 2006).

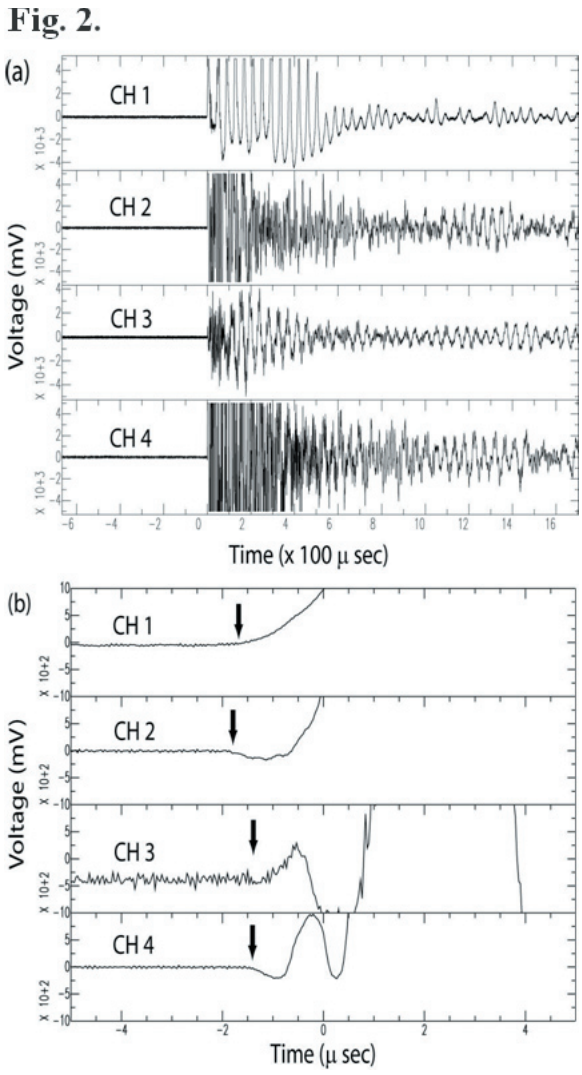

Fig. 2. (A) Acoustic signals with four channels of a shear event when a specimen, tungsten carbide rod, was broken near the center at P = 1 GPa (M529). (B) Magnified view of (A). Please note that the polarity of the first arrival is different at different channels. Arrival time difference between the first and the last arrived signal is ~ 0.4 ms. Note also that the resolution in the waveform is better than ~ 0.1 ms.

Jung, H., Y. Fei, P. G. Silver, and H. W. Green, System for detecting acoustic emissions in the multianvil experiments: Application to deep seismicity in the earth, *Review of Scientific Instruments*, 77, 014501-1~ 7, 2006.
Jung, H., Y. Fei, P. G. Silver, and H. W. Green, Detecting acoustic emissions with/ without dehydration of serpentine outside P-T field of conventional brittle failure, *AGU 2005 Fall Meeting*, MR31B-08, 2005.

This study was supported by the National Science Foundation under grants EAR0125938 & EAR0135411. The experiments were performed using the Presnall Press at the Geophysical Laboratory in preparation for developing in situ synchrotron AE experiments as part of the COMPRES Grand Challenge in Rheology..

Deformation of serpentinite with implications for dehydration-induced earthquakes and subduction zone processes

Haemyeong Jung *Institute of Geophysics and Planetary Physics,* **Larissa F. Dobrzhinetskaya** *Department of Earth Sciences, University of California, Riverside, CA,* **Harry W. Green, II** *Institute of Geophysics and Planetary Physics and Department of Earth Sciences, University of California, Riverside, CA*

Dehydration embrittlement of serpentine was investigated using triaxial deformation experiments at high pressure and temperature (P = 1 - 6 GPa; T = 550 – 820 ºC). A modified Griggs apparatus was used up to 3.4 GPa and a Walker-type multi-anvil apparatus was used 3.5 - 6 GPa. Dehydration of serpentine under a differential stress resulted in faults associated with ultra fine-grained solid reaction products, formed as byproducts of antigorite dehydration. This phenomenon was observed under all conditions tested (1 – 6 GPa, 630-820 ºC), independent of pressure, even though the sign of total volume change (ΔV) of the reaction changes from positive to negative at 2.2 GPa. This observation confirms that dehydration embrittlement is a viable mechanism for triggering earthquakes independent of depth, so long as there is a hydrous mineral breaking down under a differential stress. Aligned Mode-I cracks and fluid inclusion trails are commonly observed in relict olivine in the deformed serpentinite. We suggest that some of the puzzling observations including a seismic low velocity zone (LVZ) at the top of subducting slabs can be attributable to aligned fluid-filled Mode-I cracks and enhanced defect mobility in olivine in the presence of water. In addition, low seismicity regions in subduction zones may be explained by "superplastic" flow under low stress along the ultra fine-grained solid reaction products that are produced during dehydration reactions.

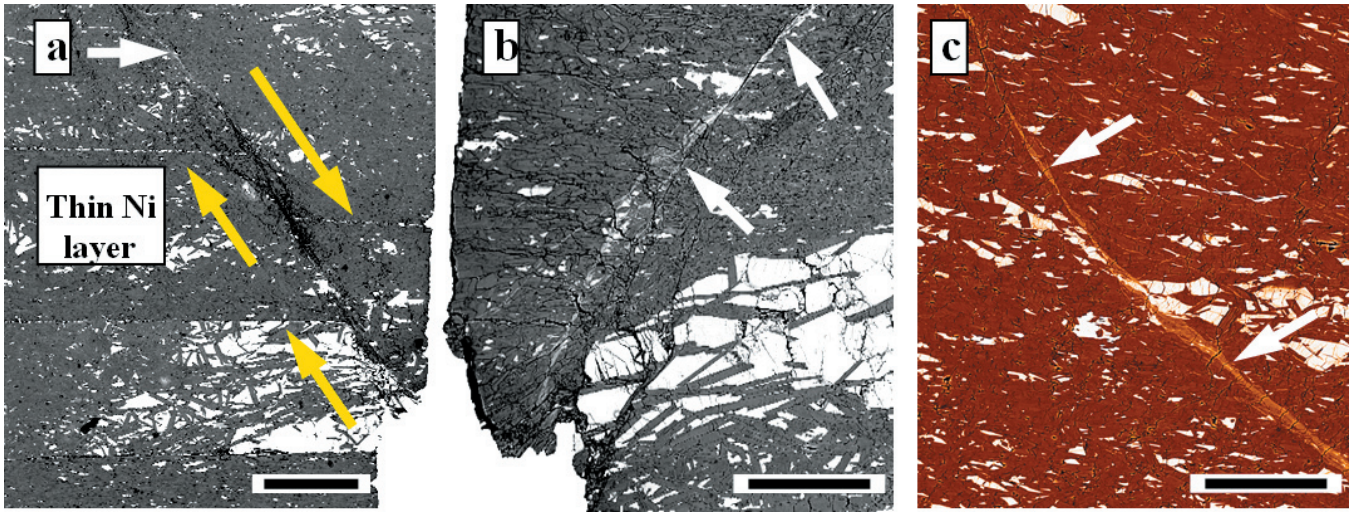

Microstructures of faulted specimens. (a) Fault displacing thin Ni marking layers (yellow arrows) (1.0 GPa, 720˚C; $\Delta V>0$). (b) Similar to (a) but 3.3 GPa, 750˚C; $\Delta V<0$. (c) False color image showing dehydration products (orange color), relict olivine (white), and serpentine (red). Dehydration products along faults in a-c indicated by white arrowheads. Scale bars: 200 μm (a, b, c). (Jung et al., 2004).

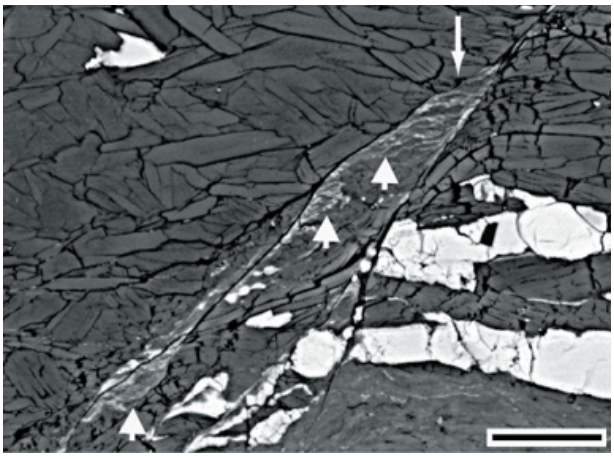

Back-scattered electron images of fault microstructures. Sample deformed at 1.0 GPa and 650 ºC ($\Delta V > 0$). Convergence zone (arrow) is under compression and exhibits a concentration of solid dehydration products (gray 'wisps') oriented normal to the orientation of s1. The multiple 'wisps' are anticracks recording volume loss in the compressed zone (arrowheads). Maximum compression direction NS in images. Scale bar 20 μm. (Jung & Green, 2004)

Jung, H., H. W. Green, and L.F. Dobrzhnetskaya, Intermediate-depth earthquakes faulting by dehydration embrittlement with negative volume change, *Nature*, 428, 545-549, 2004.

Jung, H., and H. W. Green, Experimental faulting of serpentinite during dehydration: implications for earthquakes, seismic low velocity zones, and anomalous hypocenter distributions in subduction zones, *International Geology Review*, 46, No 12, 1089-1102, 2004.

This study was supported by the National Science Foundation under grants EAR0125938 & EAR0135411 to HWG. The experiments were performed using the 5-GPa Griggs-type piston cylinder deformation apparatus at UC Riverside in preparation for in situ experiments as part of the COMPRES Grand Challenge in Rheology.

Plastic Deformation and Deformation Microstructures under Deep Mantle Conditions

Shun-ichiro Karato, Yu Nishihara, Yousheng Xu, David Tinker, Takaaki Kawazoe

Understanding of rheological properties and deformation microstructures of mantle minerals is critical for our understanding of dynamics of this planet. However, quantitative studies of these properties have been limited to low pressure conditions (<1 GPa). The RDA (rotational Drickamer apparatus) was designed in order to extend the P-T range of these studies to deep mantle conditions. In the RDA, a thin sample is squeezed between two anvils and heated by a disk-shape heater. A sample is then annealed to remove defects introduced by initial stage pressurization. Then the top anvil is rotated relative to the bottom one to allow shear deformation to occur. Because the anvil support during a deformation experiment is similar to the one for static experiments, we expect that the maximum pressure of operation is close to that for static experiments. Furthermore the geometry of deformation with this apparatus allows us to conduct deformation experiments to large strains, which is critical to the study of deformation fabrics (lattice-preferred orientation). The goal of this study at the initial stage of operation is to establish the experimental procedures and the sample assembly to achieve this goal to the transition zone conditions. We have developed sample assembly to allow this type of experiments, and have been able to conduct quantitative deformation experiments to 50-100% under the transition zone conditions (~15 GPa, ~1800 K). Although the quality of stress measurements is not high due primarily to the poor set-up of X-ray detectors, with an improved facility we will be able to obtain the first quantitative data set on rheological properties and the deformation microstructures under the transition zone and deeper mantle conditions.

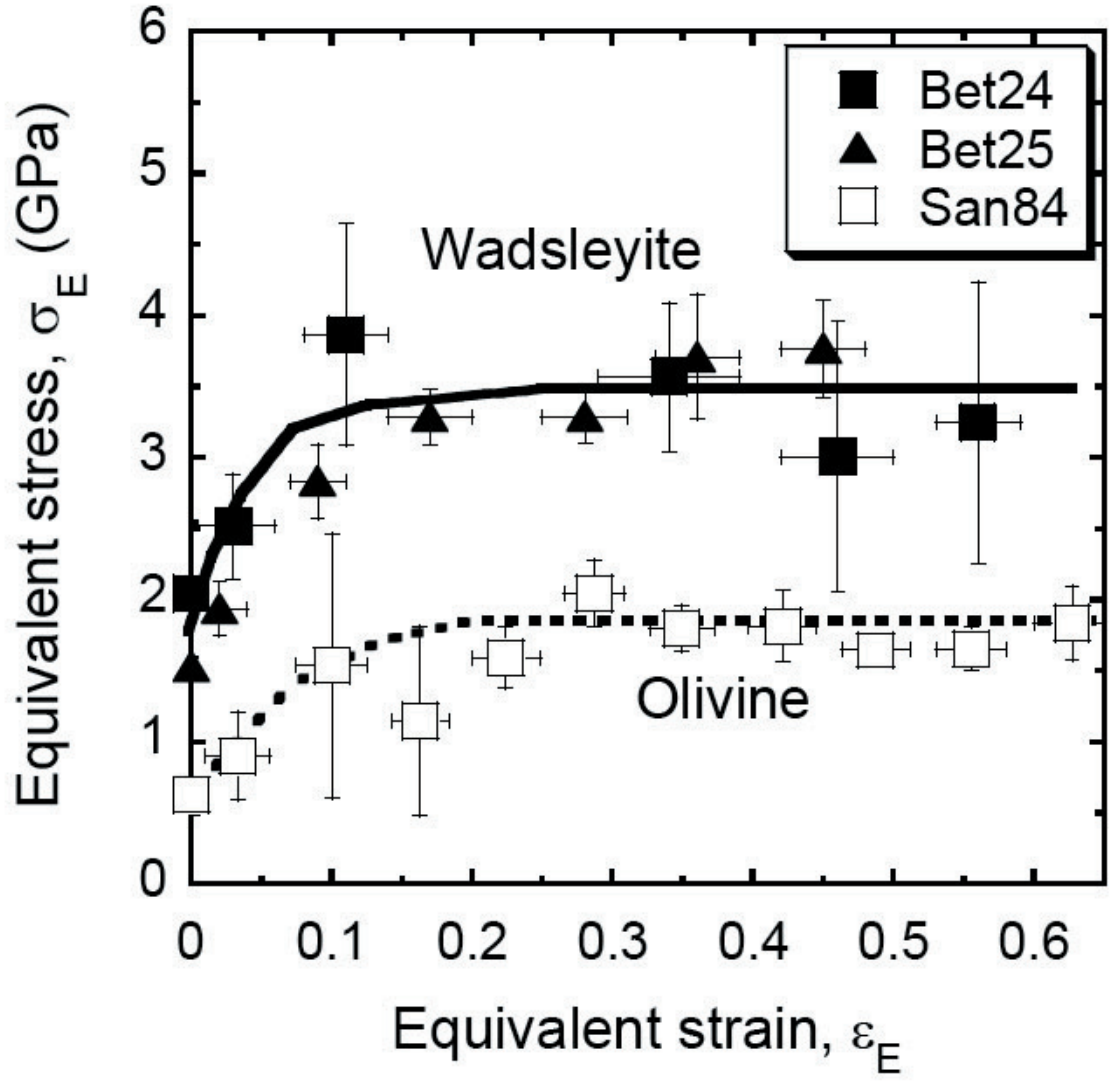

Stress-strain relationships obtained using a RDA for wadsleyite and olivine. The stress-strain curves are characterized by a transient period followed by the quasi-steady state deformation. Wadsleyite is significantly stronger than olivine under these conditions.

High Pressure High Temperature Phase Stability of Fe_2SiO_4

Abby Kavner and Michelle Weinberger

University of California, Los Angeles

Fe_2SiO_4 fayalite is the iron-end member olivine, with Mg-based forsterite pinning down the other end-member. Our goal in this study was to investigate the high pressure/temperature behavior of the Fe-rich end. We studied the phase stability of Fe_2SiO_4 starting composition from 5 GPa to 25 GPa in situ in the laser heated diamond cell and synchrotron x-ray diffraction at the ALS. The fayalite-spinel transformation proceeds differently depending on whether it is pressure-induced at room temperature, or temperature-induced with laser heating. The former generates highly oriented spinel crystals; while the latter generates a finer randomly oriented powder aggregate. The breakdown of spinel to oxide phases was also observed during laser heating. Preliminary results are shown from two sets of experiments: one using NaCl and a second with Au as pressure calibrants. The results will provide information about a possible Fe-rich silicate phase at the core/mantle boundary, and also constrain the ability to measure phase transformation pressures in situ during X-ray diffraction and laser heating.

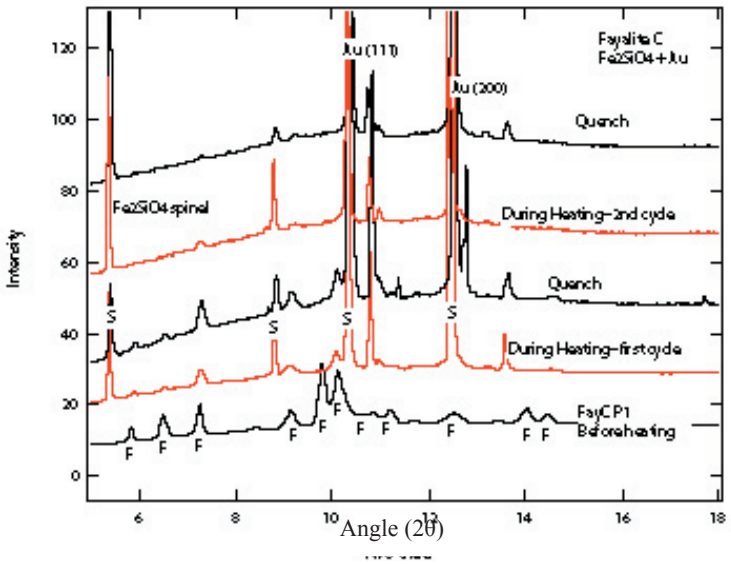

Angle-dispersive X-ray diffraction patterns of fayalite sample before (black pattern), during (red pattern), and after heating with a YAG laser at high pressures. Peaks are labeled F for the olivine phase, and S for the spinel-structured phase.

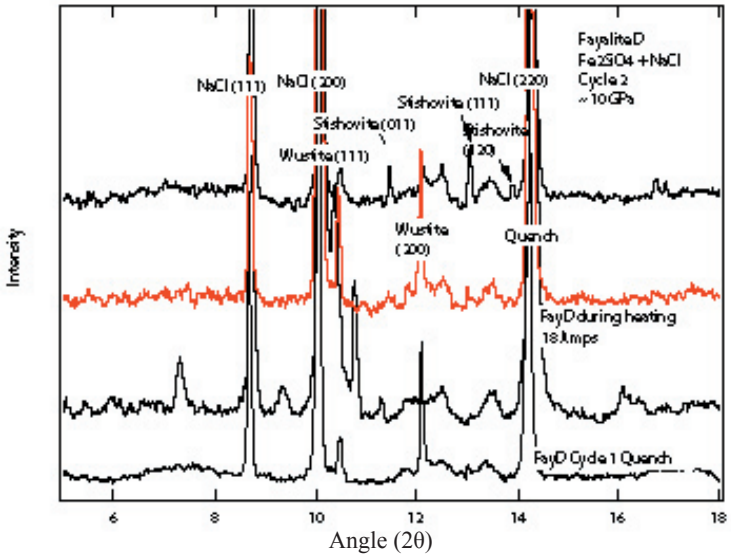

Angle-dispersive X-ray diffraction patterns of fayalite sample before (black pattern), during (red pattern), and after heating with a YAG laser at high pressures. The breakdown to the oxide phases are shown—wustite and sitishovite peaks are labeled.

Work Performed at: ALS, beamline 12.2.2.

Strength, elasticity and equation of state of cubic silicon nitride from radial x-ray diffraction in a diamond cell

Boris Kiefer, Sean R. Shieh, and Thomas S. Duffy *Princeton University*
Toshimori Sekine *National Institute for Materials Science, Tsukuba, Japan*

Spinel nitrides hold considerable technological promise due to their high strength and thermal stability. In this study, lattice strains in nano-crystalline cubic silicon nitride were measured using energy-dispersive x-ray diffraction under non-hydrostatic loading to 68 GPa. The high-pressure elastic properties were also investigated using density-functional theory. The differential stress, t, between 30 and 68 GPa increases from 7 to 23 GPa and can be described beyond 40 GPa as t = 7(4) + 0.24(7)P, where P is the pressure in GPa. The differential stress supported by γ-Si_3N_4 increases with pressure from 3.5% of the shear modulus at 21 GPa to 7.6% at 68 GPa. γ-Si_3N_4 is thus one of the strongest materials yet studied under extreme compression conditions. The elastic anisotropy of γ-Si_3N_4 is large and only weakly pressure dependent. The elastic anisotropy increases from A=1.4 to A=1.9 as the parameter α that characterizes stress-strain continuity across grain boundaries is decreased from 1 to 0.5. The high elastic anisotropy compares well with our first principle calculations that lead to A=1.92-1.95 from ambient pressure to 70 GPa.

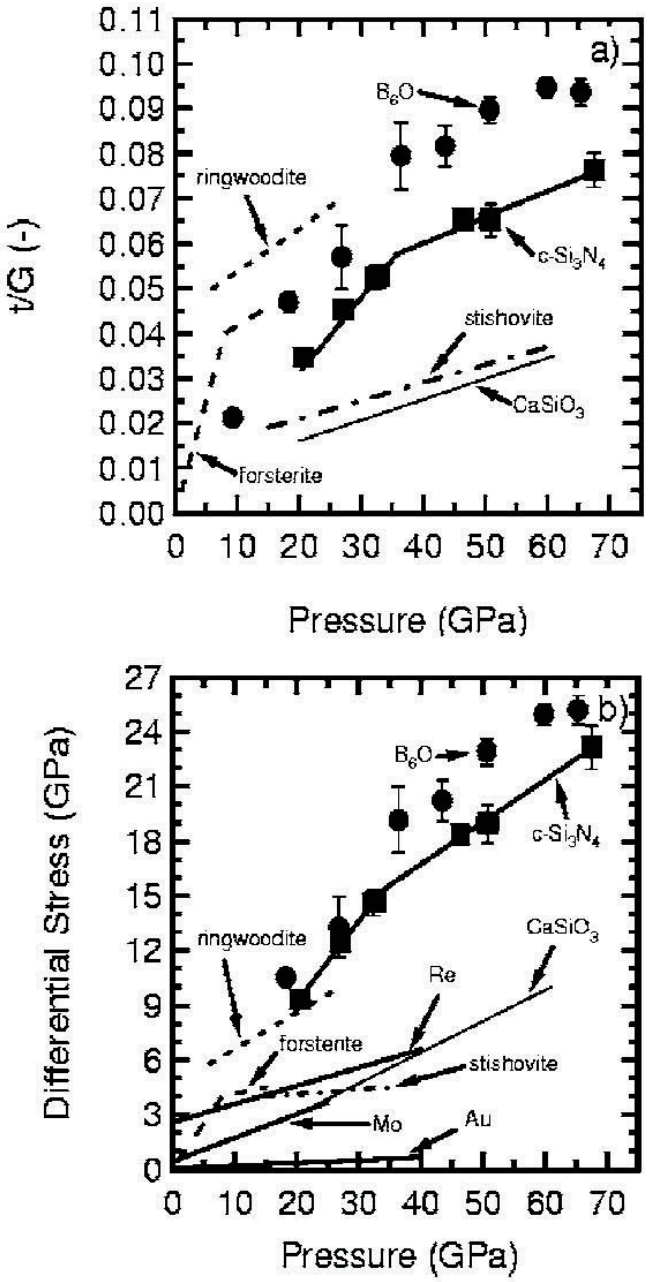

Ratio of differential stress to shear modulus (top) and differential stress (bottom) as a function of pressure for cubic silicon nitride and comparison with other materials

Kiefer, B., S. R. Shieh, T. S. Duffy, and T. Sekine, Strength, elasticity, and equation of state of nanocrystalline cubic silicon nitride (c-Si_3N_4) to 68 GPa, *Physical Review B*, 72, 014102, 2005.

This research was supported by the NSF and DOE. Experiments were conducted at the X17C beamline of NSLS which is supported by COMPRES, the Consortium for Material Property Research in the Earth Sciences under NSF Cooperative Agreement EAR01-35554.

Research Achievements

Boris Kiefer

Department of Physics, New Mexico State University

The primary focus of my research is to explore the physical and chemical properties of earth and planetary materials at relevant pressure and temperature conditions. To reach this goal I use primarily state-of-the-art computational tools. One of the most important characteristics of these methods is that they are independent of experiment and therefore provide independent and complimentary insight into the composition of planets and their dynamical state.

One of my major interests is the formulation of consistent compositional models for the Earth's interior. Many previous research efforts have concentrated on the properties of endmembers in solid solution series and/or the effect of solid solutions on the equation of state. In contrast comparatively little is still known about the effects of solid solutions on the elastic constant tensor. Thus major seismological constraints such as compressional and shear-wave velocities and elastic anisotropy are not utilized to their full potential.

In an effort to further our understanding of elasticity in relation to solid solution I have investigated several systems: the effect of iron the elastic properties on MgSiO3-perovskite, the most abundant mineral in the Earth's lower mantle. Since the discovery of the post-perovskite phase in 2004, I have considered the effect of aluminum substitution in perovskite and post-perovskite lower mantle pressures at static (low temperature) conditions and at high temperatures.

Over the past few years I have diversified my research interests both towards ambient pressures and towards the Earth's core. At ambient pressure I am investigating the relation between crystallography and properties of sulfates. Understanding the crystal chemistry of sulfates is particularly important in relation to acid mine drainage. Understanding the bonding in these minerals in detail enhances our understanding of the formation of solid solutions in these minerals and their affinity for the uptake and storage of often toxic metals. Additionally first-principle calculations can provide initial guesses for structure refinements. This is needed since many sulfates possess large unitcells and low symmetry. Thus the interpretation observations from x-ray diffraction and neutron diffraction experiments are complicated and often non-unique.

The other venue considers core materials and their physical properties. The first results (calculated by Ben Eimer, a student of mine) show that at low pressures ($P < 50$ GPa) an antiferromagnetic spin arrangement is favored. While this has been observed before, our calculations investigated the effect of the spin-arrangement on the complete elastic constant tensor. It is found that the bulk modulus is much stronger affected by the spin-arrangement than the shear modulus. Current efforts try to understand the differences of the observed and predicted shear-modulus. Encouraged by these results I have begun to investigate iron alloys and their effect on elasticity at inner core pressures. The preliminary results show very good agreement with the limited number of available experiments in the overlapping pressure range. Thus theory can provide insights into the effect alloying on elasticity and provide better constraints on the nature of the light element in the Earth inner core.

Finite Element Simulations of the Laser-Heated Diamond Anvil Cell

Boris Kiefer, *New Mexico State University*
Thomas S. Duffy, *Princeton University*

Finite element simulations of the temperature field in the laser-heated diamond anvil cell have been used to evaluate the parameters that control axial and radial temperature gradients. We have performed simulations for a typical experimental geometry consisting of an optically thin sample separated from the diamond anvils by an insulating medium of varying thickness and heated by the Gaussian mode from an infrared laser. Axial temperature gradients are primarily determined by two factors: (1) the ratio of sample thickness to gasket thickness (sample filling fraction); and (2) the ratio of thermal conductivities of sample and insulator. To obtain axial temperature decreases of 10% or less across the sample thickness, it is necessary to have a sample-filling fraction of less than 0.5 when the thermal conductivity of the sample is ten times greater than the conductivity of the insulator. If the sample-filling fraction is 0.2, then the same temperature drop can be maintained for thermal conductivity ratios of the sample to insulator as low as three. Finite element simulations of this type are well suited to model the growing complexity of the experimental geometries employed in laser heating.

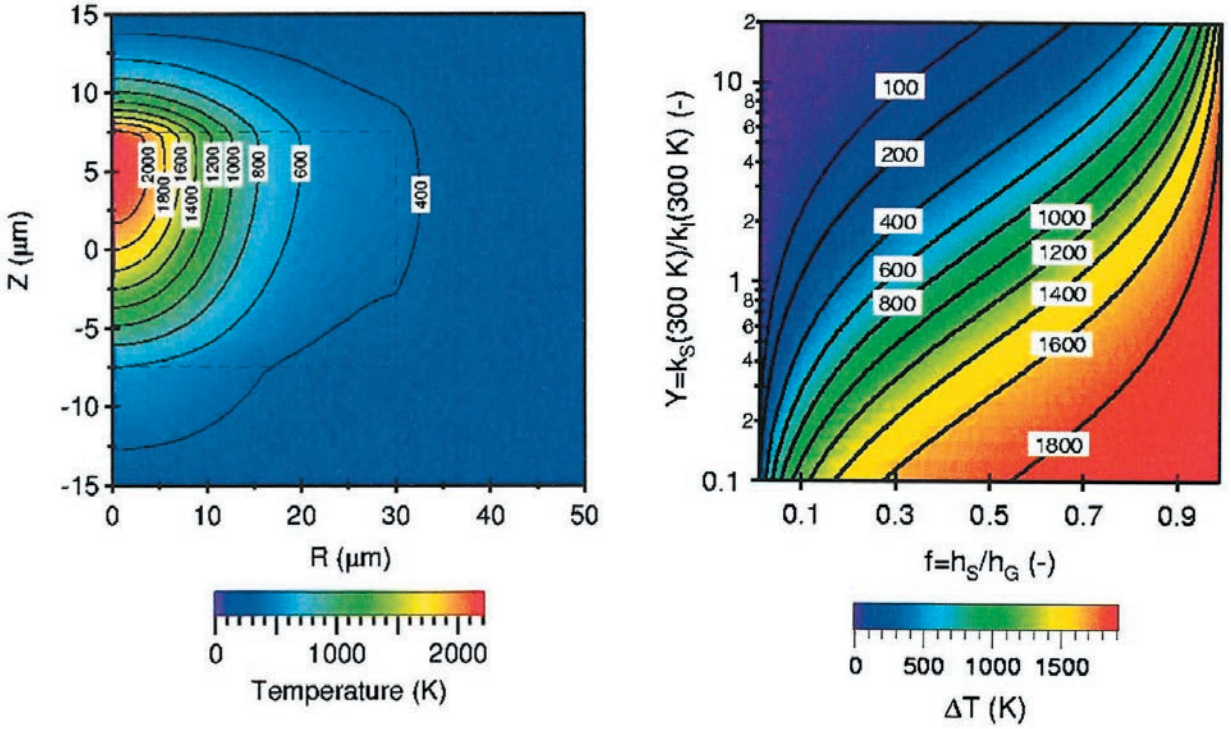

The left figure shows the thermal structure in a typical simulation with sample filling of 50% and the sample resting on an Al_2O_3 support and surrounded by argon. The figure on the right shows the axial temperature drop from 2200 K peak temperature as a function of filling fraction (f) and thermal conductivity ratio (Y).

Kiefer, B. and T. S. Duffy, Finite element simulations of the laser-heated diamond anvil cell, *Journal of Applied Physics,* 97, 114902, 2005.

This research was supported by COMPRES, the Consortium for Material Property Research in the Earth Sciences under NSF Cooperative Agreement EAR01-35554.

Synchrotron far-IR spectroscopy and the Anomalous Transformation in Ice VIII

D D. Klug *National Research Council of Canada, Ottawa, Ontario, Canada K1A 0R6*
J. S. Tse *University of Saskatchewan, Saskatoon, Saskachewan, Canada S7N 5E2*
Z. Liu, R. J. Hemley *Carnegie Institution of Washington, Washington, D.C. 20015, USA*
X. Gonze *Unité de Physico-Chemie et de Physique des Matériaux, Université Catholique de Louvain, Louvain-la-Neuve, Belgium*

New far-IR measurements were carried out by Klug et al. [1] at the U2A beamline of the National Synchrotron Light Source (NSLS) at the Brookhaven National Laboratory to test proposed pressure-induced phase transformations in H_2O and D_2O ice VIII at low temperatures up to 20 GPa and compared with the results of a series of first-principle studies for this phase transformation [2]. The beamline capability has expanded into the new far-IR region at low-T and high-pressure that enables us to study the pressure and temperature dependence of far-IR active modes and complement our ab initio linear response phonon studies. Surprisingly, both the low-T high-pressure far-IR and theoretical calculations give an anomalous transformation in ice VIII that support the experimental results from a high-pressure neutron diffraction study [3]. Our study provides a detailed and definitive new interpretation regarding this phase transformation. Further studies of dense ice phases will continue to characterize possible new phase transition behavior using our combination of theoretical and experimental methods at extreme conditions. Our ultimate goal is far-IR studies above 100 GPa at variable temperatures.

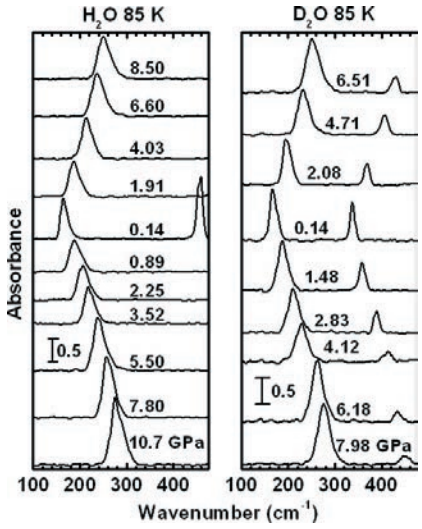

1. The measured low-temperature far-infrared spectra of ice VIII in a diamond anvil cell. The low frequency peak is the infrared active E_u mode. The higher frequency peak is an infrared active peak due to molecular librations.

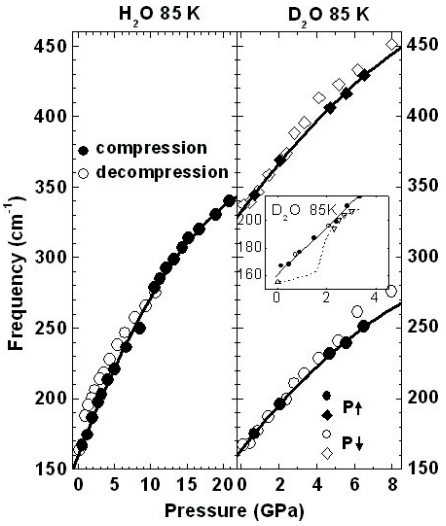

2. The frequency versus pressure results for the E_u infrared active mode compared with previous measurements and suggested pressure dependence in Ref. 3 (Inset).

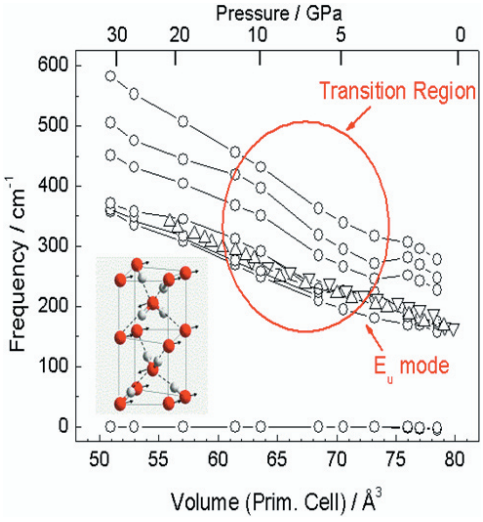

3. The calculated pressure dependence of the lattice modes of ice VIII.

D D. Klug, J. S. Tse, Z. Liu, X. Gonze, and R. J. Hemley, *Phy. Rev.B* 70, 144133, 2004).
J.S. Tse and D.D. Klug. *Phys. Rev. Lett.* 81, 2466-2469 (1998).
J. M. Besson, S. Slotz, W.G. Marshall, R.J. Nelmes, and J.S. Loveday, *Phys. Rev. Lett.* 78, 3141 (1997).

Infrared Absorption and First-Principles Study of Hydrogen-Bond Symmetrization and in Methane Filled Ice

D.D. Klug, *National Research Council of Canada, Ottawa, Ontario, Canada K1A 0R6* **J.S. Tse** *University of Saskatchewan, Saskatoon, Saskachewan, Canada S7N 5E2,* **Z. Liu, X. and R. J. Hemley** *Carnegie Institution of Washington, Washington, D.C. 20015, USA*

Clathrate hydrates are compounds consisting of cages of hydrogen bonded water molecules surrounding guest molecules or atoms. Recent studies revealed the formation of new high-pressure phases of the CH_4 clathrate[1]. This finding has important implications for hydrogen bond research as well as providing a new model for astrophysical studies such as the formation and evolution of the composition of Titan, a moon of Saturn. There has been an intense interest in this area of research. The CH_4 clathrate is also of significant importance as a potential energy source. Since the clathrate is significantly more compressible than dense ice phases, this raises the possibility of whether it may be possible to achieve the condition where the hydrogen bonds in the cages formed by the water molecules could be driven to a symmetric state as that observed in a high pressure form of pure crystalline ice, ice VIII. A series of far- and mid-IR measurements were carried out by Klug et al. [2] at beam-line U2A of the NSLS to identify the predicted phase transition from non-symmetric to symmetric hydrogen bonds at both room and low temperatures up to 40 GPa. Pressure dependence of the C-H and uncoupled O-H stretching vibrational modes indicates that the possible center symmetric hydrogen bonds as well as quantum phase may initiate at about 20 GPa. This finding is consistent with theoretical density functional studies of the stability and phonons for this clathrate system. Another important feature of these experiments was the characterization of the significant temperature dependence of Fermi resonance in this system.

FTIR Spectroscopy of Methane Clathrate Hydrate: Pressure induced symmetrization of hydrogen bonding

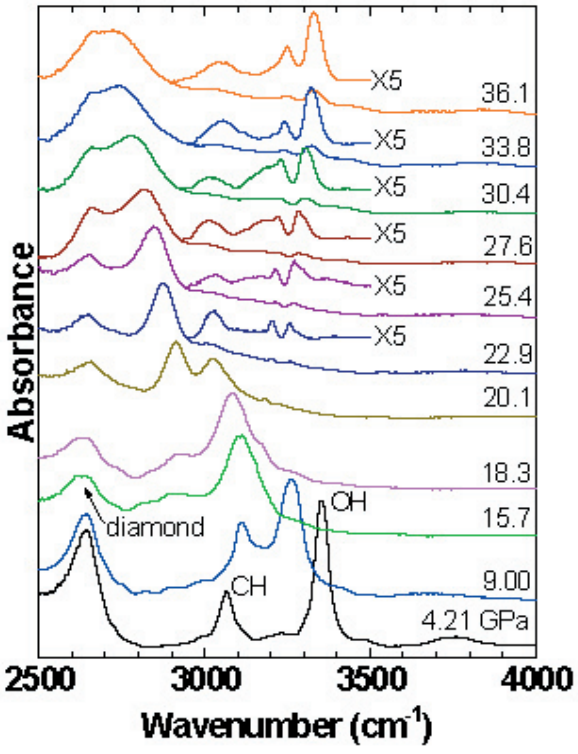

1. Infrared spectra of the clathrate MH-III prepared with 98.3% D_2O and 1.7% H_2O and CH_4 as a function of pressure at 300 K

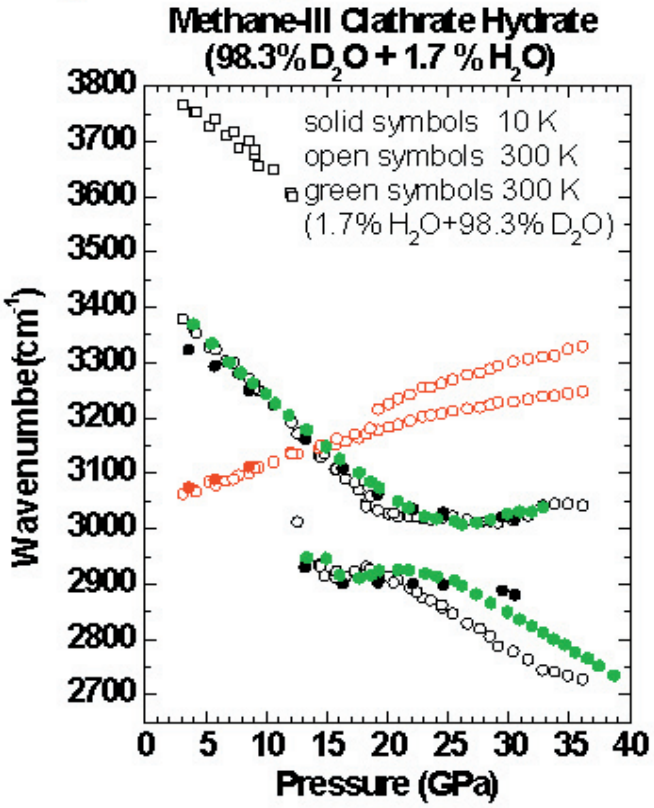

2. Pressure dependence of the mid-infrared OH stretching peaks and internal CH_4 vibrational modes for the MH-III clathrate at 10 K (solid black symbols) and 300 K (open circles) and ice VII (green symbols) at 300 K

J. S. Loveday, R. J. Nelmes, M. Guthrie, S. A. Belmonte, D. R. Allan, D. D. Klug, J. S. Tse, Y. P. Handa, *Nature*, 410, 661 (2001).
D.D. Klug, J.S.Tse, Z. Liu, and R.J. Hemley, Submitted.

Ultrasonic Observations of Elasticity Changes across Phase Transformations in $MgSiO_3$ Pyroxenes

Jennifer Kung*, Baosheng Li and Robert C. Liebermann •*Stony Brook University*

Using ultrasonic interferometry in conjunction with synchrotron X-radiation techniques in a multi-anvil, high-pressure apparatus, the elastic behavior of $MgSiO_3$ pyroxene has been continuously monitored as the specimens undergo phase transformations from the orthoenstatite to the high-pressure clinoenstatite phase and from HP-CEN to the low-pressure clinoenstatite phase. In the former case, elastic softening and amplitude attenuation is observed for both compressional (P) and shear (S) waves when the pressure exceeds 9 GPa at room temperature, which we suggest is associated with a transition to a metastable phase intermediate between OEN and HP-CEN. In the latter case, both P and S wave velocities decrease rapidly as the back-transformation from HP-CEN to LP-CEN occurs on decrease of pressure below 4 GPa at room temperature; this is accompanied by an increase in attenuation of the P waves in the specimen, but not the S waves.

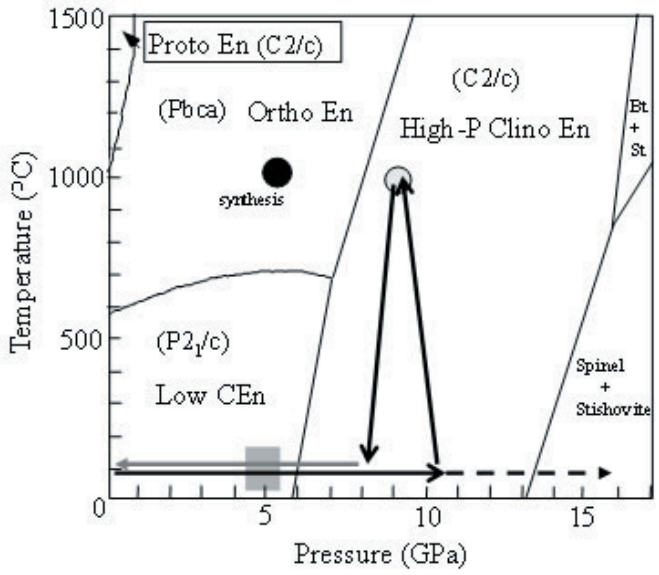

Phase diagram for $MgSiO_3$ with synthesis conditions for the orthoenstatite OEN (black circle) and high-pressure clinoenstatite HP-CEN (grey circle) phases. The P-T paths for the two ultrasonic experiments are indicated by the solid line (for T350) and the dashed line (T354).

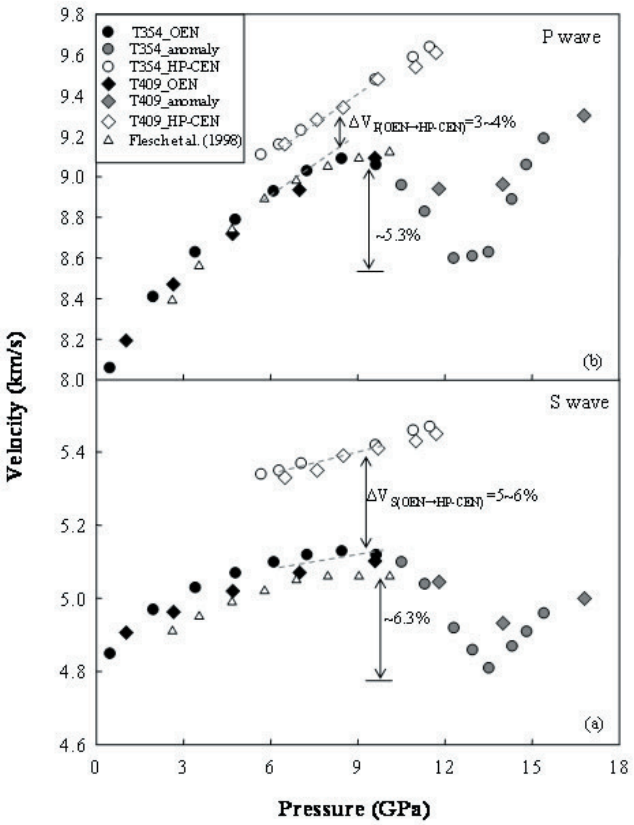

P and S wave velocities of $MgSiO_3$-enstatite as function of pressure at room temperature in runs T350 and T354.

Reference: Kung, J., B. Li, and R.C. Liebermann, Ultrasonic Observations of Elasticity Changes across Phase Transformations in $MgSiO_3$ Pyroxenes, *Journal of Physics and Chemistry of Solids*, revised January, 2006.

Acknowledgements: This study is supported by the National Science Foundation under the Grants EAR0003340 to B.L. and EAR0229704 to R.C.L.. We thank J. Hu, H. Liu and Z. Liu for assistance in conducting the in-situ X-ray DAC experiment on beamline X17C and the Raman study on beamline U2A at National Synchrotron Light Source (NSLS). We also thank the staff of beamline 13-ID, GSECARS, and especially T. Uchida and Y. Wang for their support of the original ultrasonics experiment.

Elasticity of $(Mg_{0.83},Fe_{0.17})O$ ferropericlase at high pressure: Ultrasonic measurements in conjunction with X-radiation techniques

Jennifer Kung, Baosheng Li, Donald J. Weidner, Jianzhong Zhang, Robert C. Liebermann *Stony Brook University*

The elasticity of ferropericlase with a potential mantle composition of $(Mg_{0.83},Fe_{0.17})O$ is determined using ultrasonic interferometry in conjunction with in-situ X-radiation techniques (X-ray diffraction and X-radiography) in a DIA-type cubic anvil high-pressure apparatus to pressures of 9 GPa (NaCl pressure scale) at room temperature. In this study, we demonstrate that it is possible to directly monitor the specimen length using an X-ray imaging technique and show that these lengths are consistent with those derived from X-ray diffraction data when no plastic deformation of the specimen occurs during the experiment. By combining the ultrasonic and X-ray diffraction data, the adiabatic elastic bulk (KS) and shear (G) moduli and specimen volume can be measured simultaneously. This enables pressure scale-free measurements of the equation of state of the specimen using a parameterization such as the Birch-Murnaghan equation of state. The elastic moduli determined for $(Mg_{0.83},Fe_{0.17})O$ are KS0=165.5(12) GPa and G0=112.4(4) GPa, and their pressure derivatives are KS0'=4.16(20) and G0'=1.89(4). If these results are compared with those for MgO, they demonstrate that KS0 and KS0' are insensitive to the addition of 17 mol% FeO, but G0 and G0' and are reduced by 14% and 24%, respectively. We calculate that the P and S wave velocities of a perovskite plus ferropericlase phase assemblage with a pyrolite composition at the top of the lower mantle [660 km depth] are lowered by 0.8 and 2.3%, respectively, when compared with those calculated using the elastic properties of end-member MgO. Consequently, the magnitudes of the calculated shear wave velocity jumps across the 660 km discontinuity are reduced by about 11% for P waves and 20% for S waves, if this discontinuity is considered as a phase transformation boundary (ringwoodite->perovskite + ferropericlase) only.

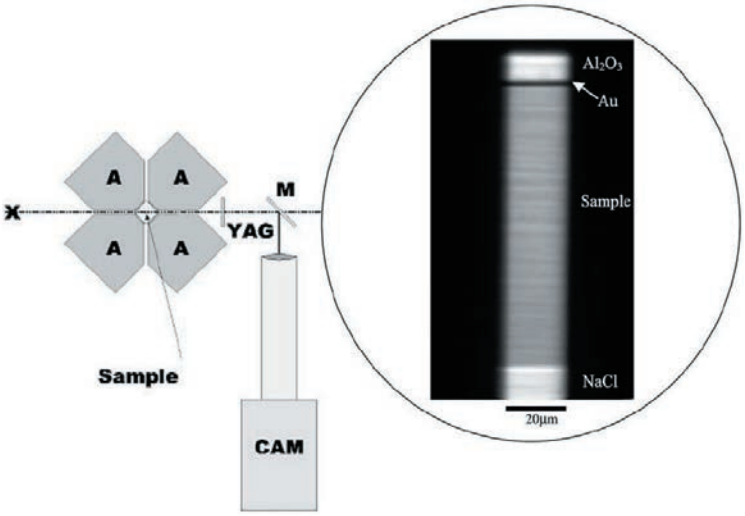

Schematic of X-radiographic image system on SAM-85, a DIA-type, high-pressure apparatus.

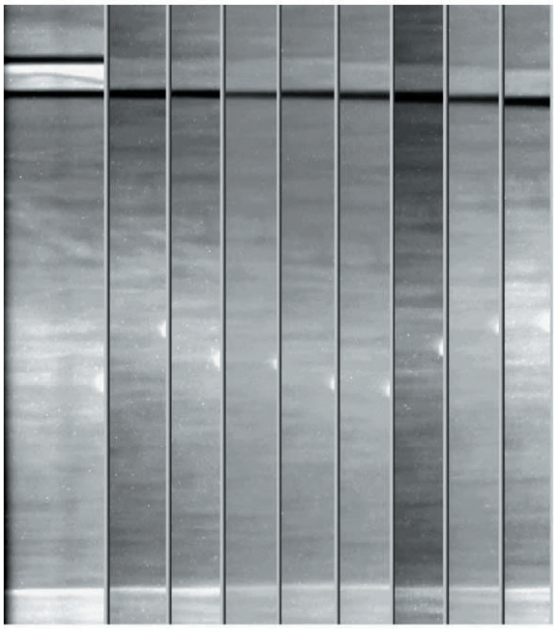

X-radiographic images of polycrystalline sample of ferropericlase as a function of pressure to 9 GPa.

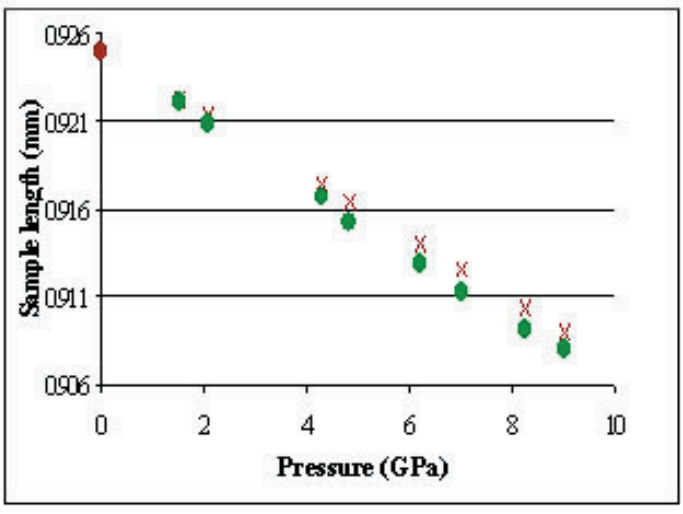

Sample lengths at high pressures using both X-radiographic images and X-ray diffraction patterns.

Reference: Kung, J., B. Li, D.J. Weidner, J. Zhang, R.C. Liebermann, Elasticity of $(Mg_{0.83},Fe_{0.17})O$ ferropericlase at high pressure: Ultrasonic measurements in conjunction with X-radiation techniques *Earth and Planet. Sci. Letters*, Vol 203, pp. 557-566, 2002.

This study was supported by the National Science Foundation under grants EAR 99-80491 and 02-29704 to RCL. The insitu ultrasonic and X-ray experiments were carried out at the X-17B2 beamline of the National Synchrotron Light Source (NSLS) which is supported by the US Department of Energy, Division of Materials Sciences and Division of Chemical Sciences under Contract No. DE-AC02-76CH00016 and by COMPRES, the Consortium for Materials Properties Research in Earth Sciences under contract number EAR 01-35554.

A Beamline for High Pressure Studies at the Advanced Light Source with a Superconducting Bending Magnet as the Source

Martin Kunz, Wendel A. Caldwell, Arianna E. Gleason *Lawrence Berkeley National Laboratory, Department of Earth and Planetary Sciences, University of California, Berkeley*, **Alastair A. MacDowell, Daniella Cambie, Richard S. Celestre, Edward E. Domning, Robert M. Duarte, James M. Glossinger, Nicholas Kelez, David W. Plate, Howard A. Padmore, Simon M. Clark** *Lawrence Berkeley National Laboratory*, **Tony Yu, Joeseph M. Zaug** *Lawrence Livermore National Laboratory*, **Raymond Jeanloz** *Department of Earth and Planetary Sciences, University of California, Berkeley,*, **A. Paul Alivisatos** *Department of Chemistry, University of California, Berkeley*

A new facility for high-pressure diffraction and spectroscopy using diamond anvil high-pressure cells has been built at the Advanced Light Source on Beamline 12.2.2. This beamline benefits from the hard X-radiation generated by a 6 Tesla superconducting bending magnet (superbend). Useful x-ray flux is available between 5 keV and 35 keV. The radiation is transferred from the superbend to the experimental enclosure by the brightness preserving optics of the beamline. These optics are comprised of: a plane parabola collimating mirror (M1), followed by a Kohzu monochromator vessel with a Si(111) crystals (E/□E ~ 7000) and a W/B4C multilayers (E/□E ~ 100), and then a toroidal focusing mirror (M2) with variable focusing distance. The experimental enclosure contains an automated beam positioning system, a set of slits, ion chambers, the sample positioning goniometry and area detectors (CCD or image-plate detector). Future developments aim at the installation of a second end station dedicated for in situ laser-heating on one hand and a dedicated high-pressure single-crystal station, applying both monochromatic as well as polychromatic techniques.

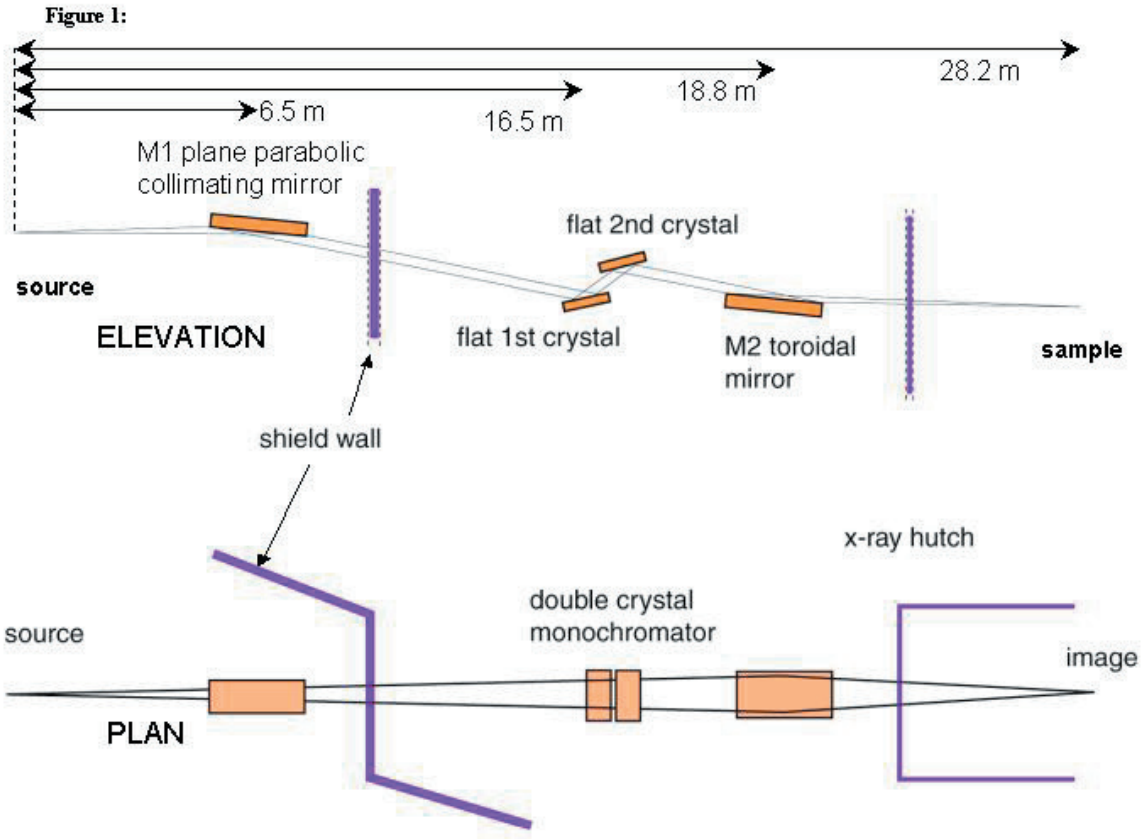

Schematic layout of the new high pressure beamline with a superbend dipole magnet source. The beamline acceptance is 1.0 x 0.22 mrad (h x v). The toroidal M2 mirror demagnifies in the horizontal in a 2:1 ratio.

The Advanced Light Source is supported by the Director, Office of Science, Office of Basic Energy Sciences, Materials Sciences Division, of the U.S. Department of Energy under Contract No. DE-AC03-76SF00098 at Lawrence Berkeley National Laboratory and University of California, Berkeley, California. COMPRES, the Consortium for Materials Properties Research in Earth Sciences under NSF Cooperative Agreement EAR 01-35554 supported this project through funding of MK, WAC and AEG as well as crucial beamline-equipment.

High-temperature single-crystal neutron diffraction study of natural chondrodite.

Martin Kunz
Advanced Light Source, Lawrence Berkeley Laboratory, MS 4R 0230, 1 Cyclotron Rd, Berkeley, CA 94720, USA; and Department of Earth and Planetary Science, University of California, Berkeley, CA 94720, USA.
George A. Lager
Department of Geography and Geosciences, University of Louisville, Louisville, KY 40292, USA.
Hans-Beat Bürgi
Labor für chemische und mineralogische Kristallographie, Universität Bern, CH-3012 Bern, Switzerland.
Maria Teresa Fernandez-Diaz
Institut Laue-Langevin, F-38042 Grenoble, France.

The H-atom environment in a Tilly Foster chondrodite was analyzed using single-crystal neutron-diffraction data collected at 500, 700 and 900 K and previously published low temperature data collected at 10 K, 100 K and 300 K on the same crystal ($Mg_{4.64}Fe_{0.28}Mn_{0.014}Ti_{0.023}(Si_{1.01}O_4)2F_{1.16}OH_{0.84}$, Friedrich et al. 2001). The full mean square displacement matrix □ of the O-H pair was determined from the temperature dependence of the anisotropic displacement parameters, enabling a proper correction of the O-H bond for thermal vibration without assumptions about the correlation of O and H movements. The results show that the perpendicular O-H motions in chondrodite are intermediate between the riding and the independent motion models. The corrected O-H bond lengths do not change with temperature whereas the corrected H•••F distances show an increase of ~0.02 Å with temperature, as do the Mg-O distances. This result shows that spectroscopic observations on the strength of the covalent O-H bond cannot be interpreted unambiguously in terms of a corresponding behaviour of the associated H•••O/F hydrogen bond.

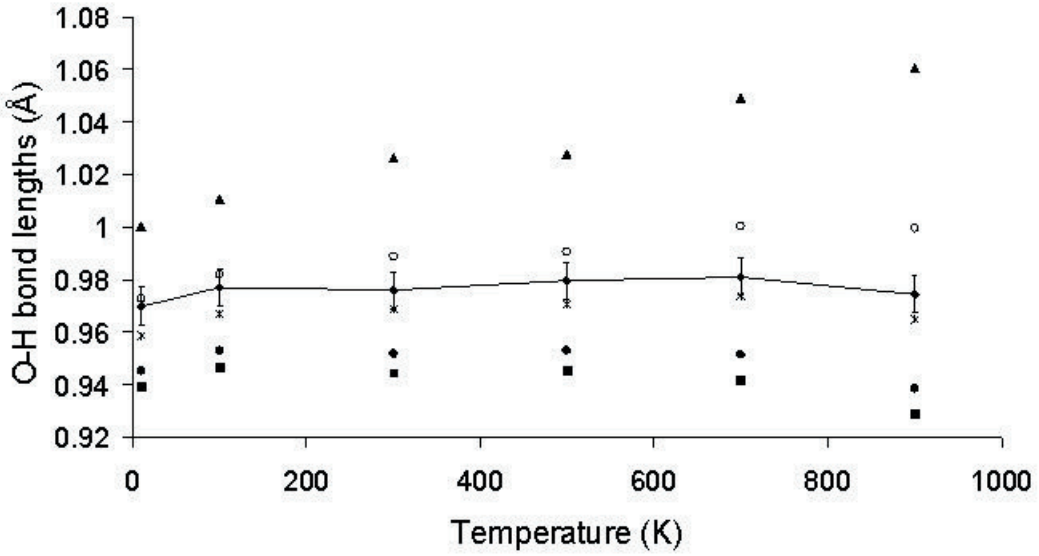

Effect of various models of motion on the O-H distance correction for Tilly Foster chondrodite between 10 K and 900 K. ▲ upper limit; O independent motion; ◆ according to Bürgi and Capelli (2000); * riding model; ● lower limit; ■ uncorrected. Error bars indicate one estimated standard deviation.

The authors acknowledge the support of the ILL staff ensuring a successful experiment. GL is supported by NSF grant No. EAR-0073734. MK's work was supported by COMPRES, the Consortium for Materials Properties Research in Earth Sciences under NSF Cooperative Agreement EAR 01-35554. HBB acknowledges support by the 'Schweizerischer Nationalfonds'.

P-V single crystal- and P-V-T powder-diffraction study on metamict zircon ($ZrSiO_4$)

Martin Kunz, *ALS, LBL, MS 4R 0230, 1 Cyclotron Rd, Berkeley CA*
Petra Simoncic, *NEAT ORU/Thermochemistry, University of California, Davis CA*

Zircon ($ZrSiO_4$) is of interest due to its capabilities to retain radioactive elements such as U and Th in the crystal structure. This makes it an ideal material for U-Pb dating in geology. Zircon is also an interesting model phase to study the mechanism and properties of structural damage inflicted by self-radiation (metamictization). This is important in view of the attempts for chemical inertialization of radioactive isotopes using ceramic nuclear waste forms. While there are numerous studies on the metamictization of zircon at ambient conditions and elevated temperatures (i.e. Rios et al. 2000; Mursic et al. 1992), the effect of pressure on the radiation induced structural damage is not well understood as yet (e.g. Ono et al. 2004). Diverging results are published on the compressibility of non-metamict zircon (Hazen and Finger, 1979, Van Westrenen et al. 2004). Here we present a structural study of metamict zircon (~ 900 ppm U, ~ 1.5 x 10^{18} alpha decay events g^{-1}) at elevated pressure and simultaneously elevated pressure and temperature and compare it with literature data of non-metamict zircon (Hazen and Finger, 1979; Kolesov et al, 2001, Van Westrenen et al. 2004). Data were collected on a single crystal (P-V-data, structure refinement) between 0 a 7 GPa. A powder diffraction experiment was performed in a heatable diamond anvil cell at pressures up to 10 GPa and temperatures up to 573 K sample (P-V-T-data) on beamline 12.2.2 of the ALS.

Room temperature single-crystal compressibility data were fitted to a 3rd-order Birch Murnaghan equation of state. This gives a room-temperature compressibility of K_0 = 205.7(5) GPa, K' = 5.3(4), V_0 = 262.609(9) Å^3. When constraining K' to 4, the K_0 increases to 209.6(3) GPa with a V_0 of 262.585(8) Å^3. The a-axis is much more compressible (Ka_0 = 180.6(4) GPa) than the c-axis (Kc_0 = 304.4(18) GPa). This is in qualitative accordance with the behavior observed for non-metamict zircon, however, the axial compressibilities are slightly more isotropic in our metamict zircon compared to a non-metamict sample (Hazen and Finger, 1979). The anisotropy in compressibility is reflected in the observed change in bond-length. Between 0 and 7 GPa, we observe a decrease in bond length of 1.7 % for the Zr-O(e) bond, oriented perpendicular to the c-axis, whereas the Zr-O(c), oriented sup-parallel to c, is compressed only by 0.7 %. The four Si-O bonds compress by 1 % in the same pressure range. The softer behavior of the a-b-plane relative to the c-axis is somewhat surprising in view of the well known larger swelling of the c-axis upon metamictization.

The single-crystal diffraction peaks show a reversible decrease in peak width (FWHM) with increasing pressure from $0.085(5)º at ambient condition to $0.070(5)º at 7 GPa. A simultaneously loaded quartz crystal showed no variation in peak width. A decrease in peak-width with increasing pressure is unusual and may be related to a stronger relative compression of the metamict portions within the crystal compared to the intact bulk structure.

The analysis of temperature dependent compressibilities is ongoing and will be presented together with the P-V data.

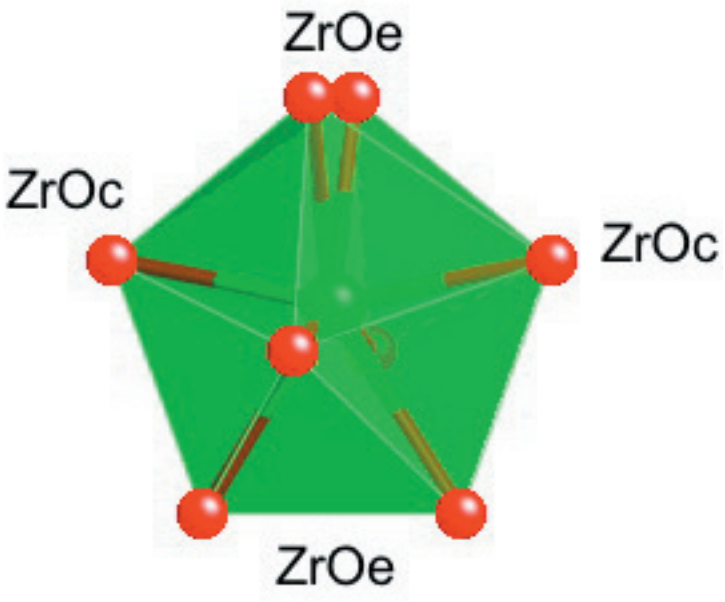

Polyedral model of the ZrO_8 coordination showing the two different Zr-O bonds.

Hazen and Finger (1979): American Mineralogist, 64, 196 – 201.
Van Westrenen et al. (2004): American Mineralogit, 89, 197 – 203.
Rios et al. (2000): Acta Crystallographica, B56, 947 – 952.
Kolesov et al. (2001): European Journal of Mineralogy, 13, 939 – 948.
Ono et al. (2004): American Mineralogist, 89, 185 – 188.
Mursic et al. (1992): Acta Crystallographica, B48, 584 – 590.

Work was partly performed on COMPRES beamline 12.2.2 at the ALS

Effect of X- and Z-site Substitutions on the High-Pressure Phase Transition in Hydrogarnet

George A. Lager, Jianrong Chen *Department of Geography and Geosciences, University of Louisville, Louisville, KY*
Zhenxian Liu *Geophysical Laboratory, Carnegie Institution of Washington, Washington D.C.*
Peter Ulmer *Institute for Mineralogy and Petrography, Swiss Federal Institute of Technology, CH-8092 Zurich, Switzerland*

High-pressure mid-infrared (IR) spectra of synthetic Sr-hydrogarnet [$Sr_3Al_2(O_4H_4)_3$] (Sr_3A) and Ca-hydrogarnet with 50% grossular component [$Ca_3Al_2(SiO_4)_{1.5}(O_4H_4)_{1.5}$] ($C_3ASi$) were collected at the U2A beam line at NSLS to determine the effect of chemical substitution on the pressure of the phase transition in hydrogarnet. It has been proposed that H-H repulsion due to the compression of H-H distances may initiate the phase transition in katoite [$Ca_3Al_2(O_4H_4)_3$] (C_3A) at 5 GPa (Lager et al. 2002). Previous experiments at the U2A beam line have shown that IR spectroscopy is very sensitive to the transition, i.e., a sharp discontinuity in OH frequency occurs at 5 GPa in C_3A (Lager et al. 2005). IR spectra collected for Sr_3A clearly show a discontinuity in vibrational frequency (3662 cm^{-1}) at ~2.5 GPa. Both OH frequencies in C_3ASi also show a significant change in slope (from positive to negative) at ~6 GPa. However, based on these results, it is not possible to determine if H-H repulsion is the driving force of the transitions. The instability of the hydrogarnet structure could also be related to a size misfit between the X-site cation and the dodecahedral cavity, i.e., the H atoms play a passive role in the transition. The nature of these transitions is being examined in more detail using both far-IR and single-crystal X-ray data.

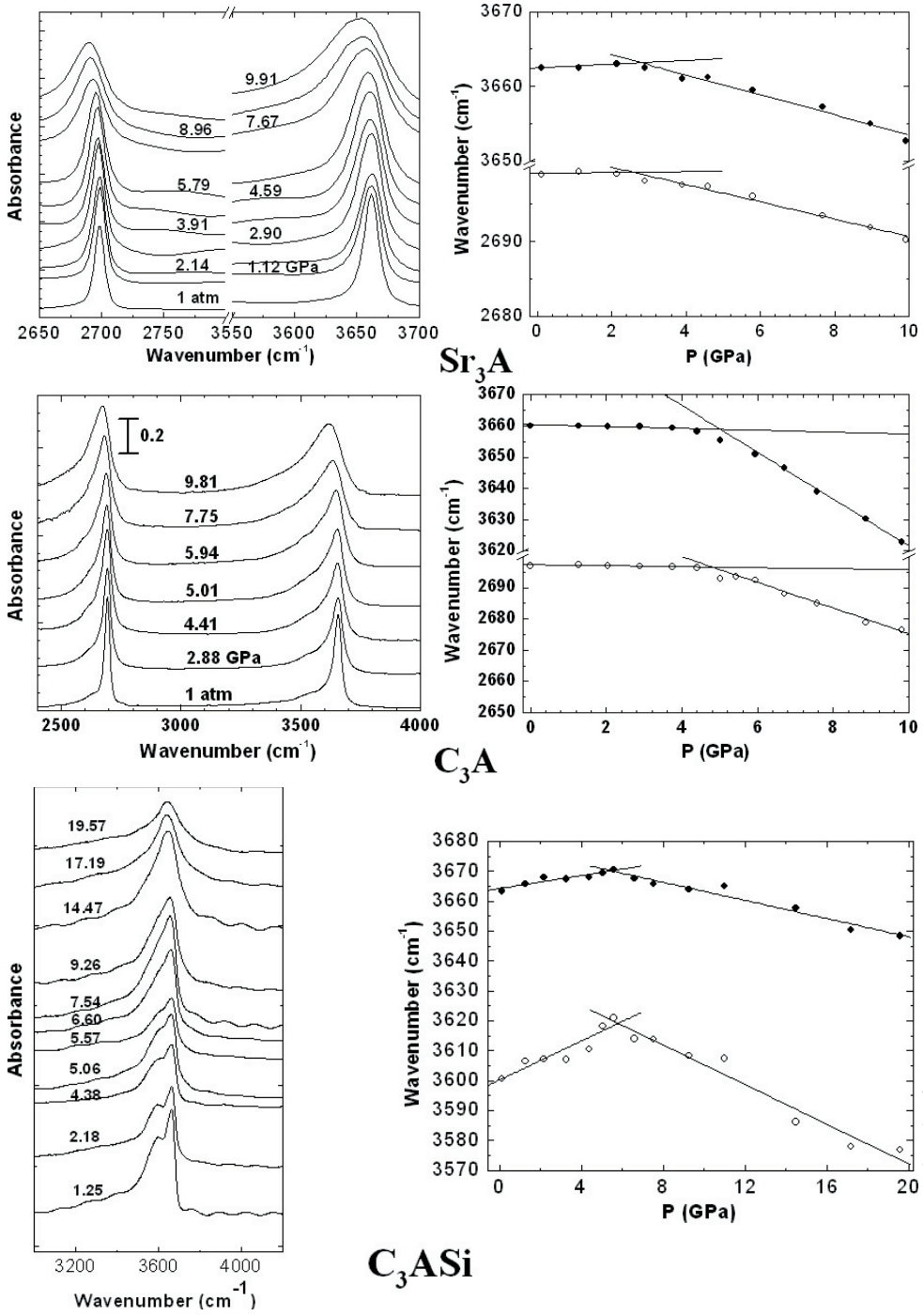

Pressure dependence of synchrotron infrared spectra and OH/OD stretching frequencies of Sr_3A, C_3A (Lager et al. 2005) and C_3ASi. KBr was used as a pressure-transmitting medium. Note the pressure of the discontinuity in O-H/O-D frequency which increases in the order $Sr_3A < C_3A < C_3ASi$. Sr_3A and C_3A are partially deuterated.

Lager, G.A., Downs, R.T., Origlieri, M., and Garoutte, R. (2002) High-pressure single-crystal X-ray diffraction study of katoite hydrogarnet: Evidence for a phase transition from *Ia3d* to *I-43d* symmetry at 5 GPa. *American Mineralogist*, 87, 642-647.

Lager, G.A., Marshall, W.G., Liu, Z., and Downs, R.T. (2005) Re-examination of the hydrogarnet structure at high pressure using neutron powder diffraction and infrared spectroscopy. *American Mineralogist*, 90, 639-644.

This research was supported by the National Science Foundation through grant EAR-0337534 to GAL.

Effect of Al^{3+} and H^+ on the Elastic Properties of Stishovite.

Dmitry L. Lakshtanov1, Konstantin D. Litasov2, Stanislav V. Sinogeikin1,*, Holger Hellwig1, Eiji Ohtani2 , Jie Li, and Jay D. Bass1

1 Department of Geology, University of Illinois at Urbana-Champaign, 1301 W Green St, Urbana, IL 61801, USA
2 Institute of Mineralogy, Petrology and Economic Geology, Tohoku University, Aza Aoba Aramaki, Sendai 980-8578, Japan
** Now at: Argonne Natl Lab, Adv Photon Source, HPCAT Carnegie Inst Washington, Argonne, IL*

X-ray diffraction, Brillouin, and Raman scattering measurements were performed on Al^{3+} and H^+-bearing stishovite at ambient conditions. Samples with different Al^{3+} and H^+ contents were used to examine the effects of these minor constituents on the density, acoustic velocities, single- and aggregate elastic moduli. The X-ray and compositional data show that the incorporation mechanism of Al^{3+} into stishovite likely involves the formation of oxygen vacancies, in addition to the incorporation H^+ in the structure. Our data show an overall linear decrease of the acoustic velocities, single crystal (C_{ij}) and aggregate (Ko, Go) elastic moduli as a function of Al^{+3} concentrations. For the sample of stishovite containing 6.07(5)wt% Al_2O_3 and 0.24(2)wt% H_2O we obtained: zero-pressure adiabatic bulk modulus, K_{S0} = 290(3) GPa, shear modulus, G_{S0} = 207(X) with the calculated density of ρ = 4.16(1). Stishovite, containing 4.37(12)wt% Al_2O_3 and 0.29(3)wt% H_2O possess higher aggregate moduli: K_{S0} = 296(3) GPa, shear modulus, G_{S0} = 213(X) with the calculated density of ρ = 4.21(1). We conclude that our data are showing the combined effects of H^+ and oxygen vacancies on elastic properties, thus explaining why the elastic properties scale with Al content rather than the H^+ content.

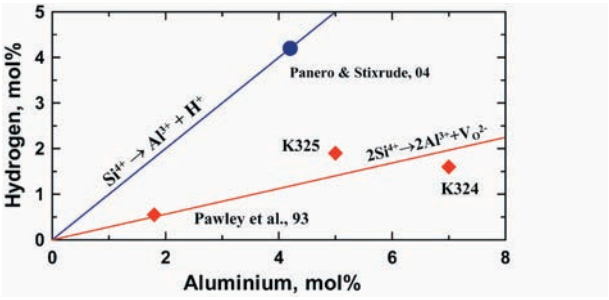

Incorporation of H^+ as a function of Al^{3+} content. Errors are smaller than symbol size

Raman modes as a function of unit cell volume of stishovite. Value of 46.51/cm³ corresponds to pure stishovite at ambient pressure (Weidner et al., 1982). Errors are smaller than symbol size.

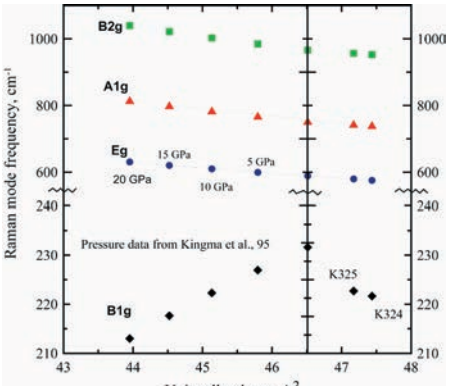

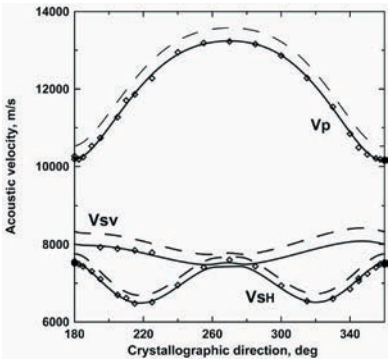

Acoustic velocities of K324 Al^{3+},H^+ -bearing stishovite (-0.982, 0.0866, 0.168). Diamonds – experimental points; broken line – velocities from pure stishovite C_{ij} (Weidner et al., 1982); solid line – velocities from measured C_{ij} (this work). Errors are smaller than symbol size.

Single-crystal elastic moduli (C_{ij}) as a function of density. Symbols – C_{ij} (high-pressure data from Carpenter et al (2000); K324, K325 – this work)
Value of 4.29g/cm³ corresponds to pure stishovite at ambient pressure (Weidner et al., 1982). Errors are smaller than symbol size.

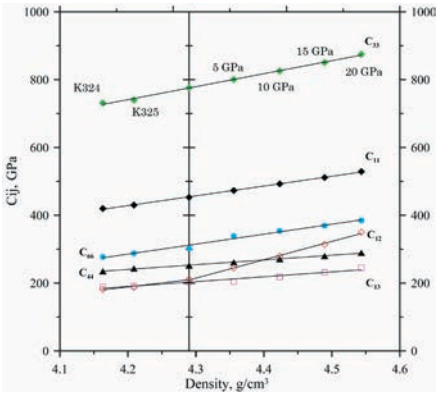

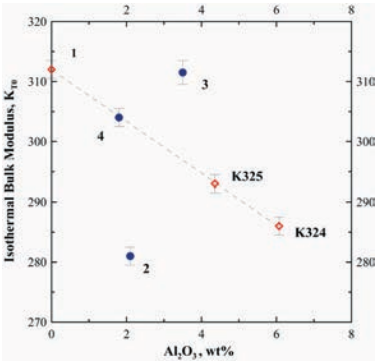

Isothermal bulk modulus (K_{T0}) as a function of Al_2O_3 content.

Diamonds: – converted from Ks, 1 – Weidner et al., 1982.

Circles: 2 - Ono et al., 2002; 3 – Panero and Stixrude, 2004; 4 – Lakshtanov et al, 2005;

Aggregate acoustic velocities as a function of Al^{3+} content. Errors are smaller than symbol size.

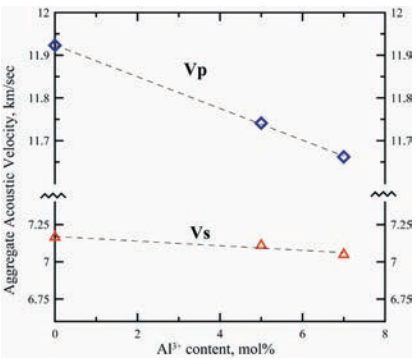

High-pressure alloying of iron and xenon: 'Missing' Xe in the Earth's core?

Kanani K. M. Lee *California Institute of Technology* **Gerd Steinle-Neumann** *Bayerisches Geoinstitut, Universität Bayreuth*

Ab-initio quantum mechanical calculations show that xenon (Xe) can be alloyed with hexagonal close-packed (hcp) iron (Fe) at high pressure through substitutional incorporation, with a favorable enthalpy of formation for the alloy relative to the elemental solids, suggesting that Xe is soluble in the Earth's iron-rich core (up to ~0.8 mol%). This alloying behavior and the possible presence of a significant amount of Xe in the core, are important for understanding the accretion and evolution of the Earth and its atmosphere.

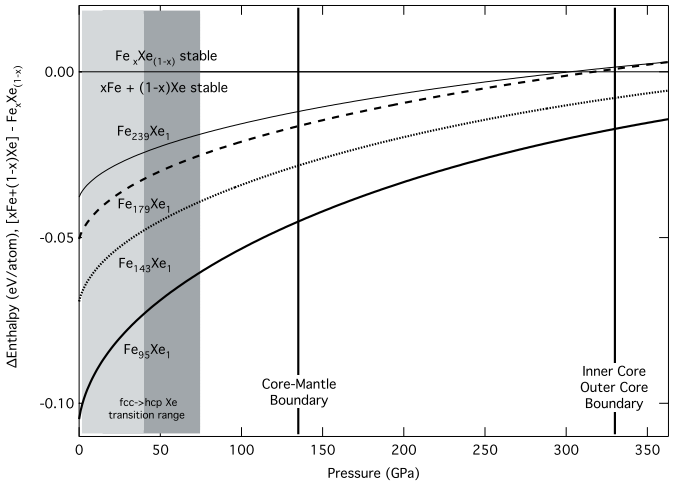

Difference in enthalpy of pure elements Fe and Xe compared to Fe-Xe alloy versus pressure: xFe + (1-x)Xe $\Leftrightarrow Fe_xXe_{(1-x)}$ where x is a value between 0.9896-0.9958 (96-240 -atom supercells). Curves are labeled for different Xe concentrations: $Fe_{0.9958}Xe_{0.0042}$ ($Fe_{239}Xe_1$, ~9,700 ppm, thin); $Fe_{0.9944}Xe_{0.0056}$ ($Fe_{179}Xe_1$, ~13,000 ppm, dashed); $Fe_{0.9931}Xe_{0.0069}$ ($Fe_{143}Xe_1$, ~16,000 ppm, dotted); and $Fe_{0.9896}Xe_{0.0104}$ ($Fe_{95}Xe_1$, ~24,000 ppm, thick). For positive values, alloy is energetically favored over pure elements. Shaded area represents the Xe fcc-to-hcp phase transition region.

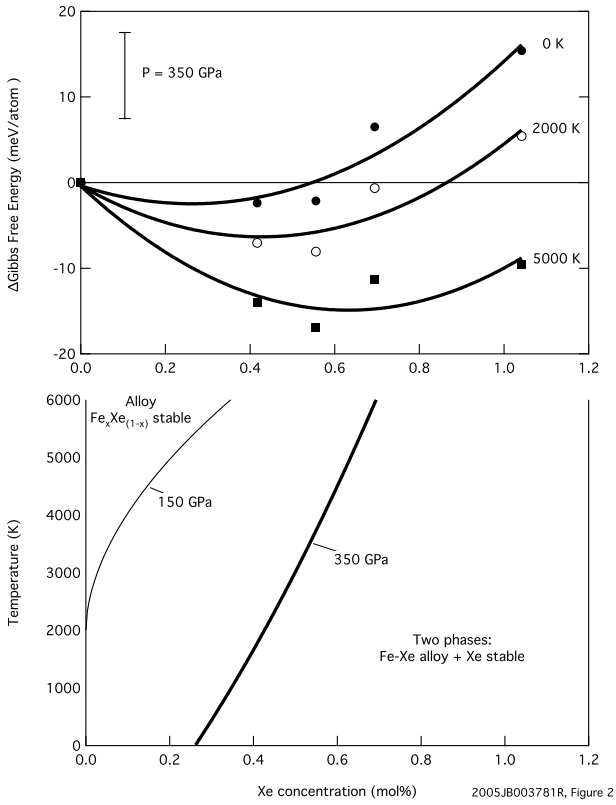

Top: Difference in Gibbs free energy of pure elements Fe and Xe compared to Fe-Xe alloy versus Xe concentration (mol%) at 350 GPa: xFe + (1-x)Xe $\Leftrightarrow Fe_xXe_{(1-x)}$ where x is a value between 0.9896-1.000 at 0 K (solid circles), 2000 K (open circles) and 5000 K (solid squares). Curves through data are third-order polynomial fits used to construct the phase diagram. Representative error bar for energy convergence uncertainty is shown (± ~5 meV).

Bottom: Fe-Xe alloy phase diagram of temperature versus Xe concentration. Thick curve delineates the stability boundary between Fe-Xe alloy and two-phase space at 350 GPa. The boundary at 150 GPa (thin curve) is also included.

Lee, K. K. M., and G. Steinle-Neumann (2006), High-pressure alloying of iron and xenon: "Missing" Xe in the Earth's core?, J. *Geophys. Res*., 111, B02202, doi:10.1029/2005JB003781.

This work was supported by the O. K. Earl postdoctoral fellowship, the Bayerisches Geoinstitut and the Alexander von Humboldt Foundation.

Simultaneous Equation of State, Pressure Calibration and Sound Velocity Measurements to Lower Mantle Pressures

Baosheng Li, Jennifer Kung *Mineral Physics Institute and Department of Geosciences, Stony Brook University,T*. **Uchida, Yanbin Wang** *Center for Advanced Radiation Sources, The University of Chicago*

Multiple techniques for measuring acoustic travel times using ultrasonic interferometry, sample unit-cell volume using X-ray diffraction, and specimen length using X-radiography were adapted simultaneously to a double-stage, large-volume high pressure apparatus (Li et al., 2004), allowing measurements of acoustic velocities under high pressure and temperature. Combined analysis of the ultrasonic velocities and density data enables us to determine elastic properties and their pressure derivatives independent of pressure up to lower mantle conditions. Furthermore, sample pressure can be directly calculated using the measured velocity and density data and finite-strain equations of state and compared with those obtained from a pressure standard adjacent to the sample, providing a means to calibrate the pressure scales currently in use. Complete experimental procedures and data analysis are demonstrated using data on a polycrystalline wadsleyite sample to 20 GPa. It is possible now to directly measure sound velocities of mantle minerals at lower mantle pressures with precise pressure determination and study the composition of the Earth's interior.

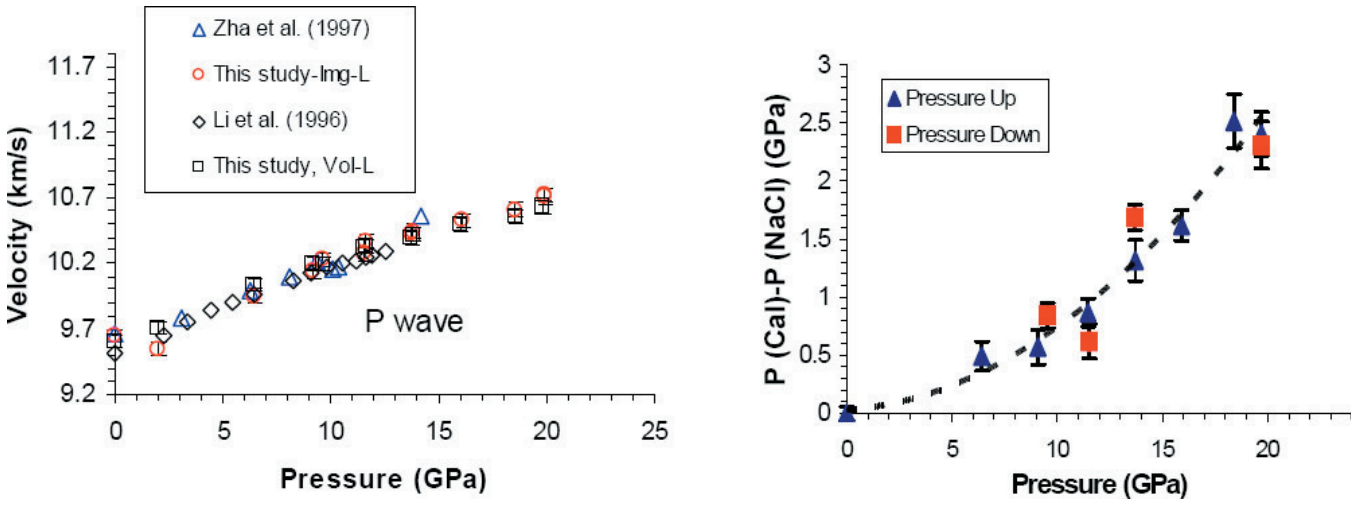

Comparison of P wave velocities with previous results (left) and the difference between absolute pressures obtained on sample and those inferred from secondary pressure standard NaCl in the present study (right).

Zha, C-S, Duffy, T.S., Downs, R.T., Mao, H-K., Hemley R.J., Weidner, D. J., 1998b. Single-crystal elasticity of the α and β of Mg_2SiO_4 polymorphs at high pressure, In: Manghnani, M.H., Yagi, T. (Eds), *Properties of Earth and Planetary Materials at High Pressure and Temperature*. American Geophysical Union, Washington, DC, pp. 9-16.

Li., B., Kung, J., Liebermann, R.C., 2004. Modern techniques in measuring elasticity of Earth materials at high pressure and high temperature using ultrasonic interferometry in conjunction with synchrotron X-radiation in multi-anvil apparatus, *Phys. Earth Planet. Interi.*, 143-144, 559-574.

This work is supported by NSF grant: EAR000135550. The experiments are conducted at COMPRES supported beamlines at NSLS(X17B2) and GSECARS (13-ID-D)/APS.

Pressure and temperature dependence of elastic wave velocity of $MgSiO_3$ perovskite and the composition of the lower mantle

Baosheng Li *Mineral Physics Institute, SUNY Stony Brook,* **Jianzhong Zhang** *LANSCE Division, Los Alamos National Laboratory*

Simultaneous measurements of compressional (P) and shear (S) wave velocities and unit cell volume (density) have been conducted on $MgSiO_3$ perovskite to 9.2 GPa and 873K using ultrasonic interferometry in conjunction with X-ray diffraction (e.g., Liebermann and Li, 1998). Finite strain analysis of current data allowed us to determine the elastic moduli and their pressure derivatives independent of the pressure measurement. The results are KS=253(2) GPa, G=173(1) GPa, $\partial KS/\partial P$=4.4(1), and $\partial G/\partial P$=2.0(1). The temperature derivatives of the bulk and shear moduli were tightly constrained from acoustic velocity measurements, yielding $\partial KS/\partial T$=-0.021(2) GPa/K and $\partial G/\partial T$=-0.028(2) GPa/K. P and S wave velocities and density profiles for a pyrolite compositional model consisting of magnesium silicate perovskite and magnesiowustite are calculated at lower mantle depths along a 1600K adiabatic geotherm, the results agree with those of seismic model PREM within 0.5%, 0.5% and 0.3%, respectively, from 800 to ~2600km. Simultaneous constraints from P and S wave velocities and density support for a homogeneous lower mantle with pyrolitic composition.

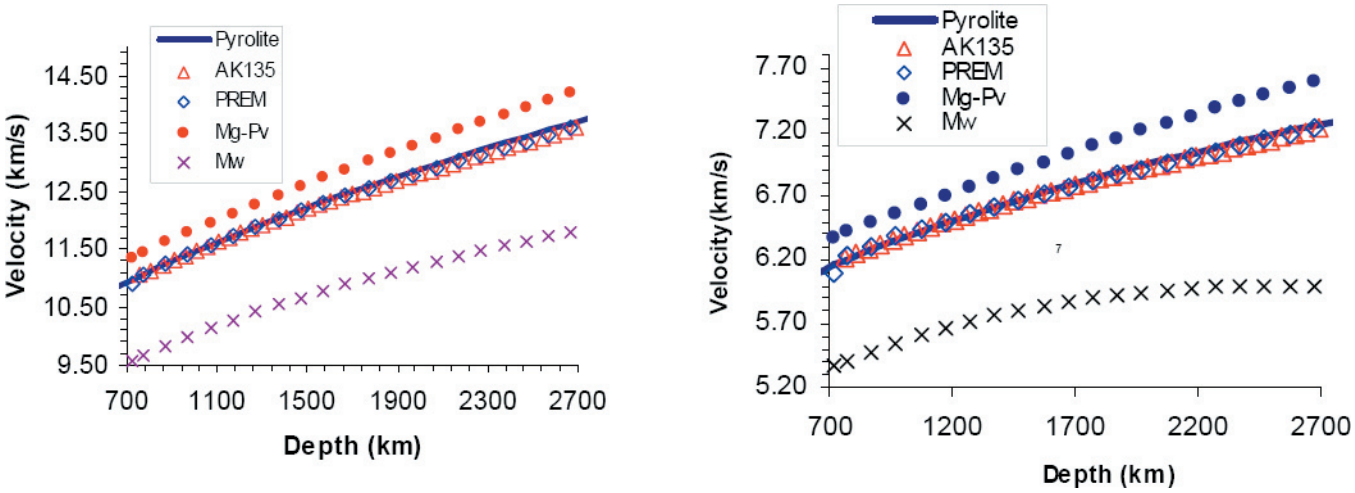

Comparison of P (left) and S (right) wave velocities of pyrolite (line) along 1600K adiabat with seismic models PREM and AK135 as a function of depth.

Liebermann, R.C. and Li, B., 1998. Elasticity at high pressures and temperatures. In: R. Hemley (Editor), *Ultrahigh-Pressure Mineralogy: Physics and Chemistry of the Earth's Deep Interior*. 37, 459-492.

This work is supported by NSF grant EAR000135550 to BL. The experiments are conducted at COMPRES supported beamline X17B2 at NSLS.

Electronic Spin State of Iron in Lower Mantle Perovskite

Jie Li *Carnegie Institution of Washington, University of Illinois,* **Viktor V. Struzhkin, Ho-kwang Mao, Jinfu Shu, Russell J. Hemley, Yingwei Fei, Bjorn Mysen, Przemek Dera** *Carnegie Institution of Washington,* **Vitali Prakapenka, Guoyin Shen** *University of Chicago*

The electronic spin state of iron in lower mantle perovskite is one of the fundamental parameters that governs the physics and chemistry of the most voluminous and massive shell in the Earth. We present first experimental evidence for spin-pairing transition in aluminum-bearing silicate perovskite $(Mg,Fe)(Si,Al)O_3$ under the lower mantle pressures. Our results demonstrate that as pressure increases, iron in perovskite transforms gradually from the initial high-spin state towards the final low-spin state. At 100 GPa, both the aluminum-free and aluminum-bearing samples exhibit a mixed spin state. The residual magnetic moment in the aluminum-bearing perovskite is significantly higher than that in its aluminum-free counterpart. The observed spin evolution with pressure can be explained by the presence of multiple iron species and the occurrence of partial spin-paring transitions in the perovskite. Pressure-induced spin-pairing transitions in the perovskite would have important bearing on the magnetic, thermoelastic, and transport properties of the lower mantle, and on the distribution of iron in the Earth's interior.

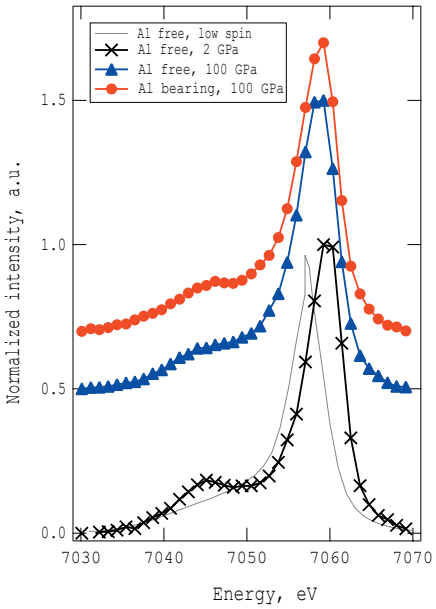

X-ray emission spectra of two perovskite samples at 100 GPa compared to the reference low-spin spectrum of an Al-free perovskite.

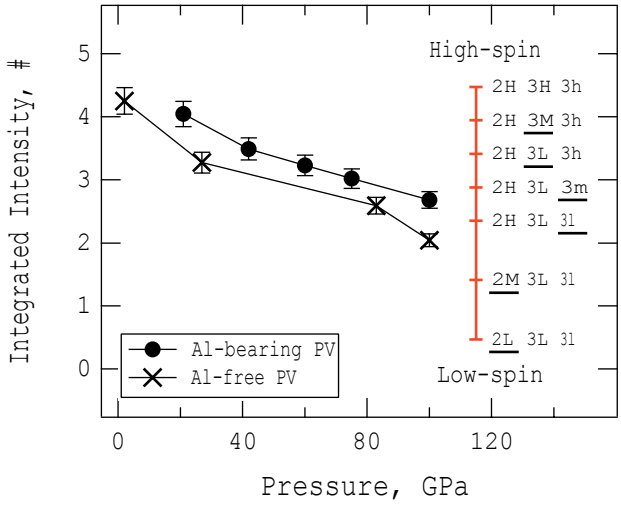

Integrated intensities of the satellite peak as a function of pressure. Vertical lines with bars are the expected intensities for the Al-bearing perovskite, based on the apparent numbers of unpaired electrons.

Reference: Li J, Struzhkin VV, Mao H-K, Shu J, Hemley RJ, Fei Y, Mysen B, Dera P, Prakapenka V, Shen G (2004) Electronic spin state of iron in lower mantle perovskite. *Proceedings of National Academy of Science* 101(39):14027-14030

We acknowledge the use of GeoSoilEnviroCARS and High Pressure Collaborative Access Team facilities at the Advanced Photon Source, Argonne National Laboratory. This work was supported by DOE-BES, DOE-NNSA through the Carnegie-DOE Alliance Center, NSF EAR-01-6009, DOD-TACOM, and W. M. Keck Foundation. V.V.S. acknowledges financial support from DOE. We thank Don Anderson, Chi-Chang Kao, Boris Kiefer, Ronald Cohen, Jennifer Jackson, Wolfgang Sturhahn, and Holger Hellwig for stimulating discussions and valuable comments.

Deformation of olivine at mantle pressure using the D-DIA

Li Li[1,2]*, Donald Weidner[1,2], Paul Raterron[2], Jiuhua Chen[1], Michael Vaughan[1], Shenghua Mei[3], Bill Durham[3]

1. Mineral Physics Institute, Department of Geosciences, State University of New York at Stony Brook, Stony Brook, NY, 11794-2100, USA.
2. Laboratoire de Structure et Propriétés de l'État Solide (associated to CNRS), Université des Sciences et Technologies de Lille, F-59655, Villeneuve d'Ascq Cedex, France.
3. Lawrence Livermore National Laboratory, Livermore, CA 94550

Knowledge of the rheological properties of mantle materials is critical in modeling the dynamics of the Earth. The high-temperature flow law of olivine defined at mantle conditions is especially important since the pressure dependence of rheology may affect our estimation of the strength of olivine in the Earth's interior. In this study, steady-state high-temperature (up to 1473 K) deformation experiments of polycrystalline olivine (average grain size ≤ 10 μm) at pressure up to 9.6 GPa, were conducted using a Deformation-DIA (D-DIA) high-pressure apparatus and synchrotron X-ray radiation. The oxygen fugacity (f_{O2}) during the runs was in-between the iron-wustite and the Ni/NiO buffers' f_{O2}. The water content of the polycrystalline samples was generally about 150 – 200 wt. ppm but was as low as 35 wt ppm. Typically, 30 % strain was generated during the uniaxial compression. Sample lengths during the deformation process as well as the differential stresses were monitored in situ by X-ray radiography and diffraction, respectively. The strain rate was derived with an accuracy of 10^{-6} s^{-1}. Differential stress was measured at constant strain rate (~ 10^{-5} s^{-1}) using a multi-element solid-state detector combined with a conical slit. Recovered specimens were investigated by optical and transmission electron microscopy (TEM). TEM shows that dislocation glide was the dominant deformation mechanism throughout the experiment. Evidence of dislocation climb and cross-slip as active mechanisms are also reported. Deformation data show little or no dependence of the dislocation creep flow with pressure, yielding to an activation volume V* of 0 ± 5 cm^3/mol. These new data are consistent with the high-temperature rheological laws at lower pressures, as reported previously.

Li, L., D. Weidner, P. Raterron, J. Chen, M. Vaughan, S. Mei, and W. Durham, Deformation of olivine at mantle pressure using D-DIA, *European Journal of Mineralogy*, 18, 7-19, 2006.

This research was carried out in part at NSLS, which is supported by the U. S. Department of Energy, Division of Material Sciences and Division of Chemical Sciences under contract No. DE-AC02_98CH10886 and COMPRES for support of the beam lines X17 and U2A (EAR0135554). This research was supported by the NSF Grant EAR-9909266, EAR0135551, and EAR0229260 and the Centre National de la Recherche Scientifique, CNRS/INSU Grants "DyETi 2003" and "DyETi 2004". MPI publication No. 340.
Beamline: X17B2 and U2A

Plastic flow of pyrope at mantle pressure and temperature

Li Li[1,2*], Paul Raterron[2], Donald Weidner[1,2]

1. Mineral Physics Institute, Department of Geosciences, State University of New York at Stony Brook, Stony Brook, NY, 11794-2100, USA.
2. Laboratoire de Structure et Propriétés de l'État Solide (associated to CNRS), Université des Sciences et Technologies de Lille, F-59655, Villeneuve d'Ascq Cedex, France.

Despite the abundance of garnet in deforming regions of the Earth such as subduction zones, its rheological properties are not well defined by laboratory measurements. Here we report measurements of steady-state plastic properties of pyrope in its stability field (temperature up to 1573 K, pressure up to 6.8 GPa, strain rate ~10^{-5} s^{-1}) using a Deformation-DIA apparatus (D-DIA) coupled with synchrotron radiation. Synthetic pyrope (Py100) and natural pyrope ($Py_{70}Alm_{16}Gr_{14}$) are both studied in a dry environment. Transmission electron microscopy (TEM) investigation of the run products indicates that dislocation glide, assisted by climb within grains and dynamic recrystallization for grain-boundary accommodation, is the dominant deformation process in pyrope. Both synthetic-and natural-pyropes' stress and strain-rate data, as measured in situ by X-ray diffraction and imaging, are best fitted with the single flow law:

$$\dot{\varepsilon}(s^{-1}) = 3.5\begin{pmatrix}+4.8\\-2.0\end{pmatrix}\times 10^{6}\times\sigma(GPa)^{(3.2\pm0.7)}\exp-\frac{(270\pm40)\times10^{3}}{RT(J/mol)}$$

where is the strain rate, $\sigma = |\sigma 1-\sigma 3|$ is the differential stress, R is the gas constant and T the absolute temperature. Forsterite and synthetic pyrope were stacked along the uniaxial compression direction in the same cell assembly during deformation in order to compare their strength at mantle condition. Forsterite is observed to be stronger than pyrope, deforming at a rate about 10% slower than the pyrope at 5.2 GPa and 1573 K. San Carlos olivine and natural pyrope were compared in a similar fashion at 6.8 GPa and 1473 K. In this case, San Carlos olivine deformed 2~3 times faster than natural pyrope. The experimental data suggest that pyrope is stronger (less than a factor of 5) than the dominant mineral (olivine) in the mantle where temperature higher than 1273 K.

Li, L., H. Long, D.J. Weidner, and P. Raterron, Plastic flow of pyrope at mantle pressure and temperature, *American Mineralogist*, 91, 517-525, 2006.

The authors thank Gabriel Gwan-mesia (Delaware State University, Delaware), Takaya Nagai (Ozaka University, Japan), and Liping Wang (Stony Brook University, New York) for kindly providing some of the materials studied here. The synthetic pyrope was made under NSF grants EAR0106528 and EAR0135431. This research was carried out in part at the NSLS, which is supported by the U.S. Department of Energy, Division of Material Sciences and Division of Chemical Sciences under contract no. DE-AC02_98CH10886, and COMPRES for support of the beam lines X17 and U2A (EAR0135554). This research was supported by the NSF grant EAR-9909266, EAR0135551, and EAR0229260 and the Centre National de la Recherche Scientifique, CNRS/INSU Grants "DyETI 2003" and "DyETI 2004". MPI publication no. 450.

Beamline: X17B2 and U2A

Phase stability of $CaSiO_3$ perovskite at high pressure and temperature: Insights from ab initio molecular dynamics

Li Li[a, b], , Donald J. Weidner[a, b], John Brodholta, Dario Alfè[a], G. David Price[a], Razvan Caracas[c] and Renata Wentzcovitch[c]

aDepartment of Earth Sciences, University College London, Gower Street, London WC1E6BT, UK
bMineral Physics Institute, Department of Geosciences, University of New York at Stony Brook, Stony Brook, NY 11790, USA
cDepartment of Chemical Engineering and Material Science, Minnesota Supercomputing Institute, University of Minnesota, Minneapolis, MN 55455, USA

We report the dynamics of the structure of $CaSiO_3$ perovskite from ab initio molecular dynamics (AIMD) calculations at high pressure (P up to 130 GPa) and high temperature (T up to 5000 K). Our calculations indicate three separate stability fields: orthorhombic, tetragonal and cubic, with the tetragonal phase dominating the pressure and temperature region between room temperature and 4000 K. These regions are defined by the stress symmetry of the AIMD calculation. The boundary between the orthorhombic and the tetragonal structures is found to have a positive Clapyron slope and is close to room temperature at low pressure. The boundary is marked by the transition from stable, constant octahedral tilts, to dynamically varying tilts that change sign with time. The calculated atom positions indicate that the orientation of the octahedra can be noted as a−a−c+ in the orthorhombic phase (T = 150 K). The magnitude of the octahedra rotation varies little over the entire P–T range at high T (1000 K and above) while, at elevated temperature, the rotation angles of the octahedra oscillate positively and negatively with time. The tetragonal structure is probably due to a shortened Si O bond distance along one axis. Calculated X-ray diffraction patterns indicate small super-lattice reflections that could result from the octahedral rotations throughout the P, T region investigated. The small spontaneous strain of the tetragonal phase relative to the aristotype, cubic phase, throughout conditions appropriate to the lower mantle, creates the possibility for seismic energy absorption (low Q) in the deep Earth.

Li, L., D.J. Weidner, J. Brodholt, D. Alfè, G.D. Price, R. Caracas, and R. Wentzcovitch, Phase stability of $CaSiO_3$ perovskite at high pressure and temperature: insights from ab initio molecular dynamics, *Phys Earth Planet Sci*., 155 (3-4), 260-268, 2006.

This work is support by NERC (Grant Nos. NER/T/S/2001/00855; ER/O/S/2001/01227), and computer facilities provided by NERC at University College London, and the High Performance Computing Facilities of the University of Manchester (CSAR) and the Daresbury Laboratory (HPCx). DJW acknowledges the Leverhulme Trust for support through the visiting Professor program. DJW and LL acknowledge NSF EAR-9909266, EAR0135551, EAR0135550. MPI publication 360. R. Wentzcovitch acknowlege NSF EAR-0135533 and ITR-0428774 (VLab).

Elasticity of $CaSiO_3$ perovskite at high pressure and high temperature

Li Li[a, b], Donald J. Weidner[a, b], John Brodholt[a], Dario Alfèa, G. David Price[a], Razvan Caracas[c] and Renata Wentzcovitch[c]

aDepartment of Earth Sciences, University College London, Gower Street, London WC1E6BT, UK
bMineral Physics Institute, Department of Geosciences, University of New York at Stony Brook, Stony Brook, NY 11790, USA
cDepartment of Chemical Engineering and Material Science, Minnesota Supercomputing Institute, University of Minnesota, Minneapolis, MN 55455, USA

Ab initio molecular dynamic (AIMD) simulations were performed to calculate the equation of state (EOS) of $CaSiO_3$ perovskite at mantle pressure–temperature conditions. At temperatures above 2000 K, even though the hydrostatic crystal structure is metrically tetragonal in the pressure range of 13–123 GPa, the symmetry of the elastic moduli is consistent with cubic symmetry. Our results show that elastic constants and velocities are independent of temperature at constant volume. Referenced to room pressure and 2000 K, we find: Grűneisen parameter is $\gamma(V) = \gamma_0(V/V_0)^q$ with $\gamma_0 = 1.53$ and $q = 1.02(5)$, and the Anderson Grűneisen parameter is given by $(\alpha/\alpha_0)=(V/V_0)^{\delta T}$ in which $\alpha_0 = 2.89 \times 10^{-5}\ K^{-1}$ and $\delta T = 4.09(5)$. Using the third order Birch Murnaghan equation of state to fit our data, we have for ambient P and T, $K_0 = 236.6(8)$ GPa, $K'_0=3.99(3)$, and $V_0 = 729.0(6)$ Å3. Calculated acoustic velocities show the following P–T dependence: $(\partial \ln V_P/\partial V)_{T\ or\ P} = -1.9 \times 10^{-3}$; $(\partial \ln V_S/\partial V)_{T\ or\ P} = -1.5 \times 10^{-3}$; $(\partial \ln V_\Phi/\partial V)_{T\ or\ P} = -2.4 \times 10^{-3}$; $(\partial \ln V_S/\partial \ln V_P)_{T\ or\ P} = 0.79$; $(\partial \ln V_S/\partial \ln V_\Phi)$T or P = 0.63, indicating that the variations in bulk modulus overpower the variations in shear modulus. The bulk modulus of $CaSiO_3$ perovskite is up to 10% lower than $MgSiO_3$ perovskite under lower mantle conditions. The difference diminishes with pressure and temperature. The shear modulus of $CaSiO_3$ perovskite is almost 25% lower compared with $MgSiO_3$ perovskite for shallow lower mantle pressures and temperatures and about 3% lower at the base of the lower mantle. The difference in density of these two perovskite is about 3–4% for all conditions. Both the density and bulk modulus differ from PREM by less than 2% throughout the lower mantle. The shear modulus is 10% lower at shallow depths grading to 5% by the core-mantle boundary. Thus, the seismic velocity of $CaSiO_3$ perovskite will be lower (0–6%) than PREM.

Li, L., D.J. Weidner, J. Brodholt, D. Alfè, G.D. Price, R. Caraca, and R. Wentzcovitch, Elasticity of $CaSiO_3$ perovskite at high pressure and high temperature, *Phys Earth Planet Sci*., 155 (3-4), 249-259, 2006.

This work is support by NERC (Grant Nos. NER/T/S/2001/00855; ER/O/S/2001/01227), and computer facilities provided by NERC at University College London, and the High Performance Computing Facilities of the University of Manchester (CSAR) and the Daresbury Laboratory (HPCx). DJW acknowledges the Leverhulme Trust for support through the visiting Professor program. DJW and LL acknowledge NSF EAR-9909266, EAR0135551, EAR0135550. MPI publication 360. R. Wentzcovitch acknowlege NSF EAR-0135533 and ITR-0428774 (VLab).

Electronic Spin State of Ferric Iron in Al-bearing Perovskite in the Lower Mantle

Li Li[1,2], John P. Brodholt[1], Stephen Stackhouse[1], Donald J. Weidner[1,2], Maria Alfredsson[1], G. David Price[1]

1. Department of Earth Sciences, University College London, Gower Street, London WC1E6BT, UK
2. Mineral Physics Institute, Department of Geosciences, University of New York at Stony Brook, Stony Brook, NY, 11790, USA

We investigate the effect of pressure on the electronic spin state of ferric iron on Al-bearing $MgSiO_3$-perovskite using first-principle computations. Ferric iron (6.25 mol%) and Al (6.25 mol%) substitute for Mg and Si respectively. Five substitution models on different atomic position pairs are examined. Our results show that spin state transition from high spin (HS) to low spin (LS) occurs on the Fe^{3+} ions at high pressure, while there is no stability field for the intermediate spin state. Fe^{3+} alone can be responsible for the spin state transition. The five models witness a transition pressure ranging from 97-126 GPa. Differential stress can change the pressure for the spin collapse. The lowest pressure spin state transition occurs where Al^{3+} and Fe^{3+} are in adjacent sites. These results are one explanation to the reported experimental observations that the spin transition occurs over a wide pressure range. This finding may have important implications for the dynamics and seismic signature of the lower mantle.

This work is support by NERC (Grant Nos. NER/T/S/2001/00855; NER/O/S/2001/01227), and computer facilities provided by NERC at University College London, and the High Performance Computing Facilities of the University of Manchester (CSAR) and the Daresbury Laboratory (HPCx). DJW acknowledges the Leverhulme Trust for support through the visiting Professor program. DJW and LL acknowledge NSF EAR-9909266, EAR0135551, EAR0135550.

Elasticity of (Mg, Fe)(Si, Al)O_3-perovskite at high pressure

Li Li[1,2], John P. Brodholt[1], Stephen Stackhouse[1], Donald J. Weidner[1,2], Maria Alfredsson[1], G. David Price[1]

1. Department of Earth Sciences, University College London, Gower Street, London WC1E6BT, UK
2. Mineral Physics Institute, Department of Geosciences, University of New York at Stony Brook, Stony Brook, NY, 11790, USA

We have calculated the single crystal elastic moduli (c_{ij}) for (Mg, Fe^{3+})(Si, Al)O_3 perovskite using density functional theory in order to investigate the effect of chemical variations and spin state transitions of the Fe^{3+} ions. Considering the favored coupled substitution of Mg^{2+} - Si^{4+} by Fe^{3+} - Al^{3+}, we find that the effect of ferric iron on seismic properties is comparable with the same amount of ferrous iron. Ferric iron lowers the elastic moduli relative to the Al charge-coupled substitution. Substitution of Fe^{3+} for Al^{3+}; giving rise to an Fe/Mg ratio of 6%; causes 1.8% lower longitudinal velocity and 2.5% lower shear velocity at ambient pressure and 1.1% lower longitudinal velocity and 1.8% lower shear velocity at 142 GPa. The spin state of the iron for this composition has a relatively small effect (< 0.5% variation) on both bulk modulus and shear modulus.

Li, L., J.P. Brodholt, S. Stackhouse, D.J. Weidner, M. Alfredsson, and G.D. Price, Electronic Spin State of Ferric Iron in Al-bearing Perovskite in the Lower Mantle, *Geophys. Res. Lett.*, 32, L17307, doi:10.1029/2005GL023045, 2005.

This work is support by NERC (Grant Nos. NER/T/S/2001/00855; NER/O/S/2001/01227), and computer facilities provided by NERC at University College London, and the High Performance Computing Facilities of the University of Manchester (CSAR) and the Daresbury Laboratory (HPCx). DJW acknowledges the Leverhulme Trust for support through the visiting Professor program. DJW and LL acknowledge NSF EAR-9909266, EAR0135551, EAR0135550.

Elasticity of Mg_2SiO_4 ringwoodite at mantle conditions

Li Li[1,2], Donald J. Weidner[1,2], John Brodholt[1], Dario Alfè[1], G. David Price[1]

1. Department of Earth Sciences, University College London, Gower Street, London WC1E6BT, UK
2. Mineral Physics Institute, Department of Geosciences, University of New York at Stony Brook, Stony Brook, NY, 11790, USA

The themoelastic properties of Mg_2SiO_4 ringwoodite at mantle pressure and temperature conditions are reported based on ab initio molecular dynamic simulations. A third-order Birch-Murnaghan equation at a reference temperature of 2000K is defined by K_0 = 138 GPa, K_0' = 5.2, and V_0(2000K) = 560.3 Å^3. The Grűneisen parameter is determined to be $\gamma(V) = \gamma_0(V/V_0(298K))^q$ with γ_0 = 1.22 and q = 1.44(5), with V_0(298K) = 524.56 Å^3. The thermal expansion is determined to be $(\alpha/\alpha_0) = (V/V_0(298K))\delta_T$ in which $\alpha_0 = 2.74 \times 10^{-5}$ K^{-1} and δ_T = 5.2 (1). The bulk modulus is temperature independent at constant volume, while the shear moduli vary with temperature at constant volume. Elastic anisotropy decreases with both pressure and temperature becoming isotropic by the bottom of the upper mantle.

reference: Li, L., D.J. Weidner, J. Brodholt, D. Alfè, and G.D. Price, Elasticity of Mg_2SiO_4 ringwoodite at mantle conditions, *Physics of the Earth and Planetary Interior*, in press, 2006.

This work is support by NERC (Grant Nos. NER/T/S/2001/00855; NER/O/S/2001/01227), and computer facilities provided by NERC at University College London, and the High Performance Computing Facilities of the University of Manchester (CSAR) and the Daresbury Laboratory (HPCx). DJW acknowledges the Leverhulme Trust for support through the visiting Professor program. DJW and LL acknowledge NSF EAR-9909266, EAR0135551, EAR00135550.

Olivine Flow Mechanisms at 8 GPa

Li Li[1*], Paul Raterron[1,2], Donald Weidner[1], Jiuhua Chen[1]

1. Mineral Physics Institute, Department of Geosciences, State University of New York at Stony Brook, Stony Brook, NY, 11794-2100, USA.

2. Laboratoire de Structure et Propriétés de l'État Solide (associated to CNRS), Université des Sciences et Technologies de Lille, F-59655, Villeneuve d'Ascq Cedex, France.

The mechanisms responsible for high-temperature olivine deformation are investigated at a pressure of 8 GPa and temperatures up to 1780 K. San-Carlos olivine specimens of different average grain size (0.5 μm and 5 μm) were deformed simultaneously between hard-alumina pistons during relaxation experiments. These experiments are carried out in a multi-anvil high-pressure apparatus coupled with synchrotron x-ray radiation. The different grain-size specimens experienced identical P-T-stress condition at any given time. A new method for measuring strains and strain rates ($\geq 10^{-6}$ s^{-1}) of specimens at high pressure is documented. This method uses time-resolved in situ x-ray imaging and an image-analysis computation. The microstructures of run products, recovered after being quenched at different temperatures were characterized by transmission electron microscopy (TEM). We find that high-temperature olivine flow is grain-size insensitive at 8 GPa, which suggests that dislocation creep dominates olivine deformation at high pressure. This result is confirmed by the TEM investigation of our deformed specimens in which we find evidences of the activation of olivine dislocation slip-systems. Specimen microstructures are consistent with dynamic recrystallization as an assisting process in olivine deformation during the high-pressure experiments. Extrapolation of our results to the low-stress level and large grain-size expected in the mantle suggests that dislocation creep assisted by dynamic recrystallization may also dominate natural olivine deformation in the upper-mantle.

Reference: Li, L., P. Raterron, D. Weidner, and J. Chen, Olivine Flow Mechanisms at 8 GPa, *Physics of the Earth and Planetary Interior*, 138 (2), 113-129, 2003.

This research was carried out in part at the NSLS, which is supported by the U. S. Department of Energy, Division of Material Sciences and Division of Chemical Sciences under contract No. DE-AC02_98CH10886 and COMPRES for support of the beam lines X17 and U2A (EAR0135554). This research was supported by the NSF Grant EAR-9909266, EAR0135551, and EAR0229260 and the Centre National de la Recherche Scientifique (CNRS). MPI publication No. 309.

Beamline: X17B2 and U2A

Stress Measurements of Deforming Olivine at High Pressure

Li Li[1*], Donald Weidner[1], Paul Raterron[2], Jiuhua Chen[1], Michael Vaughan[1]

1. Mineral Physics Institute, Department of Geosciences, State University of New York at Stony Brook, Stony Brook, NY, 11794-2100, USA.
2. Laboratoire de Structure et Propriétés de l'État Solide (associated to CNRS), Université des Sciences et Technologies de Lille, F-59655, Villeneuve d'Ascq Cedex, France.

Rheological properties of mantle minerals are critical for understanding the dynamics of the Earth's deep interior. Due to limitations in experimental technique, previous quantitative studies of the rheological properties of mantle minerals are limited to either low pressure or low temperature. The present understanding of mantle flow is mostly inferred from the extrapolation of relatively low-pressure data to mantle high-pressure conditions. However, the effect of pressure (represented by activation volume) on the rheological properties of olivine is still controversial. Therefore, deformation experiments, carried out at mantle pressures, are necessary to understand and model mantle flow. Here we report an experimental study of plastic deformation of San Carlos olivine $(Mg, Fe)_2SiO_4$ under upper mantle conditions. Macroscopic differential stress and strain rates have been measured in situ in a large-volume high-pressure apparatus using newly developed techniques. The differential stress at high temperature and high pressure that we measured is significantly lower than that estimated by many currently accepted olivine flow laws. We document the first in situ experimental differential stress results in a multi-anvil press. Our results give direct evidence for a relatively small activation volume (less than 10^{-5} m^3/mol). This shows that the effect of pressure on dislocation creep is small.

Reference: Li, L., D. Weidner, P. Raterron, J. Chen, and M. Vaughan, Stress measurements of deforming olivine at high pressure, *Physics of the Earth and Planetary Interior*, 143-144, 357-367, 2004.

This research was carried out at the NSLS, which is supported by the U. S. Department of Energy, Division of Material Sciences and Division of Chemical Sciences under contract No. DE-AC02_98CH10886. Operations of the beam lines X17 and U2A are supported by COMPRES (EAR0135554). This research was supported by the NSF Grant EAR-9909266, EAR0135551, and EAR0229260 and the Centre National de la Recherche Scientifique (CNRS). MPI publication No. 313.

Beamline: X17B2 and U2A

X-ray Stress Analysis in Deforming Materials

Li Li[1], Donald J. Weidner[1], Jiuhua Chen[1], Michael T. Vaughan[1], Maria Davis[1], and William B. Durham[2]

1 Department of Geosciences and Mineral Physics Institute, Stony Brook University, Stony Brook NY 11794-2100
2 University of California, Lawrence Livermore National Laboratory, P.O. Box 808, Livermore CA 94550

The factors that control the stress-strain state of a polycrystal under differential stress depend on whether or not plastic deformation has occurred in the solid. If not, then the elastic properties with the constraints of the Reuss-Voigt bounds limit this relationship. If plastic deformation becomes important then the Taylor and Sachs models are relevant. These models assume that the plastic process is enabled by dislocation flow on specific lattice planes and specific burgers vectors. Then the relationship between stress and strain is controlled by the orientation of an individual grain with respect to the stress field, von Mises criteria, and the critical resolved stress on the dislocation that is necessary for flow. We use a self-consistent model to predict the flow-stress during plastic deformation of polycrystalline MgO with slip system of {110} <1$\bar{1}$0>, {111} <1$\bar{1}$0>, {100} <011> at different critical resolved shear stress ratios (CRSS) for the different slip systems. The prediction of the models is correlated with the results of X-ray diffraction measurements. Uniaxial deformation experiments on polycrystalline and single crystal MgO samples were conducted in situ using white X-ray diffraction with a multi-element detector and multi-anvil high-pressure apparatus at pressure up to 6 GPa and temperature of 500ºC. A deformation DIA (D-DIA) was used to generate pressure and control a constant deformation rate. Elastic strains and plastic strains were monitored using X-ray diffraction spectra and X-ray imaging techniques respectively. The correlation of the data and models suggests that the plastic models need to be used to describe the stress-strain observations with the presence of plasticity, while the Reuss and Voigt models are appropriate for the elastic region of deformation, before the onset of plastic deformation. The similarity of elastic strains among different lattice planes suggests that {111} slip system is the most significant slip system in MgO at high pressure and high temperature.

Reference: Li, L., D.J. Weidner, J. Chen, M.T. Vaughan, M. Davis, and W.B. Durham, X-ray strain analysis at high pressure: Effect of plastic deformation in MgO, *Journal of Applied Physics*, 95 (12), 8357-8365, 2004.

Funding was provided by the National Science Foundation grants: EAR0135551 and EAR0229260, an REU program EAR 0139436 and by the support to Beamline X17B2 through COMPRES (EAR 0135554). The research utilized facilities at the National Synchrotron Light Source of Brookhaven National Laboratory. This is MPI publication 320. Work by WBD performed under the auspices of the U. S. Department of Energy by the Lawrence Livermore National Laboratory under contract W-7405-ENG-48. We wish to thank Pam Burnley for her inspiring discussions and guidance. We also want to thank Dr. B. Clausen, of Los Alamos National Laboratory, for access to source codes of his self-consistent deformation model and for valuable insights regarding the self-consistent models.

Beamline: X17B2 and U2A

High pressure phase of $Al(OH)_3$: In situ XRD and IR measurements, and first-principles calculations

Haozhe Liu, *HPCAT, APS, Argonne, IL,* **Jingzhu Hu**, *X17C, NSLS, Brookhaven, NY,* **John S. Tse**, *University of Saskatchewan, Canada,* **Zhenxian Liu, Ho-kwang Mao**, *Geophysical Laboratory, Carnegie Institution of Washington,* **Jiuhua Chen, Don J. Weidner**, *Stony Brook University*

High pressure behavior of hydrous minerals: source of water in the mantle, role in earthquakes.
Gibbsite: one of the most abundant natural minerals in aluminum hydroxide and oxide families, and has attracted experimental and theoretical attention from mineralogical and industrial applications. Its high pressure phase was studied and structure was solved.

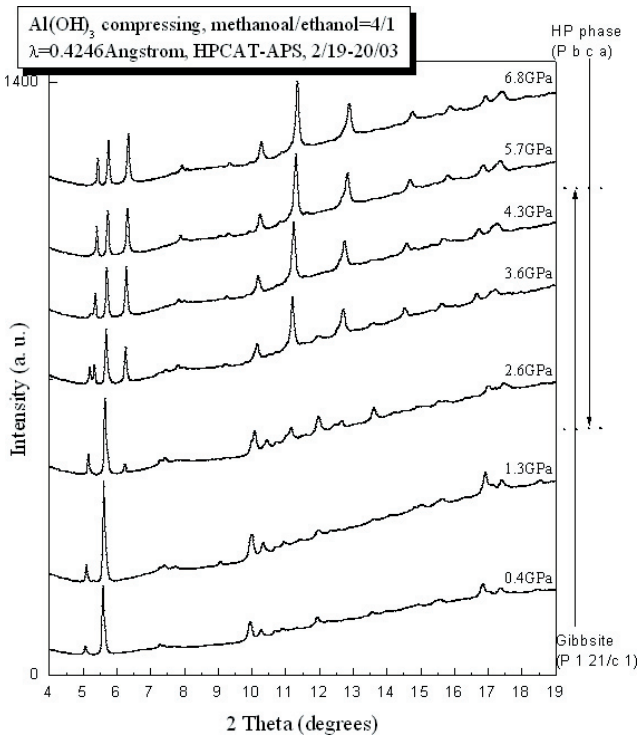

ADXRD patterns during compression procedure. Phase transition was observed at about 2.6GPa.

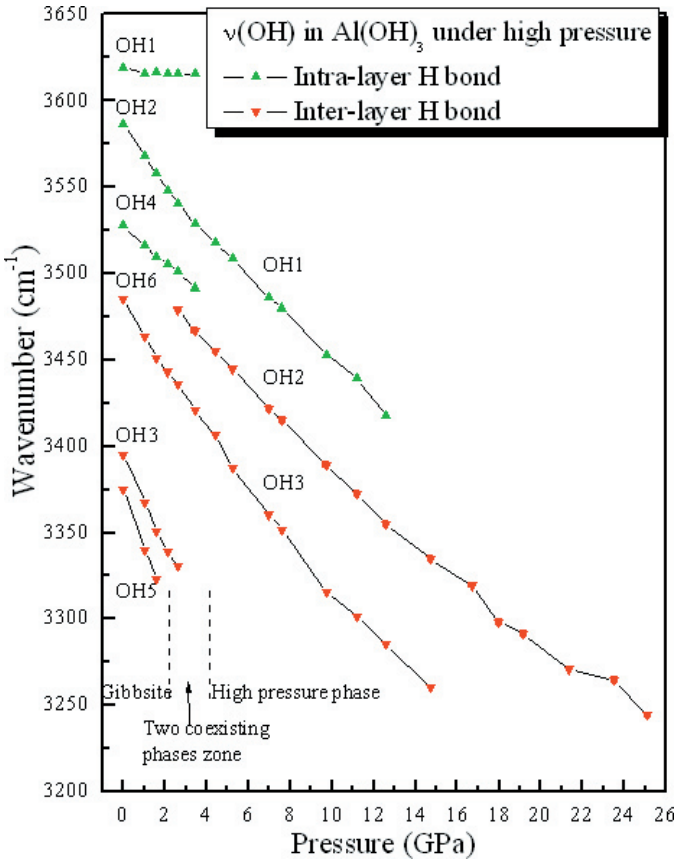

The OH stretching mode assignments for Gibbsite and the high pressure phase in IR spectra.

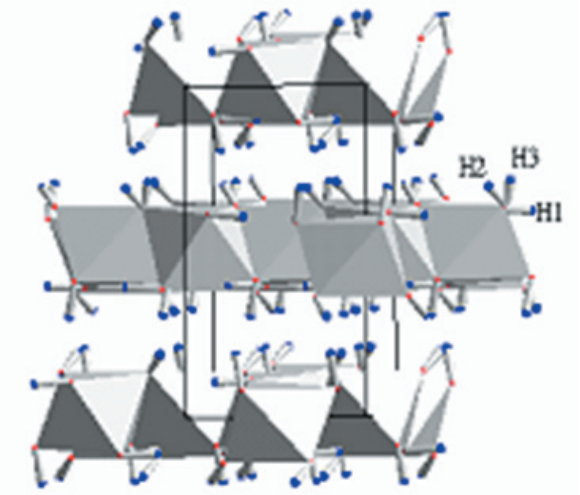

Structure of the high pressure phase, in which the hydrogen positions based on the first-principles calculations.

Haozhe Liu, John S. Tse, Jingzhu Hu, Zhenxian Liu, Luhong Wang, Jiuhua Chen, Don J. Weidner, Yue Meng, Daniel Häusermann, and Ho-kwang Mao, Structural refinement of high-pressure phase of aluminum trihydroxide: In-situ high-pressure angle dispersive synchrotron X-ray diffraction and theoretical studies, *Journal of Physical Chemistry B*, Vol. 109, No. 18, 8857-8860, 2005.

Haozhe Liu, Jingzhu Hu, Jian Xu, Zhenxian Liu, Jingfu Shu, Ho-kwang Mao, and Jiuhua Chen, Phase transition and compression behavior of gibbsite under high pressure, *Physics and Chemistry of Minerals*, Vol. 31, No. 4, 240-246, 2004.

These studies were performed at a X17C and U2A beamlines of NSLS, and ID-B station of HPCAT, APS.

$NaMgF_3$ perovskite under pressure: Octahedral tilting evolution and phase transition

Haozhe Liu, *HPCAT, APS, Argonne, IL,* **Jiuhua Chen, C. Dave Martin, Don J. Weidner,** *Stony Brook University,* **Jingzhu Hu,** *X17C, NSLS, Brookhaven, NY,* **Ho-kwang Mao**, *Geophysical Laboratory, Carnegie Institution of Washington,*

A high-pressure test of an analog for a common deep-Earth mineral may allow researchers to estimate the physical properties of materials in the planet's lower mantle. We induced pressures greater than 16 gigapascals (GPa), more than 160,000 times the normal atmospheric pressure on the Earth's surface, on a perovskite material with a similar makeup as the ubiquitous deep-mantle perovskite $MgSiO_3$ and analyzed the change in its physical makeup under the stress. We observed slight changes to its chemical bonds beginning at 6 GPa and a compression that destroyed the perovskite crystal structure at pressures approaching 20 GPa.

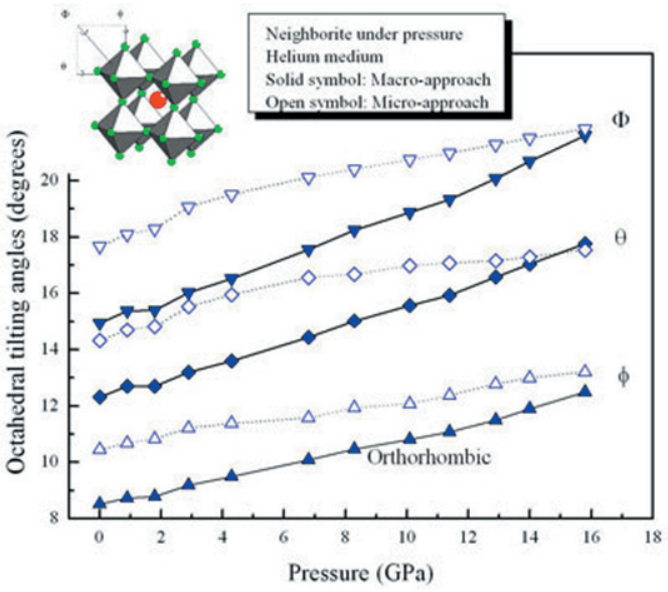

Pressure evolution of the octahedral tilting angles of $NaMgF_3$ perovskite as derived from lattice parameters (macro-approach), and atomic positions (micro-approach) plotted as solid and open symbols, respectively. Insertion shows the octahedral tilting angles referred to an ideal cubic Pm3m perovskite.

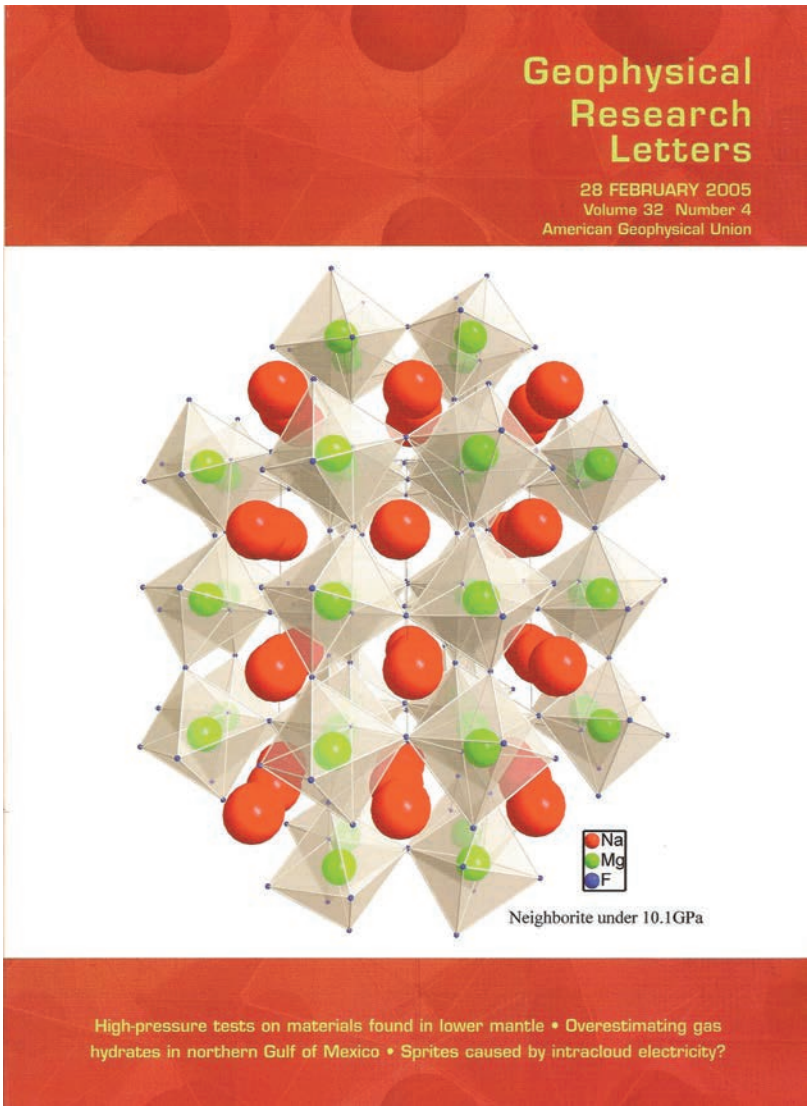

Crystalline structure of $NaMgF_3$ under pressure of 10.1GPa.

Haozhe Liu, Jiuhua Chen, Jingzhu Hu, C. Dave Martin, Don J. Weidner, Daniel Häusermann, and Ho-kwang Mao, Octahedral tilting evolution and phase transition in orthorhombic $NaMgF_3$ perovskite under pressure, *Geophysical Research Letters*, Vol. 32, No. 4, L04304, 2005.

These studies were performed at a X17C beamline of NSLS, and ID-B station of HPCAT, APS.

Synchrotron Infrared Spectroscopy of OH-Chondrodite and OH-Clinohumite at High Pressure[1]

Zhenxian Liu, Russell J. Hemley *Geophysical Laboratory, Carnegie Institution of Washington, Washington, D.C.*
George A. Lager *Department of Geography and Geosciences, University of Louisville, Louisville, KY*
Nancy L. Ross *Department of Geological Sciences, Virginia Polytechnic Institute and State University, Blacksburg, VA*

High-pressure synchrotron infrared (IR) absorption spectra were collected at ambient temperature for OH-chondrodite and OH-clinohumite up to 38 and 29 GPa, respectively, using argon as the pressure-transmitting medium. The crystal structures of both clinohumite and chondrodite are preserved up to the maximum pressure. However, disordering of the silicate framework appears to become more pronounced at high pressure based on the significant broadening of the IR bands with increasing pressure. All three OH bands in both structures shift linearly to higher frequency with pressure up to 18 GPa. Above 18 GPa, the variation of OH frequency with pressure remains linear; however, the slopes for the three OH bands are significantly different as a result of different degrees of H bonding. IR results are compared to those from recent Raman studies in which water was used as the pressure-transmitting medium.

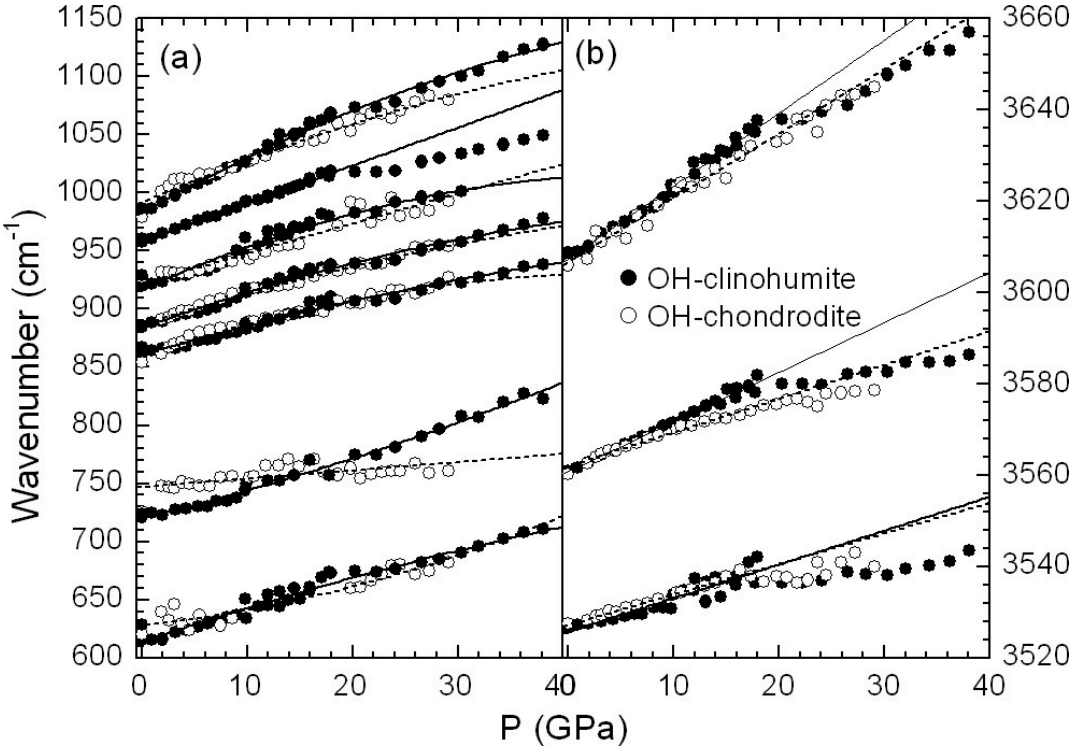

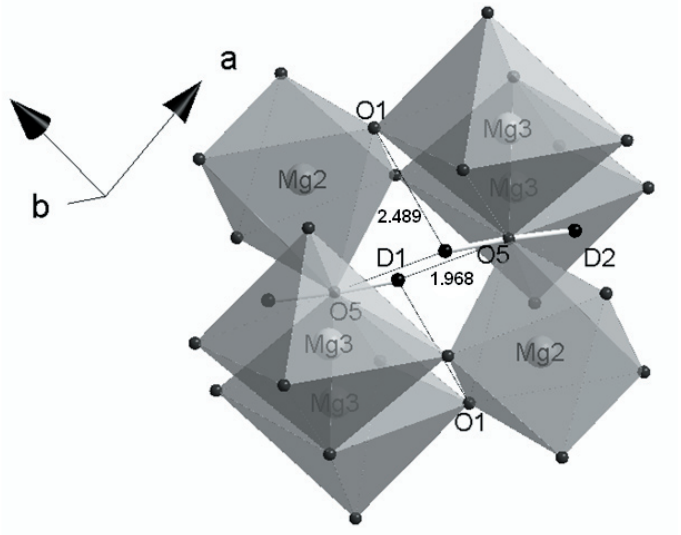

A portion of the OH(D)-chondrodite structure showing the orientation of the O-H vectors within the cavities. The two H1 sites are related by a center of symmetry and cannot be occupied simultaneously (50% occupation). When one of the H1 sites is occupied, the H2 atom is bonded to the adjacent O5 atom, i.e., the O-H vectors point in the same direction. Hydrogen bond distances D1···O5 and D1···O1 are shown on the drawing, which is based on the neutron powder diffraction data of Lager et al. (2001).

[1]Liu, Z., Lager, G.A., Hemley, R.J., and Ross, N.L. (2003) Synchrotron infrared spectroscopy of OH-chondrodite and OH-clinohumite at high pressure. *American Mineralogist*, 88, 1412-1415.
Lager, G.A., Ulmer, P., Miletich, R., and Marshall, W.G. (2001) O-D···O bond geometry in OD-chondrodite. *American Mineralogist*, 86, 176-180.

This research was supported by the National Science Foundation through grant EAR-0073734 to GAL.

Evaluating Moissonite (SiC) as a Window and Anvil for High-Pressure Infrared Spectroscopy

Z. Liu, J. Xu, *Geophysical Laboratory,* **H.P. Scott**, *Indiana U. South Bend,* **Q. Williams**, *UCSC,* **H.K. Mao and R.J. Hemley**, *Geophysical Laboratory*

The optical properties of SiC-moissonite and its performance as an anvil material for high-pressure infrared spectroscopic measurements have been examined to pressures of 53 GPa. For some frequencies, moissonite represents a less expensive and more transparent anvil material than diamond. In particular, the region between 1900 and 2300 cm^{-1} is found to be far more transparent in moissonite than in diamond, as expected from the strong characteristic phonon absorption of diamond in this region. Moissonite's utility as an infrared window also extends to frequencies associated with hydroxyl stretching vibrations. Finally, the pressure dependence of the moissonite absorption spectrum has a minimal effect on the transmissivity of SiC anvils at high pressures.

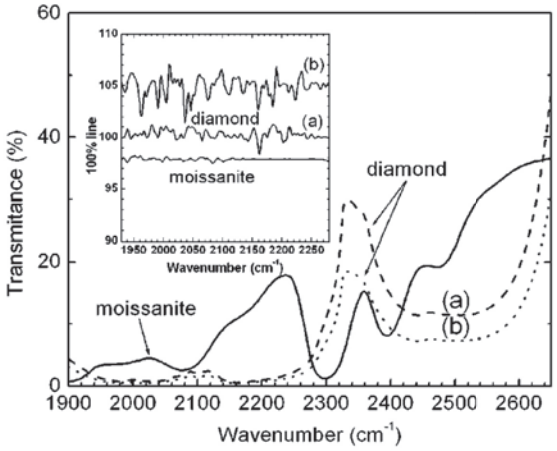

Transmission spectra of moissonite (solid lines) and type-II diamond anvils. Inset shows the signal-to-noise ratios for the different anvils.

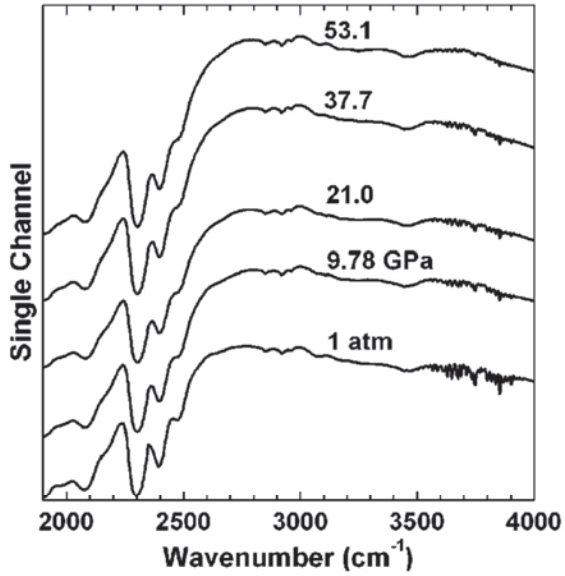

Uncorrected transmission spectra through moissonite anvils.

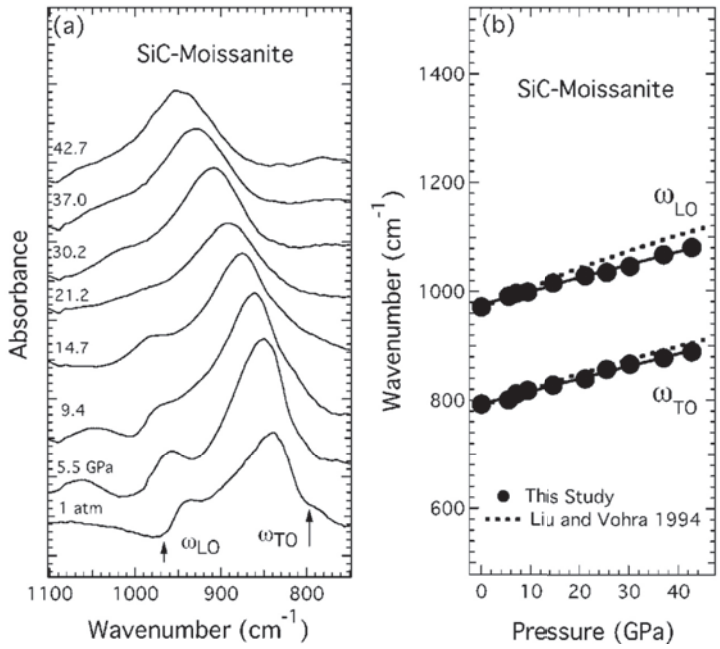

Pressure dependence of SiC phonon modes, compared with previous Raman data.

References: Liu, Z., J. Xu, H.P. Scott, Q. Williams, H.K. Mao and R.J. Hemley, Moissonite (SiC) as windows and anvils for high-pressure infrared spectroscopy, *Review of Scientific Instruments*, 75, 5026-5030, 2004.

Acknowledgment: Work supported by NSF grant EAR-0135554. This study was conducted at Beamline U2A of Brookhaven National Laboratory.

Elasticity of San Carlos Olivine to 8 GPa and 1073 K

Wei Liu, Jennifer Kung, Baosheng Li *Mineral Physics Institute, Stony Brook University, Stony Brook, NY 11794-2100*

Elasticity of San Carlos olivine, $(Mg_{0.9}, Fe_{0.1})_2SiO_4$, has been measured at simultaneous high pressure and high temperature to 8.2GPa and 1073K using ultrasonic interferometry in conjunction with synchrotron X-radiation. The elastic moduli and their pressure and temperature derivatives are precisely determined using a pressure standard free fit using third-order finite strain equations to the velocity and unit cell volume data in the entire pressure and temperature range, yielding K_{S0}=130.3(4) GPa, G_0=77.4(2) GPa, $K_{S0'}$=4.61(11), G_0'=1.61(4), $\partial KS/\partial T$=-0.0164(5) GPa/K, and $\partial G/\partial T$=-0.0130(3) GPa/K. Combined with previous thermoelastic data on wadsleyite, the velocity contrasts between α- and β-$(Mg, Fe)_2SiO_4$ at 410-km depth are calculated along a 1673K adiabatic geotherm with plausible iron partition between the two phases. The fraction of olivine consistent with a ~5% seismic discontinuity in an anhydrous mantle is constrained to be less than ~50% with the possibility that a hydrous or a cooler mantle increases the olivine content towards pyrolitic composition.

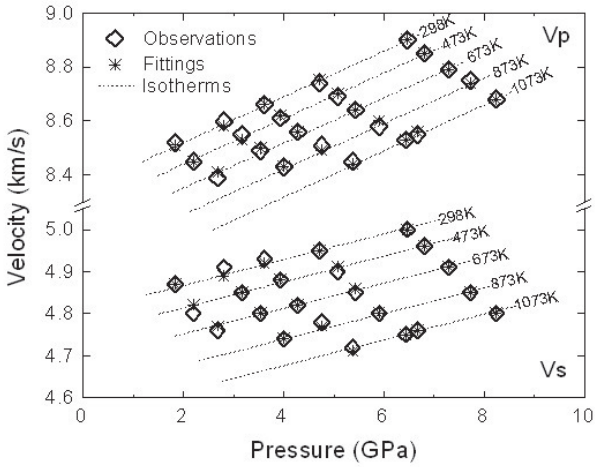

Comparison of the fitted (stars) and measured (diamonds) results of V_P and V_S as a function of pressure to 8.2GPa and temperature to 1073K. Error bars of observations are about the size of the symbols.

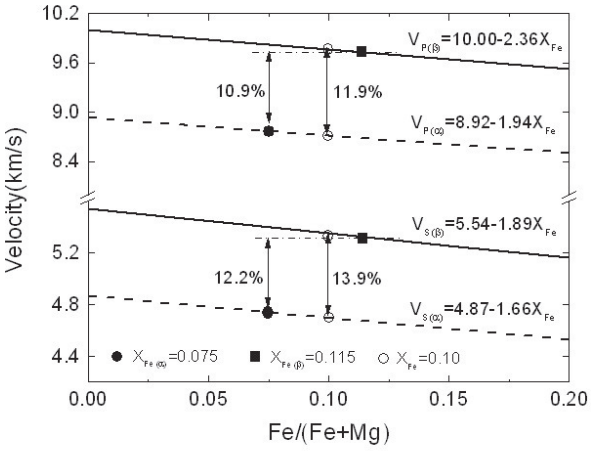

P and S wave velocities of olivine (dashed line) and wadsleyite (solid line) at the 410-km depth versus iron fraction. The iron contents in olivine (●) and in wadsleyite (■) are from the study of Irifune and Isshiki (1998).

Liu, W., J. Kung, and B. Li (2005), Elasticity of San Carlos olivine to 8 GPa and 1073 K, *Geophys. Res. Lett.*, 32, L16301, doi:10.1029/2005GL023453.

The in situ ultrasonic and X-ray experiments were carried out at the X-17B2 beamline of the National Synchrotron Light Source (NSLS) which is supported by the US Department of Energy, Division of Materials Sciences and Division of Chemical Sciences under Contract No. DE-AC02-76CH00016 and by COMPRES, the Consortium for Materials Properties Research in Earth Sciences under contract number EAR 01-35554.

Investigation on Deformation of Olivine at High Pressure and Low Temperature

Hongbo Long, Don Weidner, Li Li, Jiuhua Chen, Liping Wang *Stony Brook University*

Deep focus earthquakes reflect the rheology of the host material. Several preliminary deformation experiments of San Carlos olivine at subduction zone condition (high pressure and low temperature) have been carried out. It can be concluded that the differential stress at steady state is stable (~3 GPa) GPa relatively independent to the changes of strain rate and the temperature between 400-700°C; however, it drastically decreases to about 1 GPa and becomes temperature-dependent between 700°C and 900°C, which is similar to the results of Li et al. (2004). Further work is still needed.

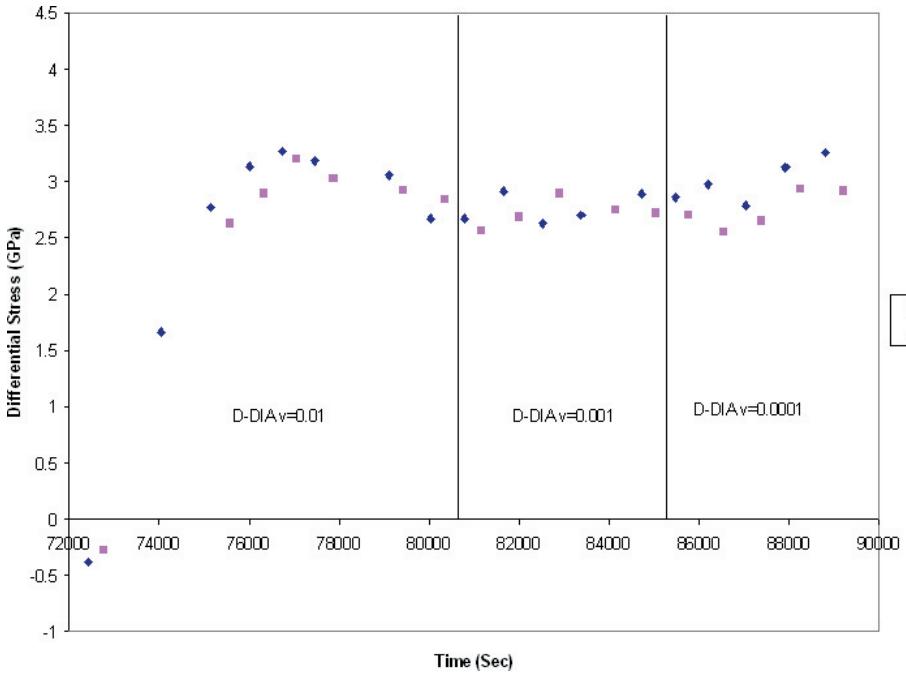

Differential stress vs. Time for deformation sample of San80 at 5 Gpa, 700C

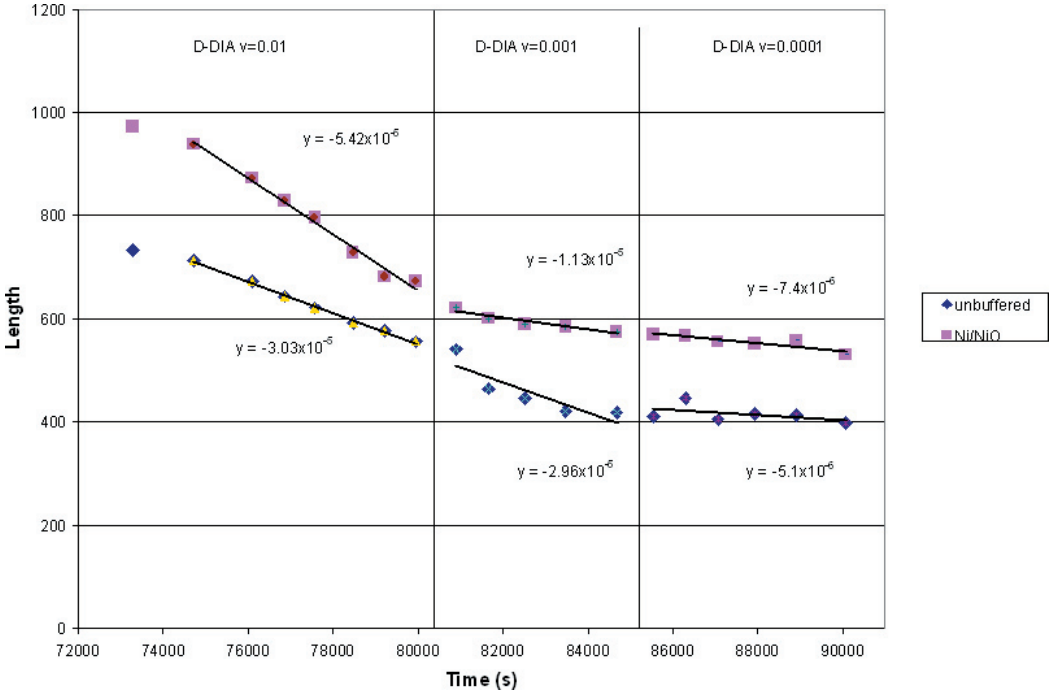

Length vs. time for deformation sample of San80 at 5GPa, 700C

This experiment is performed on the Deformation DIA apparatus at Sam85, X17B2, NSLS and is supported by the COMPRES.

Effect of shear strain on the α-ε phase transition of iron: a new approach in the rotational diamond anvil cell

Yanzhang Ma, Emre Selvi, and Valery I. Levitas
Department of Mechanical Engineering and Center for Mechanochemistry and Synthesis of New Materials, Texas Tech University, Lubbock, Texas 79409

The effect of shear strain on the iron α-ε phase transformation has been studied using a rotational diamond anvil cell (RDAC). The initial transition is observed to take place at the reduced pressure of 10.8 GPa under pressure and shear operation. Complete phase transformation was observed at 15.4 GPa. The rotation of an anvil causes limited pressure elevation and makes the pressure symmetric in the sample chamber before the phase transition. It, however, causes significant pressure increase at the center of the sample and brings about a large pressure gradient during the phase transformation. The resistance to the phase interface motion is enhanced due to strain hardening during the pressure and shear operations on iron and this further increases the transition pressure. The work of macroscopic shear stress and the work of the pressure and shear stress at the defect tips account for the pressure reduction of the iron phase transition.
Experiment was performed at X17C and X17B3, NSLS, BNL.

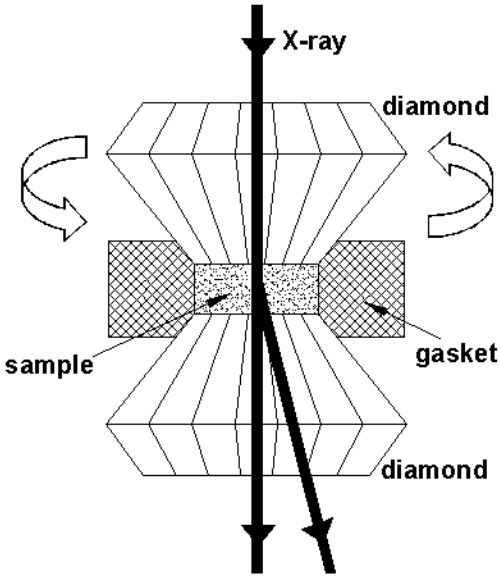

A schematic diagram of the rotational diamond anvil cell, showing the anvils, the sample chamber, and the alignment of X-ray beam for the in situ X-ray diffraction measurements.

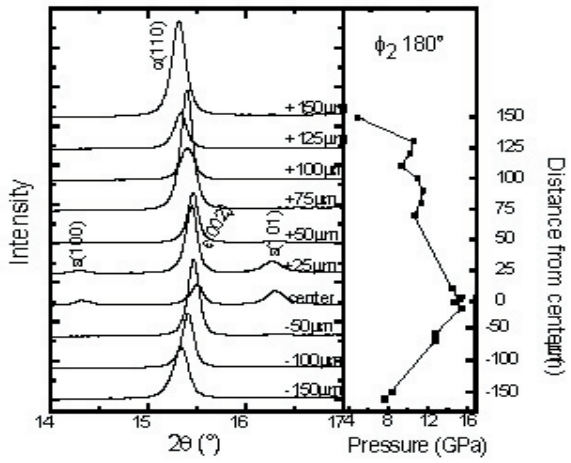

X-ray diffraction patterns after the second compression operation and rotation of 180o at different positions along the diameter of the sample plate in comparison with pressure distribution at similar positions. The values marked on the diffraction patterns indicate the distance from the center, where the diffraction was taken. The "- " and "+" signs respectively indicate the distances to the left and right side of sample center.

Hydrogen Storage in Molecular Compounds

Wendy L. Mao and Yusheng Zhao *Los Alamos National Laboratory*
Ho-kwang Mao, Viktor Struzhkin and Russell J. Hemley *Carnegie Institution of Washington*
Konstantin Lokshin *University of Tennessee*

At low temperature (T) and high pressure (P), molecular hydrogen can interact with other molecules to form crystalline compounds that may have application for energy storage. We have synthesized compounds in a number of simple molecular systems (e.g. $H_2 + H_2O$ and $H_2 + CH_4$) and found materials that contain a large amount of molecular hydrogen. Low T has allowed us to greatly expand the stability or metastability of these materials to near ambient P. We synthesized a hydrogen clathrate hydrate, $H_2(H_2O)_2$, that holds 5.3 wt% hydrogen (Mao et al., 2002). The clathrate, synthesized at 200–300 MPa and 240–249 K (Fig. 1), can be preserved to ambient P at 77 K. The stored hydrogen is released when the clathrate is warmed to 140 K at ambient P. The structure of this clathrate and the occupancy and dynamics of the molecular hydrogen clusters within different cages was studied using neutron diffraction (Fig. 2) (Lokshin et al., 2004). Low T also stabilizes other molecular compounds containing large amounts of molecular hydrogen, the stability field for $H_2(H_2O)$ filled ice (11.2 wt % molecular hydrogen) is extended from 2,300 MPa at 300 K to 600 MPa at 190 K (Mao and Mao, 2004), and that for $(H_2)_4CH_4$ (33.4 wt % molecular hydrogen) is extended from 5,000 MPa at 300 K to ambient P at 23 K (Mao et al., 2005). The unique characteristics show the potential of developing low-T molecular crystalline compounds as a new means for hydrogen storage.

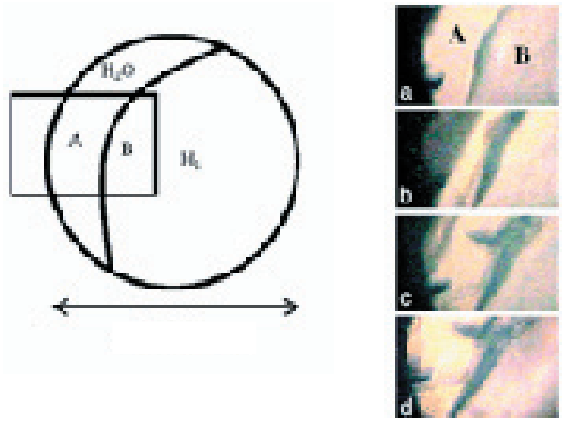

Photomicrographs at 300 MPa. (a) At 250 K, H_2O in region A is separated from H_2 in B. (b-c) Cooling to 249 K, a reaction zone of clathrate formed, and the residual water darkened as clathrate nucleated and grew until (d) the reaction was complete.

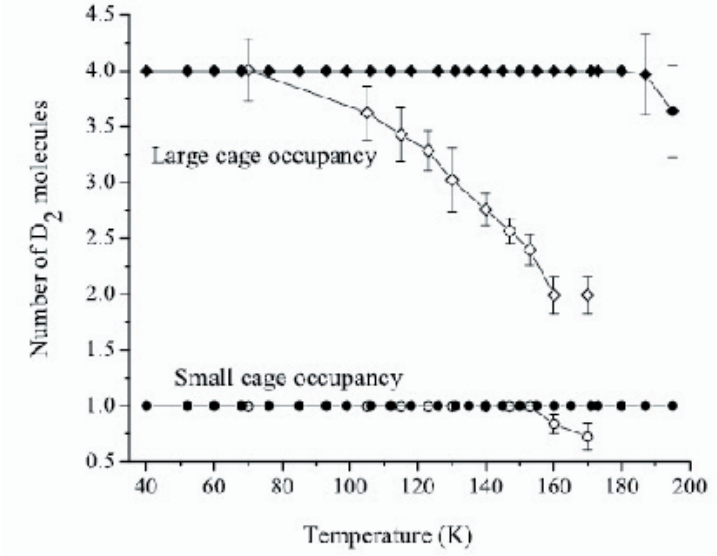

Occupancy of different cages in clathrate as a function of T at ambient P (open symbols) and 200 MPa (closed symbols). From (Lokshin et al., 2004).

Lokshin, K.A., Zhao, Y., He, D., Mao, W.L., Mao, H.K., Hemley, R.J., Lobanov, M.V., and Greenblatt, M., 2004, Structure and dynamics of hydrogen molecules in the novel clathrate hydrate by high pressure neutron diffraction: *Phys. Rev. Lett*., v. 93, p. 125503-1-4.
Mao, W., Mao, H.K., Struzhkin, V.V., Shu, J., and Hemley, R.J., 2005, Pressure-Temperature stability of the van der waals compound (H2)4CH4: *Chem. Phys. Lett*., v. 402, p. 66-70.
Mao, W.L., and Mao, H.K., 2004, Hydrogen storage in molecular compounds: *Proc. Nat. Acad. Sci*., v. 101, p. 708-710.
Mao, W.L., Mao, H.K., Goncharov, A.F., Struzhkin, V.V., Guo, Q., Hu, J., Shu, J., Hemley, R.J., Somayazulu, M., and Zhao, Y., 2002, Hydrogen clusters in clathrate hydrate: *Science*, v. 297, p. 2247-2249.
Mao, W.L. and H.-K. Mao. (2005). Hydrogen storage in molecular compounds. *Proceedings of the XX International Union of Crystallography* (IUCR2005), Florence, Italy, August 23-31, 2005.

We would like to acknowledge COMPRES (Consortium for Materials Properties Research in Earth Sciences Foundation Cooperatives Agreement EAR 01-35554) for financial support.

Experimental investigation of the creep behavior of olivine at high pressures using the deformation-DIA

Shenghua Mei and David L. Kohlstedt *University of Minnesota*
William B. Durham *Lawrence Livermore National Laboratory*
Liping Wang *Stony Brook University*

Experiments on the creep behavior of olivine at high pressures have been conducted using the deformation-DIA on a synchrotron beamline. Samples were hot-pressed from mixtures of olivine plus 5% enstatite powders. A 1 mm long x 1.1 mm diameter sample is encapsulated with 0.025-mm thick Ni foil and assembled with Al_2O_3 piston, a boron nitride sleeve, and graphite resistance heater into a 6-mm edge length cubic pressure medium. During an experiment, the cell is first pressurized isotropically to the desired level and heated to run temperature, and then deformed in compression at constant pressure. Using x-ray diffraction, we determine pressure (i.e., mean stress) and differential stress from the strain of various lattice planes measured as a function of orientation with respect to the stress field. Sample strain is computed from the length change of deforming samples measured from a series of x-radiographic images.

Experiments have been conducted at constant displacement rates ranging from 0.2 to 4 $\times 10^{-5}$ s^{-1} over axial strains of 10 - 20% at temperatures of 1373 - 1573 K and pressures of 2 - 12 GPa. Experimental results show that the creep rate of olivine depends on confining pressures with an activation volume of $V^* \approx 6 \times 10^{-6}$ m^3/mol. Comparably, this observed value of activation volume is much smaller than some other reported values of activation volume for the deformation of olivine (27×10^{-6} m^3/mol, Green and Borch, 1987; 14×10^{-6} m^3/mol, Karato and Jung, 2003) obtained with the solid-medium Griggs apparatus.

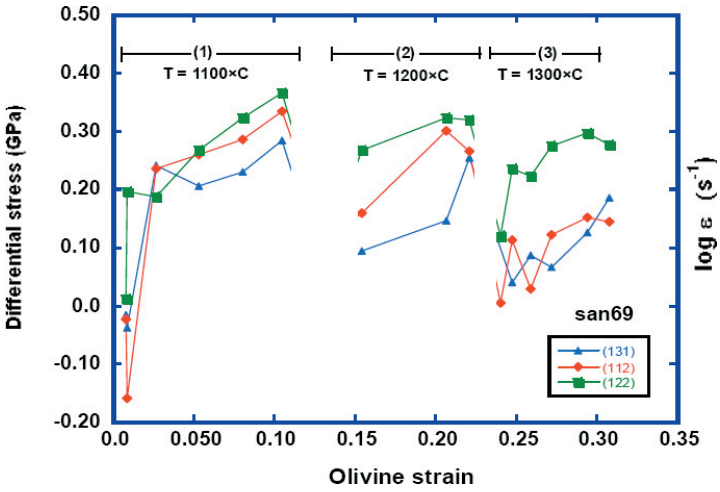

Stress vs strain for a polycrystalline olivine sample at a pressure of 5 GPa and strain rate of 2×10^{-6} s^{-1}. Plastic anisotropy of olivine results in different stresses registered for different Bragg (hkl) reflections.

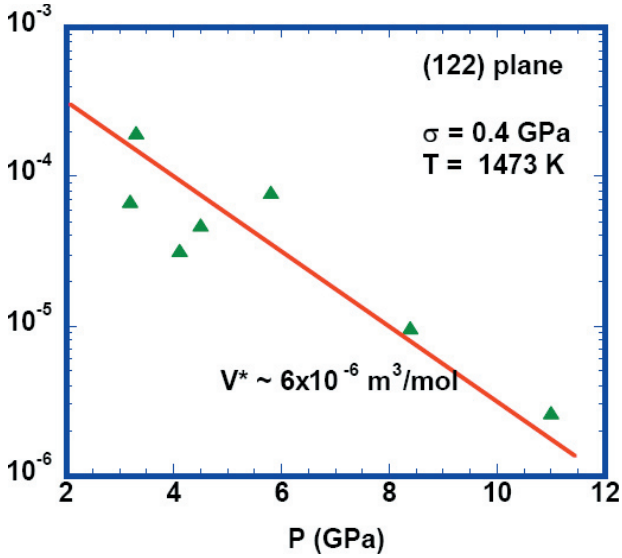

The dependence of creep rate of olivine on pressures for the (122) Bragg reflection, yielding an activation volume, $V^* \approx 6 \times 10^{-6}$ m^3/mol. Experiments were conducted at a temperature of 1473 K, normalized to a stress, σ, of 0.4 GPa.

Green, H.W. II, and R.S. Borch, The pressure dependence of creep, Acta Metall., 35, 1301-1315, 1987.
Karato, S., and Jung, H., Effects of pressure on high-temperature dislocation creep in olivine: *Philosophical Magazine*, ser. A, v. 83, 401-414, 2003.

This research was supported by US Department of Energy Office of Basic Energy Sciences under contract W-7405-ENG-48 (LLNL) and grant DE-FG02-04ER15500 (UMN). Experiments were carried out at the X17B2 beamline of the National Synchrotron Light Source, which is supported by the US Department of Energy, Division of Materials Sciences and Division of Chemical Sciences under Contract No. DE-AC02-76CH00016 and by COMPRES, the Consortium for Materials Properties Research in Earth Sciences under NSF Cooperative Agreement EAR 01-35554.

Single-crystal elastic constants of zoisite $Ca_2Al_3Si_3O_{12}(OH)$

Zhu Mao, Fuming Jiang, and Thomas S. Duffy *Princeton University*

Hydrous minerals in subduction zones are potential agents for transporting water to the deep earth. Properties of these minerals, especially elastic moduli, are needed to model seismic wave speeds in subduction zones and hence place constraints on cycling of H_2O through subduction zones. Zoisite is a metamorphic mineral of the epidote group containing 2 wt% water. It is likely to be one of the important phases in subduction zone environments. The stability field of zoisite extends up to 6.6 GPa and 950°C (Poli et al., 1998). In basaltic compositions, zoisite is found under conditions as high as 3.1 GPa and 650°C (Forneris and Holloway, 2003).

In this study, the single-crystal elastic constants of zoisite $Ca_2Al_3Si_3O_{12}(OH)$ were determined by Brillouin scattering under ambient conditions. Brillouin spectra were recorded in 37 directions for three separate crystal planes. The density of the sample and the orientation of each plane were determined by single-crystal diffraction using energy dispersive techniques at X17C of the National Synchrotron Light Source. The complete elastic tensor was then obtained by an inversion of the acoustic velocity and orientation data. The Voigt-Reuss-Hill averages of the aggregate bulk modulus, shear modulus and Poisson's ratio were determined to be KS = 125.3(3) GPa, G=71.9(1) GPa and σ=0.26, respectively. Our results are consistent with some previous static compression studies (Pawley et al., 1998; Grevel et al., 2000), although we find higher c axis compressibility. Our results provide the first determination of the shear modulus of zoisite. Compared with lawsonite, zoisite has a similar bulk modulus (~125 GPa), but a 30% larger shear modulus than lawsonite (~52 GPa). The VP/VS ratio is 1.76 for zoisite and compared with1.45 for lawsonite.

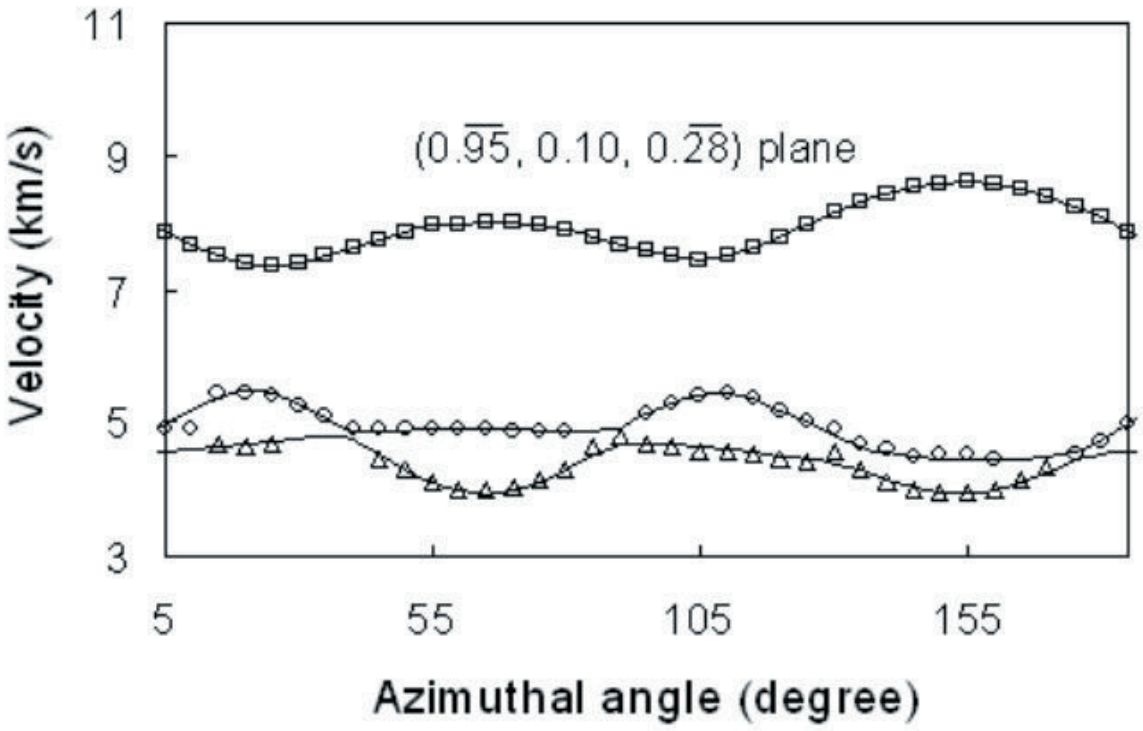

Acoustic velocities in zoisite. Symbols are measured data, lines are from best-fitting elastic constants.

Z. Mao, F. Jiang, T. S. Duffy, Single-crystal Elasticity of Zoisite $Ca_2Al_3Si_3O_{12}(OH)$ by Brillouin Scattering, EOS, *Trans AGU, Fall Meeting Suppl*., MR44A-08, 2005.

This research was supported by the NSF and DOE. Experiments were conducted at the X17C beamline of NSLS which is supported by COMPRES, the Consortium for Material Property Research in the Earth Sciences under NSF Cooperative Agreement EAR01-35554.

Quantitative high-pressure pair distribution function analysis of nanocrystalline gold.

C. David Martin and Sytle M. Antao,
Department of Geosciences, State University of New York at Stony Brook, Stony Brook NY, 11794-2100
Peter J. Chupas
Materials Science Division, MSD 223, Argonne National Laboratory, Argonne IL, 60439
Peter L. Lee and Sarvjit D. Shastri
XOR, Advanced Photon Source, Argonne National Laboratory, Argonne IL, 60439
John B. Parise
Department of Geosciences and Department of Chemistry, State University of New York at Stony Brook, Stony Brook NY, 11794-1901

Using a diamond anvil cell with high-energy monochromatic X-rays, we have studied the total scattering of nanocrystalline gold to 20 Å-1 at pressures up to 10 GPa in a hydrostatic alcohol pressure-medium. Through direct Fourier transformation of the structure function (S(Q)), pair distribution functions (PDFs) (G(r)) are calculated without Kaplow-type iterative corrections. Quantitative high-pressure PDF (QHP-PDF) analysis is performed via full-profile least-squares modeling and confirmed through comparison of Rietveld analysis of Bragg diffraction. The quality of the high pressure PDFs obtained demonstrates the integrity of our technique and suggests the feasibility of future QHP-PDF studies of liquids, disordered solids, and materials at phase transition under pressure.

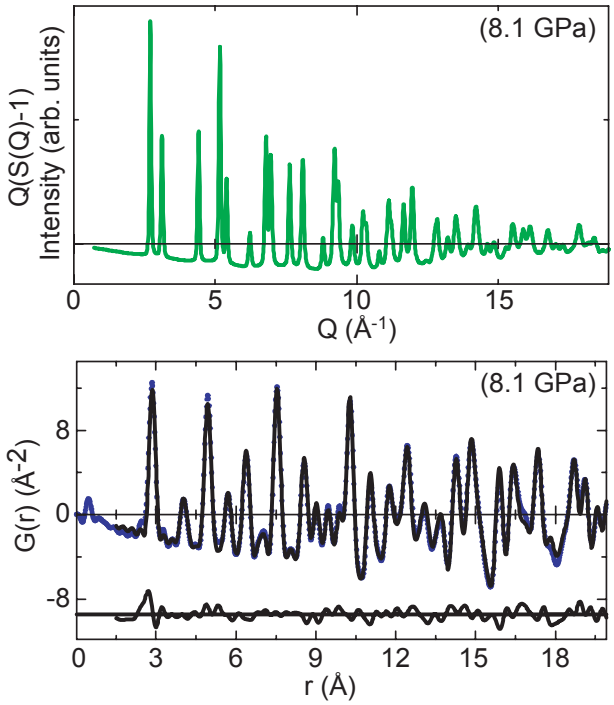

Diagrams comparing S(Q) and G(r) for gold in the diamond anvil cell (DAC) at 1 bar, with Gold in the DAC at 8.1 GPa. Full-profile fitting plots of G(r) are represented with observed data (dotted), model data (solid), and difference plot below (solid).

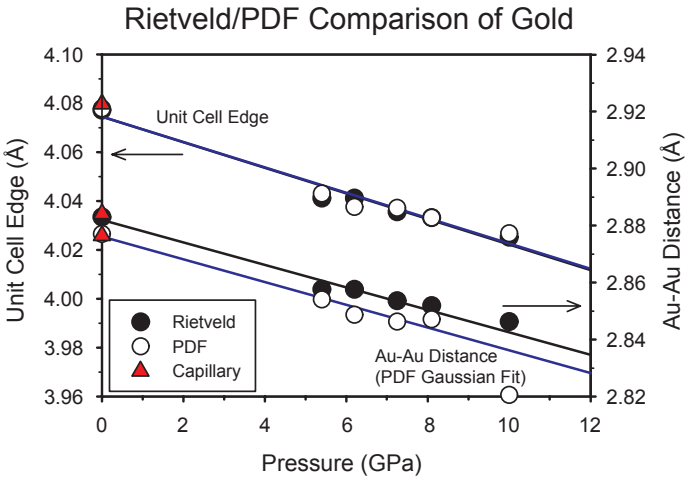

Unit cell and Au-Au distance as determined by Rietveld and HPQ-PDF analysis. The PDF-derived unit cell values were fit from the entire G(r) profile (Program PDFFIT), while a Gaussian was fit to the first Au-Au correlation to independently derive this distance. The discrepancy between the Au-Au distances may be explained as an effect of imperfect Gaussian peak-shape. The data point at the final pressure shown in the Au-Au PDF analysis was not included in the regression, due to an increase in the full-width at half-maximum in the G(r) Au-Au correlation (indicating a deviatoric-stress).

Martin, C.D., Antao, S.M., Chupas, P.J., Lee, P.L., Shastri, S.D., and Parise, J.B. (2005) Quantitative high-pressure pair distribution function analysis of nanocrystalline gold. *Applied Physics Letters*, 86(6).

Work was performed at 1-ID at APS and supported by facilities at sector 13 and was presented at the Tahoe COMPRES meeting.

Phase transitions and equations of state of $NaMgF_3$ (Neighborite) in perovskite- and post-perovskite-related structures.

C. David Martin *Geosciences Department, 255 Earth and Space Sciences Building, Stony Brook University, Stony Brook, NY, 11794-2100, USA,* **Wilson A. Crichton** *ID-27 European Synchrotron Radiation Facility (ESRF), 6 rue Jules Horowitz, BP220, 38043 GRENOBLE CEDEX, FRANCE*, **Haozhe Liu** *High Pressure Collaborative Access Team (HP-CAT), Sector 16, Advanced Photon Source, Argonne National Laboratory, Argonne, IL, 60439, USA*, **Vitali Prakapenka** *GeoSoil and EnviroCARS (GSECARS), Sector 13, Advanced Photon Source, Argonne National Laboratory, Argonne, IL, 60439, USA*, **Jiuhua Chen** *Geosciences Department, 255 Earth and Space Sciences Building, Stony Brook University, Stony Brook, NY, 11794-2100, USA*, **and John B. Parise** *Geosciences Department, 255 Earth and Space Sciences Building, Stony Brook University, Stony Brook, NY, 11794-2100, USA and Chemistry Department, Stony Brook University, Stony Brook, NY, 11794-3400, USA*

Using the diamond anvil cell with monochromatic x-radiation, perovskite structured Neighborite ($NaMgF_3$) is shown to transition to a structure resembling $CaIrO_3$-type post-perovskite between 28 and 30 GPa. Upon laser heating, the $CaIrO_3$-type structure transforms further to a possible triclinic distortion of post-perovskite (N-phase). Upon pressure release, N-phase $NaMgF_3$ becomes x-ray amorphous. N-phase may account for previous observations of extra x-ray reflections during studies of $MgSiO_3$ and $MgGeO_3$ post-perovskite and tomographic observations of an additional boundary at the bottom of the D".

Compressibility of perovskite and post-perovskite $NaMgF_3$

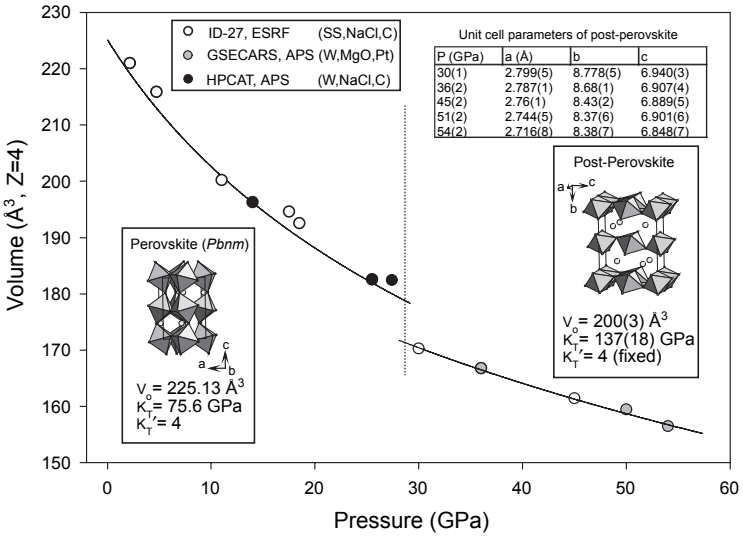

The 2nd order Birch-Murnaghan equations of state (EoS) of $NaMgF_3$ are complied from three high pressure runs. Each high pressure run contained different materials to preclude reaction with the sample (SS, stainless steel; C, graphite)

Phase transition of $NaMgF_3$ post-perovskite to N-phase

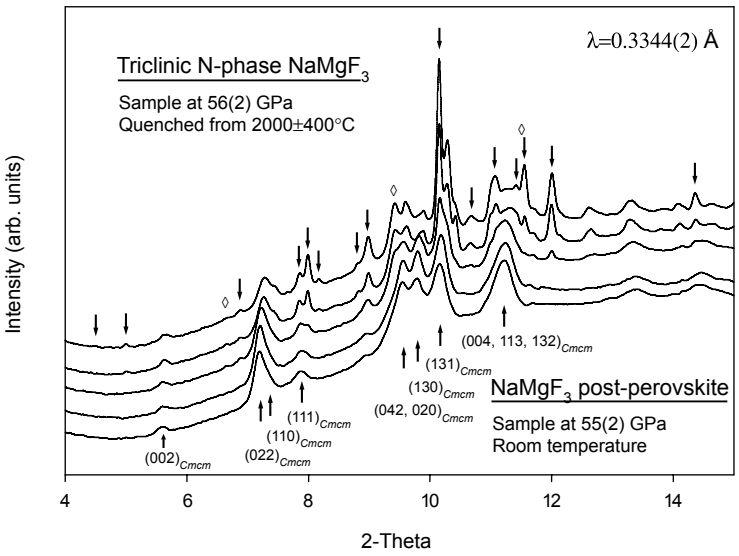

X-ray diffraction patterns of $NaMgF_3$ at high pressure before and after laser heating. Arrows pointing up show indexed peak show indexed peak positions of the post-perovskite structure, while arrows pointing down indicate peaks used to index N-phase $NaMgF_3$. Multiple unit cell solutions for N-phase $NaMgF_3$ are triclinic and include all peak positions formerly held by post-perovskite. Sample also contains NaCl (◊) and graphite (no diffraction).

Martin, C.D., Crichton, W.A., Liu, H.Z., Prakapenka, V.B., Chen, J., and Parise, J.B. (2006) Phase transitions and equations of state of $NaMgF_3$ (Neighborite) in perovskite- and post-perovskite-related structures. *Geophysical Research Letters*, Submitted.

This work supported by grant NSF-EAR-0510501 to JBP and we acknowledge the ESRF for provision of beamtime to proposal number HS-2780 at ID-27. Portions of this work were performed at GeoSoilEnviroCARS (Sector 13) as well as HPCAT (Sector 16), Advanced Photon Source (APS), Argonne National Laboratory. GeoSoilEnviroCARS is supported by the National Science Foundation - Earth Sciences (EAR-0217473), Department of Energy - Geosciences (DE-FG02-94ER14466) and the State of Illinois. Use of the HPCAT facility was supported by DOE-BES, DOE-NNSA (CDAC), NSF, DOD –TACOM, and the W.M. Keck Foundation. Use of the APS was supported by the U.S. Department of Energy, Office of Science, Office of Basic Energy Sciences, under Contract No. W-31-109-ENG-38.

In-situ Rietveld structure refinement of perovskite and post-perovskite phases of $NaMgF_3$ (Neighborite) at high pressures

C. David Martin *Geosciences Department, 255 Earth and Space Sciences Building, Stony Brook University, Stony Brook, NY, 11794-2100, USA,* **Wilson A. Crichton** *ID-27 European Synchrotron Radiation Facility (ESRF), 6 rue Jules Horowitz, BP220, 38043 GRENOBLE CEDEX, FRANCE*, **Haozhe Liu** *High Pressure Collaborative Access Team (HP-CAT), Sector 16, Advanced Photon Source, Argonne National Laboratory, Argonne, IL, 60439, USA*, **Vitali Prakapenka** *GeoSoil and EnviroCARS (GSECARS), Sector 13, Advanced Photon Source, Argonne National Laboratory, Argonne, IL, 60439, USA*, **Jiuhua Chen** *Geosciences Department, 255 Earth and Space Sciences Building, Stony Brook University, Stony Brook, NY, 11794-2100, USA*, **and John B. Parise** *Geosciences Department, 255 Earth and Space Sciences Building, Stony Brook University, Stony Brook, NY, 11794-2100, USA and Chemistry Department, Stony Brook University, Stony Brook, NY, 11794-3400, USA*

Recent high pressure experiments demonstrate $NaMgF_3$ perovskite (Neighborite) transforms to a post-perovskite phase between 28 and 30 GPa. Using Rietveld structure refinement, we are able to model the perovskite and post-perovskite structures before and after the high pressure transformation. At 28 GPa, Rietveld models indicate some extra-octahedral F-F distances rival the average intra-octahedral distance, which may cause instability in the perovskite structure and drive the transformation. The ratio of A-site to B-site volume (VA/VB) in perovskite structured $NaMgF_3$ (ABX_3), spans from 5 in the high temperature cubic perovskite phase to 4 in this high pressure perovskite phase, matching the VA/VB value in post-perovskite $NaMgF_3$. Using Rietveld refinement on post-perovskite structure models, observed discrepancies in pattern fitting may be described in terms of crystallite growth, development of sample texture in the DAC or a change of space group to Cmc21, a non-isomorphic subgroup of Cmcm; the space group describing the structure of $CaIrO_3$.

Rietveld structure refinement of perovskite and post-perovsktie $NaMgF_3$

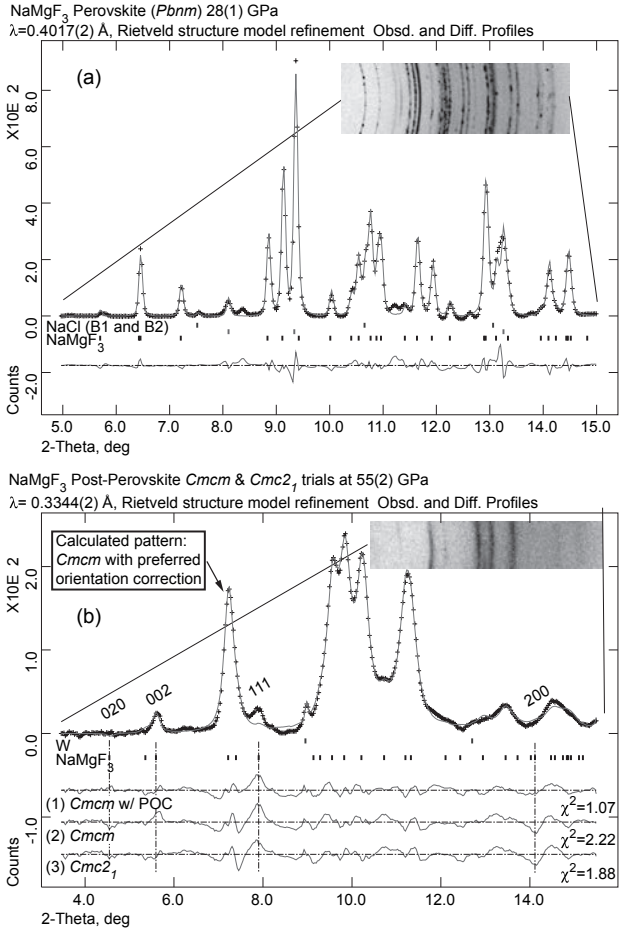

In-situ high pressure Rietveld structure modeling of (a) $NaMgF_3$ perovskite and (b) post-perovskite $NaMgF_3$. Portions of the raw two-dimensional data are inset in each plot to show sample texture. Difference curves of Rietveld structure models are plotted below the calculated (solid) and observed (dotted) background-subtracted x-ray diffraction patterns; (b) in descending order: (1) Cmcm with 4th order spherical harmonic preferred orientation correction (POC), (2) Cmcm without POC, (3) Cmc21 without POC. The volume calculated (a) for NaCl (B1, Z=4) at 28(1) GPa is 119.1(1) Å3 and 28.5(1) Å3 for the B2 phase (Z=1).

Martin, C.D., Crichton, W.A., Liu, H.Z., Prakapenka, V.B., Chen, J., and Parise, J.B. (2006) In-situ Rietveld structure refinement of perovskite and post-perovskite phases of $NaMgF_3$ (Neighborite) at high pressures. *American Mineralogist*, Submitted.

This work supported by grant NSF-EAR-0510501 to JBP and we acknowledge the ESRF for provision of beamtime to proposal number HS-2780 at ID-27. Portions of this work were performed at GeoSoilEnviroCARS (Sector 13) as well as HPCAT (Sector 16), Advanced Photon Source (APS), Argonne National Laboratory. GeoSoilEnviroCARS is supported by the National Science Foundation - Earth Sciences (EAR-0217473), Department of Energy - Geosciences (DE-FG02-94ER14466) and the State of Illinois. Use of the HPCAT facility was supported by DOE-BES, DOE-NNSA (CDAC), NSF, DOD –TACOM, and the W.M. Keck Foundation. Use of the APS was supported by the U.S. Department of Energy, Office of Science, Office of Basic Energy Sciences, under Contract No. W-31-109-ENG-38.

An X-ray diffraction study of Ilmenite ($FeTiO_3$) under high pressures and temperatures using large-volume pressure and synchrotron radiation

L.C. Ming, *Hawaii Institute of Geophysics & Planetology, University of Hawaii, Honolulu, HI 96822*
Y.H. Kim, *Department of Earth and Environmental Science, Geongsang National University, Jinju 660-701, Korea*
T. Uchida, Y.Wang , and M. Rivers, *GSE-CARS, The University of Chicago, 5640 South Ellis Avenue Chicago, IL 60637*

Two natural samples of ilmenite ($FeTiO_3$) were studied in a large volume press with T-CUP apparatus to 19.6 GPa and 800 ^oC. In situ X-ray diffraction measurements were carried using synchrotron radiation from the GSECARS beamline 13-BMD at the Advanced Photon Source (APS). The phase transformation from ilmenite to perovskite in $FeTiO_3$ was directly observed. The perovskite phase is temperature quenchable at 20 GPa and converts into the $LiNbO_3$ phase at pressures below 15 GPa at room temperature, in accord with previous observation that $LiNbO_3$ phase transforms to the perovskite phase at 16 GPa at room temperature (Levenweber et al., 1996). The $LiNbO_3$ phase transforms into the ilmenite phase at 10 GPa and 673 K. However, the back-transformation from the ilmenite to the $LiNbO_3$ phase was not observed, thus strongly suggesting that the $LiNbO_3$ phase is not thermodynamically stable but rather a retrogressive phase formed from perovskite during decompression at room temperature.

By cycling the pressure up and down at temperatures between 773 and 1023 K, the perovskite-ilmenite transformation could be observed in both directions, thus confirming that perovskite is the true high-pressure phase with respect to the ilmenite phase at lower pressures. The phase boundary of the perovskite-ilmenite transformation thus determined in this study is represented by P (GPa) = 16.0 (±1.4) – 0.0012 (±0.0014) T (K), which is inconsistent with P = 25.2 – 0.01 T (K) reported previously (Syono et al. 1980). The discrepancy could be attributed to the different experimental methods (i.e. in situ versus quench) used in the two studies. The ilmenite-perovskite phase boundary with such a small slope would potentially serve as a useful geobarometer for ilmenite-bearing rocks derived from the deep mantle or for those shocked in meteor craters.

Leinenweber, K., Utsumi, W., Tsuchida, Y., Yagi, T., and Kurita, K. (1991) Unquenchable high-pressure perovskite polymorphs of $MnSiO_3$ and $FeTiO_3$, *Physics and Chemistry of Minerals*, 18, 244-250.

Syono, Y., Yamauchi, H., Ito, A., Someya, Y., Ito, E., Matsui, Y., Akaogi, M., and Akimoto, S. (1980) Magnetic properties of the disordered ilmenite $FeTiO_3$ II synthesized at very high pressure, in *FERRITES: Proceedings of International Conference,* Japan, 192-195.

This work was published in Am. Mineralogist, 91, 120-126, 2006, and was partially supported by NSF grant No. DMR-0102215.

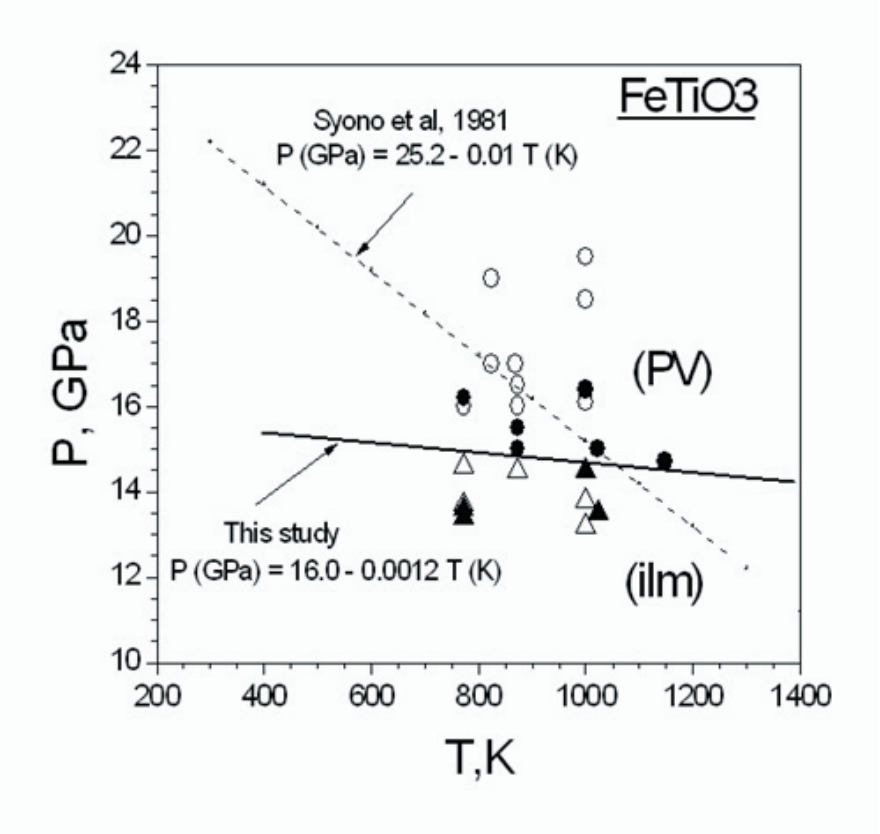

The persistence & stability of cyanuric acid in protoplanetary conditions

Wren Montgomery & Raymond Jeanloz

Department of Earth and Planetary Science, University of California, Berkeley, 307 McCone Hall, Berkeley, CA 94720-4767

Cyanuric acid, $C_3N_3O_3H_3$, which has been observed in protoplanetary systems and recovered from carbonaceous meteorites, may be a source of complex prebiotic molecules after high-pressure alteration. By documenting the structural and chemical transitions of cyanuric acid using synchrotron-source x-ray diffraction and FTIR spectroscopy in the diamond anvil cell, we can gain clues about the origins of pre-biotic material inside planets. An understanding of the spectral properties of processed materials could be used to identify their presence on extrasolar planets. Cyanuric acid is of special interest because it has a ring structure consisting of alternating C and N atoms. Critical biological components, such as nucleobases, incorporate these carbon-nitrogen rings.

Using x-ray diffraction and FTIR spectroscopy in the diamond anvil cell, we have begun a study of the stability of cyanuric acid at room temperature and pressures up to 30 GPa. Using a third-order Birch-Murnaghan equation of state, we determine a preliminary bulk modulus of K_0 = 17.16 GPa (K_0'=3.52) for pressures up to 10 GPa. The recovered samples appear to be denser than the initial sample by a factor of 3. FTIR spectroscopy up to 30 GPa suggests the formation of N-H...O and C—O...H intramolecular bonds, which could be a step towards stable molecules of greater complexity.

In conclusion, cyanuric acid is shown to be highly compressible under conditions associated with planetary embryos and planetesimals as well as cometary impacts; at the upper end of these conditions, we observe the possible formation of new bonds and more complex macro-molecules.

Synchrotron X-ray diffraction spectra of $H_3C_3N_3O_3$

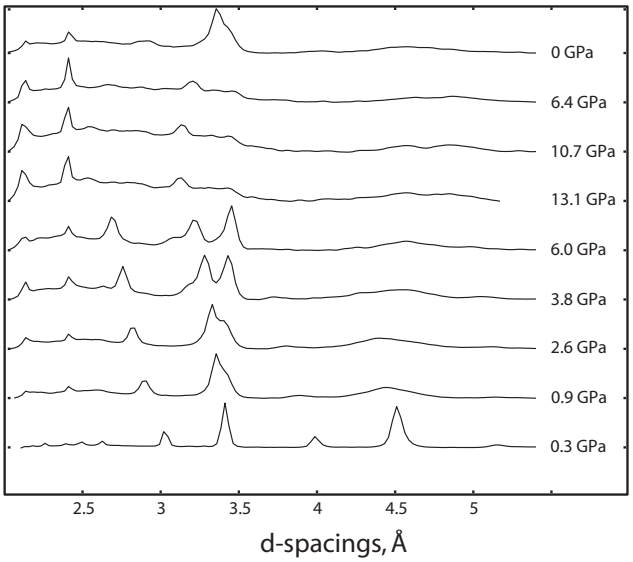

Ambient temperature (290 K) diffraction spectra of cyanuric acid show the compression of the unit cell of the material, primarily along the a-axis, reducing the spacing between the sheets of cyanuric acid molecules. At pressures above 10 GPa, the peaks are less sharply defined, suggesting amorphization of the material. This could also be due to strong texture in the sample; but, this change follows a change in the FTIR spectra. Diffraction spectra taken over 15 GPa show this amorphisation, but do not revert to the 0 GPa phase; samples which remain under 13 GPa revert as shown above. This suggests the formation of new stable bonds above a certain pressure.

Synchrotron FTIR spectra of cyanuric acid to 15 GPa

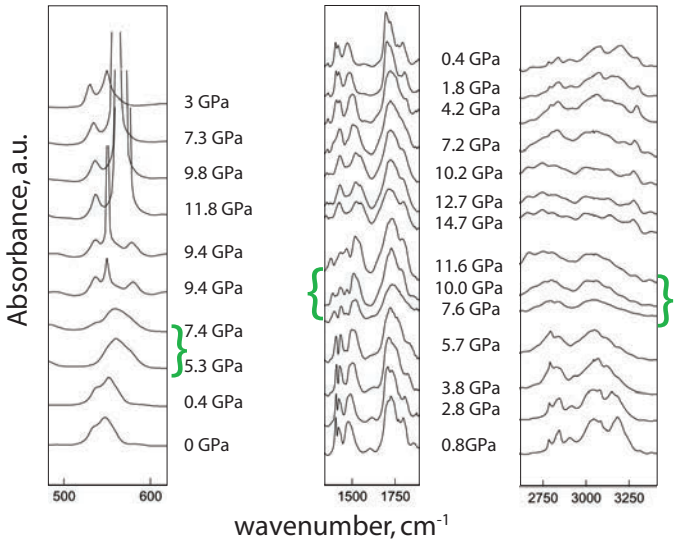

At pressures below 5 GPa, the vibrational spectra indicate that the molecule is undergoing compression: the N-H bond downshifts, indicating a strengthening of the bond and a shortening of the bond distance. The C=O bond weakens. Abruptly at 5 GPa, all of these bonds weaken or disappear, as strong peaks form at ~140 and 570 cm^{-1}. At 3000 cm^{-1}, a very broad band again consistent with intra-molecular O...H–N forms. On decompression, the FTIR spectra indicate a reversible phase transition.

Reference: The persistence & stability of cyanuric acid in protoplanetary conditions
Eos Trans. AGU, 86(52), Fall Meet. Suppl., Abstract SA53B-1173, 2005.

Acknowledgements: This research owes much to the expert assistance of Martin Kunz, Sander Caldwell, Simon Clark, Sirine Farka, and Michael Martin of the ALS, BL 11.3.3 and BL 12.2.2 and Zhenxian Liu of the NSLS, BL U2A.

Calibration based on a primary pressure scale in a multi-anvil device

Hans J. Mueller, Frank R. Schilling, Joern Lauterjung *GeoForschungsZentrum Potsdam in der Helmholtz-Gemeinschaft, Dept. 4, Telegraphenberg, D-14473 Potsdam, Germany*, **and Christian Lathe** *DESY-HASYLAB in der Helmholtz-Gemeinschaft, Notkestr. 85, D-22607 Hamburg, Germany*

A key question to all high pressure research arises from the reliability of pressure standards. There is some indication and discussion of an uncertainty of 10-20% for higher pressures in all standards. Independent and simultaneous investigation of the dynamical (ultrasonic interferometry of elastic wave velocities) and static (XRD-measurement of the pressure-induced volume decline) compressibility on a sample reveal the possibility of a standard-free pressure calibration and, consequently an absolute pressure measurement, because all required parameter are collected directly; no additional data, e.g. the volume dependence of the Grüneisen parameter etc., are needed. Ultrasonic interferometry is used to measure velocities of elastic compressional and shear waves in the multi-anvil high pressure device MAX80 at HASYLAB Hamburg enables XRD, X-radiography, and ultrasonic experiments. Two of the six anvils were equipped with lithium niobate transducers of 33.3 MHz natural frequency. NaCl was used as pressure calibrant, using the EoS of Decker (1971), and sample for ultrasonic interferometry at the same time. From the ultrasonic wave velocity data, vp and vs, we calculated the compressibility of NaCl as a function of pressure independent from NaCl-pressure calibrant. To derive the ultrasonic wave velocities from the interferometric frequencies of constructive and destructive interference requires precise in situ sample length measurements. For a NaCl-sample this is of particular importance, because the sample is the most ductile part of the whole set-up. We measured the sample length by XRD-scanning and by X-radiography. The compressibility results, derived from the ultrasonic data, were compared with data of static compression experiments up to 5 GPa (Bridgman, 1940) and up to 30 GPa (Birch, 1986) using experimental data from Boehler & Kennedy (1980) and Fritz et al. (1971). At 1.2 GPa and 5.3 GPa our velocity-derived compressibility data agree with the results of static compression. In the range between 2 and 4 GPa our dynamical data have 1.5 - 3 % higher values. In general the pressure revealed according to Decker (1971) is in accordance to our standard-free pressure calibration. Consequently, up to 8 GPa the NaCl pressure standard has a reliability of at least 1%. However, there is some evidence that at higher pressures the inaccuracy of the NaCl standard seems to exceed 1 %. Extrapolation of the compressibility data to higher pressures would also result in an increasing deviation, for EoS-fit and numerical fit of the density more than for the deformation fit.

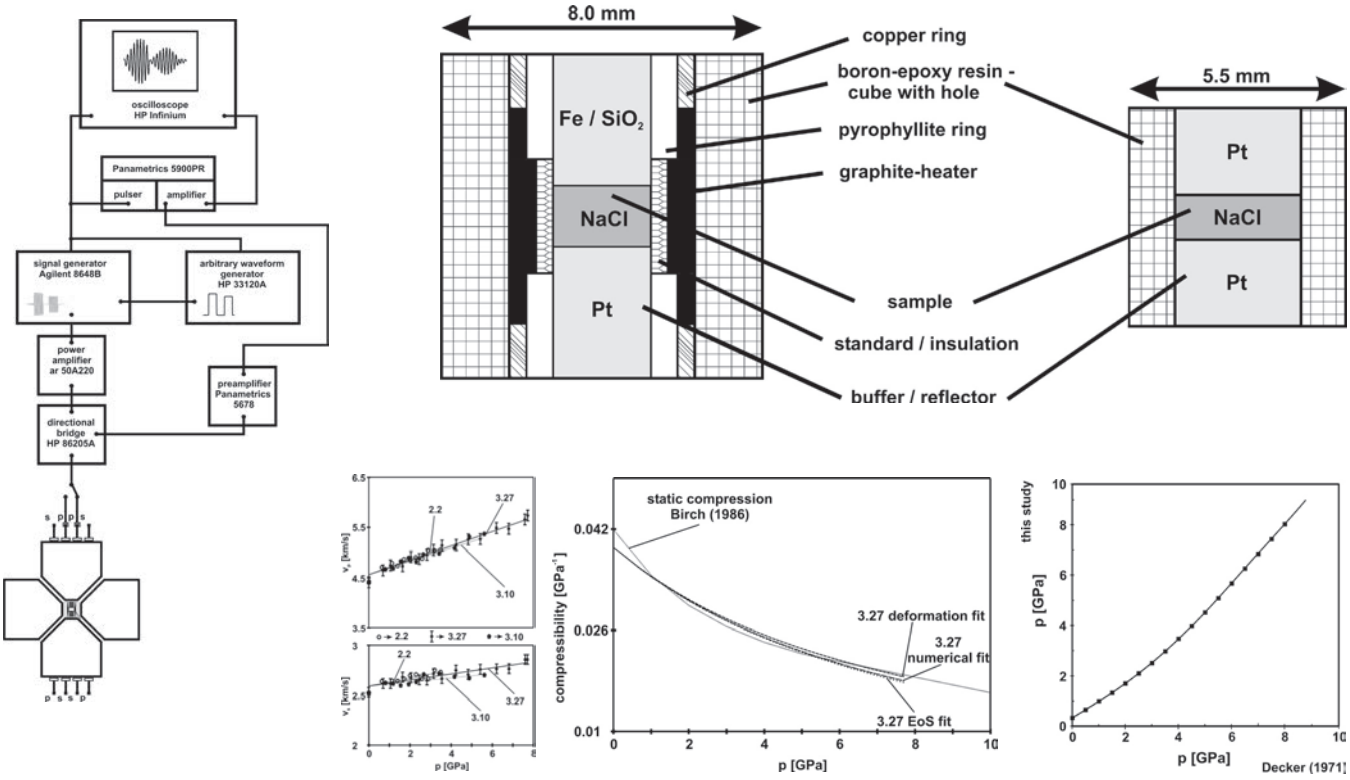

Mueller, H.J., Schilling, F.R., Lathe, C., Lauterjung, J. (2005): Calibration based on a primary pressure scale in a multi-anvil device, In: Chen, J., Wang, Y., Duffy, T., Shen, G., Dobrzhinetskaya, L. (eds.) *Advances in High Pressure Technology for Geophysical Application*, chapter 4, Elsevier B.V., pp. 427-449.

The experiments were performed at DESY-HASYLAB, beamline F2.1.
The project was funded by GFZ and BMBF.

Quantitative High Pressure Pair Distribution Function Analysis (QHP-PDF)

John B. Parise*, Sytle M. Antao, F. Marc Michel, C. David Martin • *Stony Brook University*
Peter J. Chupas, Peter L. Lee and Sarvjit D. Shastri • *APS, Argonne National Laboratory*

We have developed techniques using the diamond anvil cell (DAC) in combination with high-energy monochromatic X-rays (> 70 keV) to obtain the total scattering from crystalline, nanocrystalline and glassy materials at high pressures. Through direct Fourier transformation of the structure function (S(Q)), pair distribution functions (PDFs) (G(r)) are calculated without Kaplow-type iterative corrections. For crystalline materials, such as CeO_2 (Figure 1) QHP-PDF analysis is performed via full-profile least-squares modeling and the results are confirmed through comparison of Rietveld analysis of Bragg diffraction. The quality of the high pressure PDFs obtained demonstrates the validity of the background and sample cell corrections and suggests the feasibility of future QHP-PDF studies of liquids and disordered solids.

Many of the important transitions, substitutions, order-disorder reactions and phase transformations in Earth materials involve changes in short range order. The role of pressure and temperature in those structural changes are of primary interest. Analysis of Bragg diffraction alone however little quantitative structural information in disordered or amorphous materials, while full-profile fitting of the pair distribution function (PDF) has proven a powerful alternative in this area of structural science. Acquiring the total scattering (Bragg+diffuse) free of parasitic and inelastic (Compton) scattering so as to obtain well-normalized total structure factors, is challenging. The high-energy X-rays at beamline 1-ID, delivered by a bent double-Laue monochromator followed by vertically focusing refractive lenses, are well suited to work with the DAC. Recent developments in focused high-energy beams, and modified diamond geometries suggest quantitative data suitable for PDF analysis and the derivation of refined structure models can be obtained from samples at high P, in the DAC and other pressure vessels.

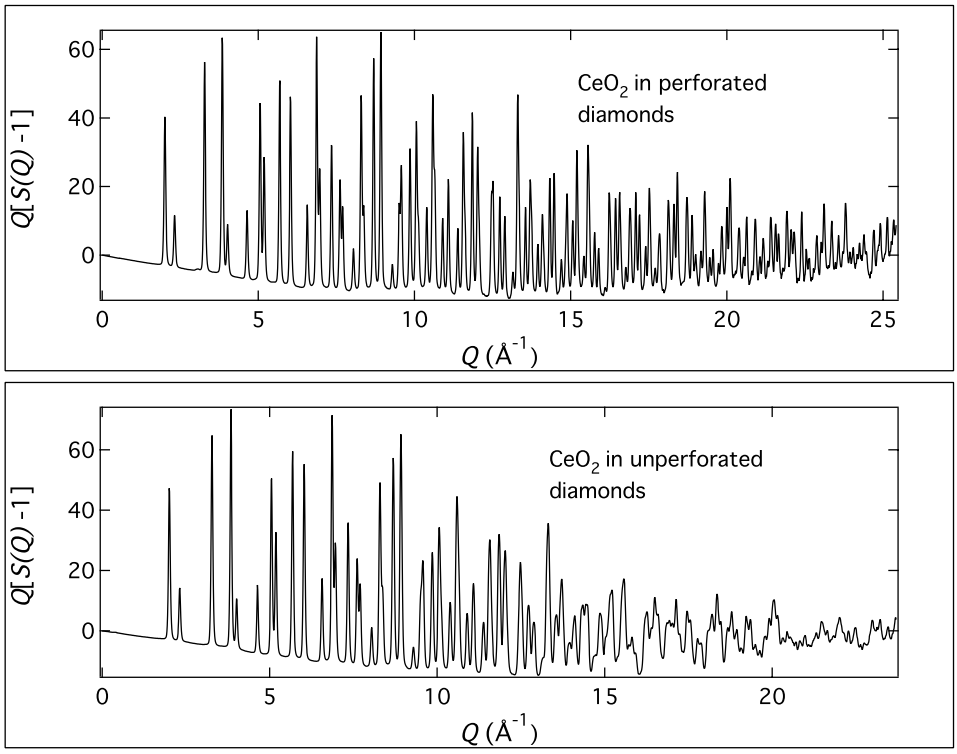

Q[S(Q)-1] for nano-CeO_2 in (top) a cell fitted with perforated diamonds and (bottom) in a standard diamond anvil cell. There is a dramatic decrease in the contribution to the overall scattering from diamonds in the perforated cell and this leads to much better signal to noise discrimination at high Q, an important factor in deriving better resolved real space correlation functions containing fewer "ripples" due to Fourier termination errors.

Martin, C. D., Antao, S. M., Chupas, P. J., Lee, P. L., Shastri, S. D. and Parise, J. B. (2005) Quantitative High Pressure Pair Distribution Function Analysis of Nanocrystalline Gold, *Appl. Phys. Lett*. 86, 061910-1 - 061910-3
Parise, J. B., Antao, S. M., Michel, F. M., Martin, C. D., Chupas, P. J. and Lee, P. L. (2005) Quantitative high-pressure pair distribution function analysis, *J. Synchrotron Rad*. 12, 554-559

This study is supported by the National Science Foundation under the Grants EAR0510501 (SMA, CDM) and DMR 0452444 (JBP) and CHE-0221934 (FMM) programs and DOE DE-FG02-03ER46085 (LE). Use of the Advanced Photon Source was supported by the U. S. Department of Energy, Office of Science, Office of Basic Energy Sciences, under Contract No. W-31-109-Eng-38. We wish to thank GSECARS at Sector 13 for use of high-pressure preparation facilities. The saw-tooth silicon refractive lenses were provided by C. Ribbing (Uppsala Univ. Sweden) and B. Cederstrom (Royal Inst. of Tech., Sweden).

An infrared spectroscopic study of 10-Å phase to 10 GPa, and comparison to talc

Stephen A. Parry, Alison R. Pawley *University of Manchester, UK*
Ray L. Jones *Daresbury Laboratory, UK*
Simon M. Clark *Advanced Light Source*

The effects of pressure on the O-H stretching frequencies of natural talc and two samples of synthetic 10-Å phase have been measured using a membrane-type diamond-anvil cell and synchrotron infrared radiation on station 1.4.3 at the Advanced Light Source, USA. The 10-Å phase was synthesized at 6.0 – 6.5 GPa, 600 ºC for 46 hours (sample 10Å-46) and 160 hours (10Å-160). Spectra were collected up to 9.0 GPa (talc), 9.9 GPa (10Å-46) and 9.6 GPa (10Å-160). The O-H stretching vibration of Mg_3OH groups in talc occurs at 3677 cm^{-1} at ambient pressure, and increases linearly with pressure at 0.97(2) cm-1 GPa^{-1}. The same vibration occurs in 10-Å phase, but shows negligible pressure shift up to 2 GPa, above which the frequency increases linearly to the maximum pressure studied, at a rate of 0.96(3) cm^{-1} GPa-1 (10Å-46) and 0.87(3) cm^{-1} GPa-1 (10Å-160). Other bands in the 10-Å phase spectrum are due to stretching of interlayer H_2O, hydrogen-bonded to the nearest tetrahedral sheet, and stretching of hydrogen-bonded Mg_3OH. These bands also show little change over the first 2 GPa of compression, as most of the compression of the structure is taken up by closing non-hydrogen bonded gaps between interlayer H_2O and tetrahedral sheets. Above 2 GPa, two additional bands are resolved and increase in intensity to 4.4 GPa, suggesting a rearrangement of structural hydroxyls in this pressure interval. At the same time, increased hydrogen bonding causes vibrations involving the interlayer to shift to lower frequencies. Above 4.4 GPa, broadening of the minor bands and lower resolution prevent further structural characterisation.

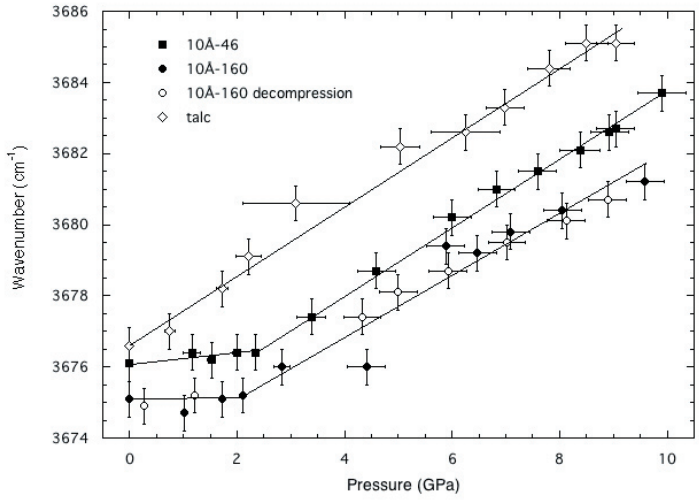

The stretching frequency of the talc-like OH group in 10-Å phase and talc as a function of pressure. The trends through the data were fit by least-squares, with the 10-Å phase data above 2 GPa fit separately from the data up to 2 GPa. Note that some 10-Å phase points below 2 GPa have not been plotted due to the peak shape being skewed by the presence of a low-frequency shoulder (see text for further discussion).

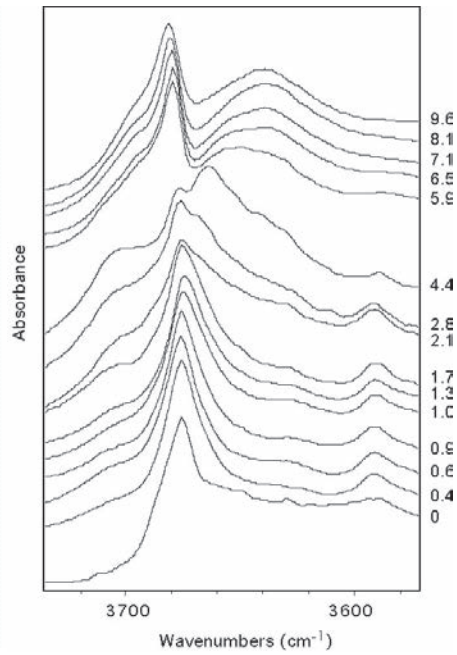

Evolution of the IR spectra of 10Å-160 during compression to 9.6 GPa. Pressures (in GPa) are shown to the right of each spectrum.

This work was supported by a UK Natural Environment Research Council studentship to S.A. Parry. We thank Dr M.C. Martin for assistance at the ALS. The ALS is supported by the Office of Basic Energy Sciences, US Department of Energy, under Contract DE-AC02-05CH11231.

Plasticity of silicon under pressure between 20°C and 425°C

J. Rabier, P.O. Renault *Laboratoire de Métallurgie Physique, UMR 6630 CNRS-Université de Poitiers, SP2MI, BP 30179, F-86962 Chasseneuil Futuroscope Cedex, France;* **J. Chen, H. Couvy, L. Wang** *Mineral Physics Institute, Stony Brook University, Stony Brook, NY 11794-2100, USA*

Plastic deformation of silicon single crystals under 5 GPa confining pressure has been characterized in-situ below the Brittle to Ductile Transition Temperature (BDTT) using synchrotron radiation. A D-DIA apparatus has been used which allows applying independently a uniaxial stress and a high hydrostatic pressure. The uniaxial stress and the pressure applied to the material have been measured in situ by using XRD on polycrystalline alumina rams as well as on polysilicon used also as a phase transformation marker. The deformation has been recorded by sample imaging. Experiments were conducted so that during the pressure application, the uni-axial stress on the samples remains as low as possible. Example of such an experiment conducted at 275°C is shown in the figure.

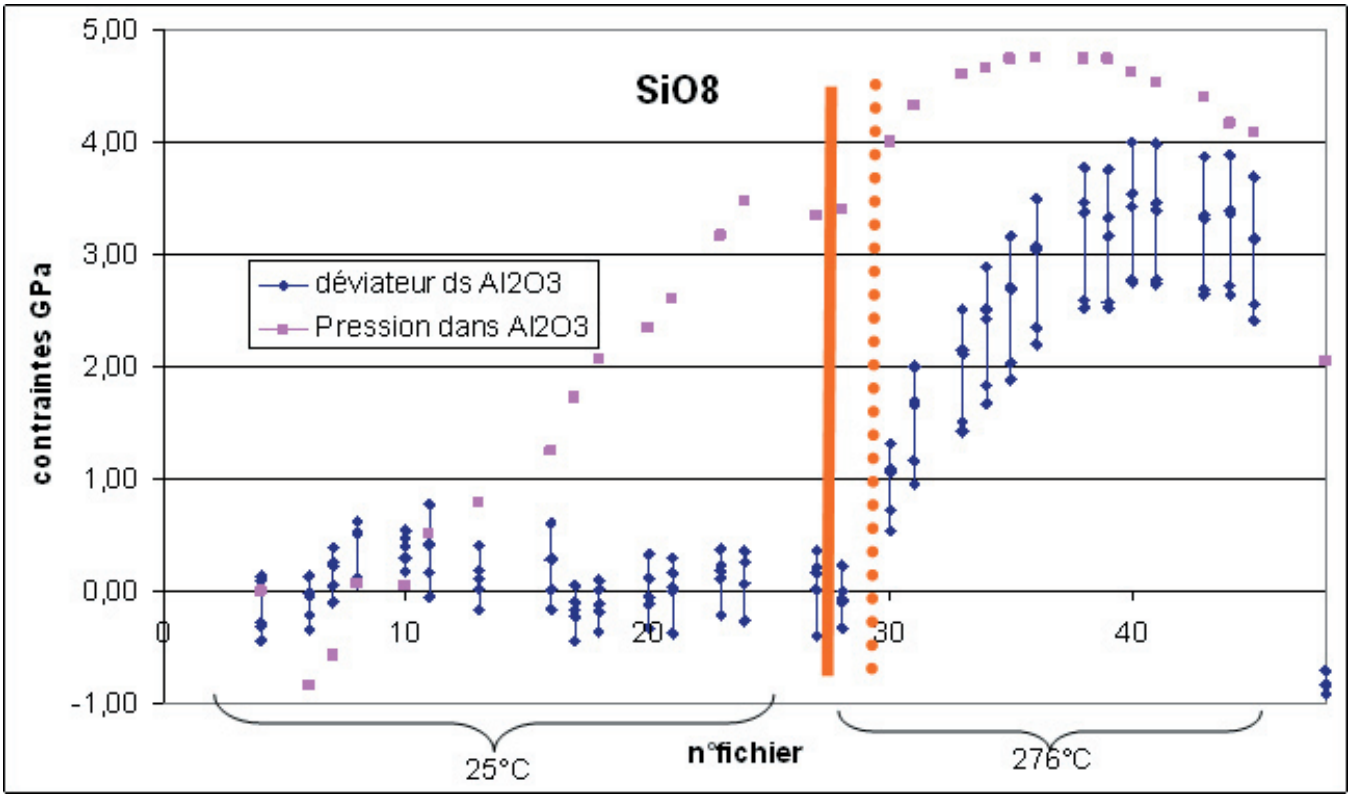

Pressure application and stress-strain curve of a FZ-Si single crystal deformed along <123> at a strain rate of the order of 10^{-5} s^{-1}

It is shown that below 300°C, the yield stress of silicon is athermal, the engineering stress being about 3GPa. This fits the results of Peierls stress derived from ab-initio and atomistic calculations for perfect shuffle dislocations in silicon.

References: J. Rabier, P.O. Renault, D. Eyidi, J.L. Demenet, J. Chen, H. Couvy and L. Wang, Plastic deformation of silicon between 20°C and 425°C, abstract accepted at EDS06, Halle, D, Sept 06.

The in-situ experiments were performed at NSLS (BNL) on the X17B2 beam line. This study was supported by CNRS and Université of Poitiers and by COMPRES, the Consortium for Materials Properties and Research in Earth Sciences under contract number EAR 01-35554

Pressure-induced slip-system transition in olivine

Paul Raterron and Patrick Cordier *CNRS and Université de Lille, France*
Jiuhua Chen, Li Li and Donald J. Weidner *Stony Brook University*

Seismic-velocity anisotropies are used to characterize convective flows in the Earth's upper mantle. They are interpreted from the lattice preferred orientations produced experimentally in olivine. Olivine dislocation slip systems have thus been extensively studied at pressure P < 3 GPa, showing that [100] slip dominates at mantle temperature, which results in aligning olivine fast velocity [100]-axis with the shear direction. Yet, recent experimental and computational reports suggest that olivine [001] slip may be dominant in the deep upper mantle where P reaches 14 GPa.

In order to quantify the effect of pressure on the activities of olivine dominant slip-system, deformation experiments were carried out using the Deformation-DIA apparatus (D-DIA) that equips the X17-B2 beam line at the NSLS (Upton, NY, USA). Single crystals of Mg_2SiO_4 forsterite (olivine Mg end-member, Fo100) were oriented in order to promote either [100] slip alone or [001] slip alone in (010) plane. They were deformed in compression two by two, one of each orientation, at upper-mantle conditions, i.e., P ranging from 2.1 to 7.5 GPa and T ranging from 1373 to 1677 K. Constant applied stress σ and sample strain rates were monitored in situ using X-ray synchrotron radiation. Deformation microstructures were investigated in the run products by TEM, which reveals that dislocation creep assisted by dislocation climb and dislocation cross slip was responsible for sample deformation. X-ray diffraction and imaging data were interpreted in terms of rheological laws, showing an increase of [001]-slip activity with pressure relative to that of [100] slip. The observed transition cannot be attributed to a possible water effect, since specimens were "dry": containing no detectable water before the runs, and less than 10±10 wt. ppm H_2O under the form of hydroxyl groups after deformation, as revealed by FTIR measurements.

Extrapolation of our data to natural P-T-σ conditions shows that along a 20-Ma oceanic geotherm, [001] slip activity increases continuously with pressure and becomes comparable to that of [100] slip at the transition zone boundary. It also shows that at P-T-σ conditions representative of subduction zone, [001] slip dominates deformation from typically 140 km depth. This may explain the seismic anisotropy attenuation observed in the Earth from 200-km depth, as well as the seismic anisotropy anomalies observed in subduction zone

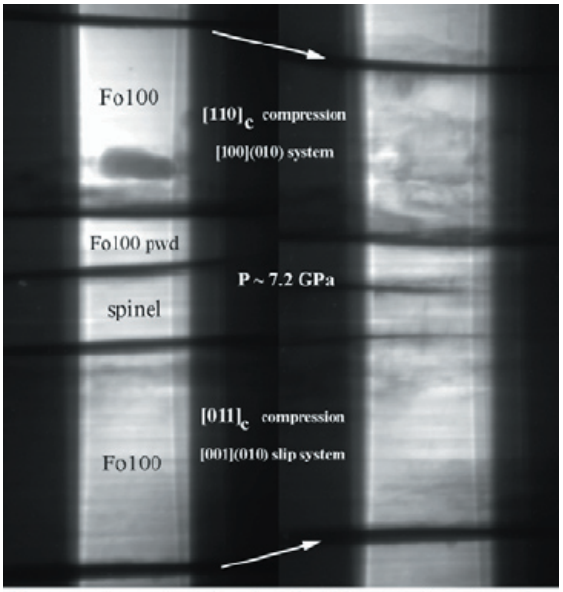

X-ray radiographs showing Fo100 crystals and strain-markers (center: Fo100 and spinel), and strains during deformation at mantle P and T

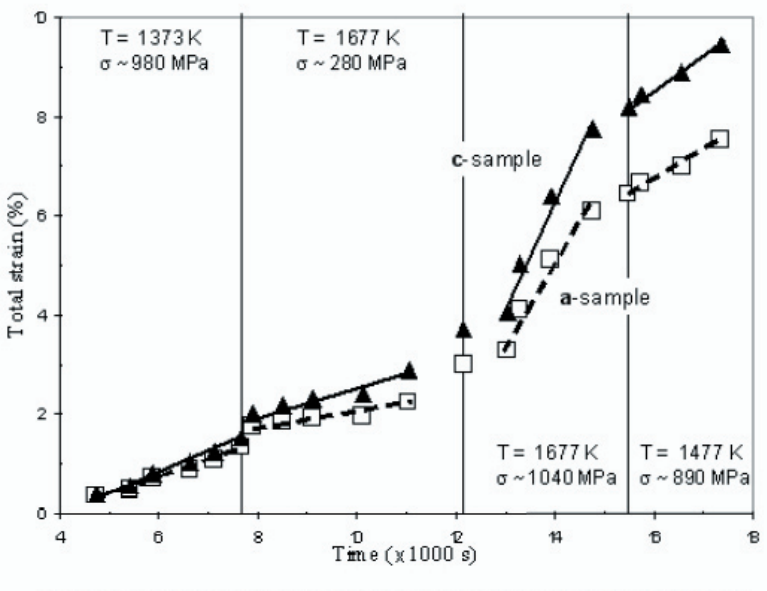

[001]-slip sample (triangles) and [100]-slip sample (squares) strainsat 7 GPa and indicated T-σ conditions, versus time. [001]-slip dominates deformation at high P, resulting in [001]-slip sample higher total strain.

Raterron, P., Chen, J., Li, L., Weidner, D.J. and P. Cordier, Pressure induced slip-system transition in olivine: high-pressure rheological measurements, microstructures and flow laws. *American Mineralogist*, submitted 2005

This research was supported by the NSF Grants EAR-9909266, EAR0135551, and EAR0229260 and the CNRS/INSU Grants DyETI 2003 and 2004. We thank Takaya Nagaï for providing the starting material, Edouard Kaminski for fruitful scientific discussions, Liping Wang, Zhong Zhong and Hongbo Long for assistance at the NSLS beam line X17-B2 (supported by the U.S. D.O.E, contract # DE-AC02_98CH10886 and COMPRES), and Christophe Depecker for his assistance with FTIR.

Single-crystal elastic properties of phase A to 12 GPa

Carmen Sanchez-Valle, Stanislav V. Sinogeikin *University of Illinois at Urbana-Champaign*
Joseph R. Smyth *University of Colorado at Boulder*
Jay D. Bass *University of Illinois at Urbana-Champaign*

The sound velocities and single-crystal elastic constants of dense hydrous magnesium silicate phase A, Mg7Si2O8(OH)6, were measured by Brillouin scattering up to 12.4(2) GPa in a diamond anvil cell. The single-crystals of phase A used in this study were synthesized at 12 GPa and 1150 ºC in a 5000-tons multi-anvil press at Bayerisches Geoinstitut (Germany). The pressure-dependence of single-crystal elastic moduli (Cij), as well as the aggregate adiabatic bulk (Ks) and shear (μ) moduli were obtained. A fit to the acoustic data using a 4th order finite-strain EOS yields the following Ks and μ and their pressure derivatives (VRH averages): Ks = 106(1) GPa, Ks' = 6.1(2), Ks" =-0.26(5), m = 61(1) GPa, μ' = 2.2(1) and μ" = -0.18(2). The present acoustic results resolve discrepancies between the bulk moduli obtained in earlier compression studies. The axial compressibility of hexagonal phase A (P63) is highly anisotropic with the c-axis, which is perpendicular to the distorted close-packed layers, approximately 21% stiffer than the a-axis, in agreement with previous static compression data. The present results on phase A help to elucidate the effect of water incorporation on the elastic properties (Ks and μ) of mineral phases along the forsterite-brucite join. The aggregate velocities (VP and VS) of phase A are ~7% lower than those of forsterite (olivine) and displays significantly distinct compressional and shear acoustic anisotropies (AP and AS) through its pressure stability range in subduting slabs. These results suggest that water may be readily identified seismologically if phase A is present in abundance at depth in the Earth, and this phase could contribute to explain the seismic low velocity zone (LVZ) that has been observed in subduction zones

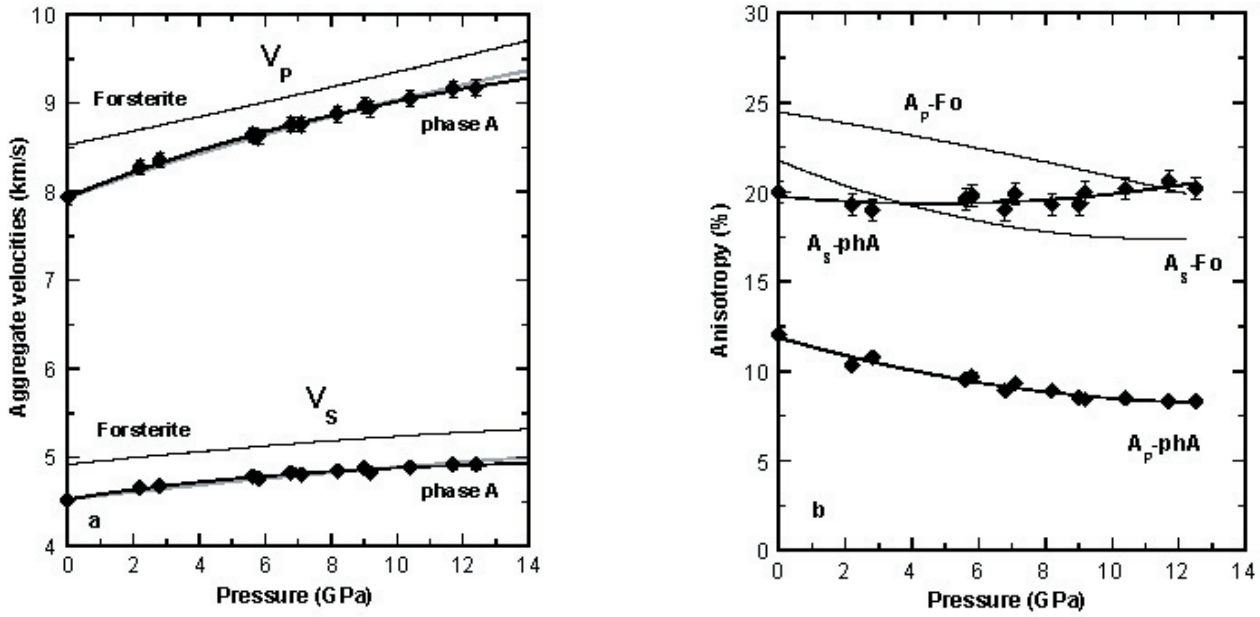

Aggregate acoustic velocities (a) and elastic anisotropy (b) of phase A and forsterite as a function of pressure. Data for Forsterite is taken from Zha et al. (1996)

Sanchez-Valle, C., Sinogeikin, S.V., Smyth J.S., and Bass, J.D. (2006) Single-crystal elastic properties of dense hydrous magnesium silicate phase A. *American Mineralogist*, in press 2006.

Sanchez-Valle, C., SV Sinogeikin, Smyth J.S., and Bass, J.D. (2006) High-pressure single-crystal elasticity of phase A and implications for water in the Earth's upper mantle

This study is supported by National Science Foundation under Grants EAR 0003383 and 0135642 to JDB.

High-pressure vibrational study of dense hydrous magnesium silicate 10Å Phase

Carmen Sanchez-Valle, Holger Hellwig, Jie Li, Jynguin Wang *University of Illinois at Urbana-Champaign*
Zhenxian Liu *Carnegie Institution of Washington*
Jay D. Bass *University of Illinois at Urbana-Champaign*

Dense hydrous magnesium silicates (DHMS) could be important hosts for H_2O in the Earth's mantle and subduction zones, and their dehydration may be responsible for deep focus earthquakes. Among these phases, the so-called 10Å phase ($Mg_3Si_4O_{10}(OH)_2.nH_2O$) is characterized by a phlogopite-like structure which accommodates molecular water in the inter-layer. However, the amount of interlayer water, its precise structural position and the response upon compression remain uncertain. Therefore, we have investigated the behavior of hydroxyl groups and interlayer water in 10Å phase as a function of pressure using synchrotron IR and Raman spectroscopy.

Thanks to the brightness of the synchrotron IR beam and the spatial resolution available at the U2A beamline at NSLS (Brookhaven National Laboratory), high-quality far- and mid-IR spectra of 10Å phase have been collected up to 20 GPa at ambient temperature in the diamond-anvil cell. The samples were synthesized at 6.7 GPa and 650 ºC in a Walker-type multianvil press at the University of Illinois. At ambient conditions, the 10Å phase IR spectrum in the OH-stretching region shows a strong band at 3675 cm^{-1} and two less intense and broader bands at 3258, 3589, 3623 and 3703 cm^{-1}. With increasing pressure up to 5.5 GPa, the band at 3675 cm^{-1} displays a linear negative frequency shift. At this pressure, a new band emerges at 3680 cm^{-1} and its intensity progressively increases with pressure up to 15.5 GPa, indicating major changes in the hydrogen bonding (Fig 1). All pressure-induced changes in the IR spectra are fully reversible upon decompression and occur without any noticeable hysteresis (Fig 2).
On the basis of combined high pressure IR and Raman results, we could reevaluate the assignment of the OH–vibrational bands of 10Å phase and constrain the response to compression of silicate tetrahedra, magnesium octahedra, hydroxyl units and molecular water.

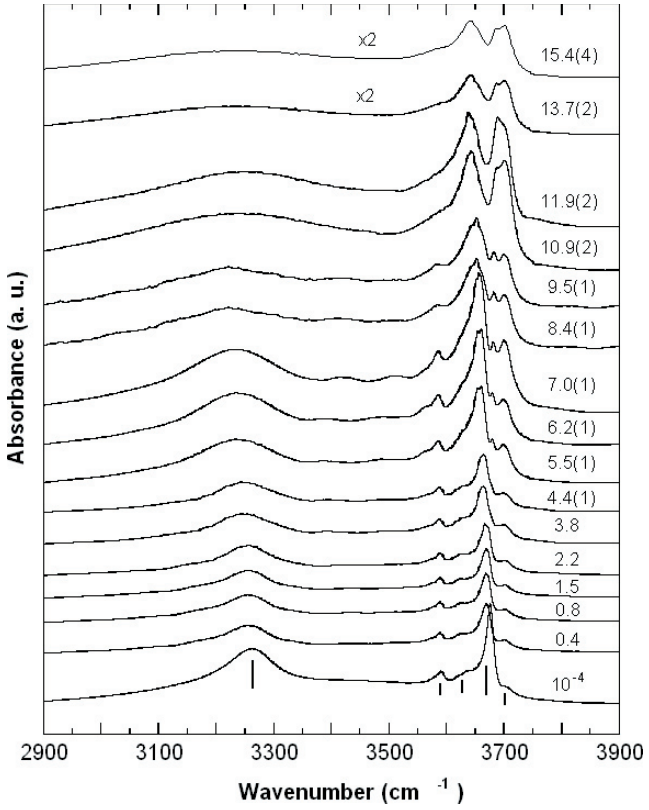

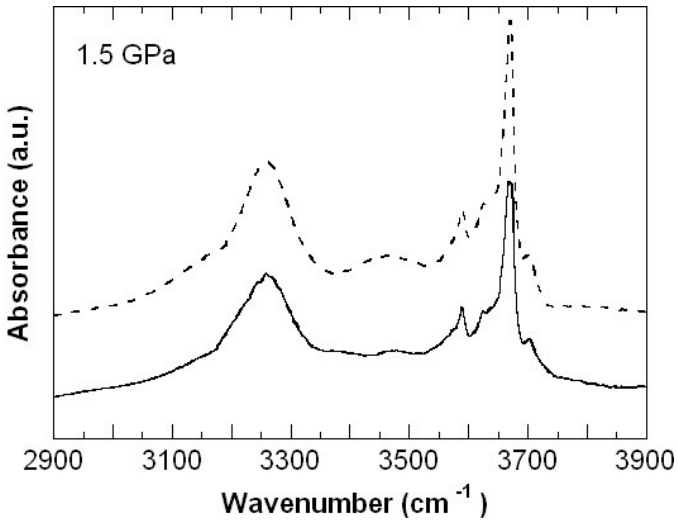

Fig2. IR spectra in the OH-stretching region of 10Å phase collected at 1.5 GPa in compression (solid line) and decompression (dashed line). Pressure-induced changes are fully reversible and occur without noticeable hysteresis.

Fig1. Representative mid-IR spectra in the OH stretching mode region of 10Å phase obtained during compression. Vertical lines indicates the position of the vibrational band at room conditions.

Sanchez-Valle, C., Hellwig, H., Li, J., Wang, J., Liu, Z., and Bass, J.D. (2006) High-pressure vibrational properties of 10Å phase. In prep.

This study is supported by National Science Foundation under Grants EAR0135642 to JDB. NSLS is supported by the Department of Energy.

High Pressure Optical Absorption Spectra of Magnesiowüstite

Tao Sun, Philip B. Allen *Department of Physics & Astronomy, Stony Brook University*
Tony Yu *Department of Geosciences, Stony Brook University*
Zhenxian Liu, Steven D. Jacobsen *Geophysical Laboratory, Carnegie Institution of Washington*

We measured room-temperature optical absorption spectra of $Mg_{1-x}Fe_xO$ (Magnesiowüstite, x=0.15, 0.24) at different pressures, using a Diamond Anvil Cell (DAC) and an HR460 spectrograph (SPEX) from 9,000 cm^{-1} to 24,000 cm^{-1}. The spectra resemble that of FeO (wüstite): a broad band at ~10,000 cm^{-1}, which corresponds to the T_{2g} - E_g crystal field excitation of Fe^{2+}, and an absorption edge at ~20,000 cm^{-1}, which is the energy gap of FeO. This similarity suggests that the d electrons of iron are quite localized and are insensitive to the surrounding metal ions. Under increased pressure, (1) the 10,000 cm^{-1} band blue shifts, (2) the 20,000 cm^{-1} edge red shifts, (3) the absorption intensifies in the whole measured frequency range. We intend to do band structure calculations to model oscillator strengths and the pressure induced peak-shifting and absorption enhancement.

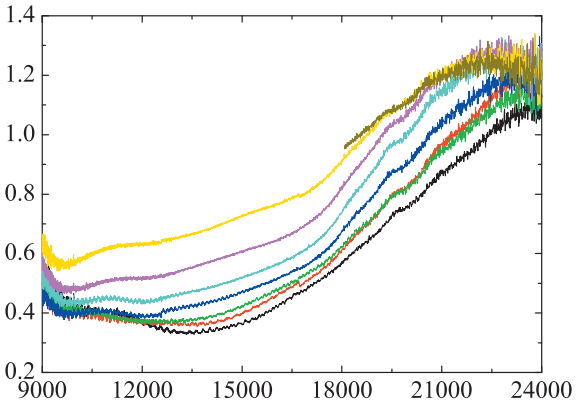

Optical Spectra of $Mg_{0.85}Fe_{0.15}O$ at different pressures. The sample thickness is 10 μm

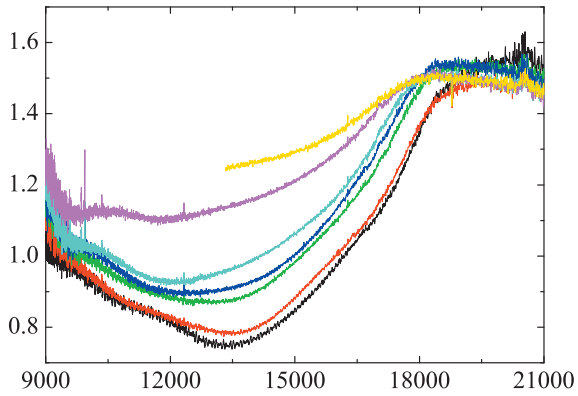

Optical Spectra of $Mg_{0.76}Fe_{0.24}O$ at different pressures. The sample thickness is 10 μm

This research is supported by National Science Foundation under grants ITR-NSF-ATM0426757. The optical absorption measurements are performed at the U2A beamline at NSLS of BNL. The U2A beamline is supported by COMPRES, the Consortium for Materials Properties Research in Earth Sciences under NSF Cooperative Agreement EAR01-35554, U.S. Department of Energy (DOE-BES and NNSA/CDAC), and NSF (EAR05-XXXX).

Stability of the Perovskite Phase and the Post-Perovskite Transition in $MgSiO_3$

Sang-Heon Shim *Massachusetts Institute of Technology,* **Thomas S. Duffy** *Princeton University,* **R. Jeanloz** *University of California,* **and G. Shen** *University of Chicago*

The development of the angle-dispersive X-ray diffraction combined with in-situ laser heating at the GSECARS of the Advanced Photon Source allowed us to measure high-resolution diffraction patterns of $MgSiO_3$ to pressure-temperature conditions related to the lowermost mantle. In this study, we confirmed the stability of $MgSiO_3$ perovskite to the P-T conditions of 2700-km depth in the lower mantle. Furthermore, we confirmed the post-perovskite phase transition at the P-T conditions of the lowermost mantle (2700-3000-km depth) proposed by Murakami et al. [2004]. This supports the existence of a major phase transition in $MgSiO_3$ under conditions close to those at the base of Earth's mantle.

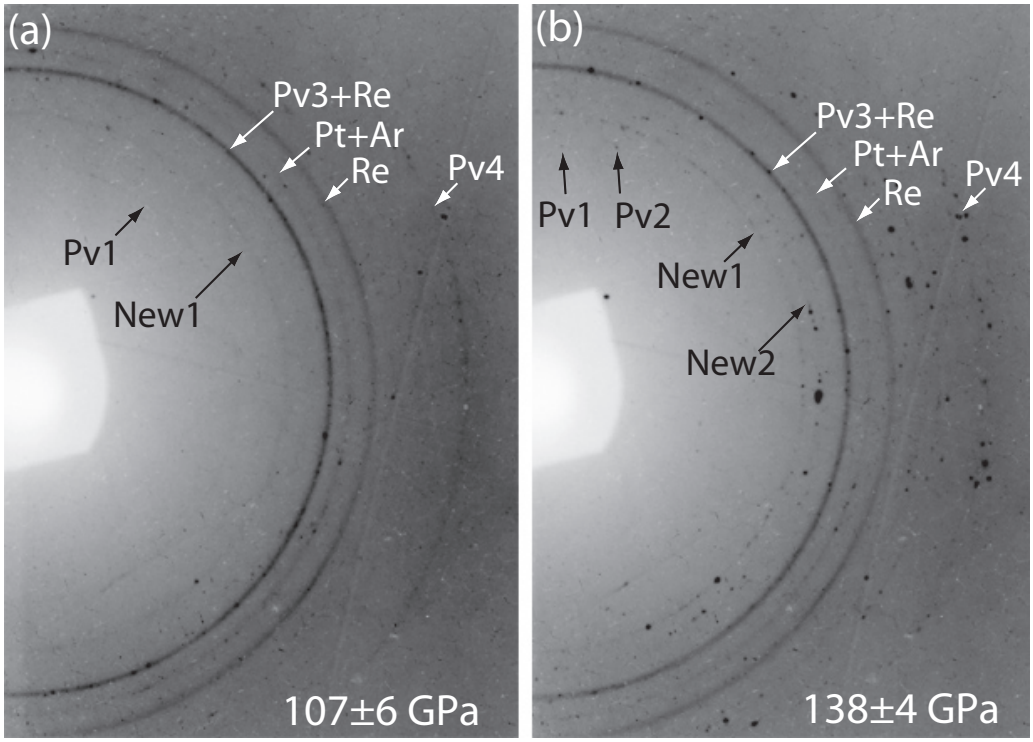

X-ray diffraction image of $MgSiO_3$ perovskite (a) and post-perovskite (b).

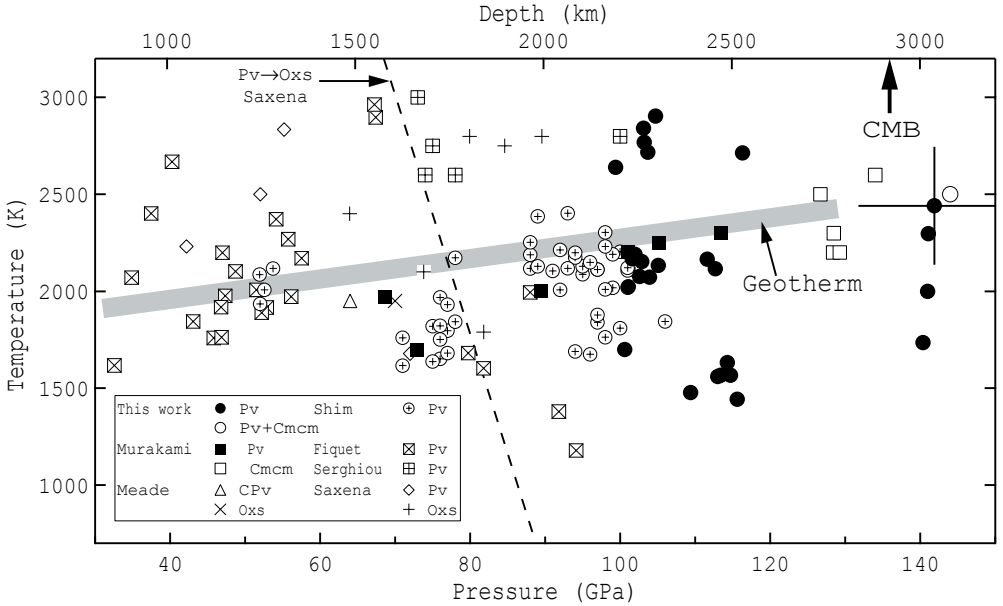

P-T range of our X-ray measurements.

S.-H. Shim, T. S. Duffy, R. Jeanloz, and G. Shen. Stability and crystal structure of $MgSiO_3$ perovskite to the core-mantle boundary. *Geophysical Research Letters* 31, L10603, 10.1029/2004GL019639, 2004.

We thank S. Shieh, V. Prakapenka, and N. Sata for their assistant in the experiments. J. Akins and T. Ahrens provided glass samples. This study is supported by NSF. SS and RJ thank the Miller Institute for support. TD thanks the Packard Foundation for support.

Strength and elasticity of SiO_2 across the stishovite-$CaCl_2$-type structural phase boundary

Sean R. Shieh, Thomas S. Duffy *Department of Geosciences, Princeton University*
Baosheng Li *Stony Brook University*

Radial x-ray diffraction, together with lattice strain theory can provide information for highpressure strength and elasticity. Stishovite, SiO_2, was regarded as a strong material at ambient conditions and was studied at pressure to 60 GPa. The yield strength is found to be nearly constant at pressures of 15-40 GPa and to drop sharply as the transition pressure is approached. The yield strength then increases rapidly in the $CaCl_2$-type phase. In contrast to its ambientpressure behavior, our measurements indicate that the yield strength of stishovite is surprisingly low at high pressures especially when compared with other silicates (e.g. ringwoodite). Our data also allow for inversion to recover a partial elastic stiffness tensor at high pressure. In general, our values of C_{11} and C_{12} lie below theoretical values, but they are qualitatively consistent with theory in that C_{11}-C_{12} is markedly reduced near the transition pressure. This provides direct experimental support for the theoretical prediction of an elastic instability involving C_{11}-C_{12} in stishovite near 50 GPa.

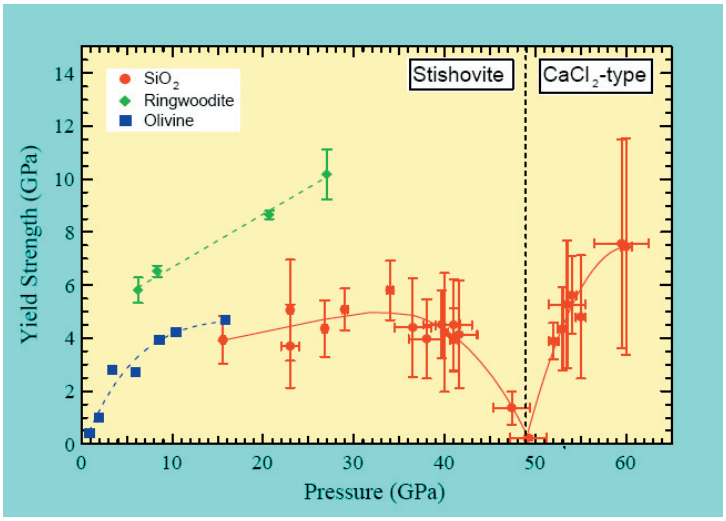

Yield strength of stishovite at high pressure. Red symbols and line are from this study; Squares and diamonds are olivine (α-Mg_2SiO_4) and ringwoodite (γ-Mg_2SiO_4) data, respectively. Black dashed line is the transition boundary of stishovite to the $CaCl_2$-type.

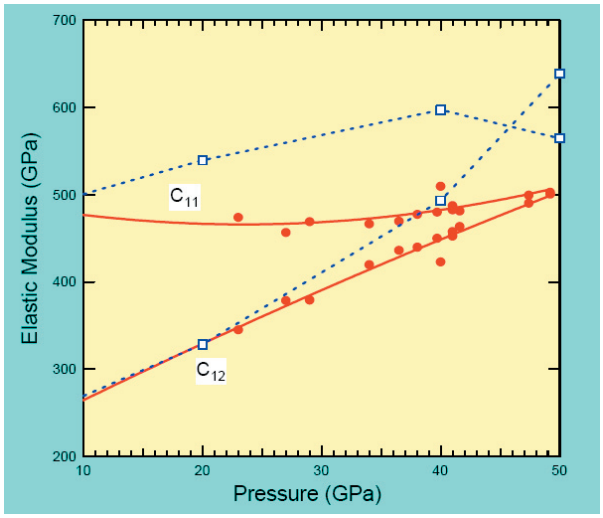

Selected elastic moduli of stishovite at high pressure. Red symbols and line are from this study; open symbols and dashed lines are from theoretical calculations.

Shieh, S. R., T.S. Duffy, and B. Li, Strength and elasticity of SiO_2 across the stishovite-$CaCl_2$-type structural phase boundary, *Phys Rev Lett*. 89(25):255507, 2002.

This work was supported by the National Science Foundation and the David and Lucille Packard Foundation.

A High Pressure Phase Transition in $CaCO_3$-Aragonite at 50 GPa and 300 K

J. Santillan and Q. Williams, *UC Santa Cruz*

$CaCO_3$-aragonite has been examined to pressures of 50 GPa using angle-dispersive synchrotron x-ray diffraction at 300 K. Pressure-induced shifts in the x-ray diffraction pattern demonstrate that aragonite undergoes a transition to a structure that is likely trigonal near 50 GPa. The occurrence of this phase transition is in general accord with systematics in aragonite-structured divalent cation carbonates, and the high pressure phase may be of importance for the sequestration of carbon within Earth's deep mantle.

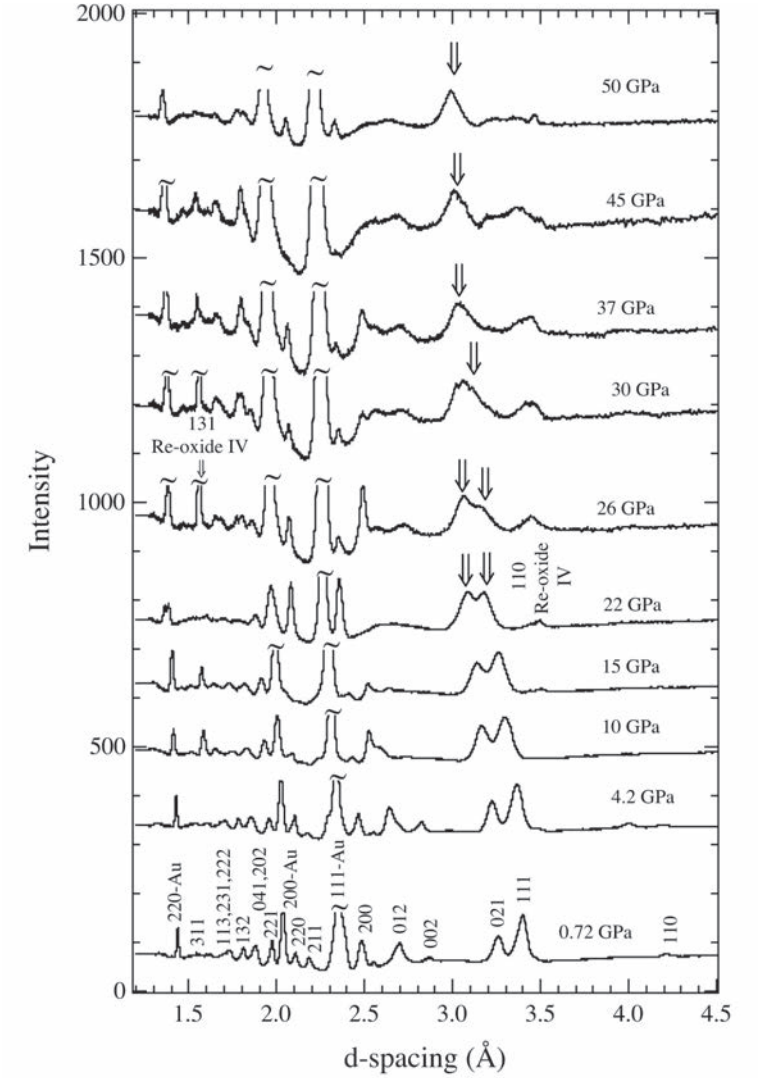

X-ray diffraction patterns of aragonite to pressures of 50 GPa. Arrows denote pressure-induced convergence of the (021) and (111) diffraction peaks.

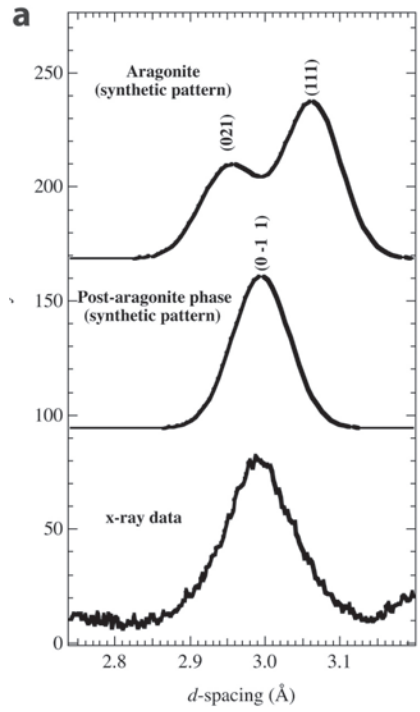

Comparison of data and synthetic patterns for the aragonite and post-aragonite phases.

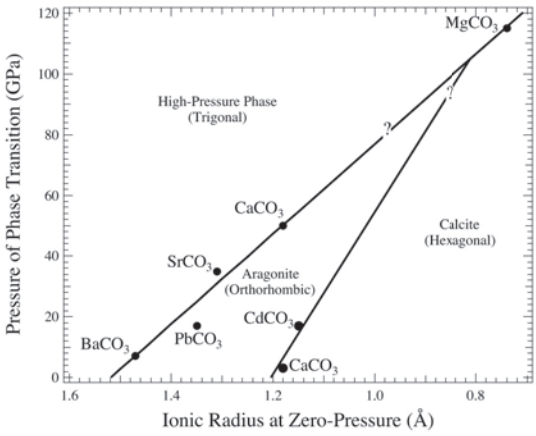

Carbonate stability fields as a function of ionic radii.

Santillan, J. and Q. Williams, A high pressure x-ray diffraction study of aragonite and the post-aragonite phase transition in $CaCO_3$, *American Mineralogist*, 89, 1348-1352, 2004.

Acknowledgment: Work supported by NSF grant EAR-0310342. This study was conducted at Beamline 10-2 of the Stanford Synchrotron Radiation Laboratory.

Densities and Partial Melting in the Fe-Fe3S System

Seagle, Christopher T. University of Chicago, Campbell, Andrew J. University of Maryland, Heinz, Dion L. University of Chicago, Shen, Guoyin HPCAT, Prakapenka, Vitali B. University of Chicago

The densities and melting relations in iron-light element binary systems provide important constraints on the light element constituents of Earth's outer core. We investigated properties of iron - iron sulfide mixtures at high pressure and temperature, using the diamond anvil cell laser heating facilities at GSECARS, Sector 13 of the Advanced Photon Source. We found that the density of iron compared to Fe3S forms a linear relationship that is independent of temperature up to 80 GPa and 2500 K. This allowed us to estimate an upper limit on the sulfur content of Earth's outer core of ~14 wt. % S. Melting temperatures in the system were also measured at a series of pressures up to 80 GPa. The Fe-Fe3S system exhibits eutectic behavior to at least 60 GPa and the eutectic temperature increases approximately linearly from 30-60 GPa with a slope of ~15 K/GPa; a lower bound on the eutectic temperature was determined to be 2150 K at 80 GPa. If sulfur is the dominant light element in Earth's outer core, the melting data suggest a minimum temperature of ~2500 K at the core-mantle boundary.

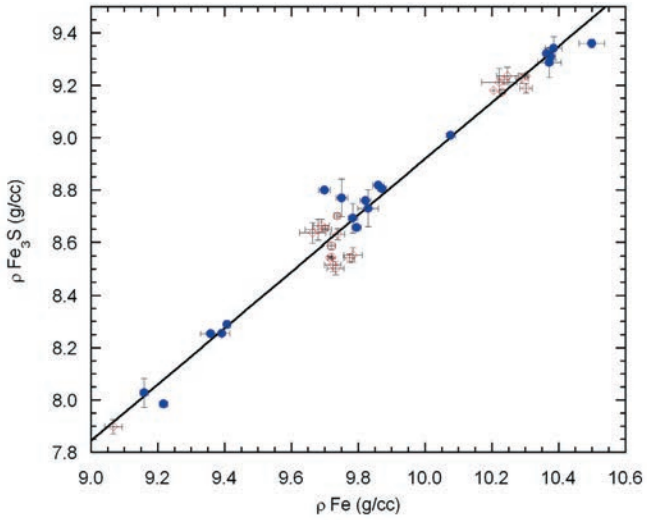

Left Figure: The density of iron and Fe3S was measured simultaneously at high pressures and temperatures. Solid line - linear fit; Red diamonds - high temperature; Blue circles - room temperature.

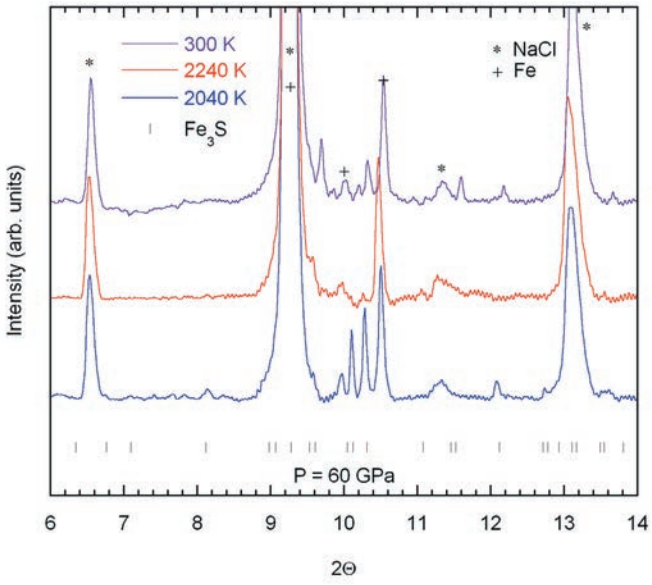

Right Figure: Series of diffraction patterns indicating partial melting. The eutectic temperature was bound between 2040 K and 2240 K. Top line, after rapid quenching.

References: Seagle, C.T., Campbell, A.J., Heinz, D.L., Shen, G., Prakapenka, V.B. (2006) Thermal Equation of State of Fe3S and Implications for Sulfur in Earth's Core. Journal of Geophysical Research – Solid Earth (in press).

Campbell, A.J., Seagle, C.T., Heinz, D.L., Shen, G., Prakapenka, V.B. (2006) Partial Melting in the Iron-Sulfur System at High Pressure: A Synchrotron X-ray Diffraction Study (in progress).

We acknowledge the use of GeoSoilEnviroCARS at the Advanced Photon Source, Argonne National Laboratory. This work was supported by NSF grants EAR 0309486 (DLH) and EAR 0600140 (AJC).

Dual Mode Ultrasonic Interferometry in Multi-Anvil High Pressure Apparatus using Single-Crystal Olivine as the Pressure Standard

Yegor D. Sinelnikov, Ganglin Chen, and Robert C. Liebermann *Stony Brook University*

Acoustic measurements of compressional (P) and shear (S) wave travel times were performed in 1000-ton uniaxial split-cylinder apparatus (USCA-1000) of the Kawai-type up to 10 GPa at room temperature, using dual mode lithium niobate transducers and ultrasonic interferometry. The cell pressures were calibrated continously by in-situ measurements of the travel times in a single crystal San-Carlos olivine buffer rod inside the cell assembly. Elastic compressional and shear wave velocities in a dense, fine-grained polycrystalline Al_2O_3 were measured simultaneously to 10 GPa; from these data, the elastic moduli and their pressure derivatives were obtained for the longitudinal modulus {L0 = 461(3) GPa, L0' = 7.0(1)}, the shear modulus {G0 = 162(2) GPa, G0' = 1.9(1)} and the bulk modulus {K0 = 245(3) GPa, K0' = 4.5(1)}.

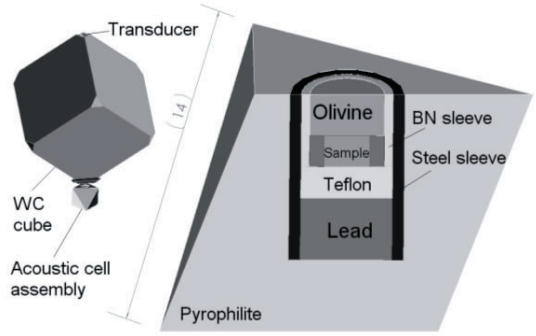

Cross-sectional view of the cell assembly for the high-pressure ultrasonic experiments in the 1000-ton uniaxial split-cylinder apparatus (UQCA-1000) using olivine single crystals as the pressure marker.

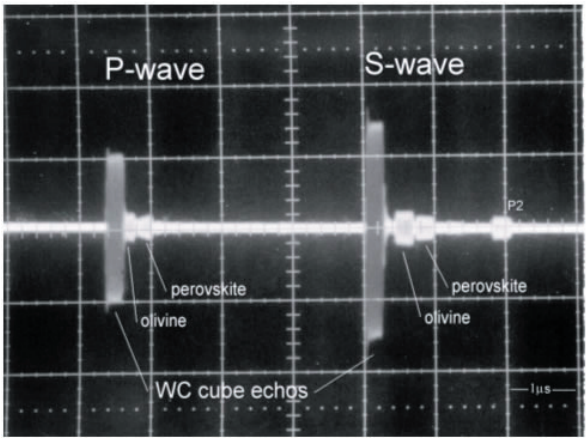

Compressional (P) and shear (S) wave echo trains at about 10 GPa produced by dual mode transducer experiments in the USCA-1000 apparatus. In each train, the first acoustic echo corresponds to the reflection from the WC cube anvil-San Carlos olivine single crystal buffer rod interface; the second echo is from the olivine-$MgSiO_3$-perovskite specimen (#3140) interface; and the third echo is from the perovskite-teflon interface. The second arrival of the P-wave reflected from the anvil-olivine interface is also visible (P2).

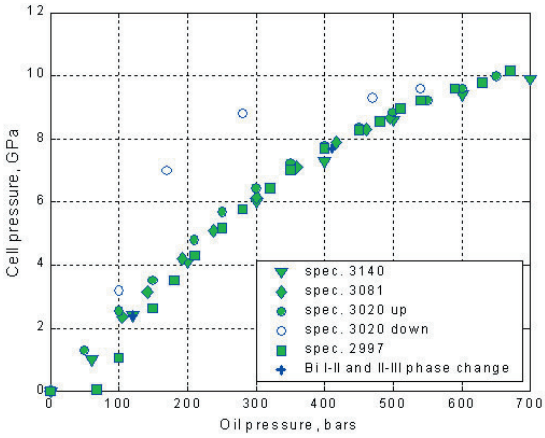

Cell pressure vs oil pressure calibration for ultrasonic interferometric experiments ar room temperature using the 14-mm cell assembly shown in Fig. 1 and a San Carlos olivine single crystal as a buffer rod and pressure marker. Several different experiments with different $MgSiO_3$-perovskite specimens yield consistent results and are in excellent agreement with the phase transitions in Bi at 2.55 GPa (Bi I-II) and 7.7 GPa (Bi III-V) in the run with specimen #3020.

Reference: Sinelnikov, Y.D., G. Chen, and R.C. Liebermann, Dual mode ultrasonic interferometry in multi-anvil high-pressure apparatus using single crystal olivine as the pressure standard, *International Journal of High Pressure Research*, 24, 183-191, 2004.

These high-pressure experiments were conducted in the Stony Brook High Pressure Laboratory, which is jointly supported by Stony Brook University and by NSF grants to RCL (under EAR 96-14612 and 99-80491), and by COMPRES, the Consortium for Materials Properties Research in Earth Sciences under contract number EAR 01-35554.

Iron spin transition in Earth's mantle

S. Speziale1*, A. Milner2, V. E. Lee1, S.M. Clark3, M. P. Pasternak2, and R. Jeanloz1
1Department of Earth and Planetary Science, University of California, Berkeley, CA 94720, U.S.A.
2School of Physics and Astronomy, Tel Aviv University, 69978 Tel Aviv, Israel
3Advanced Light Source, Lawrence Berkeley National Laboratory, Berkeley, CA 94720, U.S.A.

High-pressure Mössbauer spectroscopy on several compositions across the (Mg,Fe)O magnesiowüstite solid solution confirms that ferrous iron (Fe^{2+}) undergoes a high-spin to low-spin transition at pressures and for compositions relevant to the bulk of the Earth's mantle. High-resolution x-ray diffraction measurements document a volume change of 4-5 percent across the pressure-induced spin transition, which is thus expected to cause seismological anomalies in the lower mantle. The spin transition can lead to dissociation of Fe-bearing phases such as magnesiowüstite, and it reveals an unexpected richness in mineral properties and phase equilibria for the Earth's deep interior.

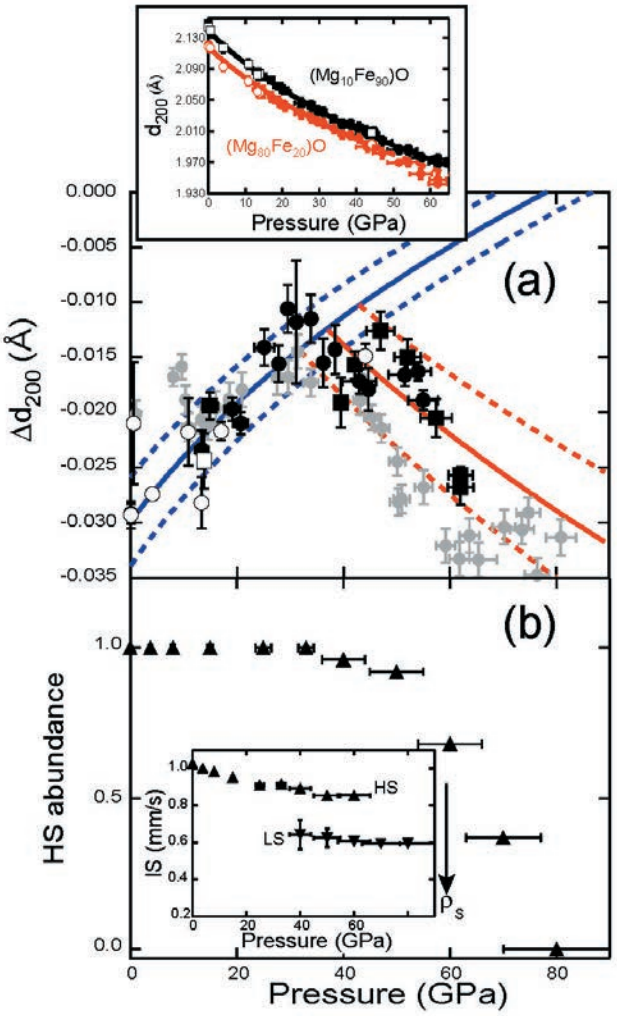

Figure 1(a) Difference in d-spacing for the 200 diffraction lines (Δd200) of $Mg_{0.8}Fe_{0.2}O - Mg_{0.1}Fe_{0.9}O$ magnesiowüstite compositions, measured as a function of pressure at 300 K. Circles indicate experiments with an alcohol mixture as a pressure medium ,and squares refer to experiments for which Ar was the pressure medium; closed symbols are for data collected on compression, and open symbols for data collected on decompression. The blue curve (with estimated 1σ uncertainty shown dashed) is obtained by fitting Δd200 measured at pressures below 35 GPa to a linear dependence of normalized pressure on the Eulerian strain (8, 9). The red line (with 1 σ envelope) is for the finite-strain fit of the observed Δd200 at pressures above 35 GPa. For comparison, the Δd200 calculated from the measurements in ref. 26 on $(Mg_{0.75}Fe_{0.25})O$ are shown in grey (these were not used to constrain the blue and red curves and error envelopes, but show good agreement with our results within mutual uncertainties). The inset shows the absolute d-spacings for the 200 lines of the two compositions: the d-spacings approach each other with increasing pressure up to the spin transition at 35 GPa, and then diverge (i. e., appearance of the low-spin state softens the equation of state of the x = 0.80 composition). (b) Abundance of Fe in the low-spin state, as determined from high-pressure Mössbauer spectra collected from $Mg_{0.8}Fe_{0.2}O$ at 6 K. The inset shows the measured isomer shift (IS) for both low- and high-spin Fe components. Note that the x-ray emission measurements exhibit spectra intermediate between those of high- and low-spin states at pressures of 54-67 GPa for an x = 0.25 sample, in good agreement (within mutual uncertainties of abundances and pressures) with our results. The isomer shift is proportional to the s-electron density at the nucleus (ρ_s), and the large difference observed between the two spin states agrees with the expectation that the radius of the Fe^{2+} ion decreases significantly across the spin transition.

S. Speziale, A. Milner, V.E. Lee, S.M. Clark, M.P. Pasternak, and R. Jeanloz, Iron spin transition in earth's mantle, *Proc. Natl. Acad. Sci. USA*, 102, 17918-17922, 2005.

This research has been supported by the National Science Foundation, Department of Energy and University of California. The Advanced Light Source is supported by the Director, Office of Science, Office of Basic Energy Sciences, Materials Sciences Division, of the U.S. Department of Energy under Contract No. DE-AC03-76SF00098 at Lawrence Berkeley National Laboratory. S. S. is supported by the Miller Institute for Basic Research in Science. The authors acknowledge the use of the facilities of beamline 12.2.2 at the Advanced Light Source, Lawrence Berkeley National Laboratory, and those of the GeoSoilEnviroCARS and the High Pressure Collaborative access Team at the Advanced Photon Source, Argonne National Laboratory. The authors would like to thank Martin Kunz, Sander Caldwell, Haozhe Liu, Madduri Somayazulu, Guoyin Shen and Vitali Prakapenka for their assistance in data collection. We also want to thank Don L. Anderson, Thomas Duffy and Russell J. Hemley for helpful discussions and comments.

High-pressure elasticity of CaO: Comparison between radial diffraction and Brillouin scattering

Sergio Speziale1, Sean R. Shieh2, and Thomas S. Duffy, *Princeton University*

1Now at University of California, Berkeley; 2Now at University of Western Ontario

Single-crystal Brillouin scattering to 25 GPa and powder X-ray diffraction to 65 GPa in a radial geometry were carried out on CaO in a diamond cell. The yield strength of CaO increases from 0.3 to 1.9 GPa in the pressure range between 5.6 and 57.8 GPa. The diffraction elastic constants are in good agreement with Brillouin data and its extrapolation up to 37 GPa. At higher pressures C_{11} appears softer and C_{12} stiffer than the extrapolation of Brillouin results. The value of C_{44} from radial diffraction is in agreement with the Brillouin data through the entire experimental pressure range. The discrepancies between Brillouin and radial diffraction data for C_{11} and C_{12} can be reconciled if α, the parameter which describes degree of stress/strain continuity across the sample's grains boundary decreases to 0.82 at 65.2 GPa. The agreement between the two methods indicates that radial diffraction with lattice strain theory is a valid probe of the mechanical properties of a moderately soft cubic solid as CaO at ultrahigh-pressures. However, more tests are required to quantify the effect of plasticity and texturing on the results of this method.

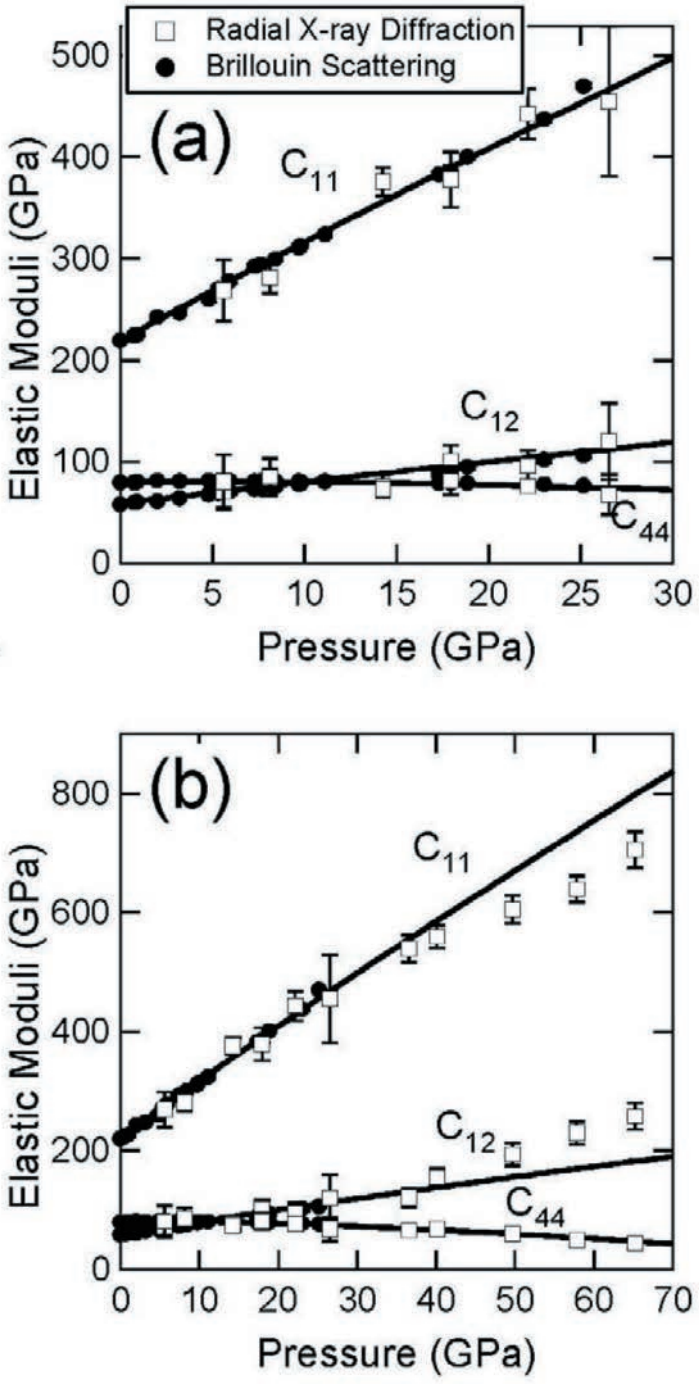

The figures compare elastic moduli of CaO from Brillouin scattering (filled symbols) and radial x-ray diffraction (open symbols). The solid lines are equation of state fits to the Brillouin data.

Speziale, S., S. R. Shieh, and T. S. Duffy, High-pressure elasticity of calcium oxide: A comparison between Brillouin scattering and radial x-ray diffraction, *Journal of Geophysical Research*, B02203, 2006.

This research was supported by the NSF and DOE. Experiments were conducted at the X17C beamline of NSLS which is supported by COMPRES, the Consortium for Material Property Research in the Earth Sciences under NSF Cooperative Agreement EAR01-35554.

Enhanced rotational ordering in molecular C_{60} retrieved from laser driven hypervelocity shock experiments

O. Tschauner1, S.-N. Luo2, T.E. Tierney2, D.C. Swift2, S.J. Chipera2, M. Kunz3, W.A. Caldwell3, S.M. Clark3

1High Pressure Science and Engineering Center and Department of Physics, University of Nevada, Las Vegas, Nevada 89154, U.S.A.
2P-24 Plasma Physics, Los Alamos National Laboratory, Los Alamos, New Mexico 87545, U.S.A.
3Advanced Light Source, Lawrence Berkeley National Laboratory, MS6R2100, Berkeley, CA 94720

C_{60} forms intermolecular bonds by 2+2 cycloaddition [1].This process can be induced by irradiation with light of suitable energy at ambient pressure leading to formation of dimers and oligomers. Cycloadditon also occurs at elevated pressures and temperatures where it yields itinerant polymers [2]. Pressure induced polymerisation is selective with respect to rotational orientation: The energy of binding between adjacent hexagonal faces is lower than for bonds involving pentagonal faces because the former allow for larger bond angles. At ambient pressure molecular C_{60} exhibits partial rotational ordering at 300 K [3]. We performed X-ray diffraction studies at ALS beamline 12.2.2 on C_{60} retrieved from laser driven hypervelocity shock experiments [4] and find rotational ordering enhanced even at 300 K. Ordering occurs in the (111) plane and is accompanied by slight rhombohedral distortion of the cubic metric. Further we observe diffuse scattering at Q-values between the (220) and (311) reflections which is interpreted as result of random polymerisation of C_{60} molecules in the (111) plane. In consequence, the remarkably high degree of rotational ordering in shocked molecular C_{60} is interpreted as result of enhanced lattice strain in the (111) plane induced by random polymerisation. The present findings provide insights into the mechanism of pressure-induced polymerisation of C_{60} and their relation to rotational ordering.

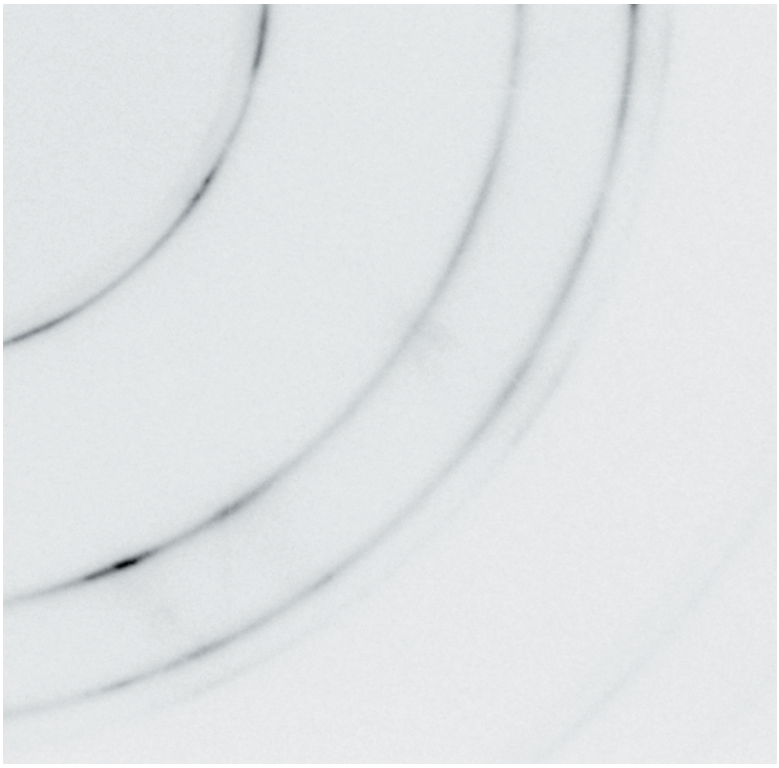

Detail of powder diffraction pattern of shocked molecular C_{60}. Splitting of the (111) reflection (in cubic metric) and pronounced diffuse scattering around (220) and (311) are clearly visible.

1: A.M. Rao et al. Science 259, 955 (1993); 2: Y. Iwasa et al. Science 264, 1570 (1994); 3: H.-B. Bürgi et al. *Acta Cryst*. B 49, 832 (1993); 4: S.-N. Luo et al. High Pressure Research, 24, 409 (2004)

This work was supported by the NNSA Cooperative Agreement DE-FC88-01NV14049. We are grateful for the invaluable support from the Trident laser facility, staff at LANL, and at ALS. The Advanced Light Source is supported by the Director, Office of Science, Office of Basic Energy Sciences, Materials Sciences Division, of the U.S. Department of Energy under Contract No. DE-AC03-76SF00098 at Lawrence Berkeley National Laboratory.

Studies of the ratio of ferrous and ferric iron in Magnesium-silicate perovskite

O.Tschauner *High Pressure Science and Engineering Center and Department of Physics, University of Nevada, Las Vegas*, **J.M. Jackson, W. Sturhahn, J. Zhao** *Argonne National Laboratory, Experimental Facilities Division*

The 'redox' state of the Earth's lower mantle is mainly constrained by the oxidation state of Fe. This is because Fe is the most abundant oxidizeable element in Mantle and Core. During formation of the Earth's core conditions must have been very reducing. However, it has been inferred from experiments that either the effective redox conditions in the present lower mantle are much more oxidizing or that disproportionation of Fe^{2+} into metallic iron and Fe^{3+} occurs under the high pressures of the lower mantle. This has significant influence on the chemical and physical properties of the Earth.
In apparent contradiction to these results, there are findings suggesting that the presence of Fe^{3+} is not the result of pressure induced changes in redox-potentials: a) The fraction of Fe^{3+} in MgSi-pervoskites with different Fe-contents remains constant as function of pressure, b) sound-velocities extracted from sidebands of nuclear resonant peaks of ^{57}Fe are inconsistent with bulk sound-velocities of MgSi-perovskite, c) Fe-bearing silicate perovskite synthesized by CO_2-laser heating of samples in equilibrium with iron is colourless or greenish. Therefore, we conducted experiments on MgSi-perovskite heated with CO_2-lasers at 30, 50, and 70 GPa in contact with metallic ^{57}Fe in order to examine the Fe^{2+}/Fe^{3+} ratio in silicate perovskite synthesized under conditions of Fe-metal silicate coexistence using the resonant nuclear forward scattering method. The experimental geometry of the synthesis experiments was the same as in.
It turned out that the conditions during the experiment were so reducing that the final Fe-content of the perovskite sample was markedly lower than in the starting material, the nuclear resonance signal was rather low and too noisy to clearly determine the Fe^{2+}/Fe^{3+} ratio from such small samples.

C.A. McCammon (1997). Perovskite as a possible sink for ferric iron in the lower mantle. *Nature* 387, 694-696

D.J. Frost et al. (2004). Experimental evidence for the existence of iron-rich metal in the Earth's lower mantle. *Nature* 428, 409-412

J.M. Jackson, W. Sturhahn, G. Shen, J. Zhao, M.Y. Hu, D. Errandonea, J.D. Bass, Y. Fei (2005), *Am.Min*. 90 (1), 199-205 (2005);
O.Tschauner et al. (1999) Partitioning of nickel and cobalt between silicate perovskite and metal at pressures up to 80 GPa. *Nature* 398, 604-607

This work was supported by the NNSA Cooperative Agreement DE-FC88-01NV14049. Use of sector 3 was supported by NSF and DOE-BES under Contract No. W-31-109-Eng-38 and by COMPRES

Compressibility of Hydrated and Anhydrous Na_2O-2SiO_2 Liquid, and Glass to 8 GPa using Brillouin Scattering

Sergey N. Tkachev, Murli H. Manghnani *University of Hawaii*
Quentin Williams *University of California Santa Cruz*
Li Chung Ming *University of Hawaii*

Brillouin scattering measurements have been carried out on a sodium disilicate aqueous solution and anhydrous sodium disilicate glass and liquid under in situ pressures to 8 GPa in the temperature range from 300 to 850 K. This temperature range spans through the glass transition of both the hydrous and anhydrous forms. The "modified" platelet scattering geometry has allowed us for the first time to determine sound velocity independently from refractive index, and hence the adiabatic compressibility and density of liquids as a function of pressure and temperature. The observed increase in density of the melt and glass phases formed at high P-T conditions is likely associated with structural effects. There is a marked change in pressure derivative of adiabatic bulk modulus between the two phases. The large values of the adiabatic bulk modulus of the liquid phase illustrate that the means of compaction of the liquid differs substantially from that of the glass, and that the liquid is able to access a wider range of compaction mechanisms. The measured bulk modulus of the aqueous sodium silicate solution is highly temperature dependent, but is much more similar to values of silicate melts than to that of end-member water, particularly at high pressures. Thus, water-rich silica-bearing solutions are likely to be difficult to distinguish from anhydrous silicate melts based solely upon their elasticity.

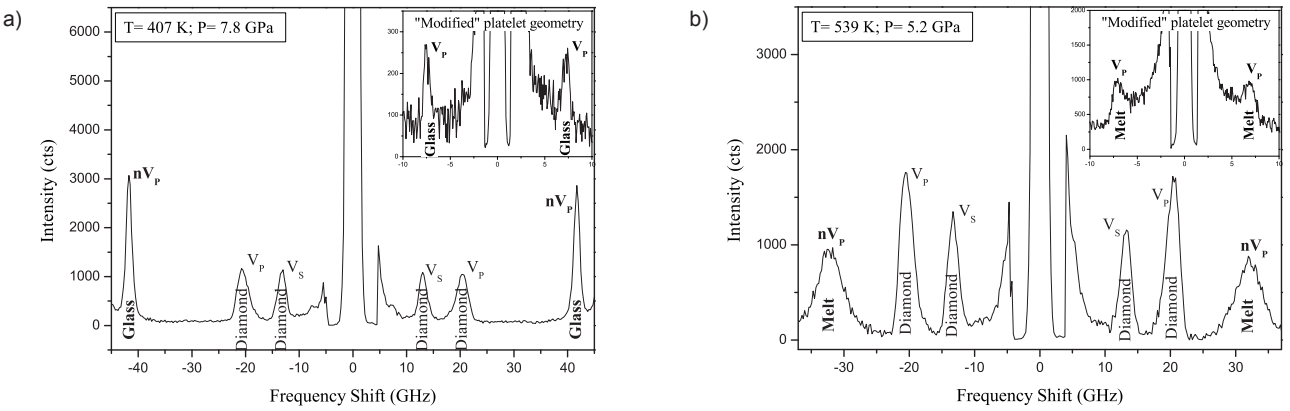

Brillouin spectra of hydrated Na_2O-SiO_2 glass and melt below (a) and above (b) glass transition temperature. Insets are the Brillouin spectra in "modified" platelet scattering geometry.

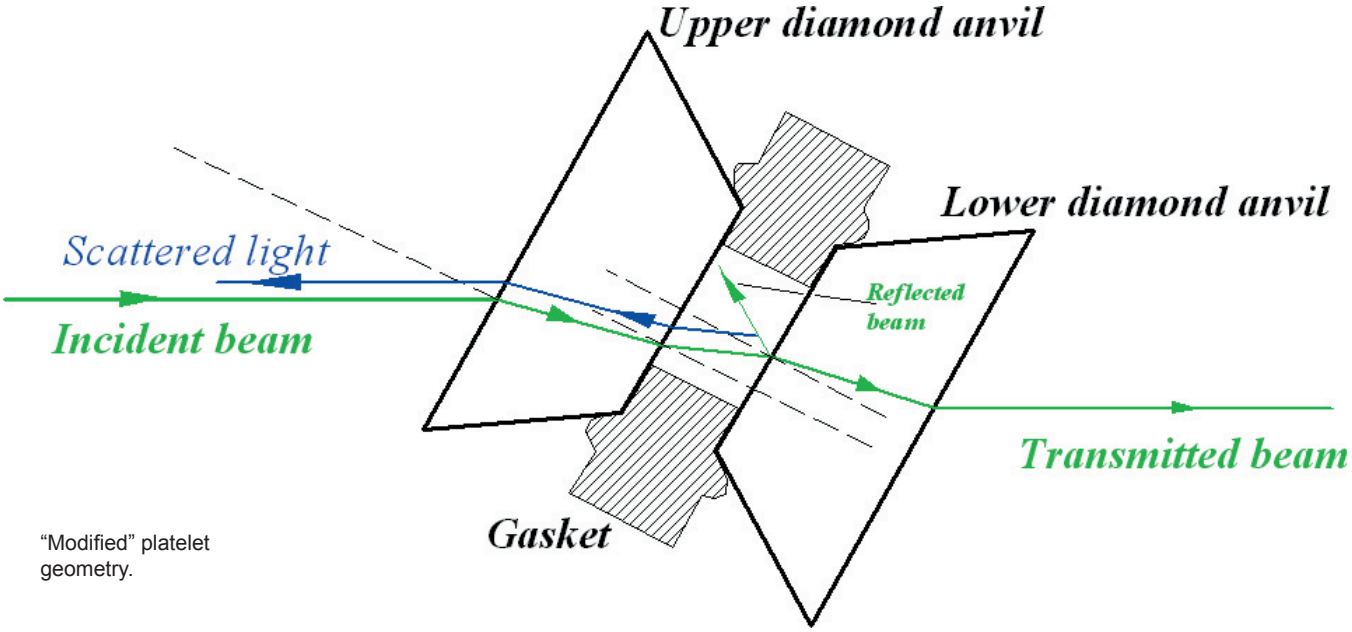

"Modified" platelet geometry.

Tkachev S.N., Manghnani M.H., Williams Q., Ming L.C., Compressibility of Hydrated and Anhydrous Na_2O-2SiO_2 Liquid and also Glass to 8 GPa Using Brillouin Scattering, *J. Geophys. Res*., 110, B07201, 2005.

This work has been carried out under the National Science Foundation Grant No. EAR-0074285, and partially supported by Federal Highway Administration Contract DTFH61-94-X-00020 and U. S. Army/TARDEC Contract DAAE07-01-L055. SOEST contribution number: 6564 and HIGP Contribution # 1379.

Thermoconsolution of the K-Na chlorides

Walker D *Lamont-Doherty Observatory, Columbia U.* **Verma PK** *Delhi University* **Cranswick LMD** *NRC, Chalk River Lab*
Clark SM *ALS, Lawrence Berkeley Lab* **Jones RL** *CLRC, Daresbury Lab* **Buhre S** *Frankfurt University*

Detailed volume systematics and 2-phase equilibrium pairs were observed across the halite-sylvite solvus at pressures up to 18 kbar. High-T thermal expansions at 1 bar across this series provide an explanation of the shift of the solvus crest with pressure that was actually observed. Excess volume systematics are strongly dependent on P&T, a complexity that is usually ignored in thermodynamic treatments for lack of information. The excess volumes of the chlorides peak in the consolute region in a deficient manner suggestive of a high concentration of vacancy defects. Full P, V, T, X, G, H, and S mixing systematics were recovered.

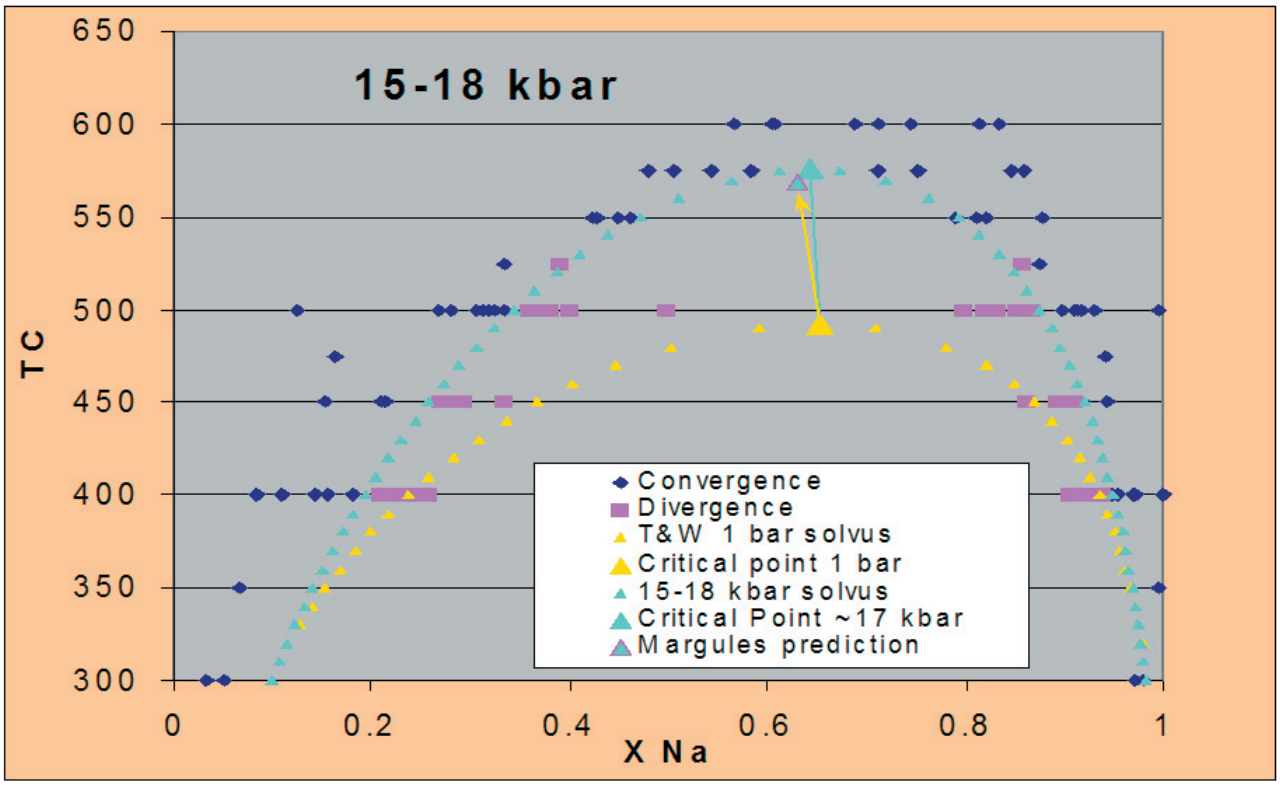

D Walker, PK Verma, LMD Cranswick, SM Clark, and S. Buhre (2004) Halite-sylvite thermoelasticity, *American Mineralogist*, **89,** 204-210.
D Walker, PK Verma, LMD Cranswick, SM Clark, RL Jones, and S. Buhre (2005) Halite-sylvite thermoconsolution, *American Mineralogist*, **90**, 229-239.

High-T thermal expansions were measured on ALS beamline 7.3.3. High-P&T volumes were measured on Daresbury station 16.4. This work was supported by the COMPRES initiative, by CRLC Daresbury, by the National Science Foundation under grant EAR02-07546 to DW, and by the Advanced Light Source, which is supported by the Director, Office of Science, Office of Basic Energy Sciences, Materials Sciences Division, of the U.S. Department of Energy under Contract No. DE-AC03-76SF00098 at Lawrence Berkeley National Laboratory.

Excess volumes in pyrope-grossular garnets

Walker D *Lamont-Doherty Observatory, Columbia U.* **Clark SM, Caldwell WA** *ALS, Lawrence Berkeley Lab* **Kunz M** *COMPRES/ALS, Lawrence Berkeley Lab*

The study of halite-sylvite chlorides showed that excess volumes were strongly T and P dependent when measured in situ at P and T, but that those excesses were not quenchable. In contrast there are very large systematic differences in quenched excess volumes in the pyrope-grossular garnets prepared in piston/cylinder (PC), multianvil (MA), or diamond anvil (DAC) devices. The systematics of our quenched excess volumes from MA and DAC are much greater and better behaved than in literature PC syntheses. These results suggest that disorder may be possible after all in this series even though previous attempts to identify it have met with quite modest success.

DAC-quenched excess volumes were measured on ALS beamline 12.2.2. MA-quenched excess volumes were measured on Daresbury station 16.4.

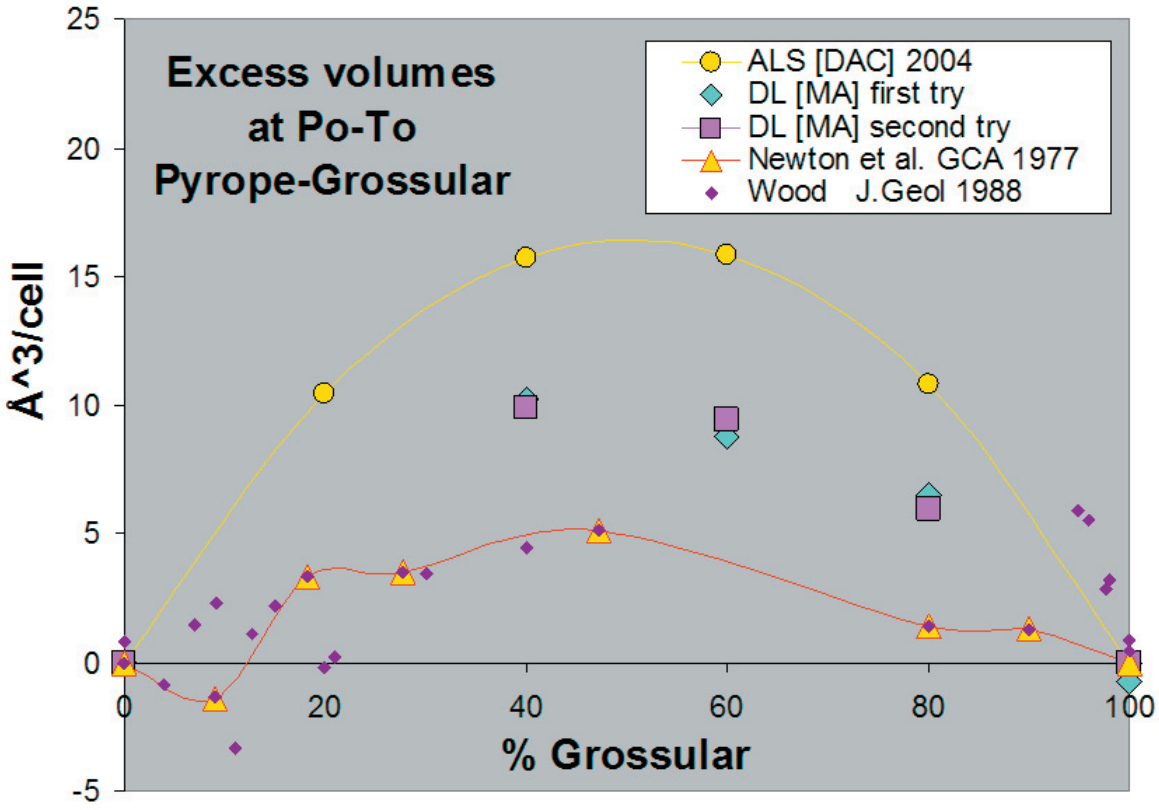

This work was supported by the COMPRES initiative, by CRLC Daresbury, by the National Science Foundation under grant EAR02-07546 to DW, and by the Advanced Light Source, which is supported by the Director, Office of Science, Office of Basic Energy Sciences, Materials Sciences Division, of the U.S. Department of Energy under Contract No. DE-AC03-76SF00098 at Lawrence Berkeley National Laboratory.

High Spatial Resolution X-ray absorption Imaging on ALS 12.2.2

Walker D *Lamont-Doherty Observatory, Columbia U.* **Clark SM** *ALS, Lawrence Berkeley Lab* **Kunz M** *Compres/ALS, Lawrence Berkeley Lab* **Walter MJ** *ALS, Lawrence Berkeley Lab & Bristol U*

ALS beamline 12.2.2 has been enhanced with the capacity to make 1-2 micron spatial resolution X-ray absorption images. Thin phosphor imaging screens and low-divergence X-ray illumination are key attributes of the system conducive to high resolution images. Our objective has been to use the imaging system to observe diamond anvil cell (DAC) experiments in progress. Laser heating to first melting of the interface between spatially-resolved crystalline starting materials produces liquids saturated in both phases. The spatial distribution of reactants and product liquids yield the sign of the melting reaction. In binary systems like Fe-FeS or Fe-FeO, the image density can be used to determine liquid chemistry. The figure shows this sort of approach to DAC melting in Fe-FeS.

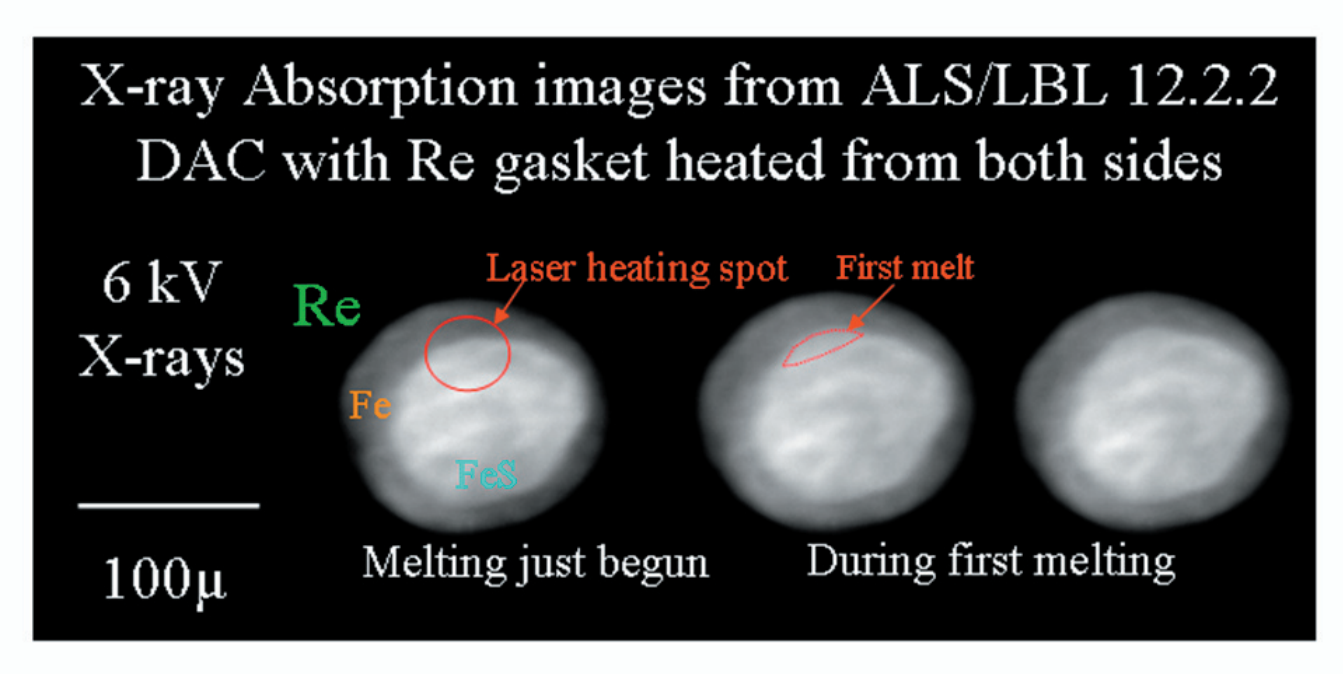

Walker D (2005) Core-mantle chemical issues. *Canadian Mineralogist*, (Fleet volume), 43(5), 1553-1564.

Imaging experiments were conducted on ALS beamline 12.2.2. We are very grateful for the development work to make possible the imaging system on 12.2.2 by R. Celestre, A. McDowell, E. Doming, and W.A Caldwell. This work was supported by the COMPRES initiative, by the National Science Foundation under grant EAR02-07546 to DW, and by the Advanced Light Source, which is supported by the Director, Office of Science, Office of Basic Energy Sciences, Materials Sciences Division, of the U.S. Department of Energy under Contract No. DE-AC03-76SF00098 at Lawrence Berkeley National Laboratory.

Elastic properties of hydrous ringwoodite at high pressures

Jingyun Wang, Stanislav V. Sinogeikin, Jay D. Bass · *University of Illinois at Urbana-Champaign Toru Inoue · Ehime University*

Phase transitions among olivine and its high pressure polymorphs, wadsleyite and ringwoodite, are thought to be responsible for the seismic velocity discontinuities in the transition zone of the mantle (400~660 km). Measurements of sound velocities in these minerals are therefore necessary to interpret seismological information on these discontinuities in terms of transition zone composition and temperature. Recent studies have demonstrated that ringwoodite can contain up to ~3% H_2O by weight, thereby making it possible to store vast quantities of water in the transition zone. It has also been shown that the incorporation of water into the crystal structure of ringwoodite results in a substantial decrease in the elastic moduli. However, there is little experimental data on the elasticity of hydrous ringwoodite under high pressure conditions. In this study we have measured the effect of pressure on sound velocities and elastic moduli of hydrous ringwoodite by Brillouin scattering. These results show how hydration affects the sound velocities of ringwoodite at high-pressures. Single crystals of hydrous Mg end-member ringwoodite containing 2.3wt% H_2O were synthesized in a multi-anvil press at 19 GPa and 1300ºC. The sound velocities and single-crystal elastic moduli of this hydrous ringwoodite were measured by Brillouin spectroscopy at pressures up to 23.4 GPa. Our results indicate that water does not significantly affect the pressure derivatives of the bulk modulus, Ks', or the shear modulus, G'. Based on the elastic properties measured at high-pressure conditions, it appears that hydration does not significantly change the velocity contrast between olivine and ringwoodite and velocity gradient of ringwoodite between dry and wet mantle conditions.

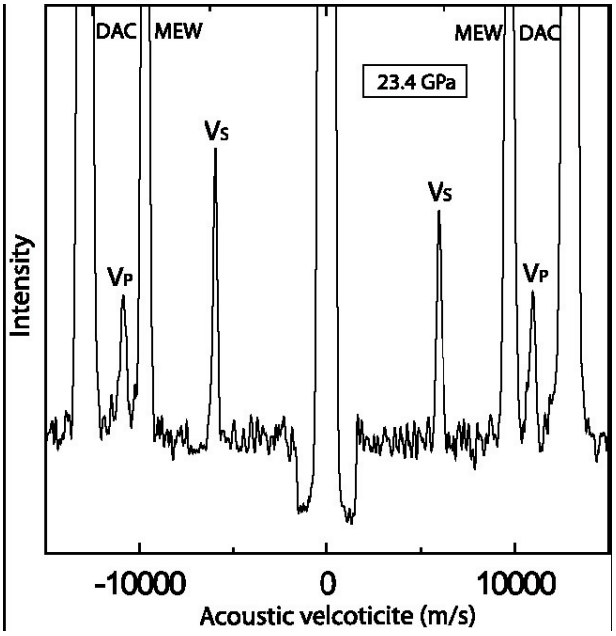

Typical Brillouin spectrum for hydrous ringwoodite measured at 23.4 GPa in the scattering plane (-0.1513, 0.7542, -0.6390). Symbol in the figure: V_P and V_S – compressional and shear modes of hydrous ringwoodite; DAC – shear mode of diamond; MEW – compressional mode of MEW.

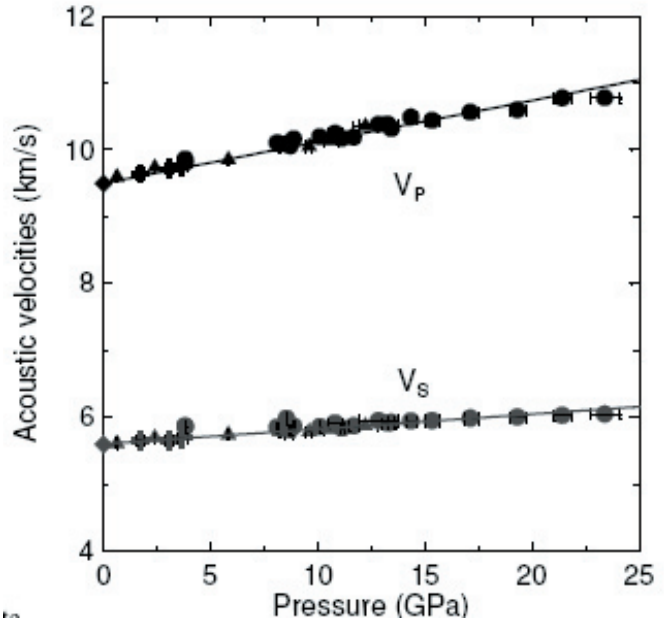

Acoustic properties of hydrous ringwoodite as a function of pressure. Symbols in the figure: diamond – ambient condition; circle – MEW; triangle – Argon; cross – fluorinet. Straight lines: linear fitting curves with fixed values at room pressure.

Reference: J. Wang, S. Sinogeikin, T. Inoue, J. D. Bass, Elastic properties of hydrous ringwoodite at high pressure conditions, in preparation.

Acknowledgements: This study is supported by the National Science Foundation under the Grants EAR-0112376 and EAR-=0003383.

IR measurements on hydrous wadsleyite

Jingyun Wang, Carmen Sanchez-Valle, Stanislav V. Sinogeikin, Jay D. Bass · *University of Illinois at Urbana-Champaign*
Zhenxian Liu · *Geophysical Laboratory*
Toru Inoue · *Ehime University*

Wadsleyite, -$(Mg,Fe)_2SiO_4$, is one of high pressure polymorphs of olivine. Phase transitions among olivine and its high-pressure polymorphs, wadsleyite and ringwoodite, and -$(Mg,Fe)_2SiO_4$, are thought to be responsible for the seismic velocity discontinuities in the transition zone of the mantle (~400-660 km in depth). Wadsleyite and ringwoodite can contain up to 3 wt% H_2O in their crystal structures, which may be the largest H reservoir in the mantle. H incorporation may play significant influences on many physical properties and processes. Quantitative measurement of H in minerals is prerequisite to constrain the extent of hydration effect on variations of physical properties and estimate the budget of H in the mantle. Current concentration of H or H_2O results from different methods, Secondary Ion Mass Spectrometry (SIMS) and Fourier Transform Infrared Spectroscopy (FTIR), are not consistent. Calibration between these 2 methods on wadsleyite has not been done. The water content of present hydrous wadsleyite was determined to be about 2.16(9) wt% by SIMS. Samples were polished with parellel surfaces normal to one principle axes. Unpolarized and polarized IR spectra were collected at the U2A beam line of NSLS. The results are shown in Fig. 1 and Table 1. Current results show IR measurement produces ~1wt% water content which is lower than 2.16wt% obtained from SIMS. The discrepancy may be explained by overestimation of water content from SIMS due to melt/fluid inclusions, boundary water, matrix effect, or underestimation from IR due to inappropriate application of Paterson's calibration on the case of wadsleyite. It is important problem to resolve which method tells the truth.

Table 1 H2O concentration from IR measurements.

Orientation	H_2O (wt%)			
	HyBt1	HyBt4	HyBt6	HyI
Unpolarized	>1.36	1.06	>0.93	0
E//[100]		0.29	>0.29	0
E//[010]	>0.35		>0.29	0
E//[001]	>0.37	>0.41		

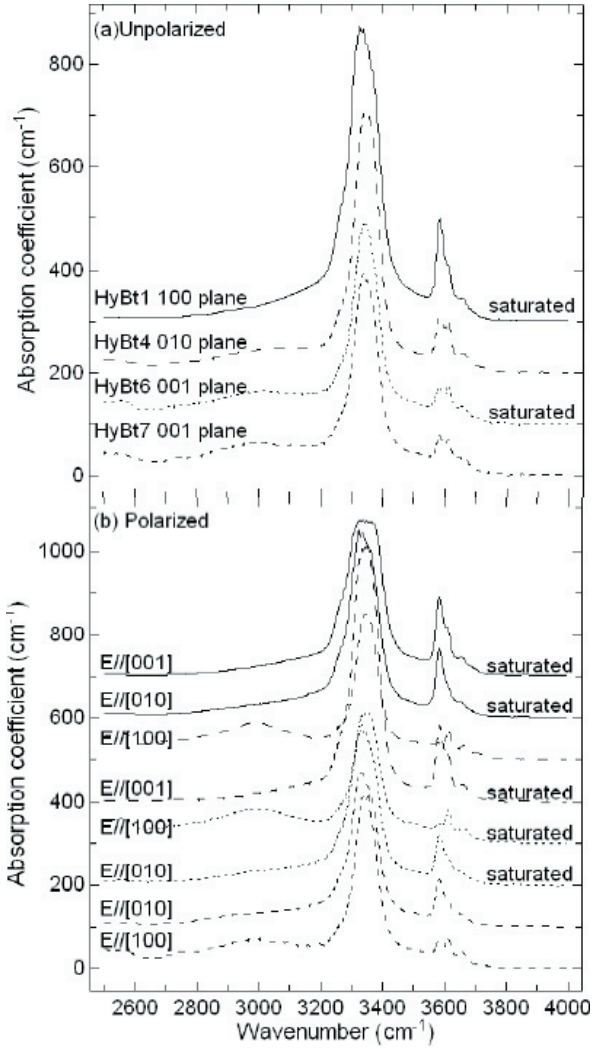

Fig. 1 FTIR spectra of hydrous wadsleyite. (a) Polarized spectra for HyBt1 (solid line), HyBt4 (long dash line), HyBt6 (dot line), and HyBt7 (short dash line). (b) Unpolarized spectra using same symbol as (a).

Reference: J. Wang, C. Sanchez-Valle, Z. Liu, S. Sinogeikin, T. Inoue, J. D. Bass, IR measurement on hydrous wadsleyite, in preparation.

Acknowledgements: This study is supported by the National Science Foundation under the Grants EAR-0112376 and EAR-0003383.

Synthesis and Characterization of a New Class of Ultra-incompressible Hard Materials

Michelle Weinberger, Robert Cumberland, Jonathan Levine, Richard Kaner, and Sarah Tolbert
UCLA Department of Chemistry and Biochemistry
Abby Kavner--*UCLA Earth and Space Sciences*
John Gilman--*UCLA Materials Science and Engineering*
Simon Clark--*Advanced Light Source, LBNL*

Ultra-incompressible, i.e. high bulk modulus, hard materials are of great interest due to their usefulness in a wide variety of industrial applications. These include abrasives, cutting tools, and coatings where wear prevention, scratch resistance, surface durability and chemical stability are a priority. To this end, we have developed a methodology to synthesize a new class of ultra-incompressible, hard materials through the optimization of valence electron density and bond covalency. The first member of this class of materials, osmium diboride (OsB_2), has been characterized via conventional diamond anvil cell high pressure experiments, by radial diffraction experiments, and by nanoindentation.

Most impressively, OsB_2 has a bulk modulus of between 365-395 GPa, where the c-axis is less compressible than the linear compressibility of diamond (see Figure 1), a hardness of greater than 25,000 kg/mm^2, and the highest elastically supported differential stress (the lower bound to yield strength) of any reversibly compressible material ever measured (see Figure 2).

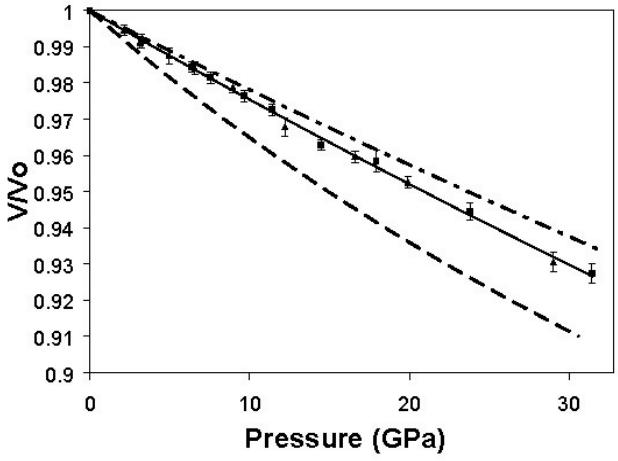

Figure 1: Pressure vs. fractional unit cell volume for OsB_2 (■ and ▲), corundum (— —), and diamond (— • —).[19] Both experimental and literature curves correspond to the third-order Birch-Murnaghan equation of state:
P = (3/2)Bo[(V/Vo)-7/3 – (V/Vo)-5/3]{ 1 – (3/4)(4 – Bo')[(V/Vo)-2/3 – 1]}

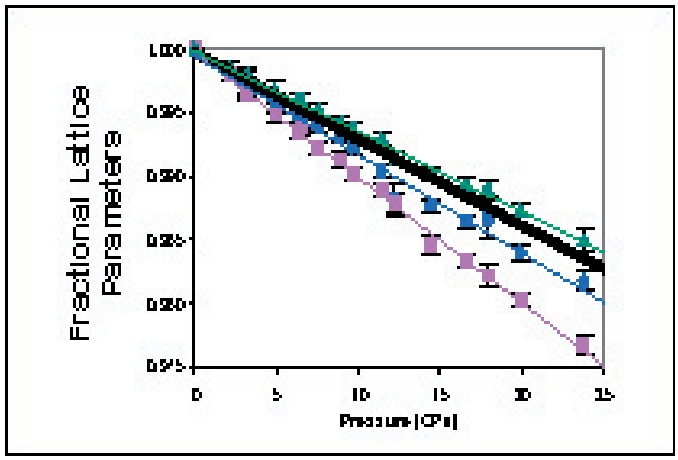

Figure 2: Comparison of the compressibility of the individual lattice parameters of OsB_2 with diamond. The a (pink), b (blue) and c (green) parameters in OsB_2 are fit to a straight line. The black line is the linear compressibility of diamond. Note that the c-axis in OsB_2 is less compressible than diamond.

Cumberland, R.W., Weinberger, M.B., Gilman, J.J., Clark, S.M., Tolbert, S.H., Kaner, R. *J. Am. Chem. Soc.*, 127(20), 7264-7265 (2005).

Weinberger, M.B., Cumberland, R.W., Levine, J.B., Conil, N., Shahar, A., Kaner, R.B., Tolbert, S.H., Kavner. A. "Strength of Osmium diboride under high pressure and nonhydrostatic stress". (manuscript in preparation for submittal to *Phys. Rev. B*.)

This work was supported by the National Science Foundation Division of Materials Research (RBK), NSF-CMS 0307322 (SHT), NSF-EAR 0440332 (AK) and the Sloan Foundation (SHT). Data was collected on Beamline X17C at the NSLS and 11.3.1 at the ALS with many thanks to Jingzhu Hu, Martin Kunz and Sirine Fakra. Use of the National Synchrotron Light Source, Brookhaven National Laboratory, was supported by the U.S. Department of Energy, Office of Science, Office of Basic Energy Science, under Contract No. DE-AC02-98CH10886. Use of the Advanced Light Source is supported by the Director, Office of Science, Office of Basic Energy Sciences, Materials Sciences Division, of the U.S. Department of Energy under Contract No. DE-AC03-76SF00098 at Lawrence Berkeley National Laboratory.

The Coesite to Stishovite Transition, Ancient Subduction, and the 300 km Seismic Discontinuity

Q. Williams, *UC Santa Cruz and* **J. Revenaugh**, *U. Minnesota*

Using phase equilibria and elasticity data on coesite and stishovite, we demonstrate that the amount of free silica expected within subducted material of basaltic chemistry (5-10 wt%) at high pressures will produce a velocity contrast near 300 km depth of 1-2.5%, and impedance contrasts of 2-5%. Approximately a dozen seismic studies have observed a velocity contrast near this depth in over thirty locations. Thus, the presence and amplitude of this seismic feature provide a means for determining how much subducted, or delaminated, formerly basaltic material is present at deep upper mantle depths, and yields a measure of mantle geochemical heterogeneity.

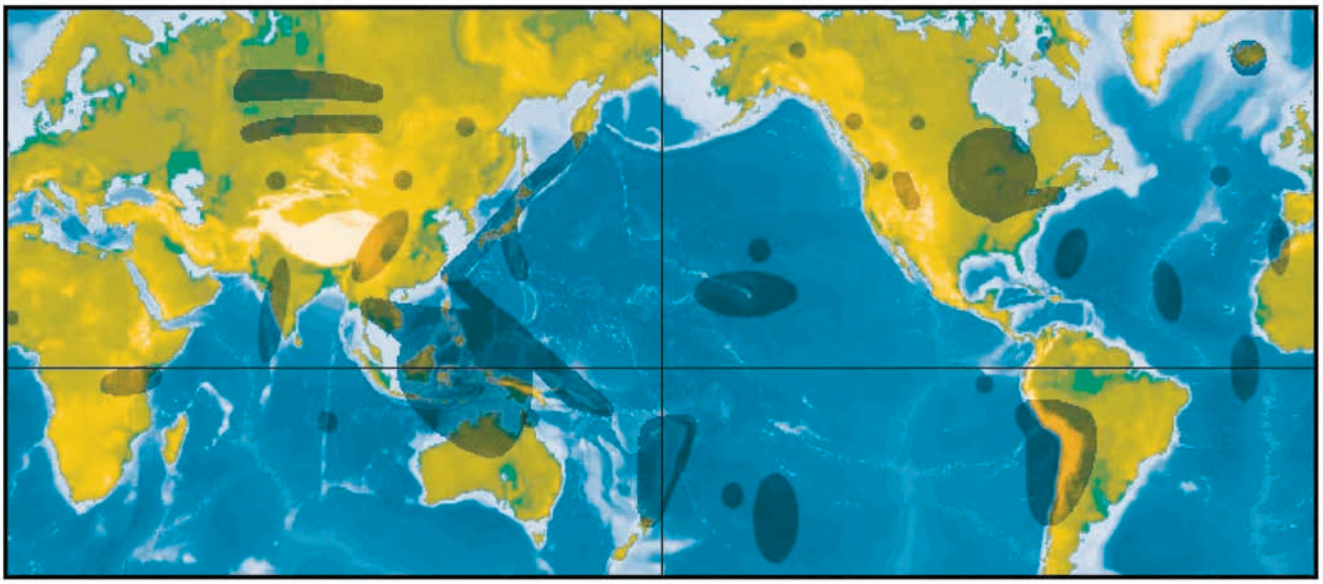

Global distribution of locations (dark regions) where the ~300 km discontinuity has been observed

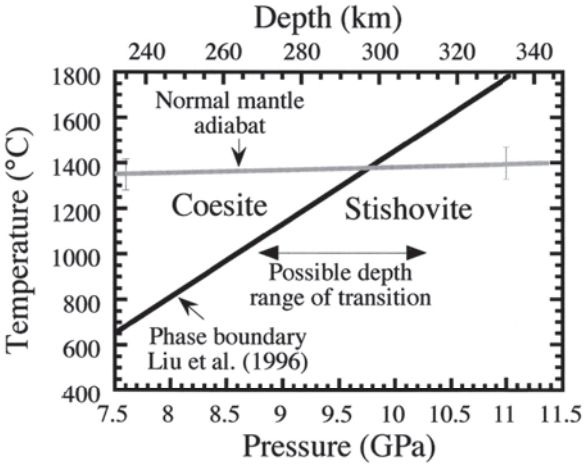

Pressure vs. Temperature dependence of phase boundary between coesite and stishovite (Liu et al., 1996).

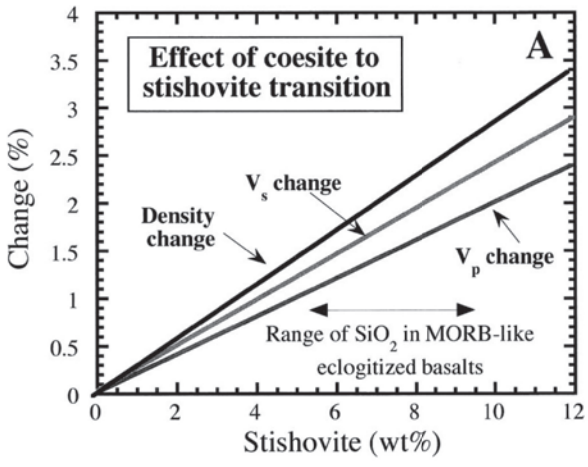

Seismic velocity and density changes associated with the coesite to stishovite transition as a function of the free silica content of eclogites with approximately basaltic chemistry.

Liu, J. et al., Calorimetric study of the coesite-stishovite transformation and calculation of the phase boundary, *Phys. Chem. Minerals*, 23, 11-16, 1996.
Williams, Q. and J. Revenaugh, Ancient subduction, mantle eclogite, and the 300-km seismic discontinuity, *Geology*, 33, 1-4, 2005.

Work supported by NSF grant EAR-0310342. This study was made possible by the existence of elastic and phase equilibria data of the type enabled by the COMPRES consortium.

Simultaneous Sound Velocity and Equation of State Measurement on MgO and Evaluation of NaCl Pressure Scale

Kelly Woody *Tennessee Department of Environment and Conservation, Division of Water Supply*

Baosheng Li *State University of New York at Stony Brook*

We measured P and S wave velocities and equation of state of MgO to conditions of 10.5 GPa and 1000^{0}C using silmultaneous ultrasonic interferometry and in-situ-X-ray diffraction techniques with a DIA-type multi-anvil high pressure apparatus (SAM85) installed at the superconducting wiggler beamline at the National Synchrotron Light Source (NSLS, X17B1). The polycrystalline specimen was hot-pressed using a 1000-ton uniaxial-split-sphere apparatus (USCA-1000) at a pressure of approximately 8 GPa and 1400^{0}C. The bulk density of the sample, 3.566 g/cm^3, is within 99.5 % of the x-ray density. Acoustic measurements at ambient pressure and temperature yield values for VP and VS of 9.78 ± 0.008 and 6.00 ± 0.005 km/s, respectively. The calculated values of the elastic moduli, KS and GS of 166.8 ± 4 and 128.6 ± 3, respectively, aggress with previously published data within 1 %. A third order Birch Murnaghan equation of state fit to the unit cell volumes at high pressure and room temperature yields a value for KT that is within 1 % of previously published data. X-ray imaging system allows us to monitor the length of the MgO specimen during the experiment at each P-T condition. Although the sample underwent plastic deformation at temperature above 800^{0}C as indicated by imaging data, acoustic velocities at high pressure and high temperature were determined precisely using sample lengths obtained from X-ray images. By combining acoustic and unit cell volume data, the elastic moduli as well as their pressure dependence determined by fitting velocity data to Eulerian Finite Strain equations without using a secondary pressure standard. Sample pressures calculated from these results are compared with these obtained using NaCl during the experiment.

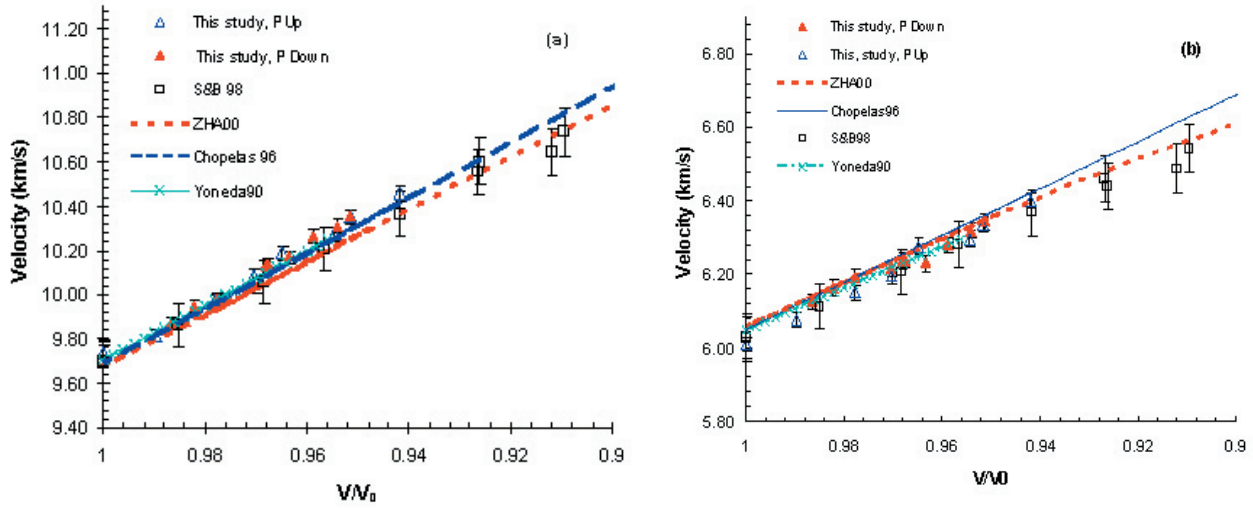

P wave (a) and S wave (b) velocities as a function of volumetric compression at 300K. Previous measurements at pressures comparable to and higher than the present study are also shown for comparison. ZHA00-Zha et al. (2000); Chopelas96: Chopelas (1996); S&B98: Sinogeikin and Bass (1998); Yoneda90: Yoneda (1990).

Li, B., K. Woody, and J. Kung. Elasticity of MgO to 11 GPa Based on Direct Measurement of Sample Pressure: Insights on Current Pressure Scales. Submitted to *Journal of Geophysical Research*, December 2005.

This study was funded by grants EAR 0003340 and EAR 00135550 to Dr. Baosheng Li. The insitu ultrasonic and X-ray experiments were carried out at the X17B1 beamline of the National Synchrotron Light Source (NSLS), which is supported by the US Department of Energy, Division of Materials Sciences and Division of Chemical Sciences under Contract No. DE-AC02-76CH00016 and by COMPRES, the Consortium for Materials Properties Research in Earth Sciences under contract number EAR 01-35554.

Image Processing for Melts Density Measurement at High Pressures

Christopher E. Young *COMPRES Beamline Intern,* **Jiuhua Chen** *Stony Brook University*

Using MATLAB it has become possible to perform a nonlinear regression for a whole image for deriving melts density based on sample x-ray absorption contract to the reference material. Before it was only possible to fit a one dimensional slice, with the new fitting scheme we can further constrain the fitting and produce more accurate results for melts density measurement at high pressures. Using simple image analysis we can also process sequential data set of a few hundred x-ray radiographs for deriving viscosity of melts in falling sphere experiments. As long as the sphere and the surrounding melt have sufficient contrast, data analysis for the sphere velocity can be done within a minute.

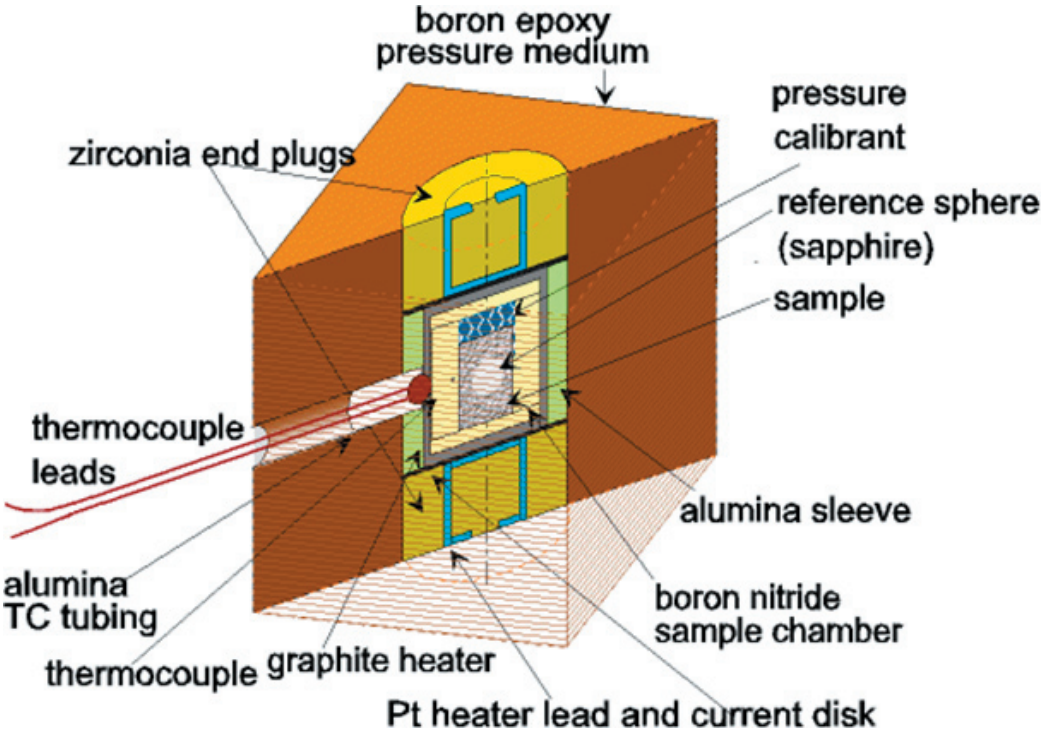

High Pressure cell assembly for melt density measurements in a cubic-type DIA apparatus.

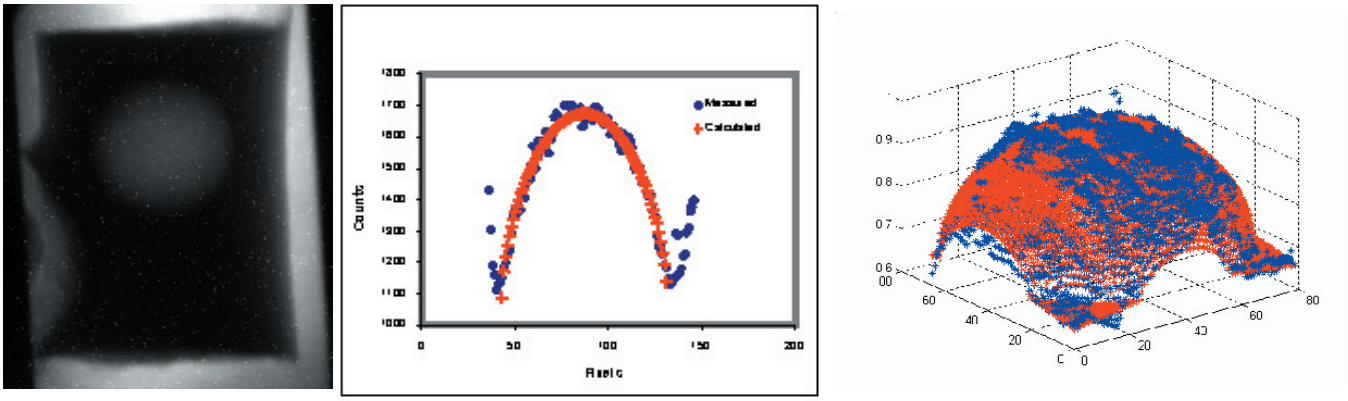

The left image is an example of the x-ray radiographs used to determine the melt density. The center is a fitting just using one column of two-dimensional data. The right is a typical fitting of the intensity of the entire x-ray radiograph. The blue points are the radiograph, the red points are the fitted data.

Chen, Jiuhua, Donald J. Weidner, Liping Wang, Michael T. Vaughan, and Christopher E. Young, Density measurements of molten materials at high pressure using synchrotron x-ray radiography: Melting volume of FeS, in *Advances in High-Pressure Technology for Geophysical Applications,* Eds. J. Chen, Y. Wang, T.S. Duffy, G. Shen and L.F. Dobrzhinetskaya, ELSEVIER, Amsterdam, pp. 185-194 (2005).

This study was supported by the National Science Foundation under grants EAR039879 to JC and COMPRES beamline internship program to CEY. The in situ x-ray experiments were carried out at the X-17B2 beamline of the National Synchrotron Light Source (NSLS) which is supported by the US Department of Energy, Division of Materials Sciences and Division of Chemical Sciences under Contract No. DE-AC02-76CH00016 and by COMPRES, the Consortium for Materials Properties Research in Earth Sciences under contract number NSF Cooperative Agreement EAR 01-35554.

Compressibility of liquid FeS by radiograph imaging

Tony Yu, Jiuhua Chen *Stony Brook University*

A new technique for density measurement of molten materials in a multi-anvil press using synchrotron x-ray radiography is described. This technique takes advantage of a linear conversion of x-ray intensity to radiograph brightness, and records two-dimensional variations in transmitted x-ray intensities across a reference sphere in the sample on a single exposure. Comparing with the existing technique of one-dimensional scan using a small beam of x-rays for the melt density measurement at high pressure, this method gains a shorter data collection time and larger data coverage (two-dimensional). By combining the radiograph technique at the NSLS and the radiograph image fitting method developed by our group at Stony Brook, we have derived density numbers of molten FeS which remains under 2% after multiple fittings of the same sample image. The isothermal density compression curve of liquid FeS up to 5.6GPa has been determined by this experiment. This study has also derived a 4.25g/cm3 zero pressure density and a 14.6GPa isothermal bulk modulus at 1673K for liquid FeS.

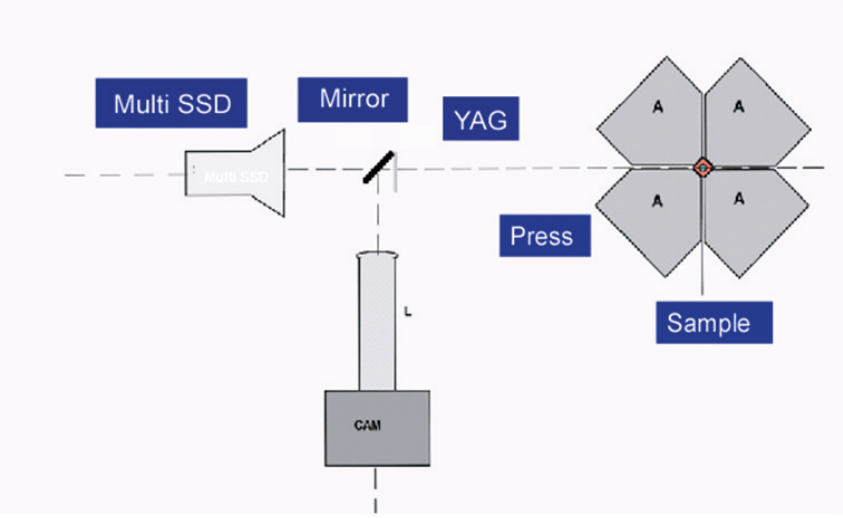

The radiograph system at Beamline X17B2, NSLS at the Brookhaven National Laboratory is an add-on system attached to the in situ x-ray beamline setup. It includes a YAG crystal as a fluorescent screen, an optical mirror, focusing-magnification lenses, and a CCD camera and/ or a video camera. The x-ray beam penetrates through the sample and impinges on the fluorescent screen, where a visible sample image based on the intensity of the transmitted x-ray is generated. The contrast of the image depends on the density difference, the mass absorption difference, and the thickness difference between the sample and the cell assembly parts.

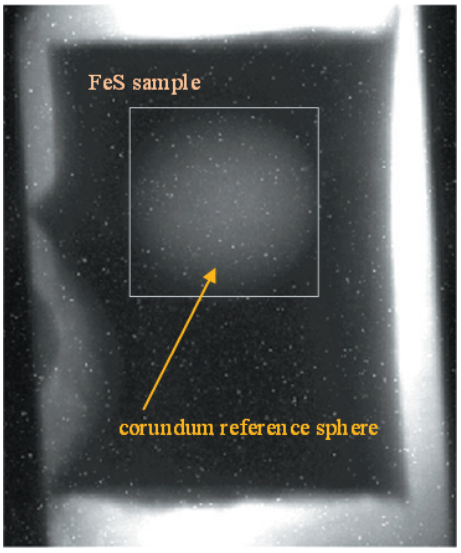

An x-ray radiograph image of the high pressure cell between the WC anvils recorded by the CCD camera. It clearly shows the corundum reference sphere (bright circle) sitting inside the FeS sample powder (dark area).

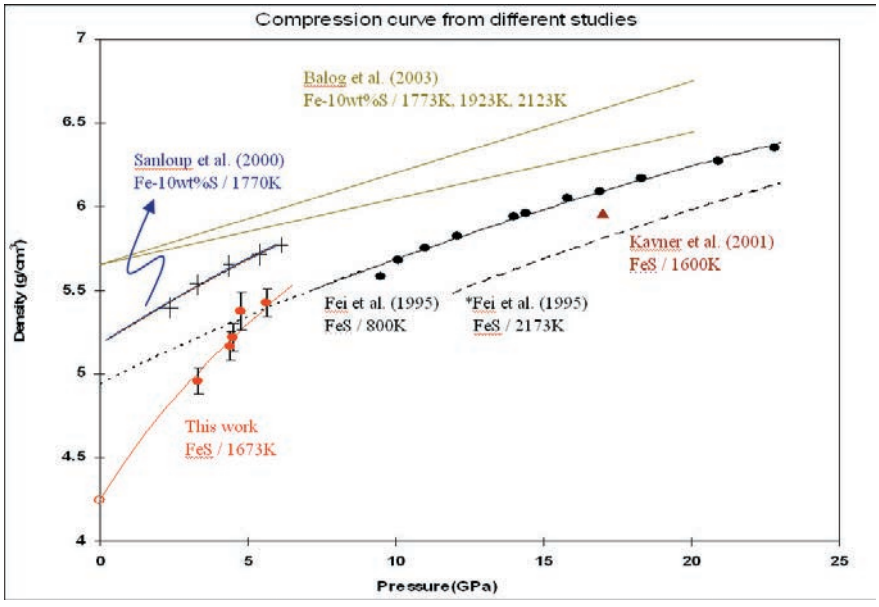

Density measurements of Fe-S alloys from different experimental studies. Kavner (2001) and Fei (1995) are solid state FeS density measurements. Others are liquid density measurements. (* : calculated result)

This study was supported by the National Science Foundation under grants EAR039879 to JC. The in situ x-ray experiments were carried out at the X-17B2 beamline of the National Synchrotron Light Source (NSLS) which is supported by the US Department of Energy, Division of Materials Sciences and Division of Chemical Sciences under Contract No. DE-AC02-76CH00016 and by COMPRES, the Consortium for Materials Properties Research in Earth Sciences under contract number NSF Cooperative Agreement EAR 01-35554

Faulting Induced by Precipitation of Water at Grain Boundaries in Eclogite – Analogue for Subducting Hot Oceanic Crust

Junfeng Zhang, Harry W. Green II, Krassimir N. Bozhilov *•University of California at Riverside*
Zhenmin Jin *•China University of Geosciences at Wuhan, China*

Dehydration embrittlement has been proposed to explain both intermediate- and deep-focus earthquakes in subduction zones. Because such earthquakes primarily occur at shallow depths or within the core of the subducting plate, dehydration at relatively low temperatures has been emphasized. However, recent careful relocation of subduction-zone earthquakes shows that at depths 100-250 km, earthquakes continue in the uppermost part of the slab (probably the former oceanic crust that has been converted to eclogite) where temperatures are higher. Here we show that at P=3GPa, T=1300-1500K, eclogite lacking hydrous phases but with significant hydroxyl incorporated as defects in pyroxene and garnet develops a faulting instability associated with precipitation of H_2O at grain boundaries and associated production of very small amounts of melt (< 1 vol%). This new faulting mechanism satisfactorily explains high-temperature earthquakes in subducting oceanic crust and potentially also could be involved in much deeper earthquakes in connection with similar precipitation of H_2O in the mantle transition zone (400-700 km). Of potentially critical importance for all proposed high-pressure earthquake mechanisms is the very small amount of fluid required to trigger this instability.

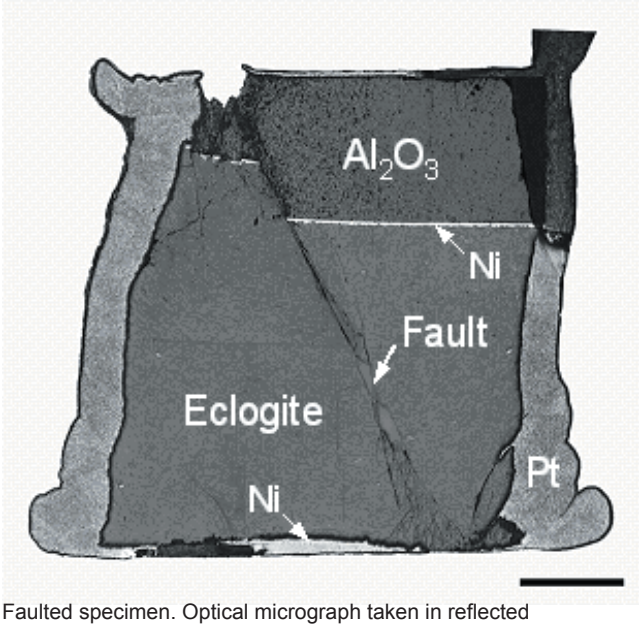

Faulted specimen. Optical micrograph taken in reflected light showing an entire faulted specimen deformed at 3 GPa, 1400 K and 1.3 X 10-4/s (GB271). Scale bar: 1mm.

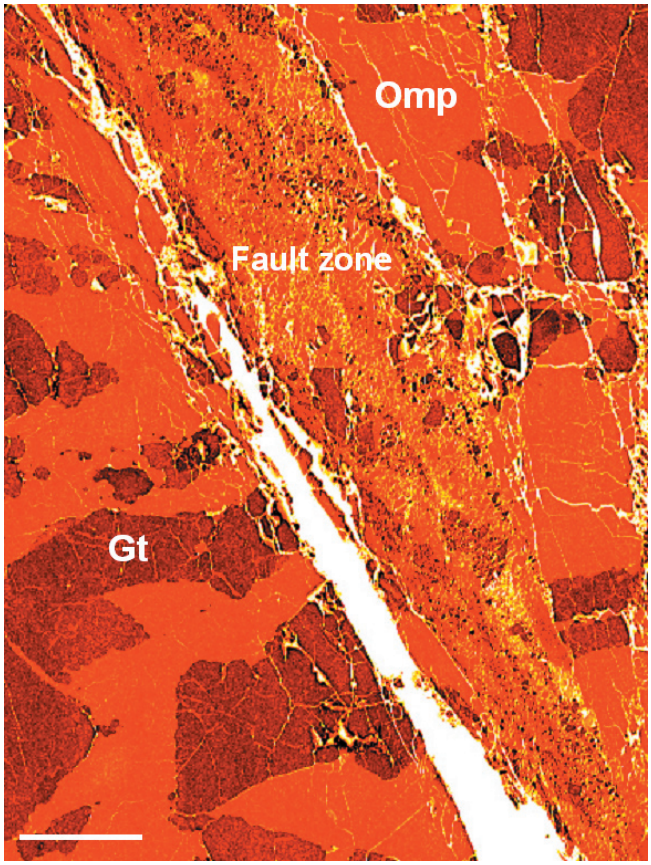

Detail. False-color SEM micrograph showing part of faulted spec- imen including microstructure. Scale bar: 25 μm

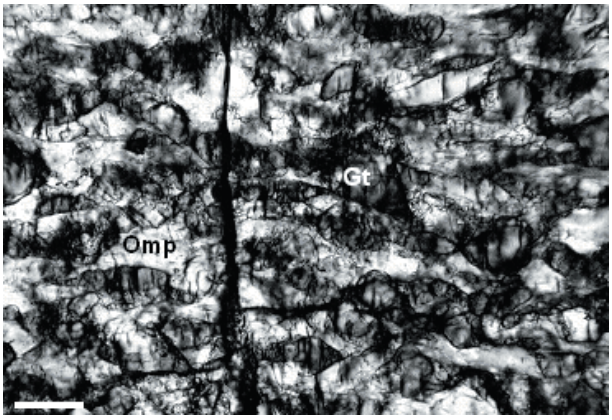

Microstructural details of faulted specimen. Optical thin section viewed in transmission shows all grain boundaries marked with glass films as well as myriads of glass-filled Mode I microcracks, demonstrating that under stress the melt + fluid generated extensive cracking preceding shear failure. Scale bar: 50μm.

Zhang, J., Green, H. W., Bozhilov, K. N. and Jin, Z. Faulting induced by precipitation of water at grain boundaries in ho subducting oceanic crust. *Nature*, vol. 428, pp. 633-636, 2004.

This study was supported by the National Science Foundation under grants EAR0003631 & EAR0135411 to HWG. The experiments were performed using the 5-GPa Griggs-type piston cylinder deformation apparatus at UC Riverside in preparation for upcoming in situ experiments to be performed in the D-DIA at NSLS or APS.

New model to predict high-pressure behavior of $GdFeO_3$-type perovskites

Jing Zhao, Nancy L. Ross, Ross J. Angel *Virginia Polytechnic Institute and State University*

Pressure-induced variations of the structures of several $GdFeO_3$-type orthorhombic perovskites (ABO_3) have been investigated by using single-crystal X ray diffraction and show that the octahedra BO_6 in some become more tilted with increasing pressure (e.g. Zhao, et. al., 2004a), whereas others become less tilted and the structure evolves towards a higher-symmetry configuration (e.g. Ross, et al.,2004). This variety of behaviour is attributed to the difference in compressibilities between the octahedral (β_B) and dodecahedral cation (β_A) sites in the perovskite structure. If the BO_6 octahedra are less compressible than the AO_{12} sites then the perovskite will become more distorted with pressure, but the perovskite will become less distorted if the BO_6 site is more compressible than the AO_{12} site. We have developed a new model, based on the bond valence concept, to predict the relative compressibilities of the cation sites in oxide perovskites (Zhao, et. al. 2004b). We introduce the site parameter Mi, the variation of the bond valence sum at the central cation in a polyhedral site due to the change of the average bond distance. Experimental data suggest that the pressure-induced changes in the bond-valence sums at the two cation sites within any given perovskite are equal. With this condition we show that the ratio of cation site compressibilities is given by $\beta_B / \beta_A = M_A/M_B$. This model, based only upon room-pressure bond lengths and bond-valence parameters correctly predicts the structural behaviour of oxide perovskites at high pressure. There is also a strong correlation between the ratio M_A/M_B and both the bulk moduli (Fig1) and the average rate of tilting (Fig.2) of the octahedra with pressure.

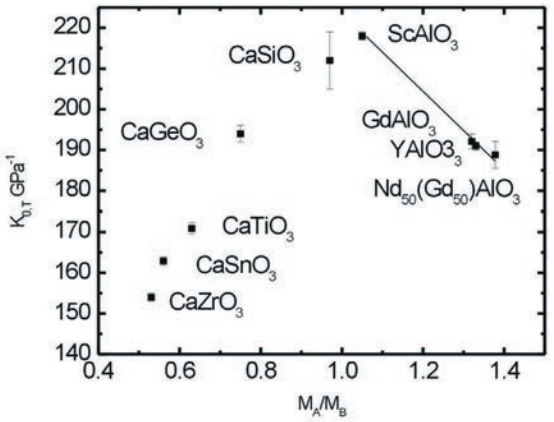

Figure 1

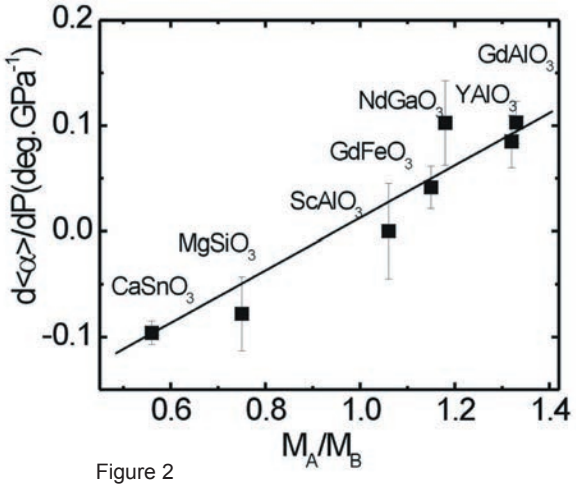

Figure 2

Ross, N. L., Zhao, J. & Angel, R. J. (2004). J. Solid State Chemistry 177,1276-1284; Zhao, J., Ross, N. L. & Angel, R. J. (2004a). Phys Chem Miner. 31,299-305; Zhao, J., Ross, N. L. & Angel, R. J. (2004b). *Acta Cryst*. B60, 263-271.

This study is supported by the National Science Foundation under the Grants EAR-0105864 to N. L. Ross and R. J. Angel.

Infrared and Raman spectroscopic studies of FeS under high pressure

Tao Zhou *New Jersey Institute of Technology;* **Zhenxian Liu** *Geophysical Lab, Carnegie Institute,* **S.W. Cheong** *Rutgers University*

Understanding of the behavior of iron sulfide, which is believed to prevail in the core of Mars under high pressure conditions, is far from being complete. Therefore, it is a great challenge and may be the key to predict the stability and time evolution of the interior structure of Mars, Earth, and other planets. Under ambient pressure, FeS is an antiferromagnetic insulator and is therefore considered to be a strongly correlated system, where competition between localization and delocalization of the d-electrons may lead to such puzzling phenomena as magnetic moment collapse, metal-insulator transition, huge volume expansion, etc.

Infrared and Raman spectroscopic methods are ideal tool to probe the metal-insulator transition, as well as to extract vibrational and structural information from the studied crystal (i.e. FeS) under pressure. By measuring the reflectance spectra at the infrared regime, one can directly detect the Drude mode, the signature of a metallic phase. Depending on its crystal structure, any crystal will exhibit either Raman or infrared active phonon modes, which can be measured by Raman or infrared spectroscopy. Thus, Infrared and Raman spectroscopic studies of FeS under high pressure will provide not only significant information for a material that is very important in geoscience, it will also help condensed matter physicists to understand better the strongly correlated electron systems, a fertile ground for exciting new physics phenomena.

The following two figures show the spectra of mid-infrared reflectance and far-infrared absorption of FeS under high pressure, respectively.

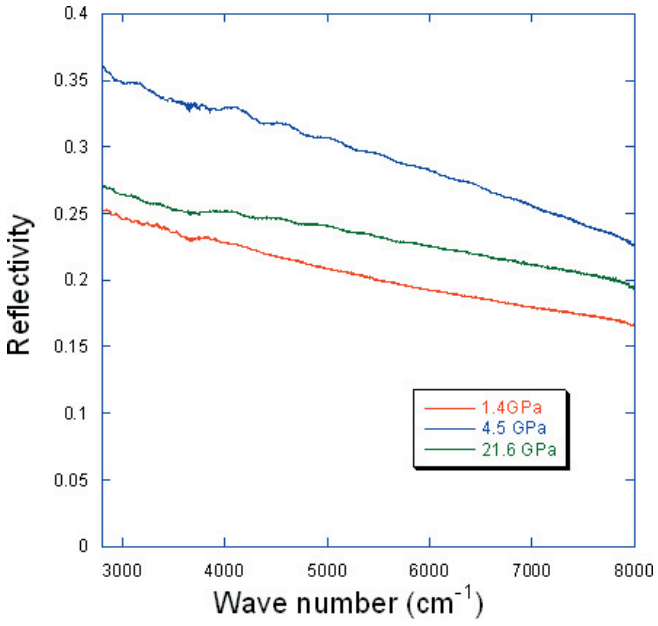

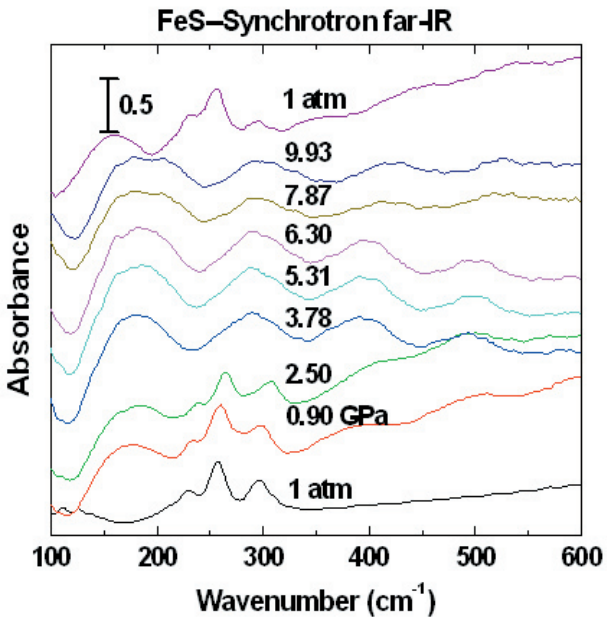

Reference: Y. Fei, C. T. Prewitt, H. K. Mao, C. M. Bertka, Structure and density of FeS at high pressure and high temperatures and the internal structure of Mars, *Science* 268, 1892 (1995).

These data were obtained from the U2A beam line at NSLS.